

**2008 DUNGENESS GROUNDWATER FLOW MODEL  
DESIGN, CONSTRUCTION, CALIBRATION AND RESULTS**

**February, 2009**

**2008 DUNGENESS GROUNDWATER FLOW MODEL  
DESIGN, CONSTRUCTION, CALIBRATION AND RESULTS**

*Prepared for:*

**Clallam County  
Dept. of Health and Human Services  
223 East 4th Street, Suite #14  
Port Angeles, WA 98362-3015**

*Prepared by:*

**Pacific Groundwater Group  
2377 Eastlake Avenue East, Suite 200  
Seattle, Washington 98102  
206.329.0141  
[www.pgwg.com](http://www.pgwg.com)**

*February 19, 2009  
JZ0601*

---

# TABLE OF CONTENTS

<b>1.0</b>	<b>INTRODUCTION.....</b>	<b>1</b>
1.1	PROJECT BACKGROUND.....	1
1.2	MODELING SCOPE.....	2
1.3	AUTHORIZATION AND WARRANTY .....	2
<b>2.0</b>	<b>SUMMARY OF FINDINGS.....</b>	<b>3</b>
<b>3.0</b>	<b>CONCEPTUAL HYDROGEOLOGIC MODEL .....</b>	<b>6</b>
3.1	PRIOR CHARACTERIZATION .....	6
3.2	SUPPLEMENTAL CHARACTERIZATION.....	7
3.2.1	<i>Deep Aquifer Occurrence.....</i>	<i>8</i>
3.2.2	<i>Flow Gains and Losses in Small Streams.....</i>	<i>9</i>
3.2.3	<i>Groundwater Inflow Along Southern Model Boundary.....</i>	<i>9</i>
3.2.4	<i>Wetlands and Evaporative Losses .....</i>	<i>10</i>
3.2.5	<i>Head Differences Between Aquifers .....</i>	<i>10</i>
3.2.6	<i>Expression of Climatic Trends as Recharge and Water-Level Responses.....</i>	<i>11</i>
<b>4.0</b>	<b>MODEL CONSTRUCTION .....</b>	<b>12</b>
4.1	PRIOR MODEL VERSIONS.....	12
4.2	MODEL REFINEMENTS .....	13
4.3	MODEL INTERFACE, CODE, SOLVER, TIMESTEPPING & REALIZATIONS .....	14
4.4	MODEL DOMAIN AND DISCRETIZATION.....	15
4.5	BOUNDARY CONDITIONS .....	15
4.5.1	<i>No-Flow Boundaries.....</i>	<i>16</i>
4.5.2	<i>Constant Head Boundaries.....</i>	<i>16</i>
4.5.3	<i>General Head Boundary.....</i>	<i>17</i>
4.5.4	<i>Specified Flux Boundary (Wells).....</i>	<i>18</i>
4.5.5	<i>Rivers.....</i>	<i>19</i>
4.5.6	<i>Drains.....</i>	<i>20</i>
4.5.7	<i>Recharge.....</i>	<i>20</i>
4.5.8	<i>Evapotranspiration.....</i>	<i>22</i>
4.6	AQUIFER AND AQUITARD PROPERTIES .....	23
4.6.1	<i>Hydraulic Conductivity and Transmissivity.....</i>	<i>23</i>
4.6.2	<i>Aquifer Storage Parameters .....</i>	<i>24</i>
<b>5.0</b>	<b>STEADY-STATE MODEL CALIBRATION.....</b>	<b>24</b>
5.1	STEADY-STATE TARGETS AND PRIOR INFORMATION.....	24
5.2	STEADY-STATE CALIBRATION PARAMETERS.....	27
5.3	STEADY-STATE CALIBRATION OBSERVATIONS .....	28
5.4	STEADY-STATE SENSITIVITY ANALYSIS .....	32
5.5	STEADY-STATE CALIBRATION RESULTS.....	33
5.5.1	<i>Realization “Dung-7e”.....</i>	<i>33</i>
5.5.2	<i>Realization “Dung-7g” .....</i>	<i>34</i>
5.5.3	<i>Overall Steady-State Calibration Assessment .....</i>	<i>35</i>
<b>6.0</b>	<b>TRANSIENT MODEL CALIBRATION .....</b>	<b>36</b>
6.1	TRANSIENT STRESS PERIODS AND INITIAL CONDITIONS .....	36
6.2	TRANSIENT CALIBRATION TARGETS.....	36
6.3	TRANSIENT CALIBRATION PARAMETERS .....	37
6.4	TRANSIENT CALIBRATION OBSERVATIONS .....	37
6.5	TRANSIENT CALIBRATION RESULTS .....	38

<b>7.0</b>	<b>PREDICTIVE ANALYSIS.....</b>	<b>39</b>
7.1	PREDICTIVE SIMULATIONS.....	39
7.2	REPRESENTATION OF AR/ASR RESPONSES .....	41
7.3	LINEARITY ANALYSIS .....	42
7.4	AR RESULTS.....	42
7.4.1	<i>Sensitivity to Site Location.....</i>	42
7.4.2	<i>Sensitivity to Specific Yield and Storativity .....</i>	43
7.4.3	<i>Sensitivity to Hydraulic Properties of Aquifers, Aquitard and Streambed .....</i>	43
7.4.4	<i>Summary of Factors Affecting AR Responses.....</i>	44
7.5	ASR RESULTS.....	44
<b>8.0</b>	<b>MODEL USES, LIMITATIONS, AND RECOMMENDATIONS .....</b>	<b>46</b>
	<b>REFERENCES .....</b>	<b>49</b>

---

## TABLES

Table 3-1	Hydrogeologic Unit Analysis of Wells Over 350 Feet Deep
Table 4-1	Summary of Solver Parameters
Table 4-2	Calibrated Hydraulic Conductivity Values for Aquifer/Aquitard Zones and Streambeds
Table 5-1	Summary of Water Level Targets
Table 5-2	Summary of Predicted Streamflow Seepage and Target Values for Steady State Calibration
Table 5-3	Summary of Head Residuals from Steady State Calibration
Table 6-1	Summary of Transient Calibration Targets
Table 7-1	Summary of Model AR Predictions and Sensitivity Analyses
Table 7-2	Distribution of Flow Augmentation Among Modeled Streams from Steady State Aquifer Recharge at 2 Cfs
Table 7-3	Maximum Head Rise Observed in Model Layers for Steady State AR Simulations
Table 7-4	Summary of Model ASR Predictions

---

## FIGURES

Figure 1-1	Vicinity Map and AR/ASR sites
Figure 3-1	Wetlands and Model Evapotranspiration Cells
Figure 3-2	Head Difference Analysis Between Shallow and Middle Aquifers
Figure 3-3	Changes in Simulated Shallow-Aquifer Heads Between Study-Period and Long-term Average Recharge
Figure 4-1	Distributions of Inactive and Constant Head Cells
Figure 4-2	Distributions of Inactive and General Head Boundary Cells
Figure 4-3	Distributions of Specified Flux Cells (Wells)
Figure 4-4	Distribution of River and Drain Cells
Figure 4-5	River Stage Departure Around Study Period Average
Figure 4-6	River Stage Departure Calculated for Transient Warm-up Period
Figure 4-7	Distribution of Steady-State Model Recharge
Figure 4-8	Transient Precipitation Recharge as Percent of Simulation Period Total
Figure 4-9	Irrigation Out-Takes and Geographic Groupings for Recharge Estimation
Figure 4-10	Kh Zonation in Layer 1 of "Dung-7e" Model Realization
Figure 4-11	Kh Zonation in Layer 1 of "Dung-7g" Model Realization
Figure 5-1	Model Water-Level Target Values
Figure 5-2	Head Target Residuals for Model Realization "Dung-7e" (Layer 1)
Figure 5-3	Head Target Residuals for Model Realization "Dung-7e" (Layers 3 and 5)
Figure 5-4	Head Target Residuals for Model Realization "Dung-7g" (Layer 1)
Figure 5-5	Head Target Residuals for Model Realization "Dung-7g" (Layers 3 and 5)
Figure 6-1	Transient Target Predictions for the Shallow Aquifer for Model Realization "Dung-7e"
Figure 6-2	Sensitivity Analysis on Transient Boundary Conditions
Figure 6-3	Transient Sensitivity to Dungeness River Streambed K <sub>v</sub>
Figure 7-1	AR Discharge to the Dungeness River at Two Rates of AR
Figure 7-2	Stream Augmentation from Steady-State AR (Model Realization "Dung-7e")
Figure 7-3	Dungeness River Augmentation from AR (Model Realization "Dung-7e")
Figure 7-4	Model Sensitivity to Key Hydraulic Properties: Sites 2 and 4
Figure 7-5	Stream Augmentation from Site 1 AR (Model Realization "Dung-7e")
Figure 7-6	Stream Augmentation from Site 2 AR (Model Realization "Dung-7e")
Figure 7-7	Stream Augmentation from Site 3 AR (Model Realization "Dung-7e")

Figure 7-8	Stream Augmentation from Site 4 AR (Model Realization “Dung-7e”)
Figure 7-9	Stream Augmentation from Site 5 AR (Model Realization “Dung-7e”)
Figure 7-10	Stream Augmentation from Site 6 AR (Model Realization “Dung-7e”)
Figure 7-11	Stream Augmentation from Site 8 AR (Model Realization “Dung-7e”)
Figure 7-12	Stream Augmentation from Site 9 AR (Model Realization “Dung-7e”)
Figure 7-13	Stream Augmentation from Site 10 AR (Model Realization “Dung-7e”)
Figure 7-14	Steady State Mounding from 2 cfs AR at Sites 1 and 2
Figure 7-15	Steady State Mounding from 2 cfs AR at Sites 3 and 5
Figure 7-16	Steady State Mounding from 2 cfs AR at Sites 6 and 7
Figure 7-17	Steady State Mounding from 2 cfs AR at Sites 9 and 10
Figure 7-18	Dungeness River Augmentation from ASR (Model Realization “Dung-7e”)
Figure 7-19	Dungeness River Augmentation from ASR (Model Realization “Dung-7g”)
Figure 7-20	Streamflow Augmentation from East-Site ASR in Layer 5 (“Dung-7e”)
Figure 7-21	Streamflow Augmentation from East-Site ASR in Layer 3 (“Dung-7e”)
Figure 7-22	Streamflow Augmentation from East-Site ASR in Layer 3 (“Dung-7g”)
Figure 7-23	Streamflow Augmentation from West-Site ASR in Layer 5 (“Dung-7e”)
Figure 7-24	Streamflow Augmentation from West-Site ASR in Layer 3 (“Dung-7e”)
Figure 7-25	Streamflow Augmentation from West-Site ASR in Layer 3 (“Dung-7g”)

---

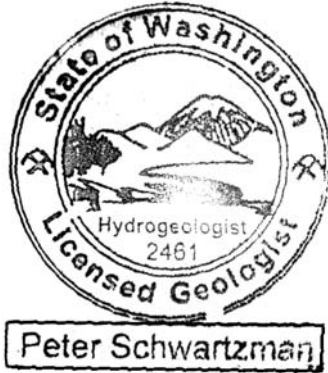
## APPENDICES

Appendix A	Model Layering, Bedrock Distribution and Marine Connections
Appendix B	Annotated List of Digital Documentation

---

## SIGNATURE

This report, and Pacific Groundwater Group's work contributing to this report, were reviewed by the undersigned and approved for release.



A handwritten signature in blue ink, appearing to read "Peter Schwartzman", is written over a horizontal line.

---

**Peter Schwartzman**  
Associate Hydrogeologist  
Washington State Hydrogeologist #2461

---

## 1.0 INTRODUCTION

This report presents the refinement and calibration of a groundwater flow model of the Dungeness Peninsula in Clallam County, Washington, and its application to predict hydrologic responses to aquifer recharge (AR) and aquifer storage and recovery (ASR). The study area and the model domain are shown on **Figure 1-1**.

---

### 1.1 PROJECT BACKGROUND

Groundwater availability and stream baseflows on the Dungeness Peninsula have been significantly affected by human activities. Irrigation diversions from the Dungeness River began in the late 19th century, and have reduced irrigation-season baseflows in the river. Groundwater recharge from leaky irrigation ditches has increased groundwater occurrence and the ability of the uppermost (“shallow”) aquifer to support baseflows in small streams and saturation in groundwater-supported wetlands. More recently, however, movements towards restoring summer baseflows in the Dungeness River by irrigation conservation (such as piping of irrigation ditches) has led to reduced groundwater recharge and has likely caused some decline in groundwater levels. In addition, population growth and increased consumption of groundwater for residential/commercial uses has further stressed study-area aquifers and contributed to the observed declines (PGG, 2002). As many of the small streams and river tributaries are fed by groundwater, groundwater level declines will ultimately cause baseflow reductions below the historic rates from times of open (leaky) irrigation ditches and lower population density. Groundwater level declines will also cause increased seepage losses from the Dungeness River. While such seepage losses will be offset by reduced diversions during the irrigation season, they are likely to cause baseflow reductions during other times of the year.

The Dungeness River Management Team (DRMT) and its Technical Advisory Group (TAG) have long discussed the possibility of maintaining the benefits of irrigation conservation on Dungeness River baseflows during the irrigation season while supporting the shallow groundwater system and associated surface-water features. AR and ASR are strategies discussed for “harvesting” a portion of flow in the Dungeness River during periods of relative availability and re-directing this water to the groundwater system. This additional recharge could support baseflows in the Dungeness River during other times of the year as subsurface “return flow”, could support baseflows in small streams and water levels in wetlands year-round, and could offset groundwater level declines due to ditch piping and increased well withdrawals. In addition, AR could be sourced with reclaimed water which is currently generated by the City of Sequim and may be generated in the Carlsborg area by the Clallam PUD in the near future.

The DRMT and TAG have pursued tools to assess the effectiveness of AR and ASR. A groundwater model commissioned in 2002 was previously used to perform preliminary evaluation of AR scenarios (TTFW, 2003). In 2006, Clallam County received a grant from Washington State Department of Ecology (Ecology) to perform a feasibility study (FS) for AR/ASR within the study area. Pacific Groundwater Group (PGG) assembled a team of consultants to prepare the FS. Prior to simulating AR/ASR scenarios, the existing “2003 Model” underwent peer review to assess its suitability for performing the simulations. The peer review recommended a number of significant modifications (ESI, 2007a), and the TAG elected to add key elements of supplemental hydrogeologic characterization and model refinement to the FS scope as permitted by available budget. PGG performed the supplemental characterization and model refinements, recalibrated the model, and worked closely with the TAG to select scenarios for AR/ASR simulation. The current model is referred to as the “2008 Dungeness Groundwater Model” (2008 Model).



---

## 1.2 MODELING SCOPE

PGG's role in model development and prediction of AR/ASR responses included the following:

- Participation in peer review and scoping of modeling activities;
- Supplemental hydrogeologic evaluation for design and construction of the 2008 Model, as described in Section 3.2;
- Refinement of elements of the 2003 Model, as discussed in Section 4.2;
- Design and construction of the 2008 Model, as discussed in Section 4;
- Steady-state and transient calibration of the 2008 Model, including various sensitivity analyses, as discussed in Sections 5 and 6;
- Communication of the design and calibration of 2008 Model to the TAG;
- Working with the TAG to identify AR/ASR scenarios to be included in model predictions;
- Performing model predictions for 10 AR scenarios and 2 ASR scenarios, as discussed in Section 7;
- Model documentation (this report) and training of project partners.

It should also be mentioned that development of the 2008 Model included collaboration between PGG and Clallam County, Environmental Simulations Inc. (ESI), and other project partners. Ann Soule at Clallam County was indispensable in tracking down hydrogeologic data and sharing local hydrogeologic knowledge and expertise. Jim Rumbaugh of ESI provided input during critical model design decisions and calibration tasks, along with adding functionality to the modeling software (Groundwater Vistas) to support specific computational tasks. Aspect Consultants and Graysmarsh provided calibration data for Gierin Creek and Graysmarsh, and Aspect provided comments on the model during the late stages of calibration. Many other project partners contributed time and information that benefited the project as a whole. An overall summary of project tasks is presented in the FS (PGG, 2009).

---

## 1.3 AUTHORIZATION AND WARRANTY

This project is funded under grant number G0600342, issued to Clallam County by Washington Department of Ecology (Ecology). PGG was authorized to perform the work discussed above (and other supporting work under the same project authorization) by Clallam County under the following contracts and amendments: 53118-06-PGG, 100511-06-PGG, 100511-06-PGG, 100511-07-PGG, 100511-06-PGG2-Amend 1, 100511-06-PGG2-Amend2, and 100511-06-PGG2-Amend3.

The work was performed, and this report prepared using generally accepted hydrogeologic practices used at this time and in this vicinity for exclusive application to the study area and for the exclusive use of Clallam County. This is in lieu of other warranties, express or implied.

---

## 2.0 SUMMARY OF FINDINGS

The following bullets summarize the main findings and recommendations of this report:

1. Supplemental characterization performed prior to preparing the model included: evaluating the occurrence of a deep aquifer from (limited) deep well logs; evaluating the distribution of flow gains and losses in small streams; evaluating groundwater inflow along the southern boundary of the model domain; evaluating the occurrence of wetlands and associated evapotranspiration; and other analyses. While deep aquifer materials were present in several places, most wells didn't penetrate sufficient depth to discern its occurrence, and one well showed its absence. Groundwater inflow along the southern boundary may be predominantly associated with the sediments that overly bedrock rather than flow within the bedrock.
2. The pre-existing version of the model (known as the "Ecology 2003 Model") was refined before and during model calibration. Refinements included: improved definition of model layering; removal of the bottom-most layer representing bedrock; restructuring the model connections between aquifers and marine water; refinement of recharge definitions; refinement of model representation of selected rivers and streams, simulation of evapotranspiration from wetlands, improved accuracy of calibration targets.
3. During model calibration it became apparent that the criteria for successful calibration could be reasonably met with more than one representation of the model. This phenomenon, known as "non-uniqueness", occurs because model parameters are seldom known precisely everywhere and more than one combination of parameters can yield similar matches to calibration targets. PGG developed two versions ("realizations") of the model to address uncertainty in the vertical hydraulic conductivity ( $K_v$ ) of the upper and lower confining beds. Calibration and prediction was performed with both model realizations.
4. Model calibration was performed in both steady-state and transient modes to target groundwater level elevations collected during the USGS study period (December 1995 through September 1997). The steady-state calibration also used estimates of streamflow gains and losses as calibration targets. The transient calibration emphasized groundwater level *changes* over the study period, rather than absolute elevations.
5. Both realizations of the model provided acceptable steady-state calibration results. The combinations of aquitard  $K_v$  values developed in these two realizations represent two possible combinations, but other combinations may exist. Whereas  $K_v$  of the upper confining bed was represented at 0.0008 ft/d and 0.008 ft/d, calibration results suggested that the  $K_v$  of the lower confining bed could not be increased significantly beyond the smaller value (0.0008 ft/d) without compromising the ability of the model to meet calibration targets in the lower aquifer. If performed, further calibration of the model to additional calibration datasets may reveal other possible combinations of aquitard  $K_v$ . Model predicted responses to AR showed low sensitivity to the modeled range in aquitard  $K_v$  values; however, model predictions of hydrologic stresses in deeper aquifers are somewhat sensitive to values of aquitard  $K_v$ .
6. Steady-state calibration revealed locations where hydrogeologic complexity in the shallow aquifer could not be adequately represented using the existing single model layer representation of this aquifer. In reality, USGS definition of the shallow aquifer includes more than one water-bearing unit separated by low permeability aquitards. This stratification sometimes results in "perched aquifers" or differing groundwater elevations in neighboring wells completed at different depths. Perched conditions are known to occur near lower Bell Creek, and were inferred during model calibration to occur

near lower Matriotti Creek. The inability of the model to simulate perched conditions in these locations introduces some inaccuracy in model predictions of pumping impacts to these streams. The model cannot be expected to simulate hydrogeologic complexities beyond the current resolution of the model grid.

7. The transient calibration revealed that model simulation of shallow-aquifer water-level variations over time is controlled predominantly by the recharge schedule specified in the model. Other time-varying model inputs, such as pumping withdrawals and Dungeness River stage variations, have much less influence on most simulated water level variations in the shallow aquifer. The magnitude and timing of recharge is influenced by many factors, including: precipitation, depth to the water table, occurrence of perching zones or low permeability soil horizons, irrigation ditch use and leakage from ditches, and irrigation applications to fields. The resulting schedule of groundwater recharge is difficult to predict based on available data. During transient calibration, predicted hydrographs for targets in the shallow-aquifer showed variable quality matches to observed hydrographs, and a significant fraction of targets did not exhibit a close match. PGG determined that further transient calibration to shallow-aquifer water-level variations could not increase the reliability of the model without a substantial additional effort towards better definition of recharge. In lieu of this approach, PGG performed transient predictions over a range of values for shallow aquifer specific yield ( $S_y$ ).
8. Both realizations of the model were used to predict hydrologic responses to AR in the shallow aquifer and responses to ASR in the middle and lower aquifers. Prior to the predictive simulations, model testing established that AR simulations are fairly linear over rates ranging from 2 to 10 cfs, such that individual AR simulations can be scaled within this range and can be summed between sites. Predictive AR simulations were performed at ten sites using two values of  $S_y$  (0.1 and 0.2), and additional sensitivity analysis was performed at two of the sites. ASR was simulated in both the lower and middle aquifers at two locations, and included both values of  $S_y$ .
9. The predicted timing of streamflow augmentation from AR, and its distribution between streams, was most sensitive to the location of the AR site and the assumed  $S_y$  value. Local variations in shallow-aquifer hydraulic conductivity also affect the pattern of streamflow augmentation. The  $K_v$  of the upper confining bed had little influence on predicted stream-flow augmentation from shallow-aquifer AR. In general, sites closer to the Dungeness River were predicted to provide greater augmentation to the river, but much of that augmentation occurs during and immediately after the AR period. AR was assumed available during the spring freshet (mid May through Mid July), and the higher rates of augmentation predicted for near-river sites typically did not extend into the most critical low-flow period (i.e. September and October). AR at sites farther from the river was predicted to provide more sustained, year-round augmentation to the Dungeness River but at fairly low rates. During the critical low-flow period, predicted Dungeness River augmentation rates ranged from 5% to 25% of the rate of AR specified over the two-month freshet period.
10. ASR was simulated as 2 cfs injection during the 2-month spring freshet, one month dormancy, and two months of recovery pumping at 2 cfs. Because the AR cycle includes both injection and withdrawal, predicted impacts to stream baseflows are both positive (augmentation) and negative (depletion). Predicted impacts to baseflows are higher for ASR conducted in the middle aquifer than for ASR conducted in the lower aquifer, and are higher with higher values of aquitard  $K_v$ . Maximum predicted baseflow impacts to the Dungeness River were no greater than  $\pm 4$  percent of the ASR rate for lower-aquifer ASR (assuming  $K_v$  values of 0.0008 ft/d), no greater than  $\pm 14$  percent of the ASR rate for middle-aquifer ASR, and no greater than  $\pm 27$  percent of the ASR rate for middle-aquifer ASR with  $K_v$  for the upper confining bed increased to 0.0008 ft/d. Predicted Dungeness River impacts were smaller for the ASR site east of the river, largely because the predicted impacts were more distributed to other streams (e.g. Cassalery and Gierin creeks).

11. Model uses, limitations, and recommendations are summarized in Section 8. The model is best suited to regional scale simulations due to its coarse grid resolution. Predictive simulations within the shallow aquifer are less affected by uncertainty regarding aquitard  $K_v$  than simulations in the middle and deep aquifers. Shallow aquifer simulations cannot replicate complexities associated with stratified groundwater occurrence, such as potentially perched conditions near Matriotti and Bell creeks. As with all models, predictive results should be interpreted as approximate, because models are inherently non-unique and include some degree of uncertainty. Nevertheless, the 2008 Dungeness Model provides the best tool currently available to estimate hydrologic impacts within the groundwater flow system.
12. Additional model development, if desired, could include additional hydrogeologic characterization in areas of uncertainty, along with further calibration. While a detailed discussion of these recommendations is provided in Section 8, recommended areas of additional characterization include: baseflow gains/losses, perched conditions along Matriotti Creek and other shallow-aquifer complexities, hydraulic property distributions in the middle and deep aquifers, aquifer connections with marine water, and occurrence of the deep aquifer. Additional calibration is recommended to better constrain uncertainty associated with aquitard  $K_v$  and other model assumptions (e.g. aquifer-marine connection). A long-term transient calibration may be more useful than the existing study-period calibration to better understand the role of aquitard  $K_v$  and time varying stresses on the aquifer system (e.g. pumping, recharge); however, sufficient data would be required to develop a calibration target dataset. The model could be converted to a higher resolution grid to support simulation of more localized conditions and improve capacity to simulate contaminant migration.

---

## 3.0 CONCEPTUAL HYDROGEOLOGIC MODEL

### 3.1 PRIOR CHARACTERIZATION

The regional hydrogeology of the Sequim-Dungeness Peninsula was recently characterized by the U.S. Geological Survey (Thomas et al., 1999). Much of the discussion in this section is summarized from this USGS study. The study describes a stratified system of geographically extensive aquifers and aquitards consisting of a “shallow aquifer” underlain by a fine-grained “upper confining bed”, a confined “middle aquifer”, a “lower confining bed”, a “lower aquifer”, and deeper undifferentiated sediments. Over most of the peninsula, all or some of these six hydrostratigraphic units overlie Tertiary bedrock of sedimentary and volcanic origin. The total thickness of unconsolidated sediments beneath the peninsula ranges from zero feet in the south (where bedrock is exposed on the land surface) to as much as 2,500 feet in the northeast.

The shallow aquifer is composed of a variety of geologic materials, including: stream alluvium, glaciomarine drift, glacial outwash, ice contact deposits, and glacial till. The alluvium was deposited by the current Dungeness River along its current floodplain and by the ancestral Dungeness River as a floodplain terrace predominantly east of the existing river channel. The glacial and glaciomarine sediments are associated with the most recent continental glaciation (Vashon stade of the Frasier glaciation), which ended approximately 13,000 years ago. Given the range of geologic materials present, the texture of the shallow aquifer can vary from fine-grained to coarse-grained, and can be highly heterogeneous (locally variable). Water-bearing zones can be separated by lower permeability zones which restrict groundwater flow, and lower permeability zones can cause perched groundwater conditions. The thickness of the shallow aquifer generally ranges from 50 to 200 feet, although greater and smaller thicknesses have been observed. The aquifer is generally unconfined but can exhibit some local confinement with the occurrence of fine-grained, low-permeability deposits. Groundwater flow directions tend to “fan out” radially beneath the Dungeness Peninsula.

The underlying “upper confining bed” is typically 30 to 110 feet thick, and is mainly composed of pre-Vashon silts and clays with locally discontinuous lenses of water bearing sand and gravel. Beneath the upper confining bed, the “middle aquifer” is typically about 10 to 70 feet thick, and contains pre-Vashon glacial outwash deposits of sand and gravel and coarse-grained interglacial deposits. Groundwater in the middle aquifer occurs under confined conditions. The middle aquifer is underlain by the “lower confining bed”, composed of till and interbedded clay, silt and fine-grained sand with possible discontinuous lenses of water-bearing sand. Because few wells penetrate this confining unit, the USGS define a broad range for its thickness (10 to 300 feet) with a “typical” thickness of 100 feet. The underlying “lower aquifer” is composed of sand with thin lenses of sand and gravel, silt and clay. Information on the lower aquifer is limited due to few well completions. The aquifer is present in the northern and eastern portions of the peninsula, and absent in the southern and western portions where bedrock occurs closer to the land surface. Its thickness is believed to range from 10 to 180 feet, with a typical value of about 90 feet. Groundwater in the lower aquifer occurs under confined conditions.

The lower aquifer is underlain by “undifferentiated deposits”, which reach thicknesses as great as 1000 feet in the northern peninsula but pinch out against bedrock in southern and southwestern portions of the peninsula. Few wells have been drilled a significant depth into this unit, and only several of these wells have encountered significant water-bearing zones (3.2.1). The underlying bedrock is composed of tertiary sedimentary and volcanic rocks, and is an unreliable source of groundwater because it yields small quanti-

ties of water to wells. In general, bedrock typically exhibits low permeability relative to unconsolidated deposits and therefore transmits a relatively small quantity of water.

The groundwater flow system is recharged at the surface from precipitation, irrigation applications to fields, septic system effluent, and seepage losses from unlined irrigation ditches, the Dungeness River and other streams. Additional recharge occurs via subsurface pathways near the foothills of the Olympic Mountains, where water-bearing zones in the bedrock discharge into the unconsolidated aquifers described above. Recharge from the land surface flows downward into the various aquifers and aquitards; and eventually discharges into marine waters, the lower reaches of various streams, portions of the Dungeness River, groundwater supported wetlands, and to wells. Groundwater flow patterns have both horizontal and vertical components. Typically, flow within aquifers is predominantly horizontal whereas flow between aquifers (through aquitards) is predominantly vertical. Downward flow generally occurs in recharge areas, whereas upward flow occurs along discharge areas (e.g. near the coast and lower stream reaches). Vertical flow rates are relatively slow due to the low permeability aquitards between aquifers.

Surface-water/groundwater interactions between the Dungeness River and the shallow aquifer were studied by the USGS and Ecology (Simonds and Sinclair, 2002). The study employed three methods to characterize interactions and estimate vertical streambed permeability along the lower 11.8 miles of the Dungeness River between September 1999 and July 2001: in-stream mini-piezometers, seepage runs, and continuous water-level and water temperature monitoring at two off-stream well transects. Vertical hydraulic gradients in the mini-piezometers generally were negative between river miles 11.8 and 3.6, indicating loss of water from the river to groundwater. Small positive gradients indicating ground-water discharge occurred in three localized reaches below river mile 3.7. Data from the seepage runs and off-stream transect wells were generally consistent with the mini-piezometer findings. An exception occurred between river miles 8.1 and 5.5 where seepage results showed a small gain and the mini-piezometers showed negative gradients. Vertical hydraulic conductivity of riverbed sediments was estimated using hydraulic gradients measured with the mini-piezometers and estimated seepage fluxes. The resulting conductivity values ranged from an average of 1 to 29 feet per day and are similar to values reported for similar river environments elsewhere.

Thomas et al (1999) reference three prior regional groundwater studies performed by Noble (1960), Drost (1983) and Sweet-Edwards/EMCON (1991). In addition to these studies, various consultants have performed local and regional hydrogeologic evaluations. Saltwater intrusion in Clallam and Jefferson Counties was studied by Forbes and CH2M-Hill (1993). PGG studied the local hydrogeology in the vicinities of the City of Sequim's Silberhorn Wellfield (1996), Port Williams Wellfield (1995, 1998, 2008), and Water Reuse Demonstration Site at Carrie Blake Park (2000). PGG (2002) also summarized hydrogeologic monitoring performed on the Sequim-Dungeness thru 2001 and will soon release an update to this monitoring report. NTI (1990) reported on testing of the PUD's Calsborg water supply well, and Robinson and Noble (1974) reported on the construction and testing of a water supply well at Weyerhaeuser seed orchard. TTFW (2003, June) performed supplemental hydrogeologic characterization in areas characterized by the USGS as lacking sufficient data, in order to define local hydrogeologic framework for construction of the 2003 Model.

---

### **3.2 SUPPLEMENTAL CHARACTERIZATION**

In order to address questions raised in the 2003 Model peer review and support further refinements for the 2008 model, PGG performed the following supplemental hydrogeologic characterization activities:

- Evaluating the occurrence of a deep aquifer in the undifferentiated sediments underlying the lower confined aquifer;
- Evaluating the distribution of flow gains and losses in small streams;
- Evaluating groundwater inflow along the southern boundary of the model domain and developing an appropriate method of representation for the 2008 model;
- Evaluating the occurrence of wetlands to identify likely areas for representing evapotranspiration in the 2008 model;
- Assessing the distribution of head differences between aquifers; and,
- Assessing how climatic trends prior to and during the study period affected groundwater recharge and the representativeness of study-period groundwater levels for model calibration targets.

### 3.2.1 Deep Aquifer Occurrence

The purpose of this analysis was to review well logs and look for evidence of a deep aquifer in the undifferentiated deposits, also known as USGS Unit 6. Unit 6 occurs beneath the lower confined aquifer (USGS Unit 5). PGG identified wells deeper than 350 feet (in some cases 300 feet) from the following databases and published tables:

- 1) Ecology online well logs database,
- 2) Clallam County well log database,
- 3) USGS National Water Information System (NWIS) database<sup>1</sup>, and,
- 4) Published tables in USGS reports by Jones et al (1996) and Drost (1983).

Well information was compiled into spreadsheets and referenced wells were mapped in the project GIS for comparison with the locations of USGS cross-section traces (Jones 1995) along with geologic contacts where bedrock truncates USGS Unit 3 (middle aquifer extent from Figure 22 of Thomas et al, 1999). PGG reviewed the logs of all the deep wells located in the areas where bedrock does not truncate Unit 3 and compared the depths of the deepest water-bearing zones on the well logs to the depths of Unit 5 shown on nearby cross-sections. This procedure was used to evaluate whether wells encountered water bearing zones beneath the depth of Unit 5 estimated by Jones. Where cross-sections were far from the deep wells, PGG spent more time reviewing the logs and attempting to differentiate hydrostratigraphic units. In some cases, logs obtained from Ecology had already been interpreted by the USGS, and PGG used their interpretations directly. Some logs referenced in the County's database were no longer available for review.

As summarized in **Table 3-1**, PGG reviewed logs from 46 deep wells. Three of the logs were oil wells which lacked detailed descriptions of the unconsolidated sediments overlying bedrock, 4 of the logs turned out to be from shallow wells improperly entered in the database(s), and 5 logs revealed relatively shallow bedrock. Of the 34 wells with data suitable for interpretation, three wells showed water bearing (aquifer) materials below Unit 5:

- Well 30N/04W-09L02 is located west of the Dungeness River along Matriotti Creek and is associated with the Weyerhauser Seed Orchard. The well is screened between 800-830 feet bls, and is definitively completed in a Unit 6 aquifer. Clay materials were noted above the production zone, separating it from Unit 5. An aquifer test on the well showed relatively high transmissivity (Robinson & No-

<sup>1</sup> <http://waterdata.usgs.gov/nwis>

ble, 1974) but incomplete recovery indicative of bounded conditions with limited recharge from overlying aquifers.

- About a mile from the Weyerhaeuser site, Well 30N/04W-3SESW<sup>2</sup> (owned by 4plus/Dungeness Golf Course) shows a water bearing zone at 509-565 feet bls; whereas the USGS show a nearby cross section with the bottom of Unit 5 at 400 feet (but no logs specifically in that area). Its completion zone could possibly occur in Unit 6, and was overlain by 60 feet of low permeability sediments.
- The actual location of Well 30N/03W-27NWSE is not certain. The well is likely east of the Dungeness River near Sequim Bay, is believed by the County to be 27NWNE rather than 27NWSE based on the street address of the well (pers com, Ann Soule). This 704-ft well is screened at 530-560 and 659-689 feet bls, and the USGS interpret Unit 5 to be absent in this area, thus suggesting completion in Unit 6. The completion zones are overlain by a significant thickness of low permeability materials.

It should be noted that most of the other wells reviewed by PGG went only a short distance into Unit 6 (e.g. 50-100 feet) without encountering an aquifer. However, several wells were drilled to considerable depth without encountering an aquifer in Unit 6. A new well at Graysmarsh (30N/03W-9SESE) is completed between 596-696 feet deep and was interpreted by Aspect as Unit 5 (pers. com., Miller). Recent drilling of Well PW-3 at the City of Sequim's Port Williams Wellfield (30N/03W-17NWSE) did not encounter a substantial aquifer in 450 feet of exploration beneath USGS Unit 5 - though several water bearing layers ranging from 5 to 20 feet were encountered. Finally, the geology at the US Coast Guard light-house well differs enough from the USGS conceptual model, that PGG could not interpret the occurrence of Unit 6.

The fact that many of the wells reviewed do not penetrate significant thicknesses of Unit 6 suggests that a definitive conclusion about the occurrence and extent of aquifer material in the unit cannot be reached at this time. The data suggest that aquifer materials occur in at least 3 locations, are likely absent in one location, and that some areas show stratigraphy that differs from the conceptual model developed by the USGS.

### **3.2.2 Flow Gains and Losses in Small Streams**

PGG evaluated groundwater-derived baseflows in small study-area streams and presented the results in a separate technical memorandum (PGG, 2008a). PGG collected available streamflow data from multiple sources (Clallam County Streamkeepers, the Jamestown S'Klallam Tribe, Graysmarsh, Ecology and the USGS, compiled the data into a master database, mapped the locations of measurement locations and evaluated the distribution of baseflow and associated gains/losses represented in the database. PGG also facilitated a meeting of project partners and conducted interviews with knowledgeable water-resource managers to obtain input for interpretation of the available data. Based on this analysis, PGG's recommendations for baseflow calibration targets are presented later in this report on **Table 5-2**.

### **3.2.3 Groundwater Inflow Along Southern Model Boundary**

The 2003 Model represented groundwater inflow into the southern model boundary with constant head cells along the boundary. This resulted in relatively large inflows where the constant head cells contacted zones of high permeability. Review of the 2003 Model indicated that this representation is unrealistic, because groundwater inflow along the boundary is ultimately limited by the permeability of bedrock, regardless of whether downgradient sediments are high or low permeability (ESI, 2007a; PGG, 2007).

---

<sup>2</sup> The well notation "3SESW" indicates the SW quarter-quarter section of the southeast quarter section of section 3.



PGG used an alternative method to represent groundwater inflow along the model’s southern boundary. Geologic maps presented by Thomas et al (1999) suggest that bedrock is likely present across the entire southern boundary of the model. In fact, Thomas defines the southern edge of his study area (which occurs north of the model boundary) as “the edge of the unconsolidated deposits at the base of the Olympic Mountains”. If bedrock is predominant along the southern edge of the model boundary, and the permeability of bedrock is the limiting factor for inflow to the model domain, then a more even pattern of bedrock inflow would be expected across the model boundary. This type of representation was selected for model design, and is further described in Sections 4.5.3 and 4.5.4.

It is important to note that the western areas along the southern model boundary are represented by till overlying bedrock, and data are lacking regarding the thickness/permeability of the till or whether aquifer materials occur between the till and the bedrock. However, given the advantages of representing an even pattern of bedrock inflow to the model in adjacent areas, this conceptual hydrogeologic model was applied to the entire southern model boundary.

### 3.2.4 Wetlands and Evaporative Losses

In order to represent evapotranspiration (ET) from groundwater supported wetlands, PGG identified relevant wetland areas and estimated ET losses from the groundwater flow system. Clallam County provided a GIS coverage of documented wetlands classified by hydrologic function ("hydro\_func"). Three of the “hydro\_func” categories (4, 5 and 6) represent wetlands associated with the groundwater flow system. **Figure 3-1** shows the distribution of wetlands obtained from the County and the model cells specified for depiction of groundwater ET losses at wetlands.

Groundwater losses to wetland ET were estimated using PGG’s proprietary spreadsheet version of the USGS Deep Percolation Model (DPM). Thomas et al (1999) used the USGS code for the DPM (Bauer & Vaccaro, 1987) to estimate ET and recharge in the study area, and PGG used the same regional parameters reported by Thomas for estimating the seasonal soil moisture balance. From this water balance, PGG estimated the soil moisture deficit (defined as the portion of potential evapotranspiration that could not be satisfied due to lack of available moisture). Theoretically, the presence of standing water in a wetland would provide the moisture required to meet this deficit during dry periods. Calculated monthly soil moisture deficits were very similar for the major composite soil groups (glaciomarine sediments, glacial outwash/alluvium, glacial till) and monthly average values are listed below (all values in inches).

Jan	Feb	Mar	Apr	May	Jun	Jul	Aug	Sep	Oct	Nov	Dec	Annual
0.00	0.00	0.00	0.43	1.30	2.32	3.47	3.06	1.57	0.00	0.00	0.00	12.14

These ET values were applied to the model cells associated with wetlands, as discussed in Section 4.5.8.

### 3.2.5 Head Differences Between Aquifers

PGG reviewed available water-level data from a variety of wells to assess head differences between aquifers with the intention of developing head-difference targets for model calibration. PGG compared groundwater elevations between nearby wells (located in the same quarter-quarter section) completed in different aquifer units. Data sources included wells inventoried by the USGS (listed in Appendix A of Thomas et al, 1999; with data available from the USGS NWIS online database), water-level and well databases maintained by Clallam County, and City of Sequim monitoring at their Port Williams Wellfield (PGG, 2001). PGG identified 22 quarter-quarter sections with wells monitored in multiple aquifers. For the USGS wells, PGG downloaded well coordinate and water-level data from the NWIS database and compared representative water-level elevation data from neighboring wells completed in different aquifer

fers. Based on the USGS-rated accuracy of the wellhead elevations, the time-proximity of representative water levels, and the amount of water-level variation observed in individual wells, PGG ranked the quality of each head difference target as high, moderate, or low. The data from the City's Port Williams Wellfield represented a long record and was ranked "high". Usable wells in the County's database were already represented in the USGS NWIS database.

In addition, PGG developed a map of head differences between the shallow and middle aquifers (layers 1 and 3) based on the head contours presented in Thomas et al (1999) in their Figures 24 and 25. Where data are available for both aquifers, head difference values (shallow minus middle aquifers) range in a continuous pattern from -32 to 420 feet. However, comparing PGG's head-difference values estimated for specific quarter-quarter section with the distribution of USGS head differences shows apparent inconsistency between data sets (**Figure 3-2**). Some of this inconsistency could be due to the accuracy of the land surface elevation from which elevations were calculated (typically 20 feet or better) and/or the representativeness of the available data relative to seasonal variations (many measurement pairs did not occur at the same time). These inconsistencies call into question the accuracy of the quarter-quarter section head difference estimates; therefore, PGG elected not to use these values as targets for model calibration and to recommend that the head comparisons be revisited at a later time when simultaneous water-level data and more accurate wellhead elevations become available.

### **3.2.6 Expression of Climatic Trends as Recharge and Water-Level Responses**

As described in Section 5.1, both the 2003 Model and the 2008 Model are calibrated to a dataset collected by the USGS between December 1995 and September 1997. This USGS study period is associated with above-average precipitation within the study area between 1995 and 1999. The USGS estimated groundwater recharge from precipitation based on study-period precipitation *and* based on long-term average precipitation (Thomas et al, 1999). Peer review of the 2003 model (PGG, 2007) questioned whether the groundwater flow system had equilibrated to the above average precipitation recharge estimated by the USGS. If not, using the study-period estimate of recharge would be inappropriate for steady-state model calibration to study-period groundwater levels. A steady state model simulation assumes that the groundwater flow system has fully equilibrated to the hydrologic boundary conditions, including recharge (see further discussion in Section 5).

PGG reviewed water-level trends in Clallam County's water-level database to ascertain whether groundwater levels appeared to respond to above average precipitation between 1995 and 1999. In most cases, PGG compared 1993-94 data with 1995-97 (study period) data to see if there was a significant rise expected with increased recharge. Where data were available through 2000, a water-level rise was sought throughout the above-average 5-year period. The database included 73 wells, of which 14 had insufficient data, 3 showed water-level declines, 44 showed no significant trend, 7 showed only a suggestion of a rise (either  $\leq 1$  foot or the suggested trend was based on insufficient data), and 5 showed discernable rises ranging from around 1 to 5 feet. Based on previous target-well aquifer assignments employed in the 2003 model (TTFW, 2003), most of the wells were completed in the shallow aquifer; however, some were completed in deeper aquifers and some did not have aquifers defined. Given the few wells showing discernable trends, it might be reasonable to conclude that increased rainfall starting in 1995 did not affect water-levels during the study period. However both PGG (2002) and Thomas et al (1999) have noted overall falling trends in groundwater levels; so it is therefore possible that above-average precipitation recharge may have counteracted (background) falling trends over the time period considered.

PGG reviewed long term water-level trends in wells near the City of Sequim's Port Williams Wellfield documented in a monitoring report prepared for the City of Sequim (PGG, 2002). Among 8 wells completed in the shallow aquifer, most showed some temporary abatement to the declining water level trend

during the 5-year higher-precipitation period; however, this abatement typically represented a difference of 1 to 2 feet from the overall trend.

PGG used an early version of the 2008 model to assess whether the difference between long-term and study-period average estimates of recharge generated by the USGS (Thomas et al, 1999) caused significant differences in model predicted water levels. Head differences of less than 3 feet were observed for 75 percent of the target wells completed in layer 1, most of which were located in the higher permeability current and older alluvial deposits of the Dungeness River. Larger differences were observed in outlying areas of the model domain in lower permeability aquifer materials (**Figure 3-3**).

PGG considered the above observations to decide which USGS estimation of recharge (long-term or study-period) to use for model calibration. The above information does not conclusively indicate whether the groundwater flow system had equilibrated to above-average precipitation during the study period. However, given the small magnitude of predicted head differences between the two recharge distributions for most of the calibration targets, PGG decided to use the average of the two distributions to represent steady-state recharge during model calibration (Section 4.5.7).

---

## 4.0 MODEL CONSTRUCTION

### 4.1 PRIOR MODEL VERSIONS

Computer modeling of groundwater flow beneath the Sequim-Dungeness Peninsula was first performed by the USGS (Drost, 1983). The model used three layers to explicitly model the shallow, middle and lower aquifers, and implicitly simulated the intervening aquitards with conductance terms between the explicitly-modeled aquifer layers. The model used an early finite-difference computer code developed by the USGS (Trescott, 1975). PGG adapted the “Drost Model” to the more recent USGS modeling code “MODFLOW” (McDonald & Harbaugh, 1988), and made some minor calibration refinements, as part of the Conservation Plan (Montgomery Water Group, 1998). PGG’s version of the Drost model explicitly represented the aquitards as model layers, and included minor adjustments to the hydraulic conductivity distribution in the shallow aquifer resulting in improved calibration statistics.

TTFW made significant modifications and improvements to the Drost Model to create the 2003 Model under contract to Clallam County with grant funding provided by Ecology (TTFW, 2003). TTFW expanded the Drost Model domain to the south (to the 48th parallel) and to the west (to Morse Creek). TTFW also increased the resolution of model cells along the Dungeness River from the (uniform) 1/4-mile square used by Drost to a north-south elongated 1/4-mile by 1/8-mile rectangle. TTFW added two layers beneath the bottom of the Drost model to represent the undifferentiated deposits and bedrock, redefined the model layer elevations based on existing data, and further adjusted the layer elevations during calibration (“grid refinement”) to avoid dry cells. The model was run with the USGS MODFLOW code, and the Dungeness River was represented using MODFLOW’s “stream package”. Other small streams were represented using MODFLOW’s “drain package”. Groundwater connection to marine water was also represented using drain cells in model layer 1. Groundwater subflow into the southern model boundary was simulated using constant head cells. The model was calibrated to hydrogeologic conditions documented by Thomas et al (1999) during their 1995-1997 study period. The calibration utilized updated estimates of pumping and USGS estimates of study-period recharge from precipitation and irrigation ditches. Calibration included steady-state simulation of study-period average groundwater elevations and groundwater/surface-water interactions, and transient calibration (by adjusting aquifer storage characteristics) to groundwater elevations observed over the study period.

---

## 4.2 MODEL REFINEMENTS

A peer review of the 2003 Model was performed at the onset of this project. Jim Rumbaugh of Environmental Simulations Inc. (ESI) performed the review and considered input from PGG, Battelle National Labs, Aspect Consultants (for Graysmarsh) and the Clallam PUD (ESI, 2007a). The peer review identified a number of areas where the 2003 Model could be improved, and a subsequent meeting of project partners was conducted to decide which refinements could be accommodated under the available project budget. In addition, some refinements were authorized during model development as issues with the 2003 model configuration were identified. The current 2008 Model includes the following adjustments and refinements:

- Model layer elevations were adjusted to better honor the USGS elevation maps, and spurious effects of “grid refinement” during TTFW calibration were removed;
- The undifferentiated deposits were initially divided into 3 sub-units (an aquifer between overlying and underlying aquitards). Based on sensitivity analysis, the bottom sub-unit and an underlying model layer representing bedrock were later removed;
- The method of simulating subsurface groundwater inflow along the model’s southern boundary was revised to prevent excessive inflows between constant head cells and adjacent high permeability sediments (alluvial sediments within bedrock terrain);
- The model was restructured to allow a marine connection between the Strait of Juan de Fuca and the shallow, middle and lower aquifers (rather than just the shallow aquifer);
- Steady-state irrigation and precipitation recharge was regenerated from the USGS coverages to fix a potential mass balance import error. Precipitation recharge employed during the steady-state calibration was reduced from the study-period values to the average between study-period recharge and long-term average recharge. Errors associated with specification of wastewater recharge were corrected;
- Transient recharge was regenerated based on consideration of a monthly soil moisture balance and the occurrence of low permeability sub-soils ;
- The Dungeness River was converted from MODFLOW’s “stream” boundary condition to a “river” boundary condition. Morse Creek and Siebert Creek were converted from MODFLOW “drains” to “rivers”. Elevations of the Dungeness River and the small streams were updated based on Lidar data;
- MODFLOW’s evapotranspiration (ET) package was used to simulate ET from wetlands;
- Steady-state head targets were revisited for accuracy of location and elevation. Transient head targets were revised to “head change” targets to allow better calibration to hydrographs. Transient hydrographs were redefined by removal of water levels collected during pumping or recovery;
- Seepage targets for small streams were revisited based on PGG’s small streams analysis (PGG, 2008a);
- The hydraulic conductivity zonation for the shallow aquifer was simplified; and,
- Transient pumping distributions were regenerated from spreadsheets accompanying the 2003 model and modified to include actual City of Sequim pumping data.

---

### 4.3 MODEL INTERFACE, CODE, SOLVER, TIMESTEPPING & REALIZATIONS

PGG used the graphical user's interface "Groundwater Vistas Version 5" (ESI, 2007b) as a platform to organize input data, run the model, and view results. During calibration, PGG used the proprietary software "MODFLOW SURFACT" (Version 3, Hydrogeologic Inc, 2006) to perform model runs. SURFACT is more robust and stable than its parent code – the USGS public domain software "MODFLOW". However, once the model was calibrated, PGG also ran the model with MODFLOW 88/96 (McDonald and Harbaugh, 1988; Harbaugh and McDonald, 1996) and with MODFLOW 2000 (Harbaugh et al., 2000) and confirmed no significant difference in model results.

MODFLOW converges considerably slower than SURFACT. Both PGG and ESI were unable to identify solver settings within MODFLOW that supported run times similar to SURFACT. SURFACT employed the PCG4 solver, whereas MODFLOW was run with the SIP and PCG2 solvers. Solver parameters are summarized on **Table 4-1**. All solvers provided acceptable mass balance errors (significantly less than 1 percent).

Both SURFACT and MODFLOW use various forms of the block-centered flow (BCF) package which requires that the initial heads provided to the model solver be fairly close to the final heads. This is because solving the model with the BCF package computes leakance (VCONT) terms based on the initial heads and does not allow them to change as the solution converges. For this reason, we recommend either using a set of initial heads that is close to the new model solution, or running the model several times to ensure that changes in leakance due to changes in initial heads become insignificant.

The model was run in both steady-state and transient modes. During steady-state simulation, all hydrologic conditions (e.g. recharge, pumping, river stage) are held constant, and the model simulates "long-term" hydrologic equilibrium to these conditions. During transient simulation, hydrologic conditions are allowed to vary over time. PGG performed calibration to both steady-state and transient simulations, and used both types of simulation for predictive analysis. Transient calibration was run over the USGS study period (December 1995 through September 1997), and was preceded by multiple runs of a 12-month "warm-up" period to simulate background conditions prior to the USGS study period. Transient predictions were performed over a 12-month cycle simulated repeatedly over a 20-year period. All transient simulations employed a monthly stress period, 30 timesteps per month, and a timestep multiplier of 1.2.

During model calibration it became apparent that the criteria for successful calibration could be reasonably met with more than one representation of the model. This phenomenon, known as "non-uniqueness", occurs because model parameters are seldom known precisely everywhere and more than one combination of parameters can yield similar predictive results. While parameter values can be constrained within reasonable limits, some degree of uncertainty is common in hydrogeologic characterization due to natural variation (heterogeneity) and insufficient data to capture this variation. PGG recognized that model predictions may be sensitive to various uncertainties, and developed two versions ("realizations") of the model to address uncertainty in the vertical hydraulic conductivity of the upper and lower confining beds. Calibration and prediction was performed with both model realizations. As described below, these realizations were named the "Dung-7e" and "Dung-7g" realizations. The two realizations only differ in the hydraulic conductivity values assigned to the aquitards, selected regions of aquifers, and the streambeds of selected streams.

---

## 4.4 MODEL DOMAIN AND DISCRETIZATION

The model domain occupies an area of 17.5 by 14.5 miles that extends from just beyond Morse Creek on the west to Sequim Bay to the east and from the foothills of the Olympic Mountains to the south to the Strait of Juan de Fuca to the north (**Figure 1-1**).

The model domain was discretized into a seven-layer, variable-spacing grid. The distribution of rows and columns remains unchanged from the 2003 model, with 64 rows and 81 columns creating 36,288 cells. As discussed in Section 4.5.1, PGG modified the distribution of inactive cells to include bedrock such that 23,607 of the model cells remain active. Column spacings range from 660 feet along the Dungeness River to 1,320 feet elsewhere, and row spacings range from 660 feet near the center of the model domain to 1,320 feet elsewhere (**Figure 4-1**). The model grid is aligned with true north (i.e. not rotated).

Model layers were defined based on the hydrostratigraphic units discussed in Section 3.1. The model represents the uppermost five hydrostratigraphic units and separates the underlying undifferentiated deposits into an upper aquitard unit and a lower aquifer unit. While the 2003 model explicitly simulated groundwater flow through bedrock, PGG's sensitivity analyses during model calibration established that the role of bedrock is very minor to the overall groundwater flow system. Rather than explicitly simulating flow through bedrock, groundwater inflow to the 7 model layers from laterally adjacent bedrock was simulated using general head boundary cells (Section 4.5.3), and groundwater flow in bedrock underlying the undifferentiated deposits was not simulated.

PGG performed major refinements on the layer elevations in the 2003 model. PGG noted that the 2003 model had areas where layer elevations were inconsistent with the USGS characterization (Thomas et al, 1999) and that TTFW had lowered the elevations of some layer contacts to avoid the occurrence of dry cells. PGG's approach to model calibration was to use the USGS layer elevations where defined, and modify aquifer properties during calibration to avoid dry cells where saturation is believed to be present. Where layer elevations were not characterized by the USGS, PGG "feathered" the nearby USGS elevations into the elevations used in the 2003 model (TTFW evaluated hydrostratigraphic units in selected outlying areas) and further hand-adjusted elevations as needed during model calibration. Detailed documentation of layering scheme development, including contour maps of layer elevations and thicknesses, is presented in **Appendix A**.

In order to simulate the hydraulic connection between hydrostratigraphic units and the Strait of Juan De Fuca, it was necessary to estimate model layer elevations north of the coastline. Data are insufficient to reasonably document this submarine layering; therefore, PGG projected the existing layering at a northward declining dip of 0.74 percent based on interpretation of USGS cross-sections. Description of this projection is presented in **Appendix A**, and simulation of the marine connection is discussed in Section 4.5.2.

---

## 4.5 BOUNDARY CONDITIONS

Boundary conditions in the model include:

- No-flow (inactive) cells corresponding to bedrock;
- Constant head cells representing marine water;
- General head cells representing groundwater inflow from bedrock across the south model boundary;

- Specified flux (well) cells representing groundwater withdrawals and shallow subflow above bedrock entering the southern model boundary;
- River cells representing the Dungeness River, Morse Creek and Siebert Creek;
- Drain cells representing the remaining small streams in the study area;
- Recharge to the uppermost model layer from precipitation, irrigation, and wastewater; and,
- Evapotranspiration in areas of groundwater supported wetlands

#### 4.5.1 No-Flow Boundaries

PGG represented bedrock located along the outer extents of the model domain with “no-flow” (inactive) model cells. Rather than explicitly simulating groundwater flow through the bedrock that “cradles” the unconsolidated aquifers and aquitards, PGG positioned general head boundary cells along the downgradient edge of the bedrock which estimated bedrock inflow based on USGS estimates of its hydraulic conductivity and other flow parameters (Section 4.5.3). Local occurrences of bedrock within the interior of the model domain *were* explicitly simulated, again using the USGS estimate of bedrock hydraulic conductivity (Section 4.6.1).

Inactive cells associated with bedrock are shown for all model layers on **Figure 4-1**. The distribution of inactive bedrock cells was based on USGS definitions presented by Thomas et al (1999). However, USGS bedrock definition for various layers has gaps west of McDonald Creek. So, after importing the USGS bedrock distributions, PGG also imported the TTFW coverages from the 2003 model in selected western portions of the model domain (**Appendix A**). The distribution of bedrock cells in the model interior explicitly simulated for active groundwater flow was derived from the most recent Washington Department of Natural Resources DGR GIS coverage downloaded online. Section 4.6.1 addresses this distribution of interior bedrock.

Although bedrock exposures are locally noted in some of the creek beds, bedrock was not explicitly simulated in the shallow aquifer along creeks, as this would prevent simulation of local groundwater/ surface-water connections through the unconsolidated deposits that overlie the bedrock.

#### 4.5.2 Constant Head Boundaries

Constant head (CH) boundaries were used to represent marine water that is in hydraulic continuity with the unconsolidated aquifers and aquitards represented by the model. Marine CH cells were identified where model layers intersected offshore bathymetry. As discussed in **Appendix A**, model layer elevations along the northern coast were projected northward with a dip of 0.74 percent to the northern boundary of the model. Beneath Sequim Bay, model layers were assumed to be flat, and elevations along the coast were maintained in an easterly direction beneath the coast. Bathymetric elevations were obtained from the Puget Sound DEM<sup>3</sup>, and were resolved to the centroids of model cells within the project GIS. The following algorithm was used to identify whether a model cell was sufficiently occupied by marine water to be represented as a marine CH cell:

- For aquifers, if the bathymetry sinks below the top surface of the aquifer then the sea is assumed to have sufficient hydraulic connection to the aquifer to justify a CH cell.

<sup>3</sup> <http://www.ocean.washington.edu/data/pugetsound/psdem2005.html>

- For aquitards, the bathymetry must penetrate 75 percent of the aquitard before the cell is specified as CH marine. This is because marine occupation of an aquitard layer will have greatest influence on heads in the underlying aquifer rather than adjacent aquitard cells that are not associated with marine conditions. An aquitard penetration of 75 percent was assumed sufficient to bring the marine condition close to the underlying aquifer layer.
- All model cells occupied by marine CH conditions are assigned high values of hydraulic conductivity (e.g. 100,000 ft/d) so that the CH cells functionally represent open-water conditions and offer no hydraulic resistance to inflow from adjacent aquifer/aquitard cells. PGG explored simulation of a submarine “skin” on the aquifer/marine interface during calibration (Section 5.3).

**Figure 4-1** shows the distribution of marine CH cells in layers 1 through 5. Layers 6 and 7 occur at elevations below the bathymetry within the model domain.

Marine CH values were set to 4.06 feet above the model datum (NAVD88), which is equivalent to the mean tidal level based on NOAA data from Ediz Hook and Port Townsend<sup>4</sup>. GV was set to perform density correction on the CH cells based on the cell midpoint elevation and a density 1.025 times greater than freshwater. This density correction increased equivalent freshwater heads from 4.06 feet NAVD88 to about 15 feet NAVD88 in the deepest layer with marine connections (layer 5).

### 4.5.3 General Head Boundary

A general head boundary (GHB) was used to represent bedrock inflow into the upgradient (southern) boundary of the model. The USGS (Thomas et al) interpreted subflow into the model domain as follows:

*“Water moves into the groundwater system in unconsolidated deposits as subsurface inflow from outside the study area. Most of this inflow probably comes from lateral flow through the southern boundary of the study area, either as near-surface flow through soils and the veneer of unconsolidated deposits overlying bedrock or as flow from fractures in bedrock into the shallow aquifer”.*

The USGS estimated a shallow-aquifer inflow of 18 cfs for the model area (USGS extended study area minus Miller Peninsula). The USGS further estimated a median bedrock permeability of 0.04 ft/d, which falls within the permeability range published for sandstone by Freeze and Cherry (1979). In order to simulate bedrock inflow into the unconsolidated sediments, PGG positioned GHB cells along the down-gradient face of the no-flow cells representing bedrock (**Figure 4-2**).

Flow from a GHB is directly proportional to the cross-sectional area, permeability and head difference associated with the “flow tube” represented by the GHB, and inversely proportional to the length of the represented flow tube. In order to simulate *regional* flow through bedrock, PGG selected a regional origination point for the flow tube about 5.7 miles south of the southern model boundary in the Olympic Mountains. Specifically, bedrock elevations 30,000 feet south of the model boundary are on the order of 3,800 feet NAVD88. Flow tubes were assigned to the southernmost active cell in each model column using the following procedure:

- The distance to the general head was calculated as the distance between the cell and the southern model boundary plus 30,000 feet;
- All general heads were set to a value of 3,800 feet NAVD88;

<sup>4</sup> [http://tidesandcurrents.noaa.gov/station\\_retrieve.shtml?type=Bench+Mark+Data+Sheets](http://tidesandcurrents.noaa.gov/station_retrieve.shtml?type=Bench+Mark+Data+Sheets)



- The width of the general head cell was set to the model width and the height of the cell was set to the saturated thickness of the cell;
- The permeability of the general head cell was set to 0.04 ft/d.

During model simulations, the height of the general head cells was updated as heads were updated by the model. As shown on the model water budget referenced in Section 5.5, bedrock inflow represented only a small portion (e.g. 1.4 cfs) of the 18 cfs inflow estimated by the USGS. The remainder of the 18 cfs inflow estimated along the southern model boundary was simulated with specified flux cells (i.e. “injection wells”) located in the same cells as the layer-1 GHB cells (see discussion immediately below).

#### 4.5.4 Specified Flux Boundary (Wells)

Specified flux boundary conditions were used to simulate groundwater withdrawals from wells and shallow subflow (inflow) to model layer 1 in the sedimentary veneer overlying bedrock. Pumping withdrawals were previously estimated by TTFW for the 2003 model, and PGG retained the same pumping distribution in the steady-state version of the 2008 model. (All TTFW wells specified for bedrock portions of the model domain were no longer simulated once bedrock regions were converted to inactive cells.) During construction of the transient model, however, PGG noticed that the pumping well distributions in the 2003 transient model (“Tranca15”) were inconsistent with both the 2003 steady-state model, and that transient pumping schedules sometimes differed significantly from those described in the 2003 model report (TTFW, 2003). PGG regenerated the model input for transient pumping wells from TTFW’s original files for import into GV. In addition, PGG modified the modeled pumping schedules at the City of Sequim’s Silberhorn and Port Williams wellfields to reflect actual monthly pumping rather than the generalized cycle of monthly pumping used on all other pumping wells simulated by the model<sup>5</sup>.

Distributions of specified flux cells for all model layers are shown on **Figure 4-3**. Layers 4 and 7 have no specified flux cells. The wells in layer 6 are relic points from the 2003 model, which simulated the layer as an extensive aquifer immediately underlying the aquifer in layer 5. While the current model has the capacity to simulate a deep aquifer below layer 5, the current configuration does not do so. Sensitivity analysis showed that leaving these relic pumping wells in layer 6 has minimal effect on model calibration, however, future refinement of the model should consider how to represent these deep aquifer withdrawals most realistically.

PGG simulated subflow to the shallow aquifer system through the veneer of sediments overlying bedrock using specified flux cells (“injection wells”) immediately downgradient of regional bedrock. The distribution of these “injection wells” located in layer 1 is shown in purple on **Figure 4-3**. The total rate of injection was about 16.6 cfs, and was calculated as the total inflow of 18 cfs estimated across the southern model boundary (Thomas et al, 1999) minus the bedrock inflow into the model simulated by the general head boundary condition (1.4 cfs). This total injection rate was distributed among the “injection wells” proportional to the column width of each cell. The rate of inflow specified for these cells was held constant over time in both the steady state and transient models.

<sup>5</sup> As noted in Section 6.1, the transient model has a “warmup” period which precedes the study period used for calibration. Port Williams pumping was not included in the warmup period (the wellfield came online during the study period) and Silberhorn pumping was based on the regenerated TTFW pumping distribution. During the calibration period, both Port Williams and Silberhorn pumping were specified as actual withdrawals on a monthly basis.

#### 4.5.5 Rivers

MODFLOW's river package was used to simulate groundwater exchanges (gains and losses) with Dungeness River, Morse Creek and Siebert Creek (**Figure 4-4**). The latter two creeks were represented as drain boundaries in the 2003 model; however, analysis of their flow regime suggested that the streams remain flowing along their entire courses within the model domain, and are therefore more appropriately represented as rivers (PGG, 2008a). Whereas drains only simulate groundwater discharge, rivers allow groundwater exchanges in both directions (gaining and losing).

For the Dungeness River, PGG estimated river elevations and lengths for each associated model cell within the project GIS. Steady-state river elevations were estimated from Lidar GIS coverage by identifying the elevation of the channel near the middle of the model cell. Channel lengths were estimated by digitizing along the midpoint of the channel within each model cell. Channel widths, previously estimated by TTFW, were maintained in the 2008 model. The riverbed was assumed to be 3 feet below the river stage, and the thickness of the riverbed was assumed to be 5 feet (the saturated hydraulic connection between groundwater and the river is therefore severed if the local water table falls more than 8 feet beneath the river surface).

During calibration, the hydraulic conductivity of the Dungeness River bed was adjusted to best match net seepage loss from the river, and all the elevations associated with the river were reduced by 4 feet. This reduction was performed to compensate for the effects of large grid cells (relative to the river dimension) and obtain a more realistic representation of the hydraulic gradient between the river and the shallow aquifer. Because seepage losses from the river are distributed over the entire area of the model cells (1320 feet by 660 feet), simulated mounding immediately beneath the river (which is only about 50 ft wide), is underestimated and the hydraulic gradient between the river and the aquifer is over-estimated. Reducing the elevation of the river allows the model to simulate more realistic gradients and maintain a saturated hydraulic connection between the river and the aquifer. This approach has been successfully used on other regional groundwater flow models (pers. com., Rumbaugh, 2008).

During transient calibration, the stage of the Dungeness River was allowed to vary. PGG specified stage variation in the river over the 23-month calibration period by calculating average monthly river stage at four sites with documented stage-discharge relationships and then calculating the difference between these monthly averages and the study-period average. This difference was termed the "stage departure", and is shown on **Figure 4-5**. PGG averaged the monthly stage departure for all four sites, and applied this set of monthly average departures to the steady-state values of river stage. For the transient warm-up period, PGG calculated average stage departures for each month using streamflow data from 1994 to 1997 and stage-discharge relationships<sup>6</sup>, and again applied these monthly 4-year average departures to the steady state values of river stage. Monthly river stage departures used for the warm-up period are shown on **Figure 4-6**.

For Morse and Siebert creeks, PGG assigned all cells a river width of 10 feet, and used the river lengths specified in the 2003 model. The top of the riverbed was assumed to be 1 foot below the river stage, and the thickness of the riverbed was assumed to be 5 feet. River elevations were estimated by averaging the lowest Lidar elevation in the given river cell with the lowest Lidar elevation in the next upgradient river cell. River elevations were held constant during both steady state and transient calibrations. Riverbed hydraulic conductivity was adjusted during calibration (Section 5).

---

<sup>6</sup> For example, the January average was the average of all January values during the 4-year period.

#### 4.5.6 Drains

All other small streams simulated by the model (Bagley, McDonald, Matriotti, Meadowbrook, Cassalery, Gierin, Bell and Johnson creeks), along with Graysmarsh, were simulated as drains. Similar to MODFLOW river cells, drains are defined by their stage elevation, length, width, drained thickness, and drained hydraulic conductivity. For all streams represented as drains, PGG used the drain widths and lengths employed in the 2003 model and drained thicknesses of 5 feet. PGG calculated drain elevations in the same manner as river elevation for Morse and Siebert creeks described above. Drain elevations remained constant during both steady-state and transient calibrations, and drained hydraulic conductivities were adjusted during calibration (Section 5.2).

PGG added several drain cells in the Bell Creek vicinity to simulate hillside springs that feed the stream. For Graysmarsh, PGG specified the drain length and width as the row and column dimension of the cells which occupy the footprint of the marsh. Model cells included in simulating the marsh footprint were varied slightly during calibration. Per information provided by Aspect Consultants, the marsh was assigned an elevation of 6 feet NAVD88. In addition, PGG added drain cells to extend McDonald and Matriotti Creeks upstream relative to the drain distribution in the 2003 model, and added drain cells to simulate Lotzgazelle and Beebe Creeks (downstream tributaries to Matriotti Creek with groundwater inflows).

#### 4.5.7 Recharge

Primary sources of recharge include precipitation, irrigation applications (seepage from ditches and fields), and infiltration of wastewater (septic systems and land application at Sunland). While recharge had been previously calculated for the 2003 model, PGG had to recalculate recharge because the previous method of recharge calculation likely had mass balance errors and because PGG's transient warm-up and calibration periods differed from those used for the 2003 model.

The USGS estimated the long-term and study-period annual average distributions of precipitation recharge, the study-period average distribution of irrigation recharge, and regression equations for estimating recharge as a function of composite soil group, precipitation, and land-surface slope (Thomas et al, 1999). PGG used area-weighted GIS calculation methods to distribute the USGS distributions of precipitation and irrigation recharge to the model cells in manner that did not add mass balance error. Because the USGS recharge coverage did not extend to all portions of the model domain, PGG used the USGS regression equations to estimate long-term and study-period precipitation recharge in outlying areas (irrigation recharge did not occur in these outlying areas). For each outlying cell, PGG extracted values of average annual precipitation and composite soil type from the USGS GIS coverages. Slope information was predominantly obtained from soil GIS coverages obtained from the Natural Resource Conservation Service (NRCS, 2005). Also, because the USGS composite soil map does not extend to the southern model boundary, PGG used WDNR surficial geology GIS coverage to correlate with soil parent types. Average annual precipitation values on the USGS isohyetal map were multiplied by 1.35 to generate study-period estimates of precipitation based on the study-period multiplier noted by Thomas et al.

Estimation of total recharge required incorporation of wastewater recharge with precipitation and irrigation recharge. TTFW estimated study-period rates of wastewater recharge per model cell, and PGG used the TTFW wastewater recharge distribution with several modifications:

- TTFW calculated septic recharge proportional to groundwater withdrawals per model cell. PGG noted one or more cells with very high rates of septic recharge, and found that these cells were associated with City of Sequim groundwater withdrawals that supply end users connected to the City's

sewer system. PGG removed the septic recharge input for these groundwater withdrawals associated with sewer wastewater disposal.

- Wastewater recharge from the Sunfield land application system was originally specified in cell 28,66 at a rate of 0.0103 ft/d. Per discussions with Ann Soule (Clallam County), the Sunfield wastewater recharge was moved from cell 28,66 to cell 29,64.

After resolving the USGS long-term average precipitation, study-period precipitation, and irrigation recharge to the model grid, PGG estimated the total recharge for both long-term conditions and study-period conditions by adding the TTFW estimates to the USGS estimates. Based on analysis of climatic and water-level trends presented in Section 3.2.6, PGG generated a total recharge distribution that summed the average (i.e. midpoint) of the long-term and study-period precipitation recharge, the irrigation recharge, and the wastewater recharge. This recharge distribution, used to calibrate the steady-state model, is shown on **Figure 4-7**.

Transient calibration required that recharge be estimated for each monthly stress period simulated by the model. The monthly distribution of precipitation recharge was estimated using PGG's proprietary version of the USGS Deep Percolation Model used by Thomas et al. Monthly values of study-period precipitation and temperature were input into PGG's DPM and precipitation recharge was calculated over a range of study-period monthly precipitation values and a range of soil available water capacity (AWC) values, both derived from data presented in Thomas et al.<sup>7</sup>. Monthly recharge was then expressed as percent of the study-period total, and plotted on **Figure 4-8**. Study-period patterns of monthly percent recharge did not vary greatly over the parameters simulated by PGG's DPM, and the average of the DPM results was used to apportion precipitation recharge per cell on a monthly basis.

The monthly distribution of irrigation recharge was estimated by TTFW for the 2003 model. TTFW estimate that the monthly distribution of irrigation recharge is roughly proportional to the monthly distribution of irrigation out-takes, and created four groups of irrigation companies from which to estimate out-take schedules. The groupings included:

- AHE – Agnew, Highland and Eureka
- CCD – Clallam, Cline & Dungeness Company
- SSP – Dungeness District & Sequim Prairie
- I - Independent

The out-take schedules and geographic distributions of groupings are shown on **Figure 4-9**. TTFW's irrigation recharge cells are presented as symbols colored by grouping. However, because PGG's method of GIS conversion between the USGS recharge grid and the model grid resulted in a slightly different recharge distribution, PGG created four recharge "zones" that closely conform to TTFW's groupings, and used these zones to assign the four monthly schedules of irrigation recharge to the associated cells. PGG's zones are shown as solid colors on **Figure 4-9**.

TTFW's correlation between irrigation out-takes and irrigation recharge is simplistic in that it assumes that all ditches (mains and laterals) are used according to the out-take schedule of the group. More specific analysis would require substantial effort, and this simplification was maintained with the caveat that

---

<sup>7</sup> Monthly precipitation data were used from USGS stations Pre-5 (lower end) and Pre-1 (moderate) and 1.75 times Pre-1 (upper end, multiplier derived from isohyetal map). AWC value ranged from 0.04 to 0.14 in/in per Table 3 in Thomas et al (1999)

it may introduce some error in the irrigation recharge distribution to the transient model. Other factors, such as presence/absence of shallow till and the thickness of the unsaturated zone can also affect the timing of recharge, and are discussed below.

Wastewater recharge was held at the average annual rates used in the steady-state model, as indoor water use (the source for septic wastewater recharge) was assumed to show little seasonal variation.

For each month in the study period, total recharge was calculated by summing up study-period precipitation recharge, irrigation recharge, and wastewater recharge. While it was beyond the scope of this modeling exercise to estimate the effects of depth to the water table on the timing of recharge arriving at the uppermost aquifer, PGG did modify the recharge schedule for model cells where recharge from the root zone had to pass through a low permeability subsoil to reach the water table. This modification was performed because low-permeability sub-soils often cause shallow perched conditions which tend to slowly release water to the underlying aquifer at relatively steady rates until seasonally perched water has fully drained. The USGS associate low permeability sub-soils with glaciomarine, fine/very-fine alluvium, and till composite soil groups (shown as low vertical permeability values on Table 3 in Thomas et al, 1999). The following algorithm was used to modify the recharge schedule for soils underlain by low permeability subsoil:

1. Where total recharge was relatively low ( $\leq 0.6$  ft/yr) and irrigation recharge was absent, total recharge was distributed evenly over 4 months (December thru March);
2. Where total recharge was relatively high ( $>1.0$  ft/yr) and irrigation recharge was absent, total recharge was distributed evenly over 6 months (November thru April);
3. Where total recharge was intermediate (between these two ranges) and irrigation recharge was absent, total recharge was distributed evenly over 5 months (December thru April);
4. Where precipitation recharge occurred in combination with irrigation recharge, PGG assumed that the opposite seasonal schedules of these two sources maintain perched conditions year-round, and total recharge was spread evenly over the entire year.

For the 12-month transient warm-up period, PGG used our proprietary version of the DPM to estimate the monthly percentage of total annual recharge based on long-term monthly average precipitation reported by the Western Regional Climate Center for the Sequim weather station<sup>8</sup> times a 1.32x multiplier to adjust Sequim precipitation upwards towards the study-area average, and applied these percentages (shown on **Figure 4-8**) to the USGS estimates of long-term precipitation recharge (Thomas et al, 1999). Irrigation recharge was distributed based on monthly average values of the percent of total irrigation out-takes shown on **Figure 4-9**. Both wastewater recharge and the method of apportioning monthly recharge in areas underlain by low-permeability sub-soils were the same as discussed above.

#### 4.5.8 Evapotranspiration

As described in Section 3.2.4, PGG defined ET cells in areas occupied by groundwater supported wetlands (categories 4, 5, and 6 from Clallam County wetland GIS coverage). ET cells were associated with both larger wetland polygons and areas containing groups of small groundwater supported wetlands. Perched wetlands (categories 1 and 3) were assumed to generally originate from rainfall or surficial runoff. **Figure 3-1** shows the distribution of wetlands and ET cells specified in model layer 1.

---

<sup>8</sup> <http://www.wrcc.dri.edu/summary/climsmwa.html>

The monthly soil moisture deficit values presented in Section 3.2.4 were used to specify potential ET for the transient model, along with an extinction depth of 3 feet. For the steady state model, PGG assigned wetland cells the annual average value of the soil moisture deficit (roughly 1 ft/yr).

It is worthwhile to note that many of the model cells to which wetland ET was applied are larger than the area of the associated wetland(s). In addition, the extinction depth of 3 feet was applied to the land surface, which is the average Lidar elevation for the model cell rather than its minimum elevation. Further refinement of the model might consider scaling the potential ET rates by the proportion of wetland area to cell area and adjusting the extinction depths to represent the fact that wetlands typically occur at the lowest elevations in the model cells. However, total wetland ET predicted by the model was small relative to total recharge (see model water budget referenced in Section 5.5), and PGG did not attempt to make these additional refinements.

---

## 4.6 AQUIFER AND AQUITARD PROPERTIES

The hydraulic properties of aquifers and aquitards are specified in the model using hydraulic conductivity (K), storage coefficient (S), and specific yield ( $S_y$ ). Hydraulic conductivity can be further separated into its horizontal and vertical components ( $K_h$  and  $K_v$ ). PGG used a method of zonation, where zones of like aquifer properties are distributed over continuous regions of active model cells. Groundwater Vistas calculates the transmissivity of a model layer based on its thickness and its  $K_h$ .

### 4.6.1 Hydraulic Conductivity and Transmissivity

Zones of like  $K_h$  and  $K_v$  were designated as sub-regions within the shallow aquifer (layer 1). In underlying hydrostratigraphic units, estimates of aquifer and aquitard properties were relatively sparse, and a single, uniform  $K_h/K_v$  zone was assigned to the entire layer. This simplified approach is justified where little information is available about hydrostratigraphic units. Not adding unwarranted complexity is referred to as the “principle of parsimony”. Anisotropy, the ratio of  $K_h:K_v$ , was maintained at about 10:1 for aquifer hydraulic conductivity zones and 100:1 for aquitard hydraulic conductivity zones. Model cells associated with seawater (represented with constant head cells, as discussed in Section 4.5.2), were all assigned a relatively high value for both  $K_h$  and  $K_v$ . Interior model cells associated with bedrock outcrops (except those in streambeds where surface-water/groundwater interactions are expected to occur) were assigned a value of 0.04 ft/d. **Figures 4-10** and **4-11** show the layer-1  $K_h$  zonation for the two model realizations, and **Table 4-2** summarizes K values per zone for all model layers.

Values of  $K_h$  and  $K_v$  for individual zones were adjusted during calibration, and the boundaries of various sub-regions were sometimes shifted within layer 1 during calibration. PGG initially designated K zones in layer 1 according to the USGS analysis (Figure 26 in Thomas et al., 1999). However, given that the USGS K zonation was largely based on specific capacity data from short-term tests in domestic wells (typically not constructed to maximize performance), the USGS interpretation was not strictly maintained during calibration. Section 5.2 discusses adjustments to K zones during calibration.

Transmissivity (T) was calculated for each layer by Groundwater Vistas as the product of  $K_h$  and saturated thickness. Therefore, T was not directly assigned to the model layers. However, the hydraulic conductivity of the lower aquifer (layer 4) was selected so that T for the 100-foot thick layer was equal to the T estimated at the Port Williams Wellfield (approximately 4,000 ft<sup>2</sup>/d).

## 4.6.2 Aquifer Storage Parameters

Transient calibration of the model focused largely on water-level variations in the shallow aquifer, which is simulated as unconfined. Values of specific yield ( $S_y$ ) were adjusted during calibration with acceptable values ranging from 0.05 to 0.25. Predictive analyses were run using  $S_y$  values of 0.1 and 0.2, in order to address uncertainty. Storage coefficient ( $S$ ) was varied between 0.0005 and 0.0005, but was maintained at 0.0002 for predictive analysis, as estimated from aquifer testing at Sequim's Port Williams Wellfield (PGG, 2008b). Because transient calibration focused mainly on hydrologic stresses and responses in the shallow aquifer, model calibration was not highly sensitive to  $S$  values in underlying layers.

---

## 5.0 STEADY-STATE MODEL CALIBRATION

Calibration is the process of adjusting model parameters (e.g.  $K_h$ ,  $K_v$ ,  $S$ ,  $S_y$ ) within acceptable, representative ranges to achieve the best match between model predictions and observations from the hydrologic system ("calibration targets"). During steady-state calibration, targets included study-period average water-level elevations measured in monitoring wells, and streamflow seepage (gains/losses) estimated from a variety of sources. During transient calibration, targets included study-period groundwater level trends measured in monitoring wells (head *changes* over time). Where possible, adjustments to model parameters were constrained by "prior information". Prior information largely consisted of knowledge gained from published hydrologic interpretation, such as an estimated hydraulic conductivity distribution for the shallow aquifer (Figure 26 in Thomas et al, 1999) and estimation of transmissivity from aquifer testing in the lower aquifer at the Port Williams Wellfield (PGG, 2008b).

Some model parameters, such as the hydraulic conductivity ( $K$ ) of aquitards, have little prior information and can only be constrained based on textural descriptions and  $K$  ranges published in textbooks. Such generic  $K$  ranges are fairly broad, and while they can be narrowed down considerably through calibration, significant uncertainty can still remain. During calibration, it became apparent that the calibration targets could be reasonably met with more than one value of aquitard  $K$ . PGG therefore developed two "realizations" of the model, one with a low-end value of aquitard  $K$  (Dung-7e) and the other with a higher  $K$  value for the upper confining bed (Dung-7g). As discussed in Section 5.3, using a higher  $K$  value for the lower confining bed provided a poorer match with calibration targets. The calibration targets specified for this model development were insufficient to further refine estimates of aquitard  $K$ ; however, other datasets are available which may aid in such refinement. Further calibration is recommended at a later date to better constrain aquitard  $K$  values and make the model more robust for predictive simulations that are sensitive to this parameter. Fortunately, prediction of AR in the shallow aquifer was not particularly sensitive to aquitard  $K$  and the model is well suited for this application (Section 7.4.3).

The following sections describe model calibration targets and prior information, parameters varied during steady-state calibration, observations made during model calibration, sensitivity analysis performed during steady-state calibration, and calibration results.

---

## 5.1 STEADY-STATE TARGETS AND PRIOR INFORMATION

Calibration targets include groundwater elevations and net baseflow gains or losses on study area streams. Groundwater elevation targets were derived from water-level monitoring performed during the USGS study period (December 1995 through September 1997). TTFW originally developed a set of 65 water-level targets that included study-period averages for 56 wells and 1979 measurements for 9 wells (from Drost, 1983). PGG performed the following refinements and increased the number of head targets to 69.

- Targets were added for 3 wells at Sequim’s Port Williams wellfield using water level from 1996-1997 and for 4 wells owned by Graysmarsh using water level data from 1997-1999. Sequim data were provided by PGG and Graysmarsh data were provided by Aspect Consulting. The locations and elevations of most (6) of these wells were based on surveyed data.
- Clallam County improved the location accuracy of 58 of the 63 non-surveyed target wells by locating the wells on the County’s GIS. Estimated accuracy was within 10 to 40 feet. PGG updated the locations of 4 of the 5 remaining non-surveyed wells based on coordinates from the USGS NWIS database<sup>9</sup>. Elevations of all non-surveyed wells were updated based on the new coordinates and Lidar land surface elevations.
- PGG revisited the study-period average water-level calculations performed by TTFW, removed two wells where measurements were predominantly taken during pumping, and adjusted representative depths to water for several additional wells by removing data collected during pumping recovery.
- PGG obtained depth-to-water measurements from the study period for 4 of the 9 targets originally derived from the Drost Model dataset, and updated these targets accordingly. In most cases, only one measurement was available during the study period.
- PGG assigned relative accuracy weights to the water-level targets. Targets with data collected during the study period were generally assigned relative weights of 1. Targets with data from the Drost study, almost 20 years prior to the calibration period, were generally assigned relative weights of 0.3. Drost targets with depth-to-water updated using (limited) data from the study period were assigned relative weights of 0.7.

**Table 5-1** and **Figure 5-1** present summaries of the water-level targets used during steady-state calibration. TTFW identified the completion aquifers of most of these wells. Along with the targets obtained from the City of Sequim and Graysmarsh, 52 of the 69 wells are estimated to be completed in the shallow aquifer, 2 in the upper confining bed, 11 in the middle aquifer, and 5 in the lower aquifer.

The accuracy of target elevations is a function of accuracy of the reference point elevation (measuring point at wellhead or land-surface) and the accuracy and representativeness of the depth-to-water used to calculate the water-level elevation. While the surveyed reference points are at least accurate to  $\pm 1$  foot, the lidar elevations of wells located by Clallam County are likely within  $\pm 5$  feet of accuracy (unless within forested areas or moderate/steep sloped areas)<sup>10</sup>, and the elevation accuracy of the five remaining wells may be on the order of  $\pm$  tens of feet (depending on local topography). Measurements of depth to water within wells are typically relatively accurate (e.g. within  $\pm 0.1$  feet); however, the extent to which the available water-level measurements accurately represents conditions during the study period is variable. As shown on **Table 5-1**, some of the targets include data collected throughout the study period, whereas other targets have data records that represent just a portion of the study period or just one measurement, and other targets have data collected outside the study period. Wells with data collected throughout the study period were typically visited monthly, although some wells have as few as 5 measurements. Most of these wells are likely to have fairly representative values for average depth to water, whereas water-levels from 1979 may be significantly less representative.

“Flooded cells” were sometimes used as a qualitative target where no head targets were available. Large areas of flooded cells in the shallow aquifer (where unconfined conditions are supposed to predominate) were generally avoided.

<sup>9</sup> <http://nwis.waterdata.usgs.gov/usa/nwis>

<sup>10</sup> The accuracy of lidar is typically within  $\pm 2$  feet; however, additional errors may result from inaccuracies in well location.



Streamflow seepage targets were estimated for the Dungeness River, 10 other streams, and Graysmarsh. Groundwater/surface-water interactions on the Dungeness River were studied by Simonds and Sinclair (2002), and TTFW reported personal communication with Bill Simonds indicating that net losses from the river are on the order of 12 to 15 cfs (TTFW, 2003). Groundwater discharge to Gierin Creek and Graysmarsh is estimated to be 0.9 cfs and 6.5 cfs respectively (pers. comm., Aspect Consulting, 2008). Target flow recommendations for groundwater discharge to other small streams within the model domain were developed by PGG (2008a), and are listed in **Table 5-2**.

Prior information for model calibration included:

1.  $K_h$  estimates developed by Thomas et al (1999), including statistics per hydrostratigraphic unit and an estimated hydraulic conductivity distribution map for the shallow aquifer;
2. T estimates for the lower aquifer in the vicinity of the City of Sequim Port Williams Wellfield;
3. T estimates for the deep aquifer at the Weyerhaeuser Seed Orchard (Robinson & Noble, 1974 and Sinclair, 2002);
4. An estimated range of streambed  $K_v$  for the Dungeness River by Simonds & Sinclair (2002);
5. Textural descriptions of aquitard properties combined with associated textbook K estimates.

The  $K_h$  estimates presented in Thomas et al (1999) were based on specific capacity data from driller's logs. The method of estimating  $K_h$  makes a number of significant simplifying assumptions that, in our opinion, make the  $K_h$  estimates highly approximate. For example, the thickness of the aquifer is assumed to be equivalent to the length of the well screen and the well is assumed to be highly efficient (minimal well loss). Neither of these assumptions are particularly applicable to small domestic wells, which are likely to represent a significant subset of the wells considered in the analysis<sup>11</sup>. Thomas also noted that in some cases the statistical differentiation between specific lower-value and moderate-value  $K_h$  zones was insignificant. For these reasons, PGG used the  $K_h$  estimates as initial values, but allowed significant departures (as needed) during model calibration.

For the middle aquifer, Thomas et al defined a  $K_h$  range of 15 to 128 ft/d (25<sup>th</sup> percentile to 75<sup>th</sup> percentile). For the lower aquifer, Thomas's estimated range of 8 to 68 ft/d (25<sup>th</sup> percentile to 75<sup>th</sup> percentile) provides reasonable agreement with the transmissivity estimates from the Port Williams wellfield. For bedrock, Thomas defined a range of 0.015 to 1.3 ft/d PGG (25<sup>th</sup> percentile to 75<sup>th</sup> percentile) with a median value of 0.04 ft/d. This median value is on the mid-to-upper end of the published range for sandstone (Freeze and Cherry, 1979). PGG did not reference Thomas' K estimates for aquitards, as they tend to represent permeable lenses in which wells are completed.

At the Port Williams Wellfield, PGG found that lower aquifer T estimates ranged from about 2,400 to 7,000 ft<sup>2</sup>/d (log average 4,100 ft<sup>2</sup>/d) and storage coefficient (S) ranged from 0.0001 to 0.0003 (PGG, 2008). At the Weyerhaeuser Seed Orchard (T30N/R4W-9L), aquifer testing data by Robinson & Noble (1974) were interpreted by Sinclair (2002) to indicate an estimated deep-aquifer T of 21,400 ft<sup>2</sup>/d, and PGG noted incomplete recovery from the aquifer testing, thus suggesting that the deep aquifer may be recharge limited in this location.

---

<sup>11</sup> Sinclair (2002) showed that T values derived from specific capacity measurements in selected study-area wells provided reasonable estimates of T values derived from aquifer testing. However, these wells were well designed production wells rather than (typically) inefficient domestic wells and Sinclair used a more sophisticated technique than referenced above.

Simonds and Sinclair estimated that the streambed  $K_v$  of the Dungeness River ranges from about 1 to 30 ft/d.

Thomas et al note that the upper confining bed is mainly comprised of silts and clays, and contains locally discontinuous lenses of water-bearing sand and gravel. They further note that the lower confining bed is composed of till and interbedded clay, silt and fine-grained sand, but may contain locally discontinuous lenses of water-bearing sand. The vertical permeability of a stratified confining bed is typically closest to its lower permeability layers. With this in mind, the  $K_v$  of the two confining beds is most likely to occur in the range of silt, clay and till. Published  $K$  ranges are broad; however, it's worthwhile to note that Freeze and Cherry (1979) estimate  $K$  ranges of about 0.0003 to 6 ft/d for silt,  $3 \times 10^{-7}$  to 0.0003 ft/d for unweathered marine clay, and about  $3 \times 10^{-7}$  to 0.003 ft/d for glacial till. The published transition between silt and clay occurs around 0.0003 ft/d.

---

## 5.2 STEADY-STATE CALIBRATION PARAMETERS

Parameters varied during the steady-state calibration included:

- Aquifer  $K_h$ ;
- Aquitard  $K_v$ ;
- Streambed  $K_v$ ;
- Dungeness River Elevation;
- Drain Cell Distributions; and,
- Constant Head Cell  $K_h$

Aquifer  $K_h$  was varied based on the prior information discussed above. During calibration, PGG noted that varying aquifer  $K_v$  had little effect on target residuals, and therefore maintained anisotropy ( $K_h/K_v$ ) at a ratio of approximately 10:1.

PGG began model calibration with the shallow-aquifer  $K_h$  zonation mapped by Thomas et al, and modified both zone values and zone boundaries during calibration. PGG attempted to maintain a similar *relative*  $K_h$  distribution by dividing Thomas's mapped distribution into 3 relative classes of  $K_h$  value: high (>100 ft/d), moderate (20-50 ft/d), and low (<10 ft/d). However, given the inaccuracies inherent in the method of  $K_h$  estimation, PGG allowed departures from Thomas's estimates by a factor of 3 (1/3 to 3-times). PGG maintained middle-aquifer  $K_h$  values within the 25<sup>th</sup> percentile to 75<sup>th</sup> percentile range defined by Thomas. Lower-aquifer  $K_h$  was initially set so that the 100-foot thick aquifer had a transmissivity equal to the representative value from Port Williams testing (about 4,000 ft<sup>2</sup>/d), but was allowed to vary 1/3 to 3-times during calibration. The model was temporarily used to simulate an aquifer in the undifferentiated deposits (layer 7), and employed  $K_h$  values that allowed simulating T values of both 21,000 and 4,000 ft<sup>2</sup>/d (this simulated aquifer was removed during calibration). PGG used Thomas's median estimate of bedrock hydraulic conductivity (0.04 ft/d) in the general head cells which simulate bedrock inflow to the model domain – no adjustment was made to this  $K$  value during calibration.

Aquitard  $K_v$  was varied over an order of magnitude. During initial calibration, best results were obtained with  $K_v$  values of 0.0008 ft/d for both the upper and lower confining beds (layers 2 and 4, respectively). The confining bed that directly underlies the lower aquifer in layer 6 was assigned the same value as layer 4. This value lies close to the published transition of hydraulic conductivity between silt and clay (0.0003 ft/d in Freeze and Cherry, 1979) and exceeds a calibrated estimate used for silt/clay aquitards in the Co-

lumbia River lowland of 0.00015 ft/d (Leighton & Porcello, 2001). However, the Drost model used an equivalent value that is still relatively low for silty materials, and PGG allowed an upper-end  $K_v$  value two orders of magnitude higher (0.08 ft/d) during calibration.

Streambed  $K_v$  was varied over a large range during calibration. The Dungeness River streambed was allowed  $K_v$  values ranging from 1 to 30 ft/d – a range estimated by Simonds and Sinclair (2002). Most other streambeds were allowed to vary over a range from 0.1 to 30 ft/d; however, Morse, Siebert and McDonald Creeks were allowed to use  $K_v$  values ranging from 0.01 to 0.1 ft/d. These low  $K_v$  values likely compensate for bedrock noted along the channels of Morse and Siebert Creeks, although the hydrogeologic conditions along McDonald Creek that require such a low  $K_v$  value are unknown.

The Dungeness River elevation was varied during calibration to compensate for errors in simulating stream-aquifer gradients due to the fact that aquifer cells are much larger than the Dungeness River footprint (Section 4.5.5). Reductions ranging from 2 to 8 feet were applied to all elevation definitions associated with the Dungeness River cells prior to selecting a 4-foot reduction during calibration.

Drain cells were originally specified per the 2003 model design. However, during calibration drain cells were added to simulate the upper reaches of McDonald and Matriotti Creeks, Lotzgazelle and Beebe Creeks (in order to obtain more flow in lower Matriotti Creek), and Bell Creek (in order to simulate off-channel springs which feed the creek). In addition, the footprint of Graysmarsh was adjusted during calibration in order to obtain inflow values reported by Aspect Consultants.

Constant head (CH) cell values of  $K_h$  were varied during calibration to simulate a resistive skin on the seafloor, potentially representing fine-grained materials that might settle out of suspension. When the aquifer/marine interface was simulated without such a skin, the CH value of  $K_h$  was relatively high (e.g. 10,000 ft/d). However, when a skin was simulated,  $K_h$  was specified as low as 7 ft/d. Given the MODFLOW equations for flow between a CH and an adjacent model cell, and the associated cell dimensions, this  $K_h$  is equivalent to a 100-foot thick skin with a  $K_h$  value of 0.5 ft/d.

---

### 5.3 STEADY-STATE CALIBRATION OBSERVATIONS

The following observations were noted during the process of steady-state model calibration:

1. It was necessary to reduce the streambed  $K_v$  of Morse and Siebert Creeks to increase heads in the western portion of the model. Streambed  $K_v$  values were 0.04 and 0.045 ft/day, respectively. Both of these streams have substantial lengths of bedrock outcrops along their channels, and the low  $K_v$  values may reflect how local bedrock hydraulically insulates the streams. With higher values of  $K_v$ , heads drop substantially near the streams and stream fluxes become much higher than target values. While optimal for meeting flux and nearby head targets, use of low  $K_v$  values cause flooded cells along the streams, which are considered an artifact of the complexity of representing bedrock-lined stream channels.
2. Simulation of Morse and Siebert creeks illustrate how streambed  $K_v$  values specified for rivers and drains can be used to compensate for hydrogeologic complexity that cannot be simulated by the simplified one-layer depiction of the shallow aquifer system. Calibrating heads and fluxes along McDonald Creek required relatively low  $K_v$  values (0.037 and 0.074 ft/d). While bedrock is not mapped along the creek, the low  $K_v$  values may reflect some other local complexity such as confined aquifer conditions in the vicinity of the creek.

3. The model had difficulty simulating observed flows on Matriotti Creek. While head targets are satisfied along the creek, the model tends to predict very small baseflow gains. In an attempt to increase baseflow gains, PGG added drain cells to simulate Lotzgazelle and Beebe Creeks, along with extending the upland portions of Matriotti Creek simulated by the model. PGG's "Small Streams Memorandum" (2008a) notes that most year-round flow occurs in the lower reach of Matriotti Creek (below river mile 1.3) and that the middle and upper reaches are seasonally dry. However, both the 2008 model and the 2003 model tend to predict groundwater inflow to the middle reach. The reasonable match of groundwater head targets, but under-prediction of flux near the lower reach suggests that the model may be reasonably simulating regional flow in the shallow aquifer system, but that single-layer simulation of the shallow aquifer may preclude simulation of perched conditions that potentially support baseflow in lower Matriotti Creek. Lower portions of the creek occur along a contact between glaciomarine/fine-alluvium sediments and outwash/coarse alluvium (Thomas et al, 1999).
4. In addition to potential perched conditions along Matriotti Creek, several additional examples illustrate how hydrogeologic complexity in the shallow aquifer system cannot be captured by a single-layer representation of the shallow aquifer:
  - A paired set of targets on the north side of Bell Hill (30N03W28C03 and 30N03W28G02) show very different target heads, the latter 80 feet higher than the former (**Figure 5-1**).
  - A large wetland complex in the Bell Creek valley, downstream of Carrie Blake Park, is supported by a perched groundwater system. This system provides inflow to Bell Creek, but cannot be explicitly represented by the single-layer representation.
  - Head targets along the upper modeled portions of the Dungeness, where adjacent targets show head differences of about 30 feet (**Figure 5-1**).
5. PGG used a variety of streambed  $K_v$  values for the Dungeness River (0.25, 1, 8, 10, and 50 ft/d). Simons & Sinclair (2002) estimate a  $K_v$  range of 1 to 30 ft/d. Values of 0.25 ft/d largely severed the hydraulic connection between the Dungeness River and the shallow aquifer, causing groundwater levels to drop beneath the bottom of the streambed. Values of 1 ft/d worked well with the steady-state calibration, but transient evaluation showed too little aquifer response to stream stage variations (Section 6.4). Values of 10 ft/d worked well during transient calibration, and were retained in the calibrated model. Values of 50 ft/d are also feasible, but increased modeled Dungeness River losses from about 20 to 24 cfs, and were not considered further during modeling.
6. During calibration, PGG lowered the Dungeness River stage and streambed bottom elevations by 4 feet to achieve a better hydraulic connection between the river and the shallow aquifer. This adjustment was performed to offset the fact that the size of the river cells (660 feet) is much larger than the width of the river (40 feet), and therefore the model does not properly simulate the mounding that would occur beneath the river and the associated reduced gradient between the river and the model cell. By spreading out the river seepage over the entire cell, mounding beneath the river is minimal, and a larger gradient (river to aquifer) is maintained than in actuality. Reducing the river elevations removes that overly large gradient.
7. PGG evaluated the effect of simulating a low permeability marine "skin" where the aquifers sub-cropped into marine waters. The skin may represent silty sediments on the seafloor, and was simulated by reducing the  $K_h$  of the CH cells. Reductions of  $K_h$  could be translated into an "equivalent skin conductance". One of PGG's simulations simulated the equivalent of a 50-foot thick "skin" with a  $K$  value of 3 ft/d. In general, addition of a marine "skin" tended to raise heads significantly in high permeability portions of the shallow aquifer, so much so that lowland model cells (with land surface elevations of 10 to 20 feet NAVD88) became flooded. PGG did not further pursue the simulation of a marine skin, and deeper aquifers did not require the increase in heads that such a skin would provide.

8. While calibrating the model using a single  $K_v$  value for all aquitards, a value of 0.0008 ft/d provided the best results. This value is close to the transition between silt and clay permeability documented in Freeze and Cherry (1979), and is higher than the 0.00015 ft/d value used for a silt/clay aquitard in the Columbia River lowland by the calibrated DAY model (Leighton and Porcello, 2001). However, higher values could be considered, and a  $K_v$  value of 0.008 ft/d allowed good target matches in the shallow and middle aquifers, but caused a 10+ foot rise in the lower aquifer which is relatively high given that the range of target values in this aquifer is only 10 feet. PGG explored a variety of means for reducing model heads in the lower aquifer (increasing  $K_h$  fourfold, eliminating “bedrock inflow” from upgradient GHB cells, and moving the connection with marine CH cells closer in toward the coast). However, heads could only be reduced in the lower aquifer by limiting leakage inflow with the lower value of  $K_v$  in the lower confining bed.
9. Model calibration to assess the interconnectedness between aquifers was based on head targets within each aquifer and consideration of head differences between adjacent aquifers. As noted in Section 5.5, head targets and head differences between aquifers were reasonably reproduced by either simulating all aquitard  $K_v$  values at 0.0008 ft/d or by increasing the  $K_v$  of the upper confining bed to 0.008 ft/d. The project’s calibration dataset did not provide additional information to further refine  $K_v$  values for the aquitards, and the project scope did not include sufficient budget for development of additional calibration datasets. However, monitoring data collected at Sequim’s Port Williams Wellfield from 1996 through 2008 illustrates head differences and simultaneous pumping responses in the shallow, middle and lower aquifers (PGG, 2009). A head difference of 15 to 20 feet was generally maintained between the middle and lower aquifers; however, seasonal variations were very similar (potentially indicating similar responses to wellfield withdrawals from the lower aquifer). PGG performed a series of preliminary steady-state simulations of water-level response to lower-aquifer pumping at the wellfield to assess how water-level responses varied over a range of  $K_v$  values for the lower confining bed. Our preliminary findings suggest additional data analysis and calibration are warranted, as follows:
  - Time-series monitoring at the Port Williams Wellfield shows ratios of seasonal water-level variation between the lower aquifer and the middle aquifer of around 2:1. Steady-state simulation of 0.4 mgd pumping from the wellfield shows a 6:1 ratio, therefore suggesting that simulated drawdown may not fully propagate from the (pumped) lower aquifer to the middle aquifer. PGG did not assess the degree to which steady-state simulations can represent seasonal drawdown ratios; however, they are likely to overestimate the ratios somewhat because time is required for pumping drawdown to propagate through the confining bed;
  - Universally increasing aquitard  $K_v$  values from 0.0008 ft/d to as high as 0.016 ft/d does not reduce this drawdown ratio significantly. Leakage from the shallow aquifer may be maintaining low drawdowns in the middle aquifer. An acceptable drawdown ratio in steady state can be achieved by only increasing the  $K_v$  of the lower confining bed (e.g. 0.008 to 0.016 ft/d) while leaving the upper confining bed at 0.0008 ft/d. However, when the  $K_v$  of the lower confining bed is increased, the head difference between the middle and lower aquifers becomes too low (1 to 3 feet, rather than the observed 15 to 20 feet).
  - Another possibility is that a portion of the seasonal fluctuation exhibited in middle aquifer is from other pumping in that aquifer. Higher pumping in the summer is common to many users, not just the Port Williams Wellfield. Summer low water levels are noted in other wells monitored by the City of Sequim at distances of 2000 and 4000 feet from Port Williams Wellfield. However, hydrographs from the Port Williams monitoring are very similar between the lower and middle aquifers.

- The  $K_v$  values used for aquitards in the 2003 model are higher than (this) 2008 model, ranging from about 0.2 ft/d to 0.01 ft/d. Such high  $K_v$  values may have been necessary in the 2003 model because the deeper aquifers had no connection with marine waters, and in order for them to discharge to the north the water was forced to come back up through the aquitards to reach the "marine drain cells" in layer 1. Drost (1983) used an aquitard  $K_v$  value of 0.005 ft/d, and did include a direct hydraulic connection between the deeper aquifers and marine waters.
  - The range of  $K_v$  values applicable to the confining beds, and the apparent contradictions within the limited calibration observations discussed above (i.e. better steady-state drawdown ratios corresponding to a poorer match in head difference between the lower and middle aquifers), suggests that more research is needed to define a good dataset for calibrating the model to the  $K_v$  of the aquitards below the shallow aquifer.
  - Sensitivity analysis on predictive simulations (discussed in Section 7.4.3) suggests that uncertainty in aquitard  $K_v$  values has little impact on predicting how AR applied to the shallow aquifer affects flow augmentation in adjacent streams. However, predicting the impacts of pumping and ASR in deep aquifers is sensitive to values of aquitard  $K_v$ .
10. PGG evaluated the effect of a "deep aquifer" in the undifferentiated deposits when the model was in its 9-layer configuration. Simulated  $K_h$  values for the deep aquifer were as high as 200 ft/d, which provided a T value of 20,000 ft<sup>2</sup>/d, similar to interpretation of aquifer testing at the Weyerhaeuser Tree Farm (Sinclair, 2001). With aquitard  $K_v$  values of 0.0008 ft/d, the maximum target head difference in layer 1 was insignificant (0.82 feet). However, when aquitard  $K_v$  values were increased an order of magnitude, the model predicts declines in the shallow aquifer of up to 5 feet which must be offset by reducing  $K_h$  values in layer 1. Further simulation of the deep aquifer was not pursued; however, the model is structured to allow its representation at a later date. If future model calibration is pursued to improve definition of the deeper flow system, simulating *some* deep aquifer occurrence may assist in better calibrating the model a higher  $K_v$  in the lower confining bed without causing overly high heads in the lower aquifer. (However, it's worth noting that a significant deep aquifer was not encountered near Sequim's Port Williams wellfield, where 3 out of 5 calibration targets occur in the lower aquifer.)
  11. PGG evaluated the effect of explicitly modeling both an aquitard layer (layer 8) and a 500-foot thick bedrock layer (layer 9) beneath the layer reserved for simulation of a deep aquifer (layer 7). The model mass balance showed that flow through the bedrock aquifer represented about one percent of the total model flux (predominantly consisting of inflow from the GHB), and that flow through layer 8 largely reflected upward transmission of groundwater from layer 9. PGG removed the two layers entirely with essentially no difference to model target values.
  12. PGG inserted several local permeability zones to allow the computer model to better simulate the conceptual model and field observations. A higher  $K_h$  zone was required in the shallow aquifer along south Sequim Bay to avoid locally flooded cells there. A band of moderately lower  $K_h$  materials was required along the downgradient side of Graysmarsh to better simulate groundwater inflow into the marsh. The model also required several transition zones that cut into the USGS K distributions to match heads. All of these features are shown on **Figures 4-10** and **4-11**.
  13. Aspect Consultants noted a prior investigation by Rongey (1992) in which a relatively high permeability channel deposit was identified in the area of middle Cassalery Creek and Graysmarsh. PGG developed a realization of the model that simulated the occurrence of this deposit with reasonable calibration results. However, this realization was not pursued further due to the general similarity with existing calibrated realizations documented in this report and limited budget available to explore additional realizations in predictive analysis.

14. While the results of an automated sensitivity analysis are discussed in Section 5.4, such analysis may not capture all of the observations made during calibration. The following observations pertain to model sensitivities observed during calibration:

- Overall, the model is very sensitive to streambed conductance, which becomes a significant calibration parameter.
- The model is not sensitive to aquifer anisotropy over a  $K_h: K_v$  range of 10 to 100. This is likely because the permeability contrast between aquifers and aquitards is much higher than the  $K_h: K_v$  ratio within a given aquifer.
- The model is not sensitive to ET. ET losses are predicted to represent about 1 percent of water budget. Predicted ET tends to occur near coastlines in areas of shallow groundwater. Where the single-layer simplification of the shallow aquifer does not permit simulation of perched conditions, ET will not be simulated. Addition of ET to the model had no significant effect on calibration head targets, and reduced discharge to Graysmarsh by only 0.1 cfs relative to a target flow of 6.5 cfs.

---

## 5.4 STEADY-STATE SENSITIVITY ANALYSIS

PGG performed an automated sensitivity analysis midway through the calibration procedure to evaluate which calibration parameters (K values and boundary conditions) have the most influence on target residuals. Calibration parameters were varied over a range of 1/5 to 5x. The analysis was indexed on the sum of squared residuals (SSR) for head targets and flux targets (mid-point values were used from the flux target range summarized on **Table 5-2**). A “residual” is the difference between the observed and modeled value of a given target.

While the automated sensitivity analysis appeared to identify some of the model sensitivities to the calibration parameters considered, it also missed some of the sensitivities observed during manual calibration. Since many of the head targets are located in the high permeability zones representing the Dungeness River alluvium, parameters that have more influence there were seen as having more global influence, although their influence is actually somewhat localized. The automated sensitivity analysis provided the following findings:

- Head residuals appeared to be most sensitive to aquifer  $K_h$  and aquitard  $K_v$  values and streambed  $K_v$  values for the Dungeness River and Bagley Creek. The head SSR was not particularly sensitive to rates of groundwater inflow along the bedrock boundary on the south of the model domain simulated via GHB's or injection wells.
- Among the  $K_h$  parameters, increases in  $K_h$  values along the Dungeness River in zones 4 and 5 had the most influence on head SSR and  $K_h$  increases in several laterally adjacent zones (1, 6 and 7) had moderate influence on head SSR (see **Figures 4-10** and **4-11** for K zone maps). These 5 zones combined contain the majority of calibration targets in model layer 1. Increasing the  $K_h$  of model layer 3 also had a moderate affect on head SSR. Responses to lowering of  $K_h$  were more moderate, with the most influential zones including 1, 2, 4, and 17. The  $K_h$  zones that had the smallest influence on head SSR included: 3, 9, 11, 12, 14, 16, and 73 in layer 1 and the  $K_h$  of layer 5 (lower aquifer).
- Whereas increasing the  $K_v$  of *all* aquitards by 5x from a uniform value of 0.0008 ft/d had little influence on head SSR, decreasing the aquitard  $K_v$  had a moderate affect on head SSR.

- Reducing the  $K_v$  of the Dungeness streambed (0.25 ft/d during this stage in calibration) by 1/5 had a moderate effect on head SSR, but increasing its  $K_z$  by 5x had very little effect<sup>12</sup>. Increasing the  $K_v$  of the Bagley Creek streambed by 5x also had a moderate effect of head SSR, but decreasing its  $K_v$  had little effect. Head SSR was not particularly sensitive to changing streambed  $K_v$  for the other modeled streams.
- Flux SSR was most sensitive to the  $K_v$  of the Dungeness River bed. The shallow aquifer along the river has sufficiently high transmissivity to accommodate whatever leakage the streambed will provide. The target value for the Dungeness River was significantly larger than the other small streams, so equivalent relative departures have a greater influence on the flux SSR.
- Increasing  $K_h$  of zone 7 in layer 1 also had a significant effect on flux SSR, probably because opening up this zone in the shallow aquifer opens up a subsurface pathway to accommodate more seepage loss from the Dungeness River towards the Gierin/Cassallary creek drainages to the northeast. Modifying the  $K_h$  of zones 4 and 5 had a moderate effect on flux SSR. Both of these  $K_h$  zones occur along the Dungeness River and control interactions between the river and nearby groundwater.

---

## 5.5 STEADY-STATE CALIBRATION RESULTS

**Table 5-2** provides a comparison of streamflow seepage targets and model simulated fluxes. Head residuals are summarized on **Table 5-3** and weighted residuals are mapped on **Figures 5-2** through **5-4**. Summary statistics are used to assess the “match” between observed and modeled heads and to evaluate whether the model is well calibrated. A well calibrated model minimizes the difference between observed and modeled heads (residual). Three statistics are generally used to evaluate the minimization of residuals. The residual mean (RM) is the sum of all residuals divided by the number of targets. Some residuals are positive and some negative and a well calibrated model that balances the two would result in a low RM-value. The Absolute Residual Mean (ARM) is the sum of the absolute values of the residuals divided by the number of targets. The ARM statistic is a measure of the overall average error. Finally, a comparison of the residual standard deviation to the overall range in target values throughout the model is assessed, with a value less than 10% generally considered good. These summary statistics are also included on **Table 5-3**. Both model realizations exhibited acceptable calibration statistics, and are discussed individually below.

*Note that residuals are defined as observed minus simulated head, so negative residuals indicate that model-simulated head is higher than observed head.*

### 5.5.1 Realization “Dung-7e”

Realization “Dung-7e” uses  $K_v$  values of 0.0008 ft/d for all model aquitards. PGG adjusted all other calibration parameters discussed in Section 5.2 to achieve acceptable calibration results for this realization.

Weighted head residuals for the shallow aquifer (**Figure 5-2**) are generally within  $\pm 5$  feet in the higher  $K_h$  zones along the Dungeness River and its former outlet channels. Slightly high head residuals (6 to 11 feet) are noted near the lower reaches of the Dungeness River and Matriotti Creek. Larger residuals ( $\pm 20$  to 60 feet) are noted in outlying areas. In some cases, residuals showing model underestimation of water levels occur near “flooded” model cells, indicating either inaccuracy in target values or confined aquifer conditions that would result in flowing wells if tapped. Flooded cells along Morse and Siebert Creeks are likely associated with complexities in simulating groundwater discharge to a stream channel with notable

---

<sup>12</sup> Note: the final streambed  $K_v$  of the Dungeness River was 10 ft/d in the calibrated model realizations.



occurrence of bedrock. In some cases, neighboring pairs of targets with significantly varying residuals indicate hydrogeologic complexity that cannot be captured by the model's single-layer simulation of the shallow aquifer system (e.g. weighted residuals of -56 and 50 feet south of lower Bell Creek, and weighted residuals of -30 and 52 immediately west of the Dungeness River).

Weighted head residuals in the middle aquifer (**Figure 5-3**) show that most weighted residuals are within  $\pm 20$  feet; however, two residuals near the bedrock occurrence estimated in the southern model domain show underestimation of head on the order of 49 to 65 feet. The larger range of residuals generated for the middle aquifer may be related to the simplified representation of the aquifer with a single value of  $K_h$  for the entire layer. As previously noted, this simplified approach is based on the "principle of parsimony" and reflects the general lack of hydraulic property data compiled for the middle aquifer. Further characterization of aquifer properties could support designation of  $K_h$  zones and improve the calibration for this aquifer. Weighted head residuals in the lower aquifer (**Figure 5-3**) range from -2 to 27 feet, and are also likely influenced by the single  $K_h$ -value representation of the aquifer.

Comparison of modeled vs. observed streamflow seepage (**Table 5-2**) shows reasonably good agreement for all streams except Matriotti Creek. Simulated net seepage loss from the Dungeness River (19.6 cfs) is 4.6 cfs higher than the estimated upper limit of the target range. However, it should be noted that streamflow measurement accuracy is on the order of  $\pm 5\%$  (pers. comm., Simonds, 2008) and measured flow rates during seepage runs were on the order of 100 to 300 cfs. Measurement accuracy is thus on the order of  $\pm 5$  to 15 cfs, and model estimated seepage is within the measurement accuracy of the target range. The poor calibration match to Matriotti Creek seepage is likely due to hydrogeologic complexity that could not be simulated by a single-layer depiction of the shallow aquifer system. As discussed in Section 5.3, groundwater contributes to baseflow in the lower reaches of Matriotti Creek, and perched conditions may occur in this area that cannot be simulated by the model. Perched conditions are known to occur along lower Bell Creek, and while the model reasonably simulates seepage flux into the Bell Creek, it is not explicitly simulating the perched flow system in this area.

A mass balance for the model is presented in **Table 5-4**. Total mass balance error is below the 1-percent value typically considered adequate for the model solver.

### 5.5.2 Realization "Dung-7g"

Realization "Dung-7g" differs from "Dung-7e" in that the  $K_v$  value of the upper confining bed (layer 2) was raised from 0.0008 ft/d to 0.008 ft/d. After making this  $K_v$  modification, PGG adjusted all other calibration parameters discussed in Section 5.2 to achieve acceptable calibration results for this realization.

Weighted head residuals are presented for the shallow aquifer (**Figure 5-4**) and the middle and deep aquifers (**Figure 5-5**). Weighted residuals for the shallow aquifer are very similar to those predicted by realization "Dung-7e". Realization "Dung-7g" has several areas where model cells are predicted to be dry. Increasing the  $K_v$  of layer 2 caused reduced heads in layer 1 which were partially compensated by reducing shallow-aquifer permeability values (**Table 4-1**), but partly resulted in the small dry-cell areas. Weighted head residuals in the middle aquifer (**Figure 5-5**) vary from those in Realization "Dung-7e", with improvements in some areas and worsening in other areas. Overall, the quality of calibration in the middle aquifer is fairly similar between the two realizations. The quality of calibration for the lower aquifer (**Figure 5-5**) is also similar to realization "Dung-7e" for the lower aquifer, although residuals at the Port Williams Wellfield (east of the Dungeness River) are slightly higher. Calibration summary statistics for head residuals are not quite as good as for realization "Dung-7e" (**Table 5-3**) with the exception of the residual mean, which suggests a slightly more balanced distribution of positive and negative residuals.

Seepage predictions are also similar to realization “Dung-7e” (Table 5-2). Slightly higher seepage loss is predicted from the Dungeness River, but the value is still within measurement error of the target range. Total mass balance error is within the 1-percent guideline.

### 5.5.3 Overall Steady-State Calibration Assessment

Overall, both model realizations are considered to have acceptable to good calibration statistics. Head target residuals are best in the shallow aquifer, where multiple  $K_h$  zones were employed using the zonation estimated by Thomas et al as an initial template. Both head residuals and stream flux residuals in the shallow aquifer reveal hydrogeologic complexities that cannot be simulated based on a single-layer depiction of the shallow aquifer system and the available degree of subsurface characterization. Head residuals are typically larger in the middle and lower aquifer, likely due to the fact that these units were simulated with uniform  $K_h/K_v$  values. Improved characterization of hydraulic conductivity distributions in both aquifers, as well as variations in the thickness of the lower aquifer would likely improve calibration statistics in these model layers.

The use of two model realizations helps to address uncertainties in aquitard  $K_v$  values; however, the two realizations likely do not represent the entire range of aquitard  $K_v$  combinations. Development of additional calibration datasets should precede additional calibration to better define the range of aquitard  $K_v$  combinations. Improving understanding of interconnectedness between aquifers in the deeper portions of the groundwater flow system will improve the accuracy of predictions associated with deep aquifer pumping.

The potential for multiple realizations, a phenomenon called “non-uniqueness”, also extends to other model calibration parameters. For instance, PGG developed a realization of the model that incorporated hydrogeologic interpretation in the Cassalery-Gierin creek area (Rongey, 1991) with similarly acceptable calibration results. This realization did not differ greatly from the two discussed above, but it shows that alternative interpretations can likely satisfy the calibration criteria and may differ when used for prediction – particularly on the local scale.

It should also be noted that the accuracy of model calibration is dependent on the accuracy of estimated inflows to and outflows from the hydrologic system, such as recharge and pumping. Whereas the accuracy of precipitation recharge estimated by the USGS (Thomas et al, 1999) is generally considered to be good, Aspect Consultants raised questions about the accuracy of irrigation recharge estimates in the vicinity of Gierin Creek and possibly in other areas (pers. comm., Miller, 2008). PGG did not attempt to review or refine the steady-state pumping estimates developed by TTFW.

Finally, the steady-state calibration assumed that the study-period average head targets and the stream-flow seepage target ranges (developed over varying time periods) are correlated with the estimates of recharge and pumping discussed above. Based on analysis presented in Section 3.2.6, steady-state calibration employed a recharge distribution averaged between the USGS long-term and study-period recharge estimates. While the calibration study period coincided with above-average precipitation, it is unclear whether the hydrologic system had fully responded to (and equilibrated with) the increased recharge. Also, given that both pumping withdrawals and piping of irrigation ditches have also increased over time, it is possible that the hydrologic system had not fully equilibrated to these changing stresses. The assumption of equilibration inherent in steady-state model simulation, paired with the potentially transient nature of hydrogeologic conditions under adjustment to changing stresses, can cause some inaccuracies in estimating hydrogeologic parameters. Transient calibration (discussed below) was performed over the 22-month study period and does not capture the long-term trends towards equilibration with changing stresses on the groundwater flow system.

---

## 6.0 TRANSIENT MODEL CALIBRATION

The steady-state calibration described above strives to adjust model parameters so that study-period average conditions are well represented in the model. A transient calibration, on the other hand, strives to adjust model parameters so that time varying stresses (e.g. seasonal changes in recharge or pumping rates) and corresponding responses to the aquifer system are well represented in the model. A transient calibration was performed for both model realizations to calibration targets developed from the study-period groundwater level data. The calibration included iterative feedback between the transient and steady state models, as transient calibration showed that values of Dungeness River streambed  $K_v$  were initially too low. The calibration exercise concluded that transient calibration residuals were predominantly sensitive to specification of transient recharge, and that predictions of transient recharge were sufficiently uncertain to warrant adjustments of other calibration parameters. Streambed  $K_v$  was adjusted based on transient sensitivity analysis, and values of aquifer storage parameters ( $S$  and  $S_y$ ) for predictive analysis were recommended based on reasonable published ranges.

---

### 6.1 TRANSIENT STRESS PERIODS AND INITIAL CONDITIONS

The USGS study period extends from December 1995 through September 1997. PGG elected to simulate a transient calibration period starting in November 1995 (rather than December) because November exhibited significant above-average precipitation that would not be represented in the initial conditions prior to simulation of the calibration period. Initial conditions were simulated with a transient warm-up period that was based on background conditions prior to the study period.

The transient calibration included monthly average river stages during the calibration period, monthly average pumping estimated by TTFW and revised to include actual City of Sequim pumping during the calibration period, monthly estimates of long-term average potential ET for wetlands, and estimated monthly average recharge during the USGS study period. Estimation of these transient boundary conditions is discussed in Section 4.5, and all other boundary conditions were held constant during the transient simulations. The transient warm-up period simulation initially included monthly average Dungeness River stages derived from a 1994-1997 dataset, monthly average pumping similar to the calibration period (with adjustments for pumping activity by the City of Sequim), monthly estimates of long-term average potential ET for wetlands, and long-term average monthly recharge. Later in the calibration, the recharge during the warm-up period was changed to study-period average monthly estimates, as the transition from long-term average recharge (warm-up) to study-period recharge (calibration) caused simulation of a rising groundwater level trend that was not observed in the calibration targets. This removed the simulated rising trend, but did not alter the simulated seasonal variation of groundwater levels.

The warm-up period extended over a calendar year, with monthly stress periods from January 1 through December 31. Each stress period was assigned 30 timesteps with a timestep multiplier of 1.2. Heads from the warm-up period at the end of October were used as an initial condition for the calibration period simulation. The calibration period extended over 23 months, and similarly used monthly stress periods and 30 timesteps per stress period.

---

### 6.2 TRANSIENT CALIBRATION TARGETS

Transient calibration was performed to water-level trends observed over the USGS study period in 57 monitored wells. **Table 6-1** summarizes the target wells used in the transient calibration, and shows that TTFW identified 48 wells as completed in the shallow aquifer, 1 well as completed in the upper confining

bed, 5 wells as completed in the middle aquifer, and 3 wells as completed in the lower aquifer. During calibration, water-level trends were expressed as “head differences” relative to the first data point in the calibration record. PGG calculated these calibration targets based on TTFW’s water-level database developed for the 2003 model, and GV calculated simulated head difference with a new feature that offsets drawdown hydrographs from model predictions relative to the first point in the target head series. PGG updated target coordinates for wells located by Clallam County (Section 5.1)<sup>13</sup>, and removed two targets where water-level measurements predominantly reflected pumping conditions.

Prior to transient calibration, PGG made a series of maps showing the hydrographs of all the targets expressed as offset from the first value in the data record. Consistency in patterns of offset vs. time among neighboring wells is needed to have successful calibration to the hydrographs. PGG noted some areas with consistent neighboring wells and other areas with differing adjacent hydrographs. Areas with significantly differing adjacent hydrographs are likely to reflect hydrogeologic complexity not simulated by the model, and will be impossible to match during transient calibration. A map of observed and modeled hydrographs is presented in **Figure 6-1**, and shows these spatial similarities and differences in hydrographs.

---

### 6.3 TRANSIENT CALIBRATION PARAMETERS

Parameters adjusted during the transient calibration included  $S$ ,  $S_y$  and streambed  $K_v$  for the Dungeness River.  $S$  and  $S_y$  were specified uniformly for all layers.  $S_y$  was varied over a range of 0.05 to 0.25, and  $S$  was varied over a range of 0.00005 to 0.0005. Streambed  $K_v$  was not varied during the calibration period simulations, but was varied during as sensitivity analysis (described below) which simulated aquifer responses to variation of Dungeness River stage.

---

### 6.4 TRANSIENT CALIBRATION OBSERVATIONS

The following observations were noted during transient model calibration:

1. Calibration focused on water-level trends in the shallow aquifer, as most of the targets are completed in this aquifer. The shallow aquifer is most influenced by recharge, and sensitivity analysis during model calibration suggested that pumping and Dungeness River stage fluctuations generally have minimal effects on simulated hydrographs. **Figure 6-2** shows the results of a sensitivity analysis performed midway through the transient calibration that systematically converted (transient) seasonal variations in recharge, pumping, and river stage to constant (steady state). Conversion of transient wells to steady state had virtually no observable impact on the hydrograph whereas conversion of transient recharge to steady state had significant effect. Conversion of both wells and recharge to steady state permits observation of (minimal) seasonal variation associated with river stage fluctuations<sup>14</sup>. Similar observations were made for 9 other shallow-aquifer targets distributed throughout the model domain. Targets immediately adjacent to the Dungeness River showed a greater river influence and the calibrated increase in Dungeness River streambed  $K_v$  (later in the calibration) likely increased sensitivity to river fluctuations. The transient model also proved sensitive to reducing  $S_y$  from 0.15 to 0.05, but did not prove sensitive to varying  $S$  from 0.00005 to 0.0005.

---

<sup>13</sup> Updating water-level elevations based on the revised coordinates and associated wellhead reference elevations was unnecessary because the transient model was calibrated to head difference rather than the absolute heads used to calibrate the steady-state model.

<sup>14</sup> The rising trend occurs because this early sensitivity analysis was performed when the warm-up period was simulated with long-term average recharge. Transition to (higher estimates of) study-period recharge causes the rise.

2. Further sensitivity analysis revealed that early-calibration values of Dungeness River streambed  $K_v$  (1 ft/d) were too low to properly simulate groundwater responses along the river. Simonds and Sinclair (2002) showed groundwater levels highly responsive to river stage variation in one location, and variably responsive in another. Sensitivity analysis to a 60-day rising and falling stage cycle showed little response with a  $K_v$  of 1 ft/d. but reasonable responses with  $K_v$  values of 10 and 50 ft/d (see example on **Figure 6-3**). Given the estimated  $K_v$  range of 1 to 30 ft/d (ibid), PGG increased the  $K_v$  to 10 ft/d in all versions of the steady-state and transient models.
3. Model predicted hydrographs in transient targets tended to exhibit one of three characteristic patterns of seasonal water levels:
  - a. Water-level rises during winter months with maximum seasonal water-levels during the winter and spring. This pattern is presumably associated with natural precipitation recharge specified predominantly during winter months.
  - b. Two water-level rises per year, with maximum water-levels occurring winter and summer. This pattern is presumably associated with recharge by both natural precipitation and irrigation.
  - c. No substantial seasonal variation. This pattern is presumably associated with little variation in recharge year-round recharge, such as where low-permeability sub-soils underlie areas of both precipitation and irrigation recharge.
4. PGG compared the characteristic trends simulated in the shallow-shallow aquifer targets with the distribution of recharge patterns discussed above and (respectively) found a very high correlation between the three trends and recharge via: a) natural precipitation recharge on areas with outwash soils and areas with low permeability sub-soils; b) natural precipitation and irrigation recharge on areas with outwash soils; and c) natural precipitation and irrigation recharge on areas with low permeability sub-soils. This correlation suggests that specification of recharge is generally controlling the pattern of the simulated water-level trends.
5. PGG mapped graphical comparisons of simulated vs. observed water-level hydrographs for several values of  $S_y$  and for model realizations “Dung-7e” and “Dung-7g”. An example of this comparison is provided on **Figure 6-1**, which shows a highly variable distribution of match quality between observed and simulated hydrographs. Variable match quality is indicated by similarity/difference in both pattern and scale. Some targets show similar patterns whereas others are completely different. The scale of variation also ranges from similar to different.

---

## 6.5 TRANSIENT CALIBRATION RESULTS

As noted above, matches between observed and simulated hydrographs for shallow-aquifer targets varied significantly, with some targets showing reasonably good matches and others being relatively far off. The observations listed above suggest that predicted hydrograph “patterns” are largely dependent on temporal patterns of recharge and that  $S_y$  can have a significant effect on the scale of variation. While transient calibration to the study-period data focused on the adjustment of aquifer storage parameters, further calibration efforts would likely have established that the scale of variation (and possibly the timing) is also dependent on aquifer hydraulic conductivity ( $K_h$ ). However, the transient calibration was discontinued after determining these sensitivities for the following reasons:

- The actual timing and distribution of recharge to the water table is not well known, and is difficult to predict. Seasonal recharge “pulses” are delayed and dispersed over time as they propagate through the vadose zone. The role of low permeability subsoils toward creating perched conditions which af-

fect recharge delivery to an underlying vadose zone is also unknown. Finally, irrigation recharge was simulated to follow temporal patterns of irrigation diversion and was assumed to be similar across large areas supplied by specific diversions. However, the routing of irrigation water through main canals, laterals and fields would be very difficult to characterize, and infiltration may vary significantly among areas of irrigation conveyance and application.

- Although the shallow aquifer is modeled as a single unconfined unit, it actually contains hydrogeologic complexities that include: perched conditions, confined conditions, and variation (heterogeneity) in hydraulic conductivity. The monitoring wells used to generate target hydrographs likely represent a variety of subsurface conditions which likely respond to recharge emanating from the land surface in different manners. This degree of hydrogeologic complexity, particularly in response to (transient) seasonal recharge, cannot be easily simulated with the existing model and the existing degree of hydrogeologic characterization.

Rather than attempting to synthesize patterns of recharge reaching the various completion zones of target monitoring wells (without sufficient data to do so) or modifying the model structure to support simulation of hydrogeologic complexities in the shallow aquifer system (again, with insufficient characterization to do so), PGG suggests performing model predictions over ranges of model parameter variation in the manner of an “uncertainty analysis”. This approach is further illustrated in the following section.

---

## 7.0 PREDICTIVE ANALYSIS

This section presents predictive simulations performed with the model to evaluate the impacts of aquifer recharge (AR) and aquifer storage and recovery (ASR) scenarios identified by the TAG. PGG met with the TAG on several occasions to present the model and select predictive scenarios. Predictive results from the scenarios discussed below were reviewed by TAG members to select three “FS scenarios” to be included in a feasibility study (FS) for AR/ASR (PGG, 2009). Additional simulations were performed for the FS, and are documented in that report.

---

### 7.1 PREDICTIVE SIMULATIONS

Both realizations of the model were used to simulate AR from 10 sites (two of which are ditches) and to simulate ASR from 2 sites on either side of the Dungeness River (**Figure 1-1**). The 10 AR sites were selected by the TAG during model development, and the 2 ASR sites were selected by PGG to be used as general indicators of ASR responses on either side of the river. None of the sites investigated with the model in this report are implied to be available as actual AR/ASR sites. Rather, the model results illustrate the hydrologic responses to AR/ASR in these general vicinities and therefore support identification which locations might best meet the needs of future AR/ASR projects.

AR was simulated at the 10 sites under both constant, year-round (steady state) and seasonal (transient) conditions. For both steady-state and transient simulations, the calibrated steady-state version of the model was used as a base case and AR/ASR was the only perturbation applied to the model<sup>15</sup>. Steady-state simulations were performed at all AR sites using AR rates ( $Q_{AR}$ ) of 2 cfs (cubic feet per second).

---

<sup>15</sup> This approach was justified based upon the principal of superposition, which states that for a linear groundwater flow system, a single perturbation can be simulated and superimposed upon the groundwater flow system. Although some non-linearities may exist, this approximation seems appropriate given the magnitude of seasonal groundwater level variations (predominantly < 5 feet during the study period on Figure 6-1) relative to the saturated thickness of the shallow aquifer and other uncertainties inherent in the model.

Seasonal AR was simulated for 2 months per year (May and June) for all sites except Site 7 (where transient simulation was not performed). Additionally, the seasonal simulations were performed twice, using values of specific yield ( $S_y$ ) for the shallow aquifer system of 0.1 and 0.2. This range in  $S_y$  values allows assessment of hydrologic uncertainty of  $S_y$ , and is believed to provide a reasonable “envelope” of predictive responses to AR. **Table 7-1** presents a summary of predictive AR simulations.

All AR/ASR simulations were conducted using model realization “Dung-7e”, but were supplemented with simulations using “Dung-7g” and other configurations of the model. The AR simulations were subjected to “linearity analysis” and “sensitivity analysis”. The linearity analysis ran steady-state and transient simulations of “Dung-7e” at selected sites using  $Q_{AR}$  values of both 2 cfs and 10 cfs. PGG evaluated model predictions of streamflow augmentation (as a percent of  $Q_{AR}$ ) and ascertained that the model will generally provide the same proportional results over the range considered. In addition, PGG compared model steady-state simulation of simultaneous operation of AR sites 1 through 4 with the summed results of the four sites individually, and obtained the same values of proportional streamflow augmentation. These observations suggest that the model behaves in a linear fashion with respect to streamflow augmentation, and that individual AR simulations can be scaled over the 2 cfs to 10 cfs range and added together in order to estimate a variety of AR-rates and AR-site combinations.

Sensitivity analysis was performed under both steady-state and transient simulations to evaluate hydrogeologic uncertainty to the hydraulic properties of the shallow aquifer, the upper confining bed, and Dungeness River streambed permeability ( $K_v$ ). Steady-state sensitivity analysis was performed on Site 3 and transient sensitivity analyses were performed on sites 2 and 4. For all sites, the horizontal hydraulic conductivity ( $K_h$ ) distribution of the entire shallow aquifer system was multiplied by 2x and 0.5x, “Dung-7g” was used to represent  $K_v$  of the upper confining bed 10x higher than “Dung-7e”, and the Dungeness River streambed  $K_v$  was multiplied by 3x. On the steady-state analysis (Site 3), the  $K_v$  of the upper confining bed was also multiplied by 0.1x. Comparison of model results under these ranges of uncertainty allowed PGG to evaluate the uncertainty inherent in the predictive model results.

ASR was simulated at both sites with injection and recovery in either the lower aquifer (model layer 5) or the middle aquifer (model layer 3). The simulations employed a storativity value of 0.0002 for all aquitards and confined aquifers, and employed the same range of  $S_y$  values (0.1 and 0.2) for the shallow aquifer. ASR injection at 2 cfs was simulated over 2 months (May-June), followed by a month of dormancy, followed by ASR recovery for 2 months at 2 cfs. Whereas “Dung-7e” was used for both lower-aquifer and middle-aquifer simulations, “Dung-7g” was also used to simulate ASR in the middle aquifer with a higher  $K_v$  for the upper confining bed (0.008 ft/d rather than 0.0008 ft/d). This range of ASR conditions provides an “envelope” of AR responses under a range of target aquifers and aquitard  $K_v$  values. However, as noted above, some uncertainty remains regarding aquitard  $K_v$  values, and further model calibration and simulations are recommended should ASR in the middle or deep aquifers be pursued. Prediction of AR in the shallow aquifer system is much less effected by uncertainty in aquitard  $K_v$  values (see Section 7.4.3).

All transient simulations of AR and ASR were run for a period of 20 years back-to-back. Initial testing of the model suggested that about 5 years of repeated simulation allowed the aquifer response to AR/ASR to approach a “cyclic steady state”, where the seasonal variations in water levels and stream discharges become the same from one year to the next. Twenty years was considered to be a conservative period to simulate AR/ASR so that model predictions are likely to represent a sustained (long-term) condition of seasonal AS/ASR rather than the transition period in response to introduction of new AR/ASR.

---

## 7.2 REPRESENTATION OF AR/ASR RESPONSES

**Table 7-1** summarizes the predictive AR and sensitivity runs. Besides describing the design of the model run, the table notes the maximum head rise in the AR cell (MODFLOW assumes that the AR is distributed evenly throughout the entire cell rather than being introduced via a well, ditch or infiltration pond), the percent of the volume recharged ( $V_{AR}$ ) discharging to the Dungeness River, the average annual rate of AR discharge to the Dungeness River expressed as a percentage of the 2-month  $Q_{AR}$ , and the seasonal range in AR discharge to the Dungeness River expressed as a percentage of the 2-month  $Q_{AR}$ . The latter term reflects whether the AR discharge to the Dungeness River is “flashy” (high range of variation) or fairly consistent (low range of variation).

**Table 7-2** summarizes the distribution of AR discharge to all the streams represented in the model for the steady-state AR predictions. Given the consistency between steady-state and transient predictions of AR discharge to the Dungeness River shown on **Table 7-1**, the relative distribution of AR discharge among streams is expected to be similar between steady-state and transient runs.

**Table 7-3** summarizes the maximum head rise observed in model layers for the steady-state AR simulations. This table supports interpretation of how mounding from AR is transferred from the layer in which AR was applied to adjacent aquifers. The table includes steady-state simulations from the 10 AR sites (i.e. year-round AR infiltration) as well as steady-state simulations of recharge only from the two ASR sites in the middle and deep aquifers. Steady-state mounding provides a maximum limit to model predictions during transient AR or ASR recharge, but does not compensate for the fact that MODFLOW distributes the AR/ASR inflow to the entire model cell. When AR is introduced in smaller footprint features (e.g. infiltration basin or ditch system) and when ASR is introduced via a well, mounding local to these facilities can be significantly higher.

**Table 7-4** summarizes the results of the ASR simulations. Besides presenting the maximum head rise in the ASR cell (with ASR recharged over the entire cell rather than at an injection well), the table summarizes how ASR injection and recovery affect local streams. For each stream where baseflows are changed by more than 2 percent of the rate of ASR ( $Q_{ASR}$ ), the table presents the maximum streamflow augmentation (associated with injection) and the maximum streamflow depletion (negative value, associated with recovery).

**Figure 7-1** presents the results of the linearity analysis on transient model runs at sites 2 and 4. **Figure 7-2** presents a graphical summary of the distribution of augmentation among streams for steady-state simulations using model realization “Dung-7e”. **Figure 7-3** presents streamflow augmentation curves for the Dungeness River for the 9 sites with transient simulations based on model  $S_y$  values of 0.1 and 0.2. **Figure 7-4** presents Dungeness River augmentation curves for the hydraulic property sensitivity analyses performed on sites 2 and 4. **Figures 7-5** through **7-13** present streamflow augmentation curves for the 9 (transient) AR sites, with augmentation to small streams shown for streams receiving significant portions of  $Q_{AR}$ . **Figure 7-14** through **7-17** present maps of groundwater level mounding associated with the AR scenarios. **Figure 7-18** presents Dungeness augmentation/depletion curves for ASR conducted in the lower and middle aquifers at the two ASR sites using model realization “Dung-7e”, and **Figure 7-19** presents Dungeness augmentation/depletion curves for ASR conducted in the middle aquifer at the two sites using model realization “Dung-7g” (higher  $K_v$  in upper confining bed). Finally, **Figures 7-20** through **7-25** present flow augmentation curves for all streams with significant responses to ASR (i.e. augmentation  $\geq 2\%$   $Q_{AR}$ ) for all 6 ASR scenarios simulated by the model.



---

## 7.3 LINEARITY ANALYSIS

Early experimentation with the model showed that steady-state AR predictions, using  $Q_{AR}$  rates of 2 cfs and 10 cfs, showed no significant difference in the relative distribution of AR discharge to the streams (rivers and drains) represented by the model. Steady-state analysis with realization “Dung-7e” also showed that the sum of streamflow augmentation simulated from sites 1 through 4 individually was essentially equal to a single model simulation with AR occurring at all 4 sites simultaneously. In addition to steady-state linearity analysis, PGG performed transient linearity analysis at AR sites 2 and 4 using realization “Dung-7e”, where  $Q_{AR}$  (2 and 10 cfs) was applied during two months of the year (May and June). **Figure 7-1** presents model estimates of AR discharge to the Dungeness River for all runs, and shows insignificant variation in the timing of Dungeness River augmentation (expressed as percent  $Q_{AR}$ ) for the two rates. This indicates that transient model results, expressed as percent  $Q_{AR}$ , can be reasonably applied to simulations of AR rates between 2 and 10 cfs (and likely values near this range) without introducing unacceptable error, and without needing to re-run the model for each individual value of  $Q_{AR}$ .

---

## 7.4 AR RESULTS

AR introduced to the shallow aquifer results in mounding (rise in groundwater levels) and increased baseflows in streams that have a saturated connection to the aquifer. For gaining streams, increased groundwater levels near the stream cause an increased (upward) gradient across the streambed, and therefore increased seepage gains. For losing streams, increased groundwater levels cause a decreased (downward) gradient across the streambed, and therefore decreased seepage losses. The sections below describe how the distribution of mounding and streamflow augmentation from any AR application depends on the location of the site relative to the groundwater-connected streams, the local transmissivity of the aquifer, the storage properties of the aquifer, and other factors considered in the model sensitivity analysis.

In reviewing the following sections, it is important to keep in mind that both the magnitude *and* the timing of AR discharge to key streams are important factors for selecting sites for future AR operations. Site selection should favor locations that deliver AR water to streams when it is needed, rather than solely considering the maximum magnitude of AR discharge to streams.

### 7.4.1 Sensitivity to Site Location

The distribution of predicted AR discharge among all streams simulated by the model is summarized on **Table 7-2** and **Figure 7-2** based on steady-state simulations by model realization “Dung-7e”. AR sites east of the Dungeness River, particularly those farther from the river, tend to deliver more water to Casalery Creek and Gierin Creek/Graysmarsh. AR sites immediately west of the river tend to deliver water predominantly to the river and to Matriotti Creek. However, as discussed in Section 5.3, the model may not accurately simulate the hydraulic connection between the shallow aquifer and Matriotti Creek due to local hydrogeologic complexity near the stream. Estimates of AR discharge to Matriotti Creek should be taken with some caution, and associated uncertainties could potentially affect associated estimates of AR discharge to the Dungeness River.

**Figure 7-3** shows model predictions of seasonal Dungeness River augmentation for 9 AR sites based on transient simulations performed with realization “Dung-7e”. The figure shows the most Dungeness River augmentation for sites close to the river (1, 4, 8) and less augmentation for sites farther away. Sites closer to the river tend to show more seasonal variation, partly because AR is concentrated near the river and therefore discharges less to other streams, and partly because the proximity of the river allows a more rapid loss of AR water from the groundwater flow system to the stream. Sites more distant from surface-

water bodies are able to load more AR water into aquifer storage, which then discharges slowly over time (and at lower rates) to distant streams. Thus, distant sites may provide higher rates of Dungeness River augmentation at times removed from the period of AR application. **Table 7-1** reports the distance between the site and the Dungeness River along with how much AR water is predicted to discharge to the Dungeness River and the seasonal variation of this discharge.

#### 7.4.2 Sensitivity to Specific Yield and Storativity

**Figure 7-3** presents Dungeness River augmentation from AR based on model realization “Dung-7e” and two different values of  $S_y$  (0.1 and 0.2). Both  $S_y$  values represent potentially reasonable depictions of the groundwater flow system, and therefore represent a range of hydrologic responses to AR. As discussed below,  $S_y$  appears to be the most important factor considered in the sensitivity/uncertainty analysis affecting model predictions of AR. The lower  $S_y$  value supports less storage of AR water in the aquifer, and therefore provides a more “flashy” response to introduction of AR water. The AR discharge reaches streams faster, discharges at higher rates during periods of AR, and decays faster after AR applications are complete. This can be observed by the shape of the curves on **Figure 7-3** along with the seasonal range of Dungeness River augmentation reported on **Table 7-1**.

Simulation of AR introduced as infiltration to the shallow aquifer (layer 1) is not significantly sensitive to the storage coefficient (S) of underlying hydrogeologic units. PGG ran a shallow-aquifer AR simulation using S values of 0.0002 and 0.00005 with no significant variation in results.

#### 7.4.3 Sensitivity to Hydraulic Properties of Aquifers, Aquitard and Streambed

**Figure 7-4** presents Dungeness River augmentation from AR over a range of hydraulic properties considered in PGG’s sensitivity/uncertainty analysis for sites 2 and 4. Relative to the parameters used in model realization “Dung-7e”, parameters varied include  $K_h$  of the shallow aquifer (2x and 0.5x),  $S_y$  of the shallow aquifer (0.1 and 0.2),  $K_v$  of the upper confining bed (10x in “Dung-7g”), and  $K_v$  of the Dungeness River streambed (3x). Run names referenced on the figure are further described in **Table 7-1**.

Site 2 is located a moderate distance from the Dungeness River (3500 feet), and all scenarios conducted with the same value of  $S_y$  (0.2) show tightly grouped results. In this case, reduction of  $S_y$  from 0.2 to 0.1 has the greatest effect on predicted Dungeness River augmentation. The  $S_y$  reduction affects the seasonality of the augmentation, but has no significant effect on the annual average baseflow augmentation to the river. Values of annual average augmentation are tightly grouped for all parameters considered (**Table 7-1**). The modeling results show very low sensitivity to the  $K_v$  of the upper confining bed (runs P2a, P2b and P2e are nearly identical).

Site 4 is located fairly close to the Dungeness River (1500 feet). Similar to Site 2, all scenarios conducted with an  $S_y$  value of 0.2 are reasonably well grouped. The model shows no sensitivity to the  $K_v$  of the upper confining bed (runs P4a, P4b and P4e practically fall along the same curve). Although the variation for all runs with the same  $S_y$  (0.2) is greater than predicted for site 2, the variation is still considered to be minor given uncertainties in the hydrologic system and the accuracy needed for designing an AR approach. Also similar to site 2, reduction of  $S_y$  from 0.2 to 0.1 has the greatest effect on predicted Dungeness River augmentation.

Site 3 is located far from the Dungeness River (5400 feet). Sensitivity analysis on this site was limited to steady-state simulation, but includes additional runs such as a 0.1x multiplier on  $K_v$  for the upper confining bed and a 3x multiplier on  $K_v$  for the Dungeness River streambed. Little difference is noted between the sensitivity runs, with the exception of P3-SSd (layer-1  $K_h$  x0.5) where augmentation to the Dungeness

River is predicted to show a moderate reduction from 81% to 69%. Variation among all other runs falls within a range of 4% of  $V_{AR}$ .

**Table 7-1** also notes the  $K_h$  of the model cell into which AR is introduced along with the modeled head rise in the cell. A clear relationship exists between lower  $K_h$  values and greater mounding at the site. Note that the cell-based predictions of groundwater rise will underestimate the mounding expected when AR is introduced over a smaller area than the cells (which range in dimension from 20 to 40 acres). **Figure 7-14** through **7-17** present maps of groundwater level mounding associated with the AR scenarios based on model realization “Dung-7e”. **Table 7-3** summarizes the maximum head rise in each layer associated with the modeled AR applications. For simulations using realization “Dung-7e”, water-level rises show little propagation into adjacent aquifers. However, with realization “Dung-7g” the higher  $K_v$  value for the aquitard allows greater propagation of mounding in the shallow aquifer to adjacent model layers.

#### 7.4.4 Summary of Factors Affecting AR Responses

As discussed above, the distribution and timing of streamflow augmentation associated with shallow-aquifer AR is most sensitive to the location of the AR site and the value of  $S_y$  used to represent the shallow aquifer. The  $K_v$  of the upper confining bed was shown to have little influence on predicted streamflow augmentation from shallow-aquifer AR. Sensitivity analysis also indicated that varying the  $K_h$  (and therefore the  $T$ ) of the shallow aquifer by a factor of 2 has a generally low effect on the sites considered. However, the sensitivity of model predictions to site location is affected not just by distance between the site and various surface-water bodies, but also by the situation of the site within the regional distribution of  $K_h$  and  $T$ . AR water tends to move preferentially through higher  $T$  zones and be somewhat retarded by lower  $T$  zones. Careful consideration of the predicted responses among the simulated AR sites can identify how the regional transmissivity distribution influences hydrologic responses to AR between sites. Finally, the degree of hydraulic connection between the shallow aquifer and any particular stream will also control the degree of streamflow augmentation associated with any particular AR site. As mentioned above, some uncertainty regarding the hydraulic connection between the shallow aquifer and Matriotti Creek, as well as the model’s inability to represent hydrogeologic complexities associated with this connection, adds to uncertainty regarding predicted augmentation to the creek (and therefore the distribution of augmentation between Matriotti Creek and the Dungeness River). Similar uncertainties are noted for simulation of hydraulic connection between the shallow aquifer and lower Bell Creek.

---

## 7.5 ASR RESULTS

ASR was simulated at two sites – one on each side of the Dungeness River (**Figure 1-1**). At each site, simulations were performed over a range of model configurations to yield a range of predicted ASR responses. ASR was simulated in both the lower and middle aquifers using realization “Dung-7e”. In order to evaluate model sensitivity to aquitard  $K_v$ , ASR was also simulated in the middle aquifer using realization “Dung-7g”, where the  $K_v$  of the upper confining bed is 10x higher than “Dung-7e”. Similar to the AR simulations, all ASR simulations were run using  $S_y$  values of 0.1 and 0.2. All model simulations employed the same ASR schedule (injection for two months, followed by one month dormancy, followed by recovery for two months) and the same rate of injection/recovery (2 cfs). The model predictions are independent of the actual calendar months in which the ASR cycle occurs, and previous analysis of model linearity suggests that results of these model predictions can be extrapolated over a reasonable range of ASR rates.

**Table 7-4** summarizes the ASR simulations. Streamflow augmentation (associated with ASR injection) is expressed as positive values, whereas streamflow depletion (negative values) is associated with recovery. In addition to the transient simulations described above, steady-state simulations of year-round injection were performed for reach model configuration to identify which streams were most affected by stressing the groundwater flow system at each ASR site. Impacts predicted for ASR injection are significantly smaller than impacts predicted for the steady-state injection because ASR injection occurs for only 2 months per year, and is offset by 2 months of ASR recovery soon thereafter. Note that model predictions of head rise are for injection into the entire ASR cell, and head-rise in the immediate vicinity of an actual ASR well will be greater. A comparison of predicted impacts to the Dungeness River from all simulations is presented on **Figures 7-17** and **7-18**. For each individual ASR simulation, predicted impacts to all streams where flow augmentation/depletion exceeds  $\pm 2\%$  of  $Q_{ASR}$  (and to selected additional streams) are illustrated on **Figures 7-19** through **7-24**.

As expected, predicted ASR impacts to the Dungeness River are greater when ASR is conducted in the middle aquifer rather than the lower aquifer. Predicted impacts associated with ASR in the lower aquifer are similar for both sites (**Figure 7-18**), likely because the combined influence of the lower and upper confining bed tends to disperse the ASR mounding and drawdown over large areas such that localization of impact is reduced within the shallow aquifer. Based on **Table 7-4**, streamflow augmentation/depletion for ASR in the lower aquifer is predicted to range from about -1.9 to +3.6 percent of  $Q_{ASR}$ , with *slightly* greater impacts from the west site. Moving the ASR to the middle aquifer and using the same model realization (“Dung-7e”) causes two noticeable effects: predicted Dungeness River augmentation/depletion is increased overall, and is significantly larger from ASR conducted at the west site relative to the east site. The larger range of ASR impact from the west site (-9.5% to +14.0%) compared to the east site (-2.9% to +5.0%) is likely due to the fact that the model simulates a greater connection to the small streams east of the Dungeness River relative to those on the west<sup>16</sup>, and because the upper confining bed tends to be thicker east of the Dungeness River within several miles of the coast (Thomas et al, 1999).

Increasing the  $K_v$  of the upper confining bed to 0.008 ft/d with model realization “Dung-7g” causes mixed changes of augmentation/depletion to the Dungeness River from middle aquifer pumping. For ASR simulated at the west site, this increase in  $K_v$  causes predicted impacts to the river to increase from -9.5%/+14.0% to -19.4%/+27.1%. The increased  $K_v$  causes both injection and recovery from the middle aquifer to have more of an effect on the shallow aquifer, and therefore more of an effect on the river. However, ASR simulated at the east site is predicted to cause *less* impact to the river than under simulation “Dung-7e”. A closer look at the east-site model predictions shows that while Dungeness River impacts are predicted to decrease, total predicted streamflow impacts are predicted to increase between “Dung-7e” and “Dung-7g” (**Table 7-4**). This overall increase is consistent with the increased hydraulic connection between aquifers represented by “Dung-7g”. The redistribution of impact among east-side streams is likely associated with the different aquifer property values required to calibrate realization “Dung-7g” relative to “Dung-7e”. It is not uncommon that more than one combination of aquifer properties can provide an acceptable model calibration – a characteristic called “non-uniqueness”. The difference in predicted impacts associated with east-site ASR in the middle aquifer illustrates how non-uniqueness can cause uncertainty in predictive results.

**Figures 7-20** through **7-25** present model predictions of streamflow impact for the six transient ASR simulations for streams with impacts exceeding 2% of  $Q_{ASR}$  (and additional selected streams). Note that the results are expressed as actual flow impacts in cfs from ASR simulated at 2 cfs, rather than as percent of  $Q_{ASR}$ . ASR at the east site predominantly affects the Dungeness River, Cassalery Creek, and Gierin

<sup>16</sup> See prior discussions about Matriotti Creek and low streambed conductances for selected west-side streams (possibly associated with bedrock occurrence).

Creek (along with Graysmarsh). ASR at the west site predominantly affects the Dungeness River and Matriotti Creek. As mentioned earlier, hydrogeologic complexity associated with Matriotti Creek introduces some uncertainty about model predictions of baseflow impacts in this vicinity; and uncertainties in Matriotti Creek impact likely causes uncertainty in the distribution of ASR impact between Matriotti Creek and the Dungeness River. Furthermore, non-uniqueness between “Dung-7e” and “Dung-7g” causes a redistribution of predicted ASR impact distribution between Cassalery and Gierin creeks from the east-site simulations. Finally, one can observe that the model predictions for ASR to the middle aquifer under “Dung-7g” show a faster response to both injection and recovery to predictions for the same configuration under “Dung-7e”.

---

## 8.0 MODEL USES, LIMITATIONS, AND RECOMMENDATIONS

The following bullets summarize the appropriate uses and limitations of the model:

1. The model can be used to evaluate the effects of adding a new hydrologic stress to the groundwater flow system. New stresses can include pumping, injection through wells, infiltration, changes in recharge due to land-use activities, etc.
2. The model is best suited to performing predictive simulations on a regional scale. The model was calculated at the regional scale, and does not necessarily represent hydrogeologic variations at the site scale. If knowledge of a particular site indicates that the model configuration is an acceptable representation, the regional resolution of the model cell spacing may affect predictive results. Techniques such as “telescopic mesh refinement” (TMR) and addition of new rows and columns can be used to increase model resolution near a site of interest.
3. The model cannot be expected to predict the effects of hydrogeologic complexities that are not explicitly represented by the model, or cannot be represented under the current model structure. Hydrogeologic variation at a smaller scale than the grid resolution cannot be explicitly simulated. In addition, single-layer representation of hydrostratigraphic units dictates that the model cannot represent vertical variations within an aquifer such as perched conditions or interbedding among multiple water-bearing and low-permeability zones.
4. The model is best suited to simulating hydrologic stresses and responses within the shallow aquifer, although such simulations cannot be expected to capture complexities in the groundwater flow system that are not (or cannot be) included in the model. When performing a predictive simulation within the shallow aquifer, the model user should consider which complexities are known, which are expected to be relevant, which are represented in the model, and how this extent of representation will affect model predictions.
5. The model can be used to simulate stresses within deeper portions of the groundwater flow system; however, these predictions are more subject to uncertainties regarding interconnections between aquifers via intervening aquitards. Predictive analysis of the effects of a stress imposed on one aquifer on hydrologic conditions in other aquifers is particularly sensitive to this uncertainty. PGG addressed this uncertainty by developing two realizations of the model, and both realizations should be used in making predictions associated with deeper portions of the flow system. However, alternative representations of aquitard  $K_v$  are likely admissible, and additional calibration is recommended to better constrain uncertainty associated with this element of the groundwater flow system.
6. The accuracy of model-predicted impacts on streamflow associated with new hydrologic stresses is limited in areas where model representation of streams is known to not reflect existing hydrogeologic complexity. Examples include: lower Matriotti Creek, where the model adequately represents shallow aquifer heads but does not represent interaction with the creek (potentially due to perched condi-

tions); and lower Bell Creek, where known perched conditions are not represented by the model. Errors in predicting how hydrologic stresses affect these streams can cause errors in prediction of effects in adjacent streams.

7. The calibrated realizations of the model (“Dung-7e” and “Dung-7g”) have different distributions of aquifer/aquitard properties, and therefore vary somewhat in their responses to hydrologic stresses. The ability to create more than one model realization capable of meeting calibration criteria (referred to as “non-uniqueness”) is quite common, and accounts for some of the uncertainty inherent in predicting impacts from hydrologic stresses. This inherent uncertainty cannot be avoided in any model or predictive approach, largely because subsurface conditions are inherently variable and available data are typically insufficient to characterize such variability. While model predictions can still be performed to obtain estimates of impact at a commonly acceptable degree of accuracy, uncertainty associated with non-uniqueness cannot be avoided and prevents prediction of “exact” values of hydrologic impact. In some cases, modelers will use stochastic analysis of multiple (i.e. many) realizations to characterize the range of uncertainty in model predictions.
8. The model can be used to evaluate the movement of contaminants or define wellhead protection zones on a regional scale using particle tracking. Uncertainties regarding the flow system (e.g. aquitard  $K_v$ ) or associated with (non)representation of known complexities will similarly affect the particle tracking results. Particle tracking on the site-scale may not adequately simulate the effects of site-scale hydrologic stresses or site-scale variations (heterogeneities) unless the model resolution is increased through grid refinement or TMR. Simulation of concentration-based contaminant transport using codes such as MT3D will be affected by the model’s large cell size, and higher resolution would likely be required to minimize errors due to numerical dispersion.
9. The contrast between the dimensions of model cells (typically 660 to 1320 feet) and the dimensions of rivers and streams (typically 5 to 50 feet wide) dictate that model resolution is insufficient to represent stream/aquifer interactions at a local scale. While regional interactions between surface-water and groundwater are represented, the model cannot be used to accurately simulate hydrogeologic responses to river-stage variation in areas immediately alongside the river.
10. Care must be taken if the model is used to evaluate how new stresses affect saltwater intrusion through connections with marine water. Model grid resolution is insufficient to simulate the dynamic location of the saltwater wedge, for instance using modeling codes such as SEAWAT. Model simulations can be performed to evaluate how new hydrologic stresses affect heads along the coast, but uncertainties regarding the offshore occurrence of deeper aquifers and their connections with marine water must be acknowledged.
11. The model can be used to simulate the presence of a deep aquifer beneath low permeability (confining) materials in the undifferentiated deposits. However, little is known about the distribution and properties of the deep aquifer, and such uncertainties must be acknowledged when performing model simulations.
12. Transient model predictions were made using the principal of superposition, and assume that the groundwater flow system and its connection with surface-water features are linear. Where seasonal water-level variations significantly alter the distribution of hydraulic connections between the shallow aquifer system and streams, non-linearity will occur and errors will be associated with the superposition approach. Errors associated with small variations in this hydraulic connection likely fall within the range of uncertainty of the model. If necessary, explicit modeling of both a transient base-case and a transient prediction scenario can be performed and the difference evaluated, so that the principal of superposition is not required.

If additional model development is desired, the following activities are recommended:

1. Additional hydrogeologic characterization would support further refinements of the model and reduction of model uncertainties. Recommended areas of additional characterization include:
  - Hydrogeologic conditions supporting groundwater/surface-water interactions along Matriotti Creek and Bell Creek, as well as other creeks where conditions are not well documented;
  - Hydrogeologic conditions in the vicinities of Cassalery Creek and Gierin Creek to follow up on subsurface characterization performed by Rongey (1991);
  - General compilation of existing (and new) information to better characterize complexities in the shallow groundwater flow system;
  - Hydraulic connections between deeper portions of the groundwater flow system and marine water can be evaluated through continuous water-level monitoring, evaluation of tidal groundwater level variations, and water quality sampling in coastal wells;
  - Spatial variability of transmissivity in the middle and lower aquifers;
  - Hydraulic properties and boundary effects within the deep aquifer, to the extent that testing of (limited) existing wells can provide this information. Installation of new wells to investigate the deep aquifer is desirable but may be prohibitively expensive;
2. Additional model calibration to better constrain hydraulic connections among deeper units within the groundwater flow system is recommended. Such calibration would focus on aquitard  $K_v$ , and would require generation of an appropriate target dataset. Simultaneous monitoring of multiple aquifers during background conditions and during aquifer tests can provide good data for such calibration. Data from the City of Sequim's monitoring of the Port Williams wellfield could be evaluated for a calibration dataset. Age dating (isotope) data could be used to evaluate groundwater flowpaths and travel times between aquifers.
3. Additional transient calibration could be performed to assess model simulation of long-term historic trends. In order to perform such calibration, a dataset would need to be developed that characterizes changes in groundwater withdrawals, irrigation recharge, precipitation recharge, and wastewater recharge over time.
4. Additional transient calibration could be performed to constrain representation of marine connection based on a dataset of groundwater responses to tidal variations.
5. Further refinement of the model grid (row and column resolution) could be performed to support predictive simulations on a more local scale. The model grid is currently considered to be fairly low resolution, but is adequate for regional analysis. Grid refinement would require some degree of recalibration, as new dimensions will change the modeled interaction between (relatively narrow) surface-water features and grid cells representing the shallow aquifer. The distribution of pumping could be refined to suit the new grid resolution. Further refinement of model layering could be performed to represent complexities in the vertical dimension – particularly in the shallow aquifer system. However, sufficient characterization of such complexities would be required to make use of the higher resolution.
6. The calibrated 2008 model could be used to re-run predictive simulations of the effects of piping of irrigation ditches associated with irrigation conservation.
7. The calibrated 2008 model could also be used to evaluate how climate change could affect groundwater levels and stream baseflows. Recharge input would need to be generated for future climatic conditions, preferably with a reasonably sophisticated tool such as the USGS Deep Percolation Model (as applied by Thomas et al, 1999).

---

## REFERENCES

- Drost, B. W., 1983. Impact of changes in land use on the ground-water system in the Sequim-Dungeness Peninsula, Clallam County, Washington. U.S. Geological Survey, Water-Res. Invest. Rep. 83-4094.
- ESI (Environmental Simulations, Inc.), 2007a. Critical Review of the 2003 Dungeness Groundwater Model, Clallam County, Washington. Technical analysis prepared for Ann Soule, Clallam County Dept. of Health & Human Services by Jim Rumbaugh, ESI dated March 14, 2007.
- ESI (Environmental Simulations Inc.), 2007b. Groundwater Vistas Version 5. <http://modflow2000.com/>
- Freeze, A. and J. Cherry. 1979. Groundwater. Prentice Hall Publishers.
- Forbes, R. and CH2MHill. 1993. Preliminary Assessment of Seawater intrusion in coastal wells in eastern Clallam and eastern Jefferson Counties. October 12, 1993
- Harbaugh, A.W. and McDonald, M.G., 1996. User's Documentation for MODFLOW-96, an update to the U.S. Geological Survey Modular Finite-Difference Ground-Water Flow Model. U.S. Geological Survey Open-File Report 96-485
- Harbaugh, A.W., Banta, E.R., Hill, M.C., and McDonald, M.G., 2000. MODFLOW-2000, the U.S. Geological Survey modular ground-water model — User guide to modularization concepts and the Ground-Water Flow Process, U.S. Geological Survey Open-File Report 00-92.
- Hydrogeologic, Inc. 2006, Modflow-Surfact software (version 3.0), overview: installation, registration, and running procedures. Hydrogeologic, Inc., Herndon, VA. USA.
- Jones, M.A. 1996. Delineation of Hydrogeologic Units in the Lower Dungeness River Basin, Clallam County, Washington. U.S. Geological Survey, Water-Res. Invest. Rep. 95-4008. 11 pp.
- Leighton, Jeff, and Porcello, John, 2001, Deep aquifer yield groundwater flow model—report on model development, calibration, and testing: Portland, Oregon, City of Portland Bureau of Water Works and CH2MHILL, July 2001.
- Miller, Erick. 2008. Aspect Consulting. Personal communication with Peter Schwartzman of Pacific Groundwater Group.
- Montgomery Water Group, 1998. Dungeness River agricultural water users comprehensive water conservation plan. Consultants report prepared by Montgomery Water Group of Kirkland, WA.
- McDonald, M.G., and Harbaugh, A.W., 1988. A modular three-dimensional finite-difference ground-water flow model (PDF), Techniques of Water-Resources Investigations, Book 6, U.S. Geological Survey, 586 p.
- NRCS (Natural Resources Conservation Service), 2005. Soil survey geographic (SSURGO) database for Clallam County Area, Washington. Published 12/23/05. [URL:http://SoilDataMart.nrcs.usda.gov/](http://SoilDataMart.nrcs.usda.gov/)



Noble, J.B., 1960. A preliminary report on the geology and ground-water resources of the Sequim-Dungeness area, Clallam County, Washington: Olympia Wash., Washington Department of Conservation, Division of Water Resources, Water Supply Bulletin No. 11.

Northwestern Territories Inc. 1990. Calsborg water supply well construction and testing report. Port Angeles WA. Northwestern Territories Inc.

PGG (Pacific Groundwater Group), 1995. Hydrogeologic evaluation and well yield analysis, City of Sequim Stone Well #1, Clallam County Washington. Consultants report prepared for City of Sequim dated December 1995.

PGG (Pacific Groundwater Group), 1996. Silberhorn Wellfield: Hydraulic evaluation and yield analysis, City of Sequim, Clallam County Washington. Consultants report prepared for City of Sequim dated October 1996.

PGG (Pacific Groundwater Group), 1998. Installation, testing and recommended operation Port Williams Well #2, Clallam County, Washington. Consultants report prepared for City of Sequim dated December 1998.

PGG (Pacific Groundwater Group), 2000. Hydrogeologic characterization and monitoring activities, City of Sequim Reuse Demonstration Site, Clallam County Washington. Consultants report prepared for City of Sequim dated October 2000.

PGG (Pacific Groundwater Group), 2002. City of Sequim 2001 hydrologic monitoring report. Consultants report prepared for City of Sequim dated May, 2002

PGG (Pacific Groundwater Group), 2007. Technical memorandum regarding review of Ecology 2003 Model. To: Jim Bay (City of Sequim) and Ann Soule (Clallam County). From: Peter Schwartzman, Pacific Groundwater Group. Dated February 9, 2007

PGG (Pacific Groundwater Group), 2008a. Assessment of baseflow in small streams of the Dungeness Watershed. Technical memorandum submitted to Ann Soule of Clallam County dated January 14, 2008.

PGG (Pacific Groundwater Group), 2008b. Construction, testing and recommended operation Port Williams Well #3. Consultants report prepared for City of Sequim dated March 18, 2008.

PGG (Pacific Groundwater Group), 2009. Aquifer recharge feasibility study for the Dungeness Peninsula. Consultants report prepared for Clallam County Environmental Health (in press).

Robinson & Noble, Inc. 1974. Development of a deep ground water source for the Weyerheuser seed orchard at Sequim, Washington. Consultants report dated April, 1974.

Rongey and Associates, 1992. Hydrogeological investigations Sunland comprehensive wastewater system plan. Prepared for Sunland Water District. Dated February 1992.

Rumbaugh, Jim. 2008. Environmental Simulations Inc. Personal communication with Peter Schwartzman of Pacific Groundwater Group.

Simonds, F.W. and K. Sinclair., 2002. Surface Water-Ground Water Interactions Along the Lower Dungeness River and Vertical Hydraulic Conductivity of Streambed Sediments, Clallam County, Washington, September 1999-July 2001. U.S. Geological Survey Water-Resources Investigations Report 02-4161.

Soule, Anne. Clallam County Department of Health and Human Services. Personal communication with Peter Schwartzman of Pacific Groundwater Group between 2007 and 2009.

Sweet-Edwards/EMCON. 1991. Sequim-Dungeness ground water characterization study. Consultants report prepared by Sweet-Edwards/EMCON of Bothell, WA.

Thomas, B. E., L. A. Goodman and T.D. Olsen. 1999. Hydrogeologic assessment of the Sequim-Dungeness area, Clallam County, Washington. USGS Water Resources Investigation Report 99-4048.

TTFW (Tetra Tech FW, Inc.), 2003. Dungeness Water Users Association comprehensive water conservation plan, groundwater model report. June 2003.

Trescott, P.C. 1975. Documentation of finite-difference model for simulation of three-dimensional ground-water flow; U.S. Geological Survey Open File Report 75-438.

**Table 3-1**  
**Hydrogeologic Unit Analysis of Wells Over 350 Feet Deep**

Well Owner	Source of Log	Depth* (feet)	Diameter (inches)	Ecology Location	QQ Section	Completion Date	Hydrogeologic Unit Analysis	Aquifer Unit**
VERNE PETTETT	Ecology	2900	7	31N/03W-30NWSW	31N/03W-30E	1/10/1984	Only have aband. report, 260' or 2900'??	n/a
GARY SMITH	Ecology	2327	6	30N/03W-22SWSW	30N/03W-22N	6/26/2006	Actually only 228' deep	n/a
CAROL GEER	Ecology	992	6	31N/04W-27SWSW	31N/04W-27M	10/27/1998	Actually only 99' deep	n/a
GRAYSMARSH LLC	Ecology	704.5	12	30N/03W-9SESE	30N/03W-9R	7/23/2006	Aspect Consulting interprets as Unit 5	5
BILL MCCORLE	Ecology	689	6	30N/03W-27NWSE (likely 27NWNE)	30N/03W-27F	2/17/1991	screened in WB zones @ 530-560 and 659-689; USGS interpret Unit 5 as absent here, could be Unit 6	6
ELLIOT CLARK	Ecology	617	12	31N/04W-35NE	31N/04W-35	8/31/1979	USGS interpreted as Unit 5, "Well S"	5
DUNGENESS ESTATES C/O BRUCE CRAMER	Ecology	607	6	30N/04W-4SE	30N/04W-4	11/24/1982	Looks like Unit 5 wrt USGS contact elevs	5
COULTER & SCOTT	Ecology	574	8	30N/03W-15NESW	30N/03W-15G	4/13/1951	USGS 15G01, interpreted as Unit 5	5
4 PLUS / DUGENESS GOLF COURSE	Ecology	565	8	30N/04W-3SESW	30N/04W-3Q	3/16/1998	WB Zone 509-565', USGS has Unit 5 bottom @ -400' but has no logs in area. Could be interpreted as 5 or 6.	5/6
ALDERWOOD HOME OWNERS	Ecology	549	6	30N/04W-8NE	30N/04W-8	11/24/1995	Based on nearby Well #76, likely Unit 5	5
MAINS FARM PROPERTY ASSN.	Ecology	537	8	31N/04W-34NESW	31N/04W-34G	6/20/1989	Completed above USGS Unit 6 Elevation	5
HOWARD TURNER	Ecology	534	6	30N/03W-28SENE	30N/03W-28J	3/18/1994	Bedrock @ 23', Unit 6 absent	n/a
PARK THOMPSON	Ecology	530	6	31N/04W-35	31N/04W-35	5/3/1997	Looks like Unit 5 wrt USGS contact elevs	5
OLD TOWN ASSOCIATES OLYMPIC STRAITS COMM	Ecology	510	8	31N/04W-26SESE	31N/04W-26R	12/20/1994	Looks like Unit 5 wrt USGS contact elevs	5
PUD #1 OF CLALLAM COUNTY	Ecology	468	8	30N/04W-7SESE	30N/04W-7R	11/20/1992	Completed above USGS Unit 6 Elevation	5
JOSEPH KEELER	Ecology	462	6	30N/03W-27NWSW	30N/03W-27E	8/13/2005	Bedrock @ 242', Unit 6 absent	n/a
GARDON MC GILD	Ecology	455	6	30N/03W-5NESE	30N/03W-5A	4/10/1991	Stratigraphy suggest Unit 5	5
DOROTHY ADAMS	Ecology	446	6	31N/04W-35SWSW	31N/04W-35N	5/24/2001	Completed above USGS Unit 6 Elevation	5
CLAYTON COUTURE	Ecology	442	6	30N/04W-4NWSE	30N/04W-4F	3/20/2006	Looks like Unit 5 wrt USGS contact elevs	5
DAVE AND DEBBIE BAKER	Ecology	431	6	30N/05W-14NWNE	30N/05W-14C	7/14/2006	Completed above USGS Unit 6 Elevation	5
MARK ASHEY	Ecology	423	6	30N/03W-5NWSE	30N/03W-5F	3/13/1992	No significantly thick WB zones noted	n/a
BRUCE VAN AUKEN	Ecology	419	6	30N/05W-10SWSE	30N/05W-10P	9/28/2006	Completed above USGS Unit 6 Elevation	5
BATTELLE PACIFIC NW LABORATORIES	Ecology	416	8	30N/03W-22SENE	30N/03W-22K	2/13/1981	Stratigraphy suggest Unit 5	5
CITY OF SEQUIM	Ecology	416	12	30N/03W-17NWSE	30N/03W-17F	10/18/1995	Port Williams PW-1, PGG interpretation, Recent drilling to 850' shows some thin (5-20') WB zones in Unit 6	5
DORTHY ADAM'S	Ecology	415	6	31N/04W-35SW	31N/04W-35	6/5/1989	Completed above USGS Unit 6 Elevation	5
SUZANNE FLEMING	Ecology	404	6	31N/04W-34NESE	31N/04W-34A	3/14/2003	Looks like Unit 5	5
QUENTIN BERQUIST	Ecology	398	6	31N/04W-35SW	31N/04W-35	2/24/1988	Looks like Unit 5	5
BRUCE VAN AUKEN	Ecology	396	6	30N/05W-10SWSE	30N/05W-10P	11/28/2005	Completed above USGS Unit 6 Elevation	5
EDUARDO GALVAN	Ecology	395	6	30N/03W-27NW	30N/03W-27	2/2/1990	Bedrock @ 127', Unit 6 absent	n/a
MICHAEL SCHMOLL	Ecology	385	6	30N/03W-6SWSE	30N/03W-6P	3/10/2005	Actually only 162' deep	n/a
JOHN KIRNER	Ecology	382	6	31N/03W-31NWSW	31N/03W-31E	6/5/2003	Looks like Unit 5 wrt USGS contact elevs	5
FLOYD MCREVEY	Ecology	381	6	30N/05W-14NWNE	30N/05W-14C	8/23/2001	Completed above USGS Unit 6 Elevation	5
CARLSBORG MOBILE ESTATES	Ecology	380	6	30N/04W-22NESE	30N/04W-22A	3/25/2007	Completed above USGS Unit 6 Elevation	5
CITY OF SEQUIM	Ecology	379	12	30N/03W-17NWSE	30N/03W-17F	11/30/1998	Port Williams PW-2, PGG interpretation, Recent drilling to 850' shows some thin (5-20') WB zones in Unit 6	5
LORA LEE ESTATE	County	558	8	30N/04W-8NWSE	30N/04W-08F02	1/10/1989	Completed above USGS Unit 6 Elevation (water bearing materials @ 466-558')	5
U.S. COAST GUARD	USGS	667	4	30N/04W-8NESW	31N/03W-18G01	9/1/1930	Dungeness Lighthouse, different geology, water bearing 484-538'	??
WYERHAEUSER CO	USGS	970	12	n/d	30N/04W-09L02	2/27/1974	WB from 790-837'. Unit 6 WB zone	6
DALTON, DAN, OIL TEST	USGS	3490	oil	n/d	31N/03W-30Q03	9/9/1950	log not available from USGS, oil well	n/d
STANDARD OIL CA, OIL TEST	USGS	5105	oil	n/d	31N/04W-24F01	8/16/1965	oil well, 1715' unconsolidated, no detail	n/d
COU, O L	USGS	395	no log	n/d	30N/04W-36B04	6/29/1977	no log available, USG interp suggests bedrock	n/a
CLARK, ELLIOT	USGS	618	12	n/d	31N/04W-35H01	8/31/1979	USGS interpreted as Unit 5	5
STANDARD, OIL CA, OIL TEST	USGS	7493	oil	n/d	30N/03W-17G01	2/6/1956	oil well, 2105' unconsolidated, no detail	n/d
PATTEN PACIFIC	County	440	6	30N/04W-34NEN		9/14/1989	bedrock (soft shale) @ 172'	n/a
CHUCK FINK	County	415	6	30N/04W-20SENE		5/3/1999	no aquifer in deeper portion of well	n/a
ARTHUR LEACH	County	384	6	30N/04W-21		12/29/1975	WB from 308-368, USGS interp below as fine grained unit 6	5
R&R Enterprises, 7/8/88	PGG	355	8	30N/03W-18NESW	30N/03W-18G51	7/8/1987	Interpreted in PGG Port Williams Rpt	5

\* Note: Ecology listings report completed depth, USGS and County listings report drilled depth.

\*\* Unit 5 = lower confined aquifer, Unit 6 = undifferentiated deposits

n/a - well not deep enough to make a determination or no log available n/d - no data to make determination n/r not reported

**Table 4-1**  
**Summary of Solver Parameters**

Model Code	MODFLOW SURFACT	MODFLOW 88/96	MODFLOW 88/96
Solver	PCG4	SIP	PCG2
Solver Parameters	Outer Iterations = 100	Maximum Iterations = 20,000	Outer Iterations = 1000
	Inner Iterations = 600	Acceleration Factor = 0.001	Inner Iterations = 25
	Maximum Orthogonalizations = 10	Iteration Parameters = 10	Relaxation Factor = 1
	Head Change Criterion = 0.001 feet	Head Change Criterion = 0.001 feet	Matrix Preconditions = Cholesky
	Newton-Raphson linearization (on)		Maximum Bound Eigenvalue = 2
	Backtracking Factor = 0.02		Head Change Criterion = 0.001 feet
	Residual Reduction Factor = 1.02		Flow Residual = 10 cubic feet per day
	Variably Saturated Flow Option (on)		

**Table 4-2  
Calibrated Hydraulic Conductivity Values for Aquifer/Aquitard Zones and Streambeds**

Aquifer Zone / Stream	Layer	Dung 7e		Dung 7g	
		Kh	Kz	Kh	Kz
1	1	22	2	18	2
2	1	7	0.7	7	0.7
3	1	20	2	15	2
4	1	400	40	400	40
5	1	100	10	100	10
6	1	10	1	10	1
7	1	250	25	250	25
8	1	40	4	40	4
9	1	15	1	15	1
10	1	80	8	80	8
11	1	11	1	20	2
12	1	20	2	20	2
13	1	50	5	50	5
14	1	100	10	50	5
15	1	30	3	30	3
16	1	80	8	60	6
17	1	40	4	30	3
18	1	75	8	75	8
19	1	5	5	5	5
70 (Bedrock)	1	0.04	0.04	0.04	0.04
73	1	44	4	44	4
20	2	0.1	0.0008	0.1	0.008
30	3	33	3	50	5
40	4	0.1	0.0008	0.1	0.0008
50	5	40	4	40	4
60	6	0.1	0.0008	0.1	0.0008
60	7	0.1	0.0008	0.1	0.0008
Morse Creek	1	n/a	0.04	n/a	0.04
Bagley Creek	1	n/a	0.274	n/a	0.274
Siebert Creek	1	n/a	0.09/0.045*	n/a	0.09/0.045*
McDonald Creek	1	n/a	0.074/0.037*	n/a	0.074/0.037*
Matriotti Creek	1	n/a	1	n/a	1
Dungeness River	1	n/a	10	n/a	10
Meadowbrook Creek	1	n/a	30	n/a	30
Cassalery Creek	1	n/a	30	n/a	30
Gierin Creek	1	n/a	10	n/a	20
Graysmarsh	1	n/a	0.5	n/a	0.4
Bell Creek	1	n/a	3.43	n/a	3.43
Johnson Creek	1	n/a	0.42	n/a	0.42

\* - Lower streambed Kz value applied to portions of upper stream reaches.

**Table 5-1  
Summary of Water Level Targets**

Target Name	X State Plane NAD83	Y State Plane NAD83	X,Y Location Source	Layer	Weight	Reference Elevation (NAVD88)	Elevation Source	DTW (ft)	DTW Period	Target Water Level Elev (NAVD88)
29N04W01M01	1075408	386099	CC	1	1	466.7	LS-Lidar	10.02	Avg 12/95 to 9/97	456.73
30N03W06M01	1082322	417058	CC	1	1	125.8	LS-Lidar	83.20	Avg 12/95 to 9/97	42.55
30N03W07P03	1082349	410875	CC	1	1	110.0	LS-Lidar	15.57	Avg 12/95 to 9/97	94.44
30N03W17D02	1086899	409785	CC	1	1	101.2	LS-Lidar	20.47	Avg 12/95 to 9/97	80.75
30N03W17M01	1086902	407057	CC	1	1	123.5	LS-Lidar	16.25	Avg 12/95 to 9/97	107.29
30N03W18A03	1085733	408882	CC	1	1	119.2	LS-Lidar	26.49	Avg 12/95 to 9/97	92.74
30N03W18F03	1083261	407839	CC	1	1	146.8	LS-Lidar	21.31	Avg 12/95 to 9/97	125.49
30N03W19D01	1080656	403545	CC	1	1	212.0	LS-Lidar	45.50	Avg 12/95 to 9/97	166.52
30N03W21A01	1096145	403814	CC	1	1	32.1	LS-Lidar	-0.59	Avg 12/95 to 9/97	32.71
30N03W28C03	1093908	398589	CC	1	1	169.3	LS-Lidar	96.52	Avg 12/95 to 9/97	72.77
30N03W28G02	1095130	397625	CC	1	1	246.6	LS-Lidar	56.87	Avg 12/95 to 9/97	189.72
30N03W31J02	1085360	390500	CC	1	1	592.2	LS-Lidar	25.43	Avg 12/95 to 9/97	566.79
30N04W01M03	1076626	417145	CC	1	1	75.7	LS-Lidar	13.67	Avg 12/95 to 9/97	62.04
30N04W02R01	1075090	416693	CC	1	1	80.7	LS-Lidar	11.27	Avg 12/95 to 9/97	69.38
30N04W03H03	1069443	419720	CC	1	1	90.4	LS-Lidar	24.76	Avg 12/95 to 9/97	65.65
30N04W04N01	1060233	416418	CC	1	1	127.7	LS-Lidar	31.19	Avg 12/95 to 9/97	96.52
30N04W07L01	1050431	412995	CC	1	1	159.9	LS-Lidar	61.83	Avg 12/95 to 9/97	98.10
30N04W08N01	1054897	411908	CC	1	1	182.0	LS-Lidar	52.28	Avg 12/95 to 9/97	129.74
30N04W10H01	1069737	414384	CC	1	1	103.3	LS-Lidar	0.39	Avg 12/95 to 9/97	102.92
30N04W11J01	1074735	411867	CC	1	1	126.1	LS-Lidar	17.15	Avg 12/95 to 9/97	109.00
30N04W12K01	1078972	412754	CC	1	1	108.5	LS-Lidar	6.99	Avg 12/95 to 9/97	101.46
30N04W14F05	1072047	408550	CC	1	1	158.7	LS-Lidar	23.46	Avg 12/95 to 9/97	135.22
30N04W14P01	1072588	406224	CC	1	1	186.1	LS-Lidar	19.40	Avg 12/95 to 9/97	166.70
30N04W14Q91	1073206	405456	CC	1	1	197.2	LS-Lidar	17.18	Avg 12/95 to 9/97	180.04
30N04W15A01	1070055	408558	CC	1	1	158.3	LS-Lidar	22.58	Avg 12/95 to 9/97	135.69
30N04W16G01	1062321	408120	CC	1	1	171.3	LS-Lidar	26.30	Avg 12/95 to 9/97	145.00
30N04W17B01	1057931	410766	CC	1	1	183.6	LS-Lidar	40.08	Avg 12/95 to 9/97	143.55
30N04W17P01	1055717	406054	CC	1	1	362.3	LS-Lidar	34.80	Avg 12/95 to 9/97	327.49
30N04W21G03	1062203	403649	CC	1	1	265.5	LS-Lidar	18.69	Avg 12/95 to 9/97	246.81
30N04W22C02	1066375	403996	CC	1	1	208.4	LS-Lidar	25.73	Avg 12/95 to 9/97	182.69
30N04W22J02	1069203	402153	CC	1	0.7	249.5	LS-Lidar	95.21	3/12/96	154.25
30N04W22R02	1068753	400273	CC	1	1	304.4	LS-Lidar	20.24	Avg 12/95 to 9/97	284.17
30N04W23L05	1072121	402235	CC	1	1	249.2	LS-Lidar	54.43	Avg 12/95 to 9/97	194.77
30N04W23Q04	1072627	400934	CC	1	1	268.2	LS-Lidar	33.51	Avg 12/95 to 9/97	234.71
30N04W24G02	1078931	402994	CC	1	1	236.7	LS-Lidar	55.11	Avg 12/95 to 9/97	181.61
30N04W25C01	1077102	398383	CC	1	0.7	322.3	LS-Lidar	58.50	12/95 - 1/96	263.83
30N04W25D03	1075276	398610	CC	1	1	323.6	LS-Lidar	45.10	Avg 12/95 to 9/97	278.47
30N04W26D02	1070276	398951	CC	1	1	353.0	LS-Lidar	94.55	Avg 12/95 to 9/97	258.49
30N04W26E03	1070371	398248	CC	1	1	373.0	LS-Lidar	113.62	Avg 12/95 to 9/97	259.42
30N04W26H02	1074578	398366	CC	1	1	291.8	LS-Lidar	19.88	Avg 12/95 to 9/97	271.92
30N04W34M04	1065602	391036	CC	1	1	680.8	LS-Lidar	1.47	Avg 12/95 to 9/97	679.33
30N05W20G01	1026694	404912	CC	1	1	512.5	LS-Lidar	88.66	Avg 12/95 to 9/97	423.84
30N05W23C02	1040693	404780	CC	1	1	466.8	LS-Lidar	90.48	Avg 12/95 to 9/97	376.30
30N05W26Q01	1041476	395514	USGS	1	1	843.7	LS-Lidar	111.46	Avg 12/95 to 9/97	732.26
31N03W31N01	1082429	421201	CC	1	1	33.9	LS-Lidar	12.17	Avg 12/95 to 9/97	21.74
31N04W35D01	1071321	425688	CC	1	1	79.4	LS-Lidar	69.60	Avg 12/95 to 9/97	9.80
31N04W35F01	1072987	423798	CC	1	1	108.8	LS-Lidar	91.95	Avg 12/95 to 9/97	16.85
31N04W36B06	1079551	425206	CC	1	1	21.7	LS-Lidar	13.30	Avg 12/95 to 9/97	8.37
Graysmarsh-1	1090609	415826	Graysmarsh	1	1	29.2	WH-Surveyed	9.07	4/98-4/99	20.13
Graysmarsh-2	1090873	416521	CC	1	1	24.5	LS-Lidar	6.10	3/97-3/98	18.39
Graysmarsh-4	1091796	416106	Graysmarsh	1	1	29.0	WH-Surveyed	18.84	3/97-3/98	10.16
Port_Williams_MW-1	1088325	407399	Sequim (C)	1	1	105.2	LS-Surveyed	9.78	1996-1997	95.41
30N03W16C01	1093451	409035	USGS	2	0.3	113.4	LS-Lidar (A)	(A)	3/22/79	37.40
30N03W17A01	1090018	409674	TTFW	2	0.3	128.6	LS-Lidar (A)	(A)	March '79	44.70
30N03W08M01	1087499	412149	CC	3	0.7	115.7	LS-Lidar	77.00	2/16/96	38.72
30N03W21K03	1094714	400686	CC	3	1	151.1	LS-Lidar	109.54	Avg 12/95 to 9/97	41.54
30N03W31R01	1083631	389595	CC	3	1	663.0	LS-Lidar	113.98	Avg 12/95 to 9/97	548.97
30N04W03L01	1066761	417383	CC	3	1	132.6	LS-Lidar	46.70	Avg 12/95 to 9/97	85.92
30N04W03Q01	1068073	416380	USGS	3	0.3	111.4	LS-Lidar (A)	(A)	3/21/79	100.40
30N04W07N01	1050010	411633	CC	3	1	171.3	LS-Lidar	96.47	Avg 12/95 to 9/97	74.87
30N04W23E03	1070204	403117	CC	3	0.3	244.1	LS-Lidar (A)	(A)	3/20/79	118.10
30N04W24R01	1080282	400341	CC	3	1	286.3	LS-Lidar	74.46	Avg 12/95 to 9/97	211.80
31N04W35E03	1071284	424140	CC	3	1	102.9	LS-Lidar	45.37	Avg 12/95 to 9/97	57.49
Graysmarsh-6	1096284	413800	Graysmarsh	3	0.1	18.9	WH-Surveyed (B)	(B)	(B)	28.86
Port_Williams_MW-3	1088325	407399	Sequim (C)	3	1	105.2	LS-Surveyed	43.75	1996-1997	61.44
30N03W08J03	1090593	411199	USGS	5	0.7	123.7	LS-Lidar	84.66	7/19/95	39.04
30N03W09R01	1095435	410342	CC	5	1	108.4	LS-Lidar	80.59	Avg 12/95 to 9/97	27.85
30N04W08F02	1057017	414713	CC	5	1	149.1	LS-Lidar	102.41	Avg 12/95 to 9/97	46.69
31N04W35N02	1070674	422224	CC	5	1	155.2	LS-Lidar	91.02	Avg 12/95 to 9/97	64.19
Port_Williams_PW-1	1088174	407364	Sequim	5	1	106.2	LS-Surveyed	61.77	1996-1997	44.41

**NOTES:**

- (A) - depth to water unknown, target is from Drost report in DATE
  - (B) - flowing well, depth to water unknown, assumed head 10 feet above land surface and assigned low weight.
  - (C) - coordinates for Sequim wells MW-1 and MW-3 are of control building nearby.
- X,Y sources include: CC = Clallam County, TTFW = Tetra-Tech Foster Wheeler (2003 Model)  
Lidar elevations from Puget Sound DEM (<http://www.ocean.washington.edu/data/pugetsound/psdem2005.html>)

**Table 5-2****Summary of Predicted Streamflow Seepage and Target Values for Steady State Calibration**

Stream	Model Seepage Gain (Dung-7e)	Model Seepage Gain (Dung-7g)	Target Range
Morse Creek	6.0	5.8	unknown
Bagley Creek	2.0	1.7	1 to 3
Siebert Creek	4.2	4.1	2 to 5
McDonald Creek	4.6	4.5	2 to 5
Matriotti Creek	0.2	0.1	8 to 10
Dungeness River	-19.6	-22.8	-12 to -15
Meadowbrook Creek	2.8	2.8	1 to 4
Cassalery Creek	1.8	2.0	2 to 4
Gierin Creek	0.6	0.6	0.9
Graysmarsh	6.6	6.0	6.5
Gierin + Graysmarsh	7.3	6.6	7.4
Bell Creek	2.3	2.4	2 to 3
Johnson Creek	1.1	1.0	0.5 to 1.5

Positive values indicate a net streamflow gain, negative values indicate a net streamflow loss.

Calibration values for Gierin Creek and Graysmarsh provided by Aspect Constultants (2008)

Calibration range for other small streams based on Small Streams Memorandum (PGG, 2008).

Calibration range for Dungeness River based on 2003 Model target (TTFW, 2003).

**Table 5-3**  
**Summary of Head Residuals from Steady State Calibration**

Name	X	Y	Layer	Weight	Observed	Dung-7e Computed	Dung-7e Residual	Dung-7e Weighted Residual	Dung-7g Computed	Dung-7g Residual	Dung-7g Weighted Residual
30N03W06M01	1082322	417058	1	1	42.55	42.02	0.53	0.53	41.07	1.48	1.48
30N03W07P03	1082349	410875	1	1	94.44	96.88	-2.44	-2.44	97.15	-2.71	-2.71
30N03W17D02	1086899	409785	1	1	80.75	87.87	-7.12	-7.12	87.27	-6.52	-6.52
30N03W17M01	1086902	407057	1	1	107.29	109.83	-2.54	-2.54	108.25	-0.96	-0.96
30N03W18A03	1085733	408882	1	1	92.74	97.50	-4.76	-4.76	96.53	-3.79	-3.79
30N03W18F03	1083261	407839	1	1	125.49	111.08	14.41	14.41	110.47	15.02	15.02
30N03W19D01	1080656	403545	1	1	166.52	165.88	0.64	0.64	164.32	2.20	2.20
30N03W21A01	1096145	403814	1	1	32.71	39.97	-7.26	-7.26	39.14	-6.43	-6.43
30N03W28C03	1093908	398589	1	1	72.77	128.96	-56.19	-56.19	111.37	-38.60	-38.60
30N03W28G02	1095130	397625	1	1	189.72	139.62	50.10	50.10	121.06	68.66	68.66
30N03W31J02	1085360	390500	1	1	566.79	557.23	9.56	9.56	530.61	36.18	36.18
30N04W01M03	1076626	417145	1	1	62.04	60.59	1.45	1.45	60.47	1.57	1.57
30N04W02R01	1075090	416693	1	1	69.38	68.45	0.93	0.93	68.38	1.00	1.00
30N04W03H03	1069443	419720	1	1	65.65	62.66	2.99	2.99	62.11	3.54	3.54
30N04W04N01	1060233	416418	1	1	96.52	88.23	8.29	8.29	86.27	10.25	10.25
30N04W07L01	1050431	412995	1	1	98.10	107.52	-9.42	-9.42	107.54	-9.44	-9.44
30N04W08N01	1054897	411908	1	1	129.74	128.35	1.39	1.39	128.42	1.32	1.32
30N04W10H01	1069737	414384	1	1	102.92	103.74	-0.82	-0.82	102.90	0.02	0.02
30N04W11J01	1074735	411867	1	1	109.00	109.05	-0.05	-0.05	109.02	-0.02	-0.02
30N04W12K01	1078972	412754	1	1	101.46	95.46	6.00	6.00	97.04	4.42	4.42
30N04W14F05	1072047	408550	1	1	135.22	135.14	0.08	0.08	134.59	0.63	0.63
30N04W14P01	1072588	406224	1	1	166.70	167.86	-1.16	-1.16	167.39	-0.69	-0.69
30N04W14Q91	1073206	405456	1	1	180.04	183.47	-3.43	-3.43	183.07	-3.03	-3.03
30N04W15A01	1070055	408558	1	1	135.69	137.33	-1.64	-1.64	136.43	-0.74	-0.74
30N04W16G01	1062321	408120	1	1	145.00	139.58	5.42	5.42	140.68	4.32	4.32
30N04W17B01	1057931	410766	1	1	143.55	144.17	-0.62	-0.62	142.24	1.31	1.31
30N04W17P01	1055717	406054	1	1	327.49	302.42	25.07	25.07	303.94	23.55	23.55
30N04W21G03	1062203	403649	1	1	246.81	247.87	-1.06	-1.06	243.29	3.52	3.52
30N04W22C02	1066375	403996	1	1	182.69	178.12	4.57	4.57	176.06	6.63	6.63
30N04W22J02	1069203	402153	1	0.7	154.25	196.60	-42.35	-29.64	195.56	-41.31	-28.91
30N04W22R02	1068753	400273	1	1	284.17	231.81	52.36	52.36	232.64	51.53	51.53
30N04W23L05	1072121	402235	1	1	194.77	215.98	-21.21	-21.21	215.46	-20.69	-20.69
30N04W23Q04	1072627	400934	1	1	234.71	238.01	-3.30	-3.30	237.67	-2.96	-2.96
30N04W24G02	1078931	402994	1	1	181.61	184.63	-3.02	-3.02	182.94	-1.33	-1.33
30N04W25C01	1077102	398383	1	0.7	263.83	272.87	-9.04	-6.33	268.89	-5.06	-3.54
30N04W25D03	1075276	398610	1	1	278.47	276.51	1.96	1.96	274.57	3.90	3.90
30N04W26D02	1070276	398951	1	1	258.49	247.35	11.14	11.14	246.89	11.60	11.60
30N04W26E03	1070371	398248	1	1	259.42	259.28	0.14	0.14	258.97	0.45	0.45
30N04W26H02	1074578	398366	1	1	271.92	278.63	-6.71	-6.71	277.62	-5.70	-5.70
30N04W34M04	1065602	391036	1	1	679.33	648.19	31.14	31.14	648.19	31.14	31.14
30N05W20G01	1026694	404912	1	1	423.84	403.67	20.17	20.17	394.46	29.38	29.38
30N05W23C02	1040693	404780	1	1	376.30	393.00	-16.70	-16.70	390.74	-14.44	-14.44
30N05W26Q01	1041476	395514	1	1	732.26	677.38	54.88	54.88	676.70	55.56	55.56
31N03W31N01	1082429	421201	1	1	21.74	24.25	-2.51	-2.51	24.10	-2.36	-2.36
31N04W35D01	1071321	425688	1	1	9.80	16.14	-6.34	-6.34	16.14	-6.34	-6.34
31N04W35F01	1072987	423798	1	1	16.85	27.99	-11.14	-11.14	27.94	-11.09	-11.09
31N04W36B06	1079551	425206	1	1	8.37	14.39	-6.02	-6.02	14.41	-6.04	-6.04
Graysmarsh-1	1090609	415826	1	1	20.13	20.97	-0.84	-0.84	21.77	-1.64	-1.64
Graysmarsh-2	1090873	416521	1	1	18.39	17.28	1.11	1.11	17.75	0.64	0.64
Graysmarsh-4	1091796	416106	1	1	10.16	12.87	-2.71	-2.71	13.23	-3.07	-3.07
Port_Williams_MW-1	1088325	407399	1	1	95.41	97.89	-2.48	-2.48	97.26	-1.85	-1.85
30N03W16C01	1093451	409035	2	0.3	37.40	49.70	-12.30	-3.69	52.13	-14.73	-4.42
30N03W17A01	1090018	409674	2	0.3	44.70	64.79	-20.09	-6.03	69.48	-24.78	-7.43
30N03W08M01	1087499	412149	3	0.7	38.72	59.75	-21.03	-14.72	67.57	-28.85	-20.20
30N03W21K03	1094714	400686	3	1	41.54	49.60	-8.06	-8.06	58.34	-16.80	-16.80
30N03W31R01	1083631	389595	3	1	548.97	483.67	65.30	65.30	502.76	46.21	46.21
30N04W03L01	1066761	417383	3	1	85.92	68.32	17.60	17.60	80.79	5.13	5.13
30N04W03Q01	1068073	416380	3	0.3	100.40	73.17	27.23	8.17	87.15	13.25	3.98
30N04W07N01	1050010	411633	3	1	74.87	78.73	-3.86	-3.86	119.54	-44.67	-44.67
30N04W23E03	1070204	403117	3	0.3	118.10	151.92	-33.82	-10.15	189.62	-71.52	-21.46
30N04W24R01	1080282	400341	3	1	211.80	163.12	48.68	48.68	208.92	2.88	2.88
31N04W35E03	1071284	424140	3	1	57.49	38.66	18.83	18.83	31.63	25.86	25.86
Graysmarsh-6	1096284	413800	3	0.1	28.86	35.03	-6.17	-0.62	22.89	5.97	0.60
Port_Williams_MW-3	1088325	407399	3	1	61.44	74.25	-12.81	-12.81	88.43	-26.99	-26.99
30N03W08J03	1090593	411199	5	0.7	39.04	42.69	-3.65	-2.56	45.29	-6.25	-4.38
30N03W09R01	1095435	410342	5	1	27.85	39.97	-12.12	-12.12	41.14	-13.29	-13.29
30N04W08F02	1057017	414713	5	1	46.69	41.42	5.27	5.27	46.48	0.21	0.21
31N04W35N02	1070674	422224	5	1	64.19	37.52	26.67	26.67	40.18	24.01	24.01
Port_Williams_PW-1	1088174	407364	5	1	44.41	46.35	-1.94	-1.94	51.08	-6.67	-6.67
Residual Mean							2.10	2.91		0.61	1.88
Res. Std. Dev.							20.22	18.84		21.78	19.25
Sum of Squares							28523	25076		32755	25821
L1 Sum of Squares							17158	16595		19083	18564
L3 Sum of Squares							9908	8421		12003	8018
L5 Sum of Squares							903	899		837	825
Abs. Res. Mean							12.79	11.43		13.69	12.00
Min. Residual							-56.19	-56.19		-71.52	-44.67
Max. Residual							65.30	65.30		68.66	68.66
Range in Target Values							723.89	723.89		723.89	723.89
Std. Dev./Range							2.8%	2.6%		3.0%	2.7%



**Table 5-4**  
**Steady State Model Mass Balance Summary**  
 (Net model inflow in cfs)

	Dung-7e	Dung-7g
Recharge	91.42	91.42
ET	-1.19	-1.21
Marine Discharge (Constant Head)	-88.40	-92.70
Rivers	9.46	12.86
- <i>Dungeness River</i>	19.62	22.80
- <i>Morse Creek</i>	-5.99	-5.83
- <i>Siebert Creek</i>	-4.17	-4.10
Drains	-22.05	-21.12
- <i>Bagley Creek</i>	-2.04	-1.67
- <i>McDonald Creek</i>	-4.56	-4.55
- <i>Matriotti Creek</i>	-0.21	-0.11
- <i>Meadowbrook Creek</i>	-2.76	-2.80
- <i>Cassalery Creek</i>	-1.84	-2.01
- <i>Gierin Creek</i>	-0.65	-0.57
- <i>Graysmarsh</i>	-6.61	-6.03
- <i>Bell Creek</i>	-2.29	-2.36
- <i>Johnson Creek</i>	-1.09	-1.01
Bedrock Inflow from GHB	1.38	1.38
Bedrock Inflow from Injection Wells	16.63	16.63
Well Withdrawals	-7.34	-7.34
Total Mass Balance Error	0.07%	0.06%

Total mass balance error calculated as sum of all terms over sum of net inflow.

**Table 6-1**  
**Summary of Transient Calibration Targets**

Target	Row	Column	Layer	Number of Data Points	Head Range (ft)	Fist Point (Days into Calibration)
29N/04W-01M01	55	49	1	18	8.12	6
30N/03W-04L03	27	69	1	1	0.00	459
30N/03W-05R01	28	67	1	6	2.54	7
30N/03W-05R3	28	67	1	1	0.00	459
30N/03W-05R4	28	67	1	1	0.00	459
30N/03W-06M01	26	58	1	20	2.28	10
30N/03W-07P03	35	60	1	20	4.03	10
30N/03W-17D02	37	64	1	7	2.09	7
30N/03W-18A03	37	63	1	19	2.98	11
30N/03W-18F03	38	60	1	5	1.41	10
30N/03W-19D01	41	57	1	17	7.27	10
30N/03W-21A01	41	71	1	16	4.63	102
30N/03W-28C03	45	68	1	17	5.96	67
30N/03W-31J02	51	62	1	18	1.33	10
30N/04W-01M03	26	50	1	17	1.30	6
30N/04W-02R01	28	48	1	7	7.42	7
30N/04W-03H03	24	40	1	7	1.43	7
30N/04W-03L01	25	38	1	16	12.21	104
30N/04W-04N01	27	33	1	19	3.78	10
30N/04W-07L01	32	26	1	7	0.68	7
30N/04W-08N01	34	29	1	7	1.81	412
30N/04W-10H01	31	40	1	17	1.04	10
30N/04W-11J01	33	48	1	7	1.43	7
30N/04W-12K01	34	54	1	19	9.82	10
30N/04W-14F05	37	44	1	19	8.05	6
30N/04W-14P01	39	43	1	19	2.76	6
30N/04W-14Q91	39	45	1	19	2.89	6
30N/04W-15A01	36	40	1	18	3.03	6
30N/04W-16G01	37	34	1	11	2.15	6
30N/04W-17B01	36	30	1	19	5.05	6
30N/04W-17P02	39	29	1	1	0.00	103
30N/04W-21G03	41	34	1	19	2.24	6
30N/04W-22C02	40	37	1	1	0.00	102
30N/04W-22R02	43	40	1	19	4.61	6
30N/04W-23Q04	44	45	1	17	2.81	6
30N/04W-24G02	42	53	1	20	60.35	10
30N/04W-25D03	45	49	1	19	12.22	6
30N/04W-26D02	44	41	1	4	1.68	10
30N/04W-26E03	45	41	1	6	4.10	10
30N/04W-26H02	46	47	1	19	4.46	6
30N/04W-34M04	50	36	1	18	1.88	67
30N/05W-20G01	40	7	1	15	5.39	104
30N/05W-23C02	40	18	1	17	5.19	104
30N/05W-26Q01	47	18	1	17	1.47	39
31N/03W-31N01	21	59	1	1	0.00	103
31N/04W-35D01	18	42	1	20	2.32	10
31N/04W-35F01	19	44	1	1	0.00	121
31N/04W-36B06	18	55	1	18	1.59	67
30N/04W-29B01	44	30	2	17	7.68	67
30N/03W-21K03	43	69	3	5	9.84	10
30N/03W-31R01	52	62	3	18	3.61	6
30N/04W-07N01	34	25	3	7	2.01	11
30N/04W-24R01	44	55	3	20	3.52	10
31N/04W-35E03	19	42	3	14	1.66	67
30N/03W-09R01	36	71	5	16	15.64	67
30N/04W-08F02	31	30	5	17	3.98	108
31N/04W-35N02	21	42	5	17	17.81	67

Note: head range may include some pumping or recovering water level measurements.

**Table 7-1**  
**Summary of Model AR Predictions and Sensitivity Analyses**

RUN NAME	BASE MODEL	Steady State or Transient	SITE	Q <sub>AR</sub> (cfs)	AR Period (mos)	Sy	Site Distance to River	Site Kh Zone (ft/d)	Description	AR Cell Maximum Head Rise (ft)	Average Dungeness River Augmentation (% of V <sub>AR</sub> )	Average Dungeness River Augmentation (% of Q <sub>AR</sub> )	Range of Dungeness River Augmentation (% of Q <sub>AR</sub> )
P1-SSa	Dung-7e	SS	1	2	12	n/a	1300	100	"Dung-7e", Steady State	12.9	97%	97%	n/a
P1a	Dung-7e	T	1	2	2	0.2	1300	100	"Dung-7e" with Sy=0.2, Q=2	10.8	96%	16%	66%
P1b	Dung-7e	T	1	2	2	0.1	1300	100	"Dung-7e" with Sy=0.1, Q=2	11.6	97%	16%	78%
P2-SSa	Dung-7e	SS	2	2	12	n/a	3500	15	"Dung-7e", Steady State	27.8	64%	64%	n/a
P2a	Dung-7e	T	2	2	2	0.2	3500	15	"Dung-7e" with Sy=0.2, Q=2	14.5	65%	11%	4%
P2b	Dung-7e	T	2	10	2	0.2	3500	15	"Dung-7e" with Sy=0.2, Q=10	72.5	65%	11%	4%
P2c	Dung-7e	T	2	2	2	0.1	3500	15	"Dung-7e" with Sy=0.1, Q=2	17.1	65%	11%	11%
P2d	Dung-7e	T	2	10	2	0.1	3500	15	"Dung-7e" with Sy=0.1, Q=10	82.3	64%	11%	11%
P2e	Dung-7g	T	2	2	2	0.2	3500	15	Sensitivity w/L2 Kz 10x ("Dung-7g"), Q=2	14.3	65%	11%	4%
P2f	Dung-7e	T	2	2	2	0.2	3500	15	Sensitivity w/ L1 Kh 2x, Q=2	8.1	69%	12%	4%
P2g	Dung-7e	T	2	2	2	0.2	3500	15	Sensitivity w/ L1 Kh 0.5x, Q=2	21.0	63%	11%	2%
P3-SSa	Dung-7e	SS	3	2	12	n/a	5400	400	"Dung-7e", Steady State	5.5	81%	81%	n/a
P3-SSb	Dung-7g	SS	3	2	12	n/a	5400	400	Sensitivity w/ L2 Kz 10x ("Dung-7g")	5.5	83%	83%	n/a
P3-SSc	Dung-7e	SS	3	2	12	n/a	5400	400	Sensitivity w/ L1 Kh 2x	3.1	84%	84%	n/a
P3-SSd	Dung-7e	SS	3	2	12	n/a	5400	400	Sensitivity w/ L1 Kh 0.5x	9.1	69%	69%	n/a
P3-Sse	Dung-7e	SS	3	2	12	n/a	5400	400	Sensitivity w/ L2 Kz 0.1x	5.5	80%	80%	n/a
P3-SSf	Dung-7f	SS	3	2	12	n/a	5400	400	Sensitivity w/ Riv Ks 3x (30 ft/d)	5.4	83%	83%	n/a
P3a	Dung-7e	T	3	2	2	0.2	5400	400	"Dung-7e" with Sy=0.2, Q=2	3.8	81%	14%	13%
P3b	Dung-7e	T	3	2	2	0.1	5400	400	"Dung-7e" with Sy=0.1, Q=2	4.3	81%	14%	27%
P4-SSa	Dung-7e	SS	4	2	12	n/a	1500	400	"Dung-7e", Steady State	1.9	88%	88%	n/a
P4a	Dung-7e	T	4	2	2	0.2	1500	400	"Dung-7e" with Sy=0.2, Q=2	1.6	88%	15%	58%
P4b	Dung-7e	T	4	10	2	0.2	1500	400	"Dung-7e" with Sy=0.2, Q=10	7.6	88%	15%	58%
P4c	Dung-7e	T	4	2	2	0.1	1500	400	"Dung-7e" with Sy=0.1, Q=2	1.6	88%	15%	67%
P4d	Dung-7e	T	4	10	2	0.1	1500	400	"Dung-7e" with Sy=0.1, Q=10	8.0	88%	15%	67%
P4e	Dung-7g	T	4	2	2	0.2	1500	400	Sensitivity w/L2 Kz 10x ("Dung-7g"), Q=2	1.6	89%	15%	58%
P4f	Dung-7e	T	4	2	2	0.2	1500	400	Sensitivity w/ L1 Kh 2x, Q=2	0.9	86%	14%	52%
P4g	Dung-7e	T	4	2	2	0.2	1500	400	Sensitivity w/ L1 Kh 0.5x, Q=2	2.7	86%	14%	53%
P5-SSa	Dung-7e	SS	5	2	12	n/a	7200	400	"Dung-7e", Steady State	3.6	66%	66%	n/a
P5a	Dung-7e	T	5	2	2	0.2	7200	400	"Dung-7e" with Sy=0.2, Q=2	2.2	68%	11%	10%
P5b	Dung-7e	T	5	2	2	0.1	7200	400	"Dung-7e" with Sy=0.1, Q=2	2.5	68%	11%	20%
P6-SSa	Dung-7e	SS	6	2	12	n/a	2900	15	"Dung-7e", Steady State	26.2	62%	62%	n/a
P6a	Dung-7e	T	6	2	2	0.2	2900	15	"Dung-7e" with Sy=0.2, Q=2	16.0	63%	11%	9%
P6b	Dung-7e	T	6	2	2	0.1	2900	15	"Dung-7e" with Sy=0.1, Q=2	19.5	63%	11%	19%
P7-SSa	Dung-7e	SS	7	2	12	n/a	7600	100	"Dung-7e", Steady State	14.3	28%	28%	n/a
P8-SSa	Dung-7e	SS	8	2	12	n/a	1250	100	"Dung-7e", Steady State	4.0	97%	97%	n/a
P8a	Dung-7e	T	8	2	2	0.2	1250	100	"Dung-7e" with Sy=0.2, Q=2	2.8	96%	16%	69%
P8b	Dung-7e	T	8	2	2	0.1	1250	100	"Dung-7e" with Sy=0.1, Q=2	3.0	97%	16%	78%
P9-SSa	Dung-7e	SS	W Ditch	3	12	n/a	~4000	400	"Dung-7e", Steady State	2.7	78%	13%	n/a
P9a	Dung-7e	T	W Ditch	3	2	0.2	~4000	400	"Dung-7e" with Sy=0.2, Q=2	1.5	78%	13%	29%
P9b	Dung-7e	T	W Ditch	3	2	0.1	~4000	400	"Dung-7e" with Sy=0.1, Q=2	1.8	79%	13%	42%
P10-SSa	Dung-7e	SS	E Ditch	3	12	n/a	varies	100/250	"Dung-7e", Steady State	9.0	30%	30%	n/a
P10a	Dung-7e	T	E Ditch	3	2	0.2	varies	100/250	"Dung-7e" with Sy=0.2, Q=2	3.2	32%	5%	2%
P10b	Dung-7e	T	E Ditch	3	2	0.1	varies	100/250	"Dung-7e" with Sy=0.1, Q=2	4.1	32%	5%	5%

**NOTES:**

Sy = Specific Yield, Kh = horizontal hydraulic conductivity, Q<sub>AR</sub> = rate of AR, V<sub>AR</sub> = annual volume of AR, Range of Q<sub>AR</sub> = maximum minimum minimum Q<sub>AR</sub>  
Tributary inflow (i.e. Matriotti Creek) is not included in Dungeness River augmentation.

**Table 7-2**  
**Distribution of Flow Augmentation Among Modeled Streams from Steady State Aquifer Recharge at 2 cfs**

SITE:	1	2	3	3	3	3	3	3	4	5	6	7	8	9	10
MODEL ROW,COLUMN:	48,50	44,52	42,39	42,39	42,39	42,39	42,39	42,39	37,44	36,37	41,52	43,58	45,44	n/a	n/a
RUN ID:	P1-SSa	P2-SSa	P3-SSa	P3-SSb	P3-SSc	P3-SSd	P3-SSe	P3-SSF	P4-SSa	P5-SSa	P6-SSa	P7-SSa	P8-Ssa	West Ditch	East Ditch
BASE MODEL:	Dung-7e	Dung-7e	Dung-7e	Dung-7g	Dung-7e	Dung-7e	Dung-7e	Dung-7h	Dung-7e	Dung-7e	Dung-7e	Dung-7e	Dung-7e	Dung-7e	Dung-7e
STREAM \ SENSITIVITY:	-	-	-	-	L1 Kh 2x	L1 Kh 0.5x	L2 Kz' 0.1x	Riv Ks 3x	-	-	-	-	-	-	-
Dungeness	96.5%	64.5%	81.1%	82.8%	84.0%	69.3%	80.4%	83.2%	88.1%	66.3%	62.4%	28.2%	96.6%	77.9%	29.6%
Morse	0.0%	0.0%	0.0%	0.0%	0.0%	0.0%	0.0%	0.0%	0.0%	0.0%	0.0%	0.0%	0.0%	0.0%	0.0%
Siebert	0.0%	0.0%	0.0%	0.0%	0.0%	0.1%	0.0%	0.0%	0.0%	0.0%	0.0%	0.0%	0.0%	0.0%	0.0%
Bagley	0.0%	0.0%	0.0%	0.0%	0.0%	0.0%	0.0%	0.0%	0.0%	0.0%	0.0%	0.0%	0.0%	0.0%	0.0%
McDonald	0.0%	0.0%	0.7%	0.8%	0.1%	1.7%	0.8%	0.7%	0.3%	1.3%	0.0%	0.0%	0.1%	0.7%	0.0%
Matriotti*	0.0%	0.1%	5.4%	2.8%	<b>DRY</b>	17.4%	6.8%	5.0%	3.7%	10.8%	0.2%	0.1%	0.8%	7.2%	0.1%
Meadowbrook	0.0%	0.1%	0.1%	0.1%	0.3%	0.1%	0.1%	0.0%	0.1%	0.2%	0.2%	0.2%	0.0%	0.2%	0.2%
Cassalery	0.9%	10.9%	0.4%	0.7%	0.2%	0.3%	0.4%	0.2%	0.4%	0.4%	15.3%	21.7%	0.1%	0.4%	26.3%
Gierin Creek	1.4%	15.0%	0.2%	0.2%	<b>DRY</b>	0.1%	0.1%	0.0%	0.1%	0.1%	12.4%	34.1%	0.1%	0.1%	29.7%
Graysmarsh	0.3%	3.7%	0.1%	0.1%	0.4%	0.0%	0.0%	0.1%	0.1%	0.1%	4.1%	6.7%	0.0%	0.1%	6.9%
Bell*	0.2%	1.9%	0.0%	0.0%	0.1%	0.1%	0.0%	0.0%	0.0%	0.0%	1.3%	4.3%	0.0%	0.0%	2.8%
Johnson	0.0%	0.0%	0.0%	0.0%	0.0%	0.0%	0.0%	0.0%	0.0%	0.0%	0.0%	0.0%	0.0%	0.0%	0.0%
Total to Streams	99.4%	96.1%	88.0%	87.4%	85.0%	89.1%	88.7%	89.3%	92.7%	79.3%	95.9%	95.4%	97.9%	86.6%	95.6%

**NOTES:**

Portion of augmentation  $Q_{AR}$  not discharged to streams is discharged to marine waters.

\* Model may not properly simulate the hydraulic connection between the shallow aquifer system and this stream.

Sensitivity analyses where L1 Kh is multiplied by 2x and 0.5x are not calibrated, and show significant departures from model calibration targets.

Transient simulations show relatively constant rates of augmentation to small streams.

Tributary inflow (i.e. Matriotti Creek) is not included in Dungeness River augmentation.

**Table 7-3****Maximum Head Rise Observed in Model Layers for Steady State AR Simulations**

(Values in cfs and feet)

SITE	RUN	AR LAYER	Q <sub>AR</sub>	MODEL RUN DESCRIPTION	LAYER 1	LAYER 3	LAYER 5
1	P1-SSa	1	2	"Dung-7e"	<b>12.9</b>	0.8	0.1
2	P2-SSa	1	2	"Dung-7e"	<b>27.8</b>	1.6	0.3
3	P3-SSa	1	2	"Dung-7e"	<b>5.5</b>	1.0	0.2
3	P3-SSb	1	2	"Dung-7g", Sensitivity: L2 Kz' 10x	<b>5.5</b>	2.5	0.3
3	P3-SSc	1	2	Sensitivity: L1 Kh 2x	<b>3.1</b>	0.7	0.2
3	P3-SSd	1	2	Sensitivity: L1 Kh 0.5x	<b>9.1</b>	NC	NC
3	P3-SSe	1	2	Sensitivity: L2 Kz' 0.1x	<b>5.5</b>	NC	NC
3	P3-SSf	1	2	"Dung-7h", Sensitivity: Riv Ks 3x	<b>5.4</b>	1.0	0.2
4	P4-SSa	1	2	"Dung-7e"	<b>1.9</b>	0.3	0.1
5	P5-SSa	1	2	"Dung-7e"	<b>3.6</b>	0.7	0.2
6	P6-SSa	1	2	"Dung-7e"	<b>26.2</b>	1.1	0.2
7	P7-SSa	1	2	"Dung-7e"	<b>14.3</b>	1.2	0.3
8	P8-Ssa	1	2	"Dung-7e"	<b>4.0</b>	0.4	0.1
9	West Ditch	1	3	"Dung-7e"	<b>2.7</b>	0.7	0.2
10	East Ditch	1	3	"Dung-7e"	<b>9.0</b>	1.3	0.3
ASR East	E-5-7e	5	2	"Dung-7e", East Side, Deep Aquifer	0.7	6.2	<b>39.1</b>
ASR East	E-3-7e	3	2	"Dung-7e", East Side, Middle Aquifer	1.6	<b>53.8</b>	7.2
ASR West	W-5-7e	5	2	"Dung-7e", West Side, Deep Aquifer	0.4	5.1	<b>40.5</b>
ASR West	W-3-7e	3	2	"Dung-7e", West Side, Middle Aquifer	1.3	<b>66.5</b>	5.2
ASR East	E-3-7g	3	2	"Dung-7g", Higher L2 Kz, East Side, Middle Aquifer	1.8	<b>25.6</b>	1.4
ASR West	W-3-7g	3	2	"Dung-7g", Higher L2 Kz, West Side, Middle Aquifer	1.8	<b>32.8</b>	1.1

## NOTES:

All simulations were run in steady state with AR inflow into the model at specified site (see Figure 1-1 for sites)

Q<sub>AR</sub> = rate of AR***Bold Italics*** indicates the model layer to which AR was applied.

NC = not calculated during model results analysis.

**Table 7-4**  
**Summary of Model ASR Predictions**

RUN NAME	BASE MODEL	Transient or Steady State	SITE	ASR Layer	Sy	Description	AR Cell Maximum Head Rise (ft)	Stream 1: Net % V <sub>AR</sub> (or) Max % Q <sub>ASR</sub> , Min % Q <sub>ASR</sub>	Stream 2: Net % V <sub>AR</sub> (or) Max % Q <sub>ASR</sub> , Min % Q <sub>ASR</sub>	Stream 3: Net % V <sub>AR</sub> (or) Max % Q <sub>ASR</sub> , Min % Q <sub>ASR</sub>	Stream 4: Net % V <sub>AR</sub> (or) Max % Q <sub>ASR</sub> , Min % Q <sub>ASR</sub>
E-5-7e	Dung-7e	SS	East	5	n/a	"Dung-7e", Steady State, Lower Aquifer	39.1	Dungeness: Net % V <sub>AR</sub> = 15.4%	Cassalery: Net % V <sub>AR</sub> = 3.4%	Gierin: Net % V <sub>AR</sub> = 3.2%	All Small Streams <  2%
P-E-5a	Dung-7e	Tran	East	5	0.2	"Dung-7e", Sy=0.2, Lower Aquifer	31.9	Dungeness: 1.9%, -1.0%	All Small Streams <  2%	All Small Streams <  2%	All Small Streams <  2%
P-E-5b	Dung-7e	Tran	East	5	0.1	"Dung-7e", Sy=0.1, Lower Aquifer	31.9	Dungeness: 3.2%, -1.8%	All Small Streams <  2%	All Small Streams <  2%	All Small Streams <  2%
E-3-7e	Dung-7e	SS	East	3	n/a	"Dung-7e", Steady State, Middle Aquifer	53.8	Dungeness: Net % V <sub>AR</sub> = 21.5%	Gierin: Net % V <sub>AR</sub> = 10.6%	Cassalery: Net % V <sub>AR</sub> = 10.3%	Bell: Net % V <sub>AR</sub> = 4.3%
P-E-3a	Dung-7e	Tran	East	3	0.2	"Dung-7e", Sy=0.2, Middle Aquifer	39.6	Dungeness: 3.2%, -1.8%	Gierin: 1.7%, -1.0%	All Small Streams <  2%	All Small Streams <  2%
P-E-3b	Dung-7e	Tran	East	3	0.1	"Dung-7e", Sy=0.1, Middle Aquifer	49.7	Dungeness: 5.0%, -2.9%, -0.0%	Gierin: 2.6%, -1.6%	Cassalery: 2.7%, -1.4%	All Small Streams <  2%
E-3-7g	Dung-7g	SS	East	3	n/a	Higher L2 Kz Model ("Dung-7g"), Steady State, Middle Aquifer	25.6	Dungeness: Net % V <sub>AR</sub> = 17.6%	Cassalery: Net % V <sub>AR</sub> = 28.9%	Gierin: Net % V <sub>AR</sub> = 20.3%	Bell: Net % V <sub>AR</sub> = 6.8%
P-E-3c	Dung-7g	Tran	East	3	0.2	Higher L2 Kz Model ("Dung-7g"), Sy=0.2, Middle Aquifer	24.2	Dungeness: 2.1%, -0.8%	Gierin: 5.5%, -4.1%	Cassalery: 5.5%, -2.5%	All Small Streams <  2%
P-E-3d	Dung-7g	Tran	East	3	0.1	Higher L2 Kz Model ("Dung-7g"), Sy=0.1, Middle Aquifer	24.3	Dungeness: 3.7%, -1.6%	Cassalery: 11.0%, -5.0%	Gierin: 7.7%, -5.7%	Bell: 3.8%, -1.5%
W-5-7e	Dung-7e	SS	West	5	n/a	"Dung-7e", Steady State, Lower Aquifer	40.5	Dungeness: Net % V <sub>AR</sub> = 17.9%	Gierin: Net % V <sub>AR</sub> = 2.0%	Cassalery: Net % V <sub>AR</sub> = 2.4%	All Small Streams <  2%
P-W-5a	Dung-7e	Tran	West	5	0.2	"Dung-7e", Sy=0.2, Lower Aquifer	34.7	Dungeness: 2.5%, -1.3%	All Small Streams <  2%	All Small Streams <  2%	All Small Streams <  2%
P-W-5b	Dung-7e	Tran	West	5	0.1	"Dung-7e", Sy=0.1, Lower Aquifer	34.7	Dungeness: 3.6%, -1.9%	All Small Streams <  2%	All Small Streams <  2%	All Small Streams <  2%
W-3-7e	Dung-7e	SS	West	3	n/a	"Dung-7e", Steady State, Lower Aquifer	66.5	Dungeness: Net % V <sub>AR</sub> = 44.8%	Matriotti: Net % V <sub>AR</sub> = 3.1%	Cassalery: Net % V <sub>AR</sub> = 2.2%	Gierin: Net % V <sub>AR</sub> = 1.5%
P-W-3a	Dung-7e	Tran	West	3	0.2	"Dung-7e", Sy=0.2, Lower Aquifer	61.3	Dungeness: 9.4%, -6.0%	All Small Streams <  2%	All Small Streams <  2%	All Small Streams <  2%
P-W-3b	Dung-7e	Tran	West	3	0.1	"Dung-7e", Sy=0.1, Lower Aquifer	61.4	Dungeness: 14.0%, -9.5%	All Small Streams <  2%	All Small Streams <  2%	All Small Streams <  2%
W-3-7g	Dung-7g	SS	West	3	n/a	Higher L2 Kz Model ("Dung-7g"), Steady State, Middle Aquifer	32.8	Dungeness: Net % V <sub>AR</sub> = 70.0%	Matriotti: Net % V <sub>AR</sub> = 3.3%	McDonald: Net % V <sub>AR</sub> = 2.1%	All Small Streams <  2%
P-W-3c	Dung-7g	Tran	West	3	0.2	Higher L2 Kz Model ("Dung-7g"), Sy=0.2, Middle Aquifer	30.2	Dungeness: 17.2%, -10.9%	All Small Streams <  2%	All Small Streams <  2%	All Small Streams <  2%
P-W-3d	Dung-7g	Tran	West	3	0.1	Higher L2 Kz Model ("Dung-7g"), Sy=0.1, Middle Aquifer	30.3	Dungeness: 27.1%, -19.4%	All Small Streams <  2%	All Small Streams <  2%	All Small Streams <  2%

**Notes:**

Model cells for site locations: East - Row 38 Column 63; West - Row 37 Column 39.

Values reported as % Q<sub>ASR</sub> unless otherwise indicated. Positive values indicate flow augmentation, negative values indicate depletion.

Streamflow augmentation reported for the 4 most affected streams in decreasing order. Impacts reported only for those streams with >|2%| augmentation/depletion.

Steady state simulations were run for sensitivity analysis to identify most affected streams using year-round injection with no recovery. Results reported as percent of annual injection volume (V) resulting in streamflow augmentation.

Transient simulations include 2 months injection (@ 2 cfs), one month dormancy, and 2 months recovery (@ 2 cfs). Results reported as max and min streamflow impact relative to rate of ASR (Q<sub>ASR</sub>) - e.g. "Max/Min % Q<sub>ASR</sub>".

Sy = Specific Yield, Storativity (S) was always 0.0002.

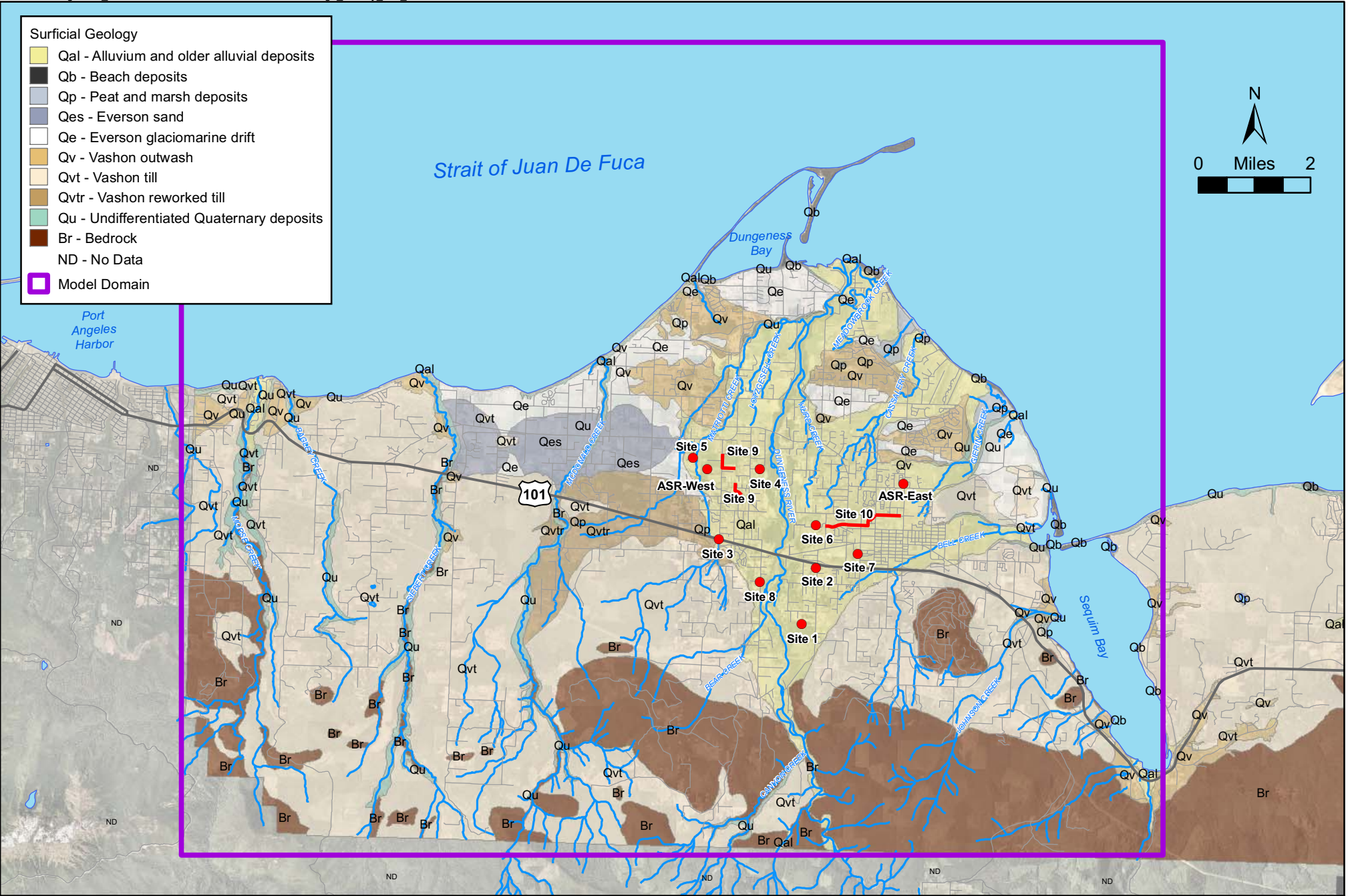


Figure 1-1 Vicinity Map and AR/ASR Sites

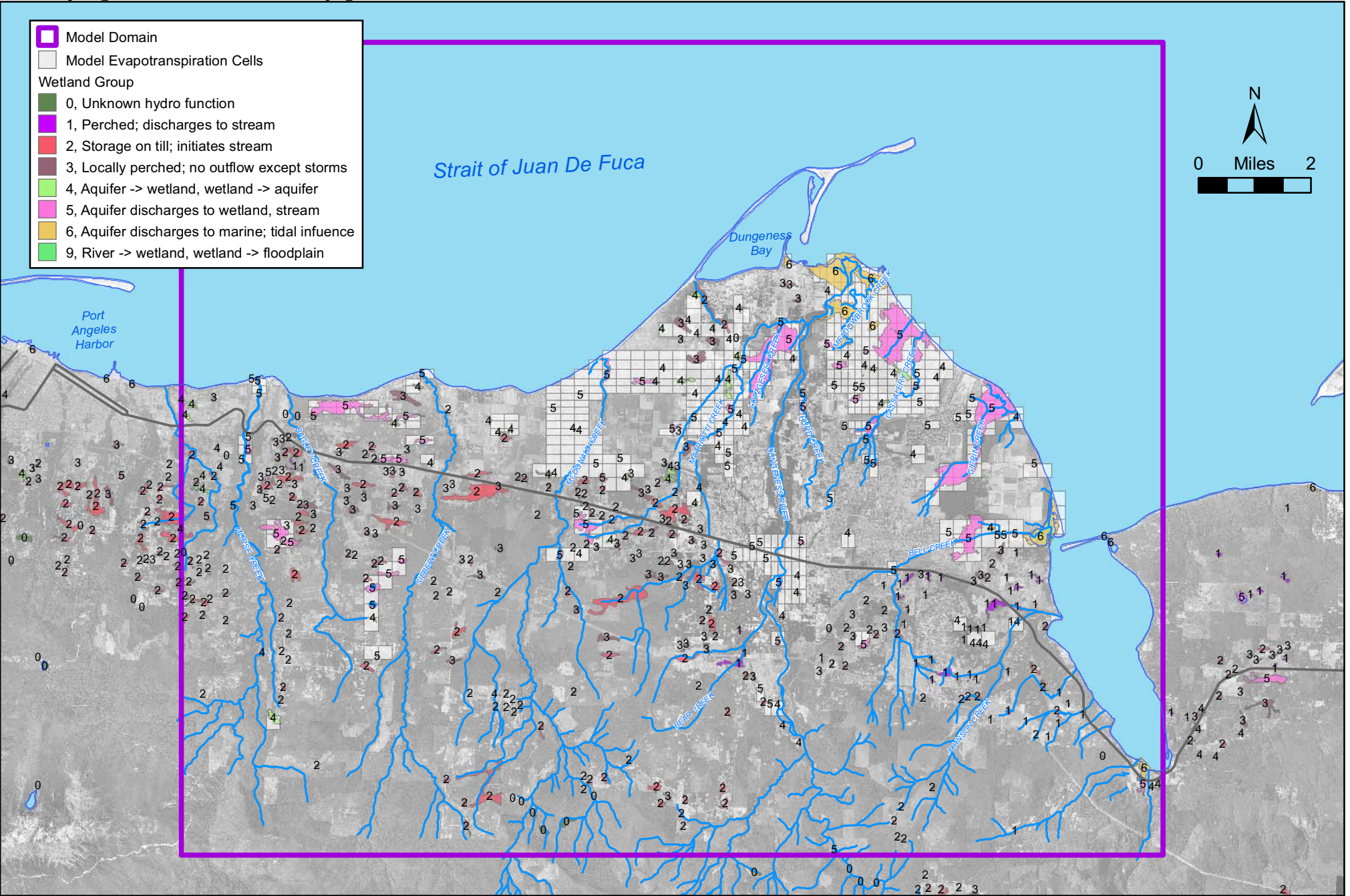
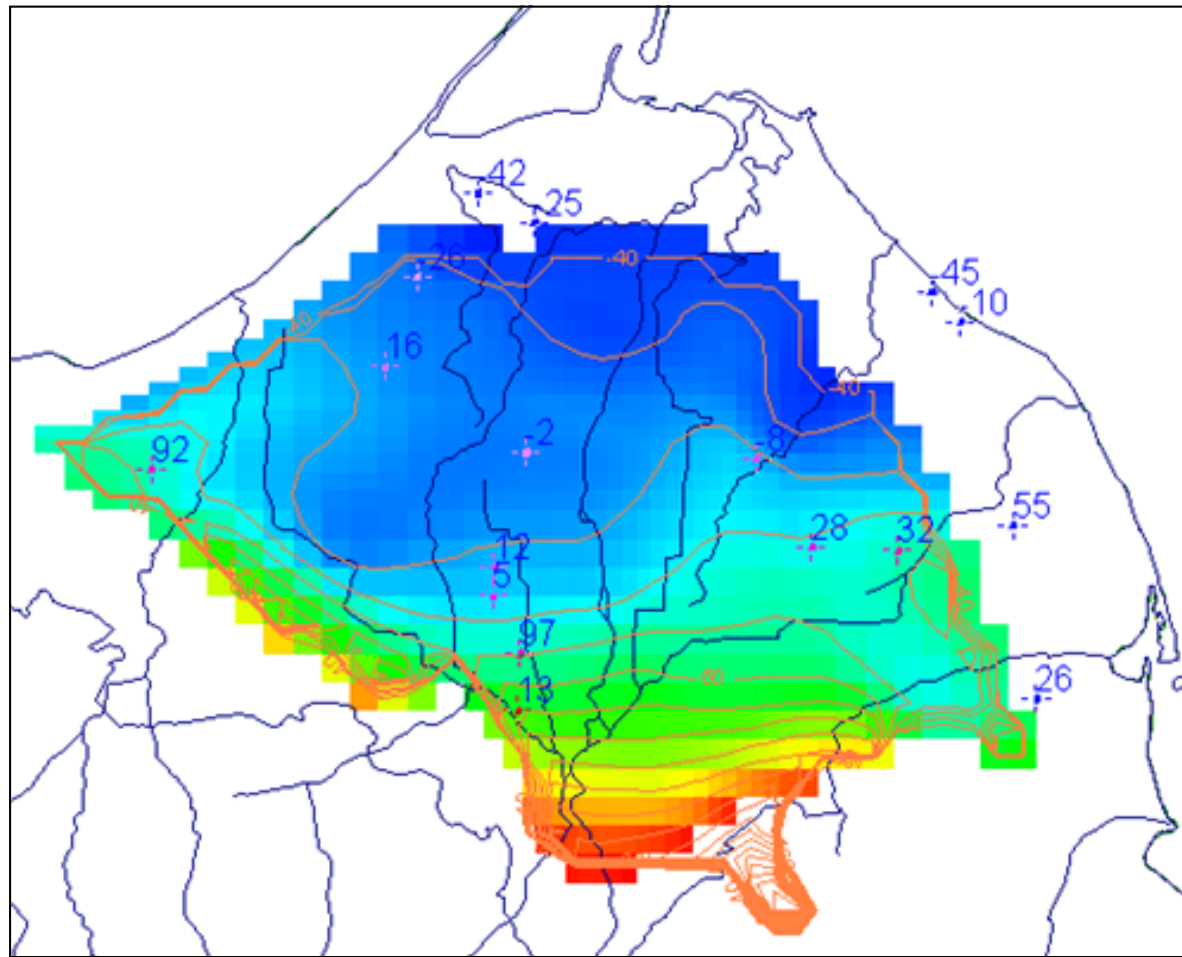
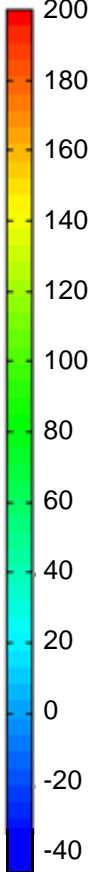


Figure 3-1 Wetlands and Model Evapotranspiration Cells





Head Difference Based on  
Contours in Drost (1999)



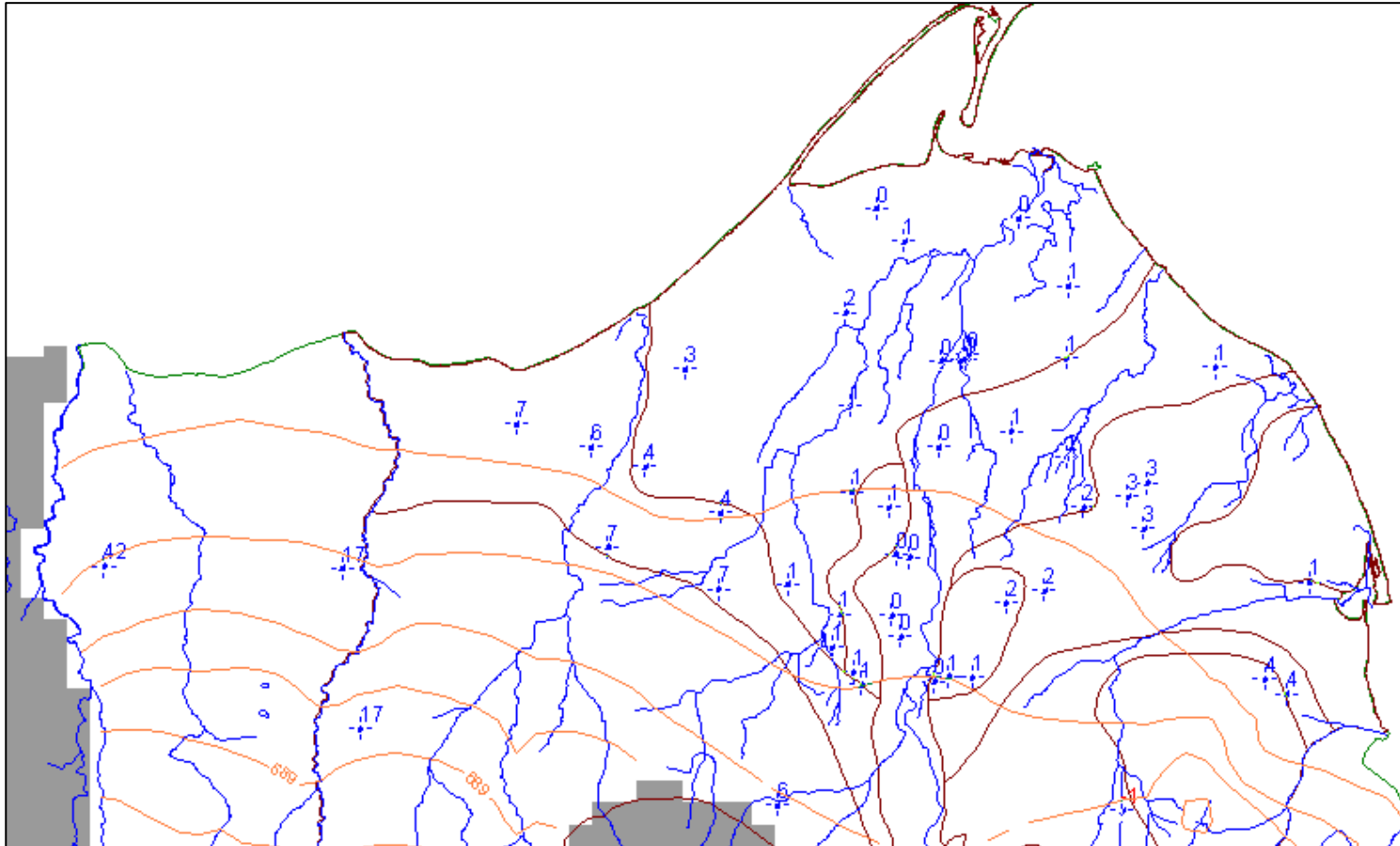
55  
Head Differ-  
ence Between  
Wells Based on  
PGG Analysis

— 20-foot Contour Interval

**Figure 3-2**  
**Head Difference Analysis Between Shallow and Middle Aquifers**

Clallam County  
2008 Groundwater Model



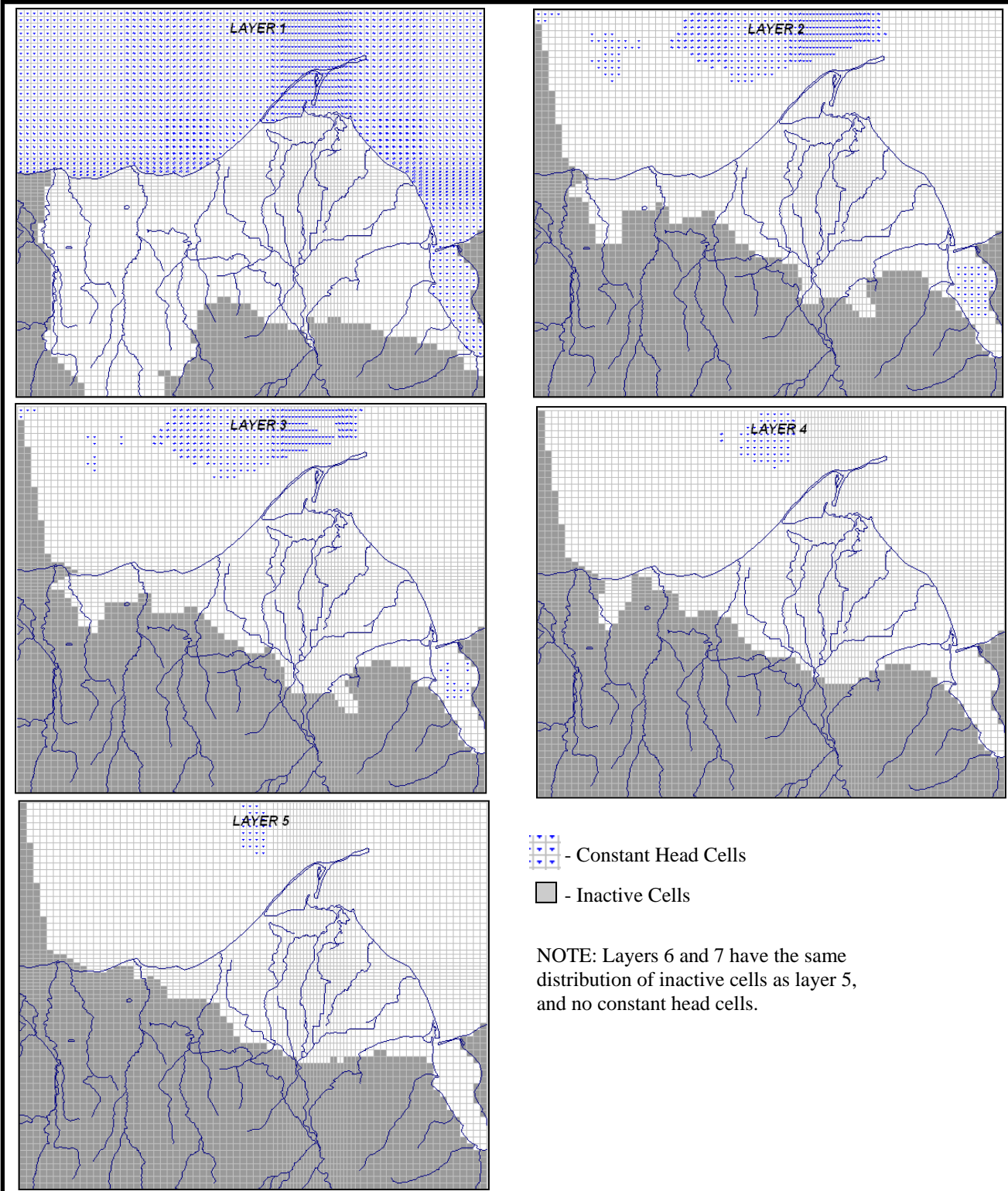


Note: head changes were estimated with an early version of the 2008 model prior to completion of calibration.

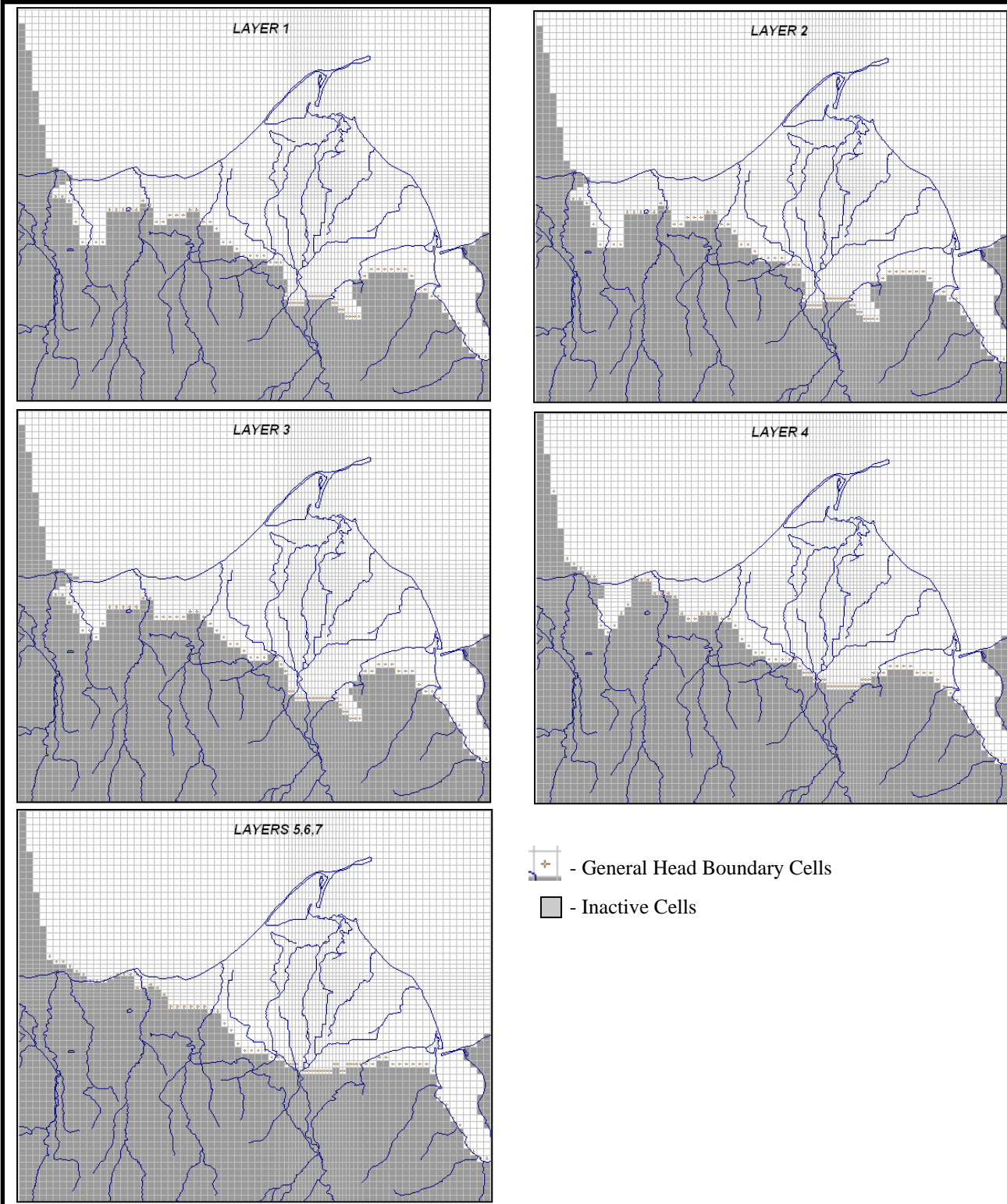
**Figure 3-3**  
**Changes in Simulated Shallow-Aquifer Heads Between Study-Period and Long-term Average Recharge**

Clallam County  
 2008 Groundwater Model



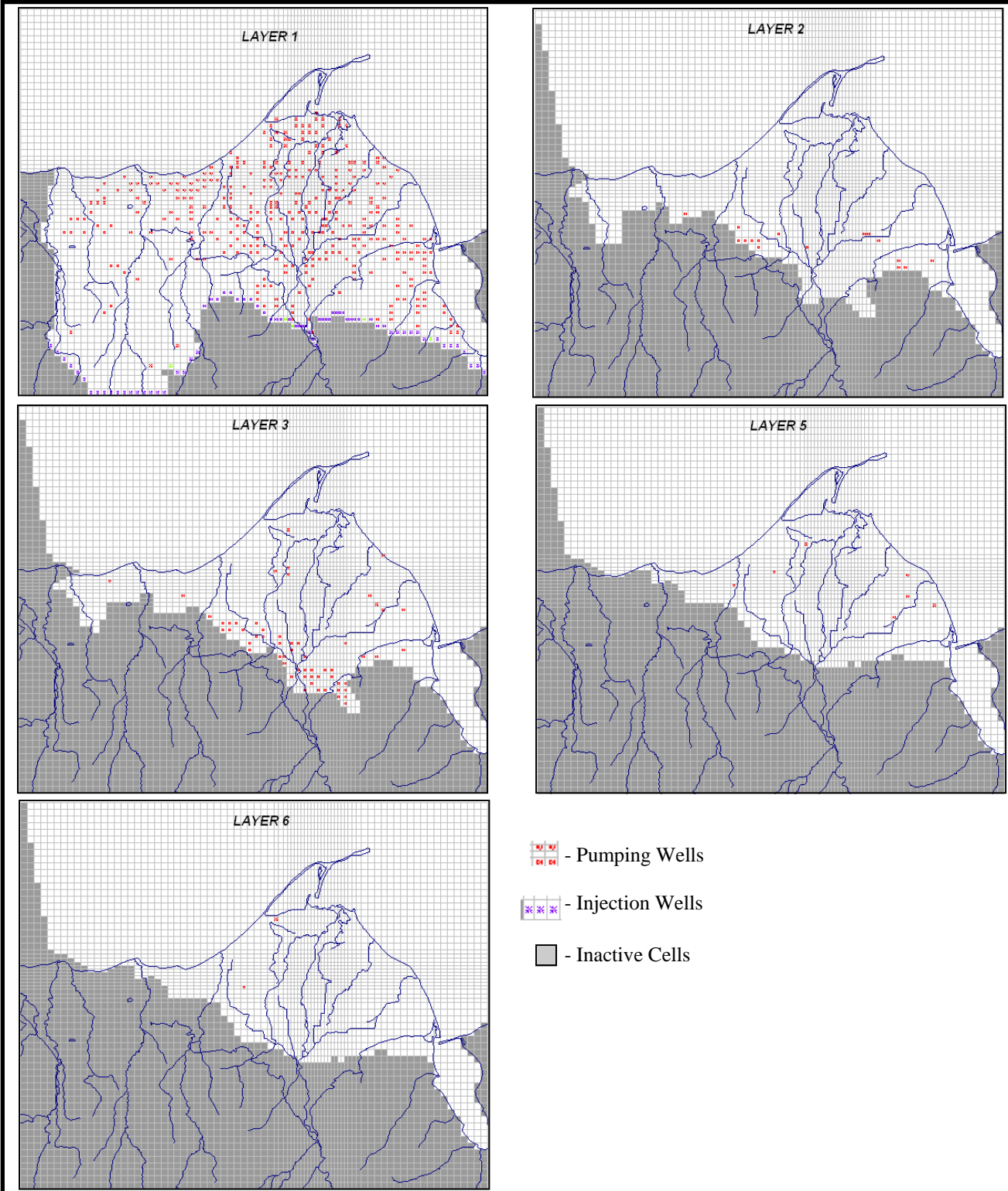


**Figure 4-1**  
**Distributions of Inactive and Constant Head Cells**



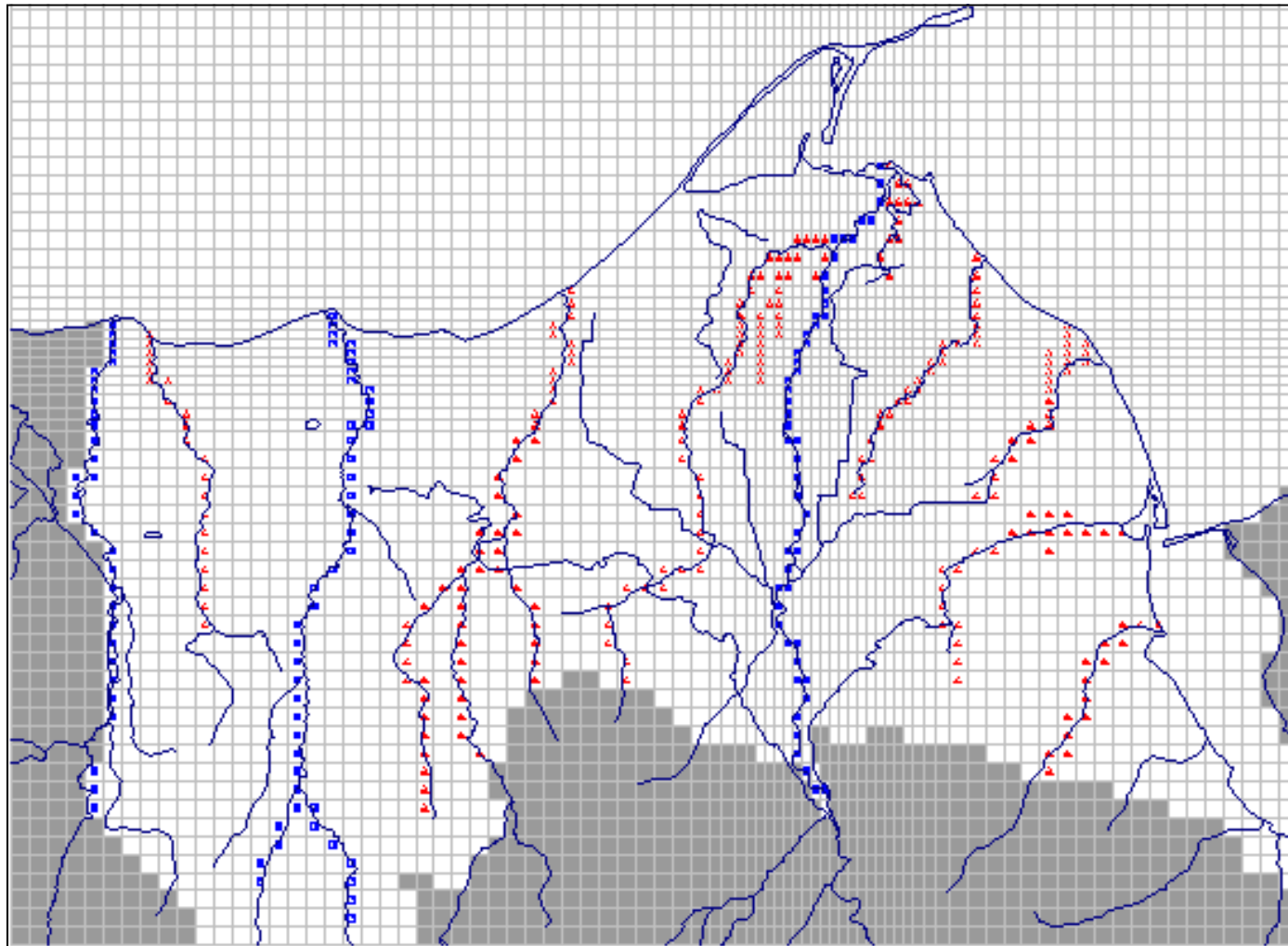
**Figure 4-2**  
**Distributions of Inactive and General Head Boundary Cells**



Clallam County  
 2008 Groundwater Flow Model



**Figure 4-3**  
**Distributions of Specified Flux Cells (Wells)**

Clallam County  
 2008 Groundwater Flow Model



-  - River Cells
-  - Drain Cells

**Figure 4-4**  
**Distribution of River and Drain Cells**

Clallam County  
2008 Groundwater Model

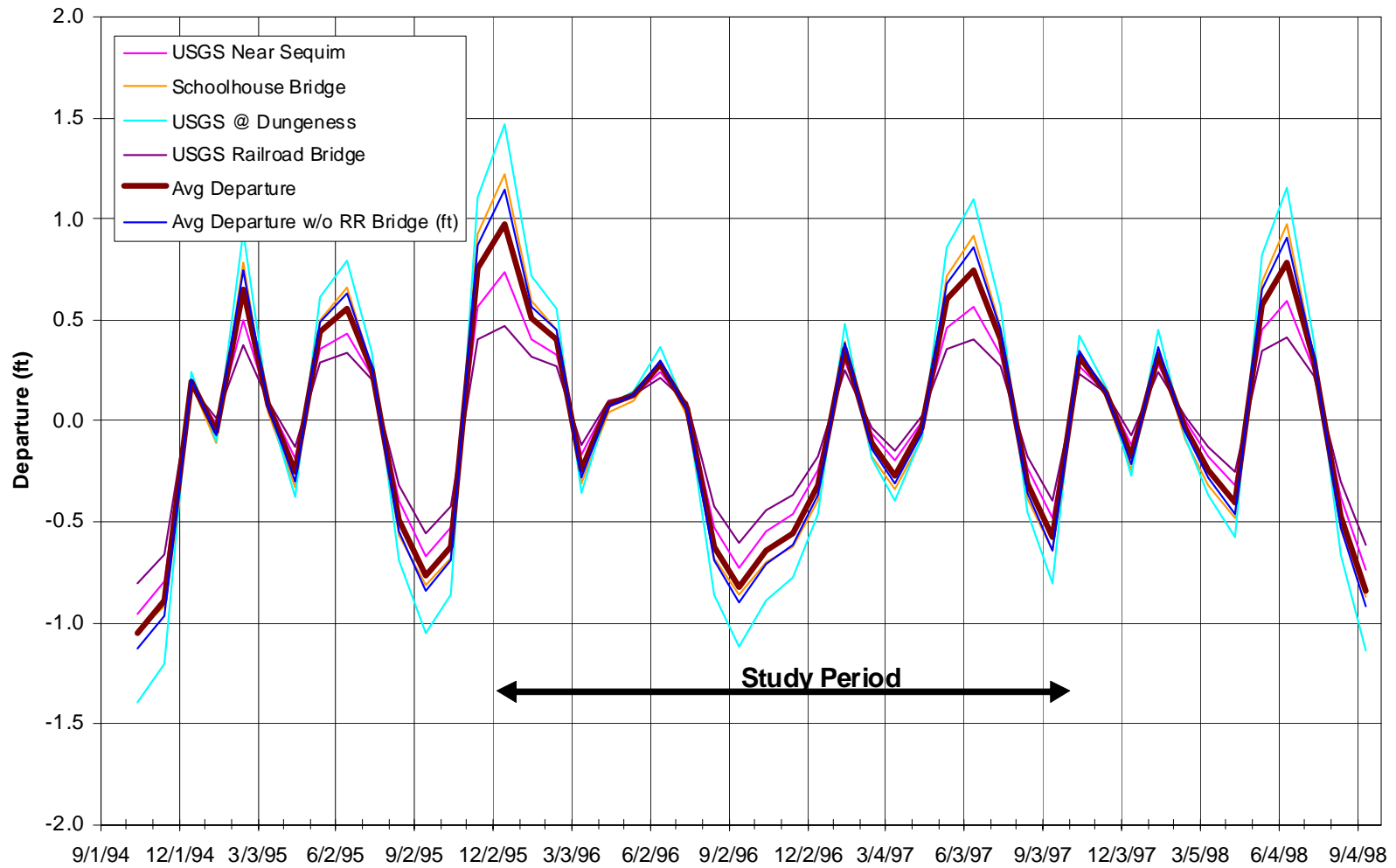


**Figure 4-5**  
**River Stage Departure Around Study Period Average**

Clallam County  
 2008 Groundwater Model



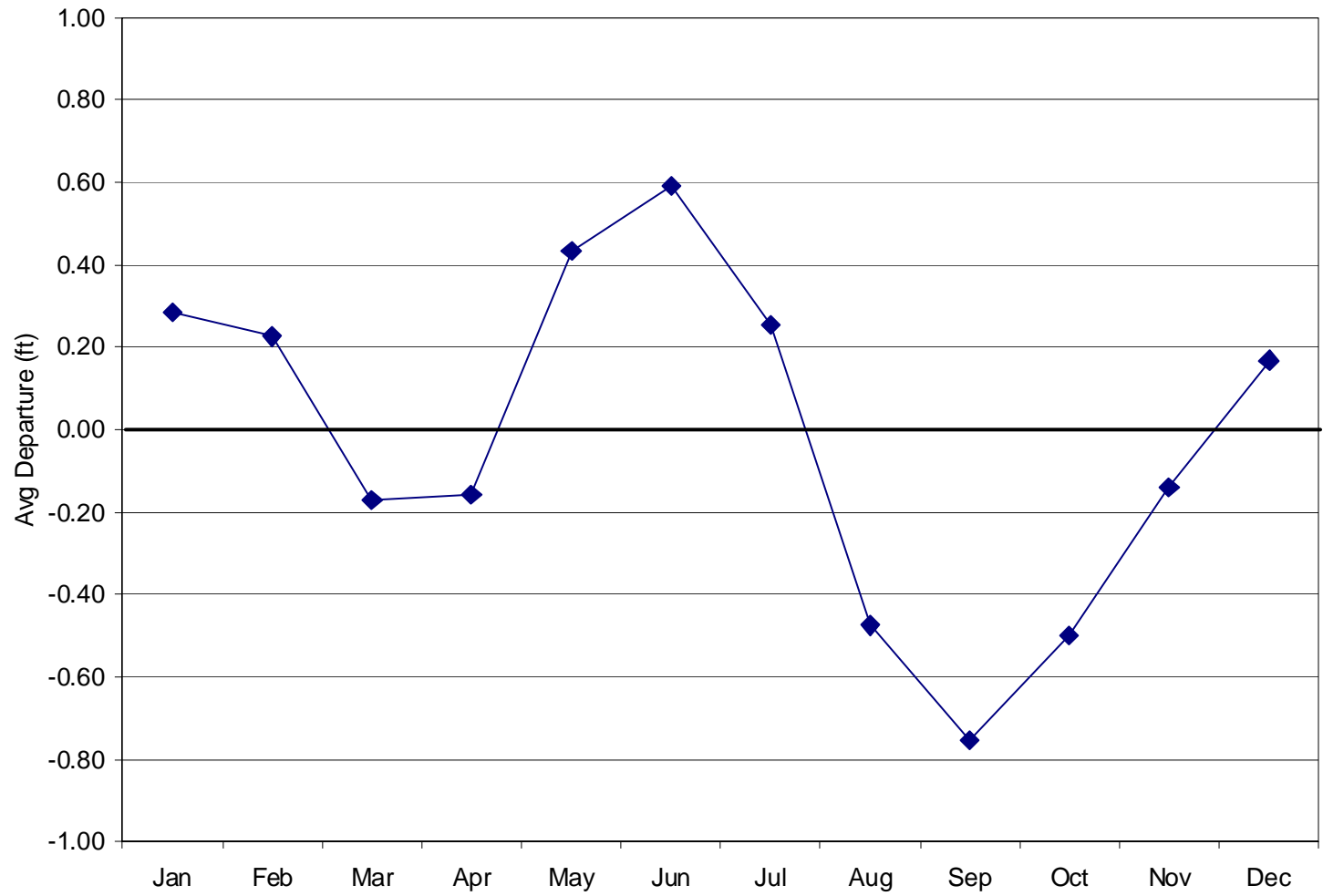


**Figure 4-6**  
**River Stage Departure Calculated for Transient Warm-up Period**

Clallam County  
2008 Groundwater Model





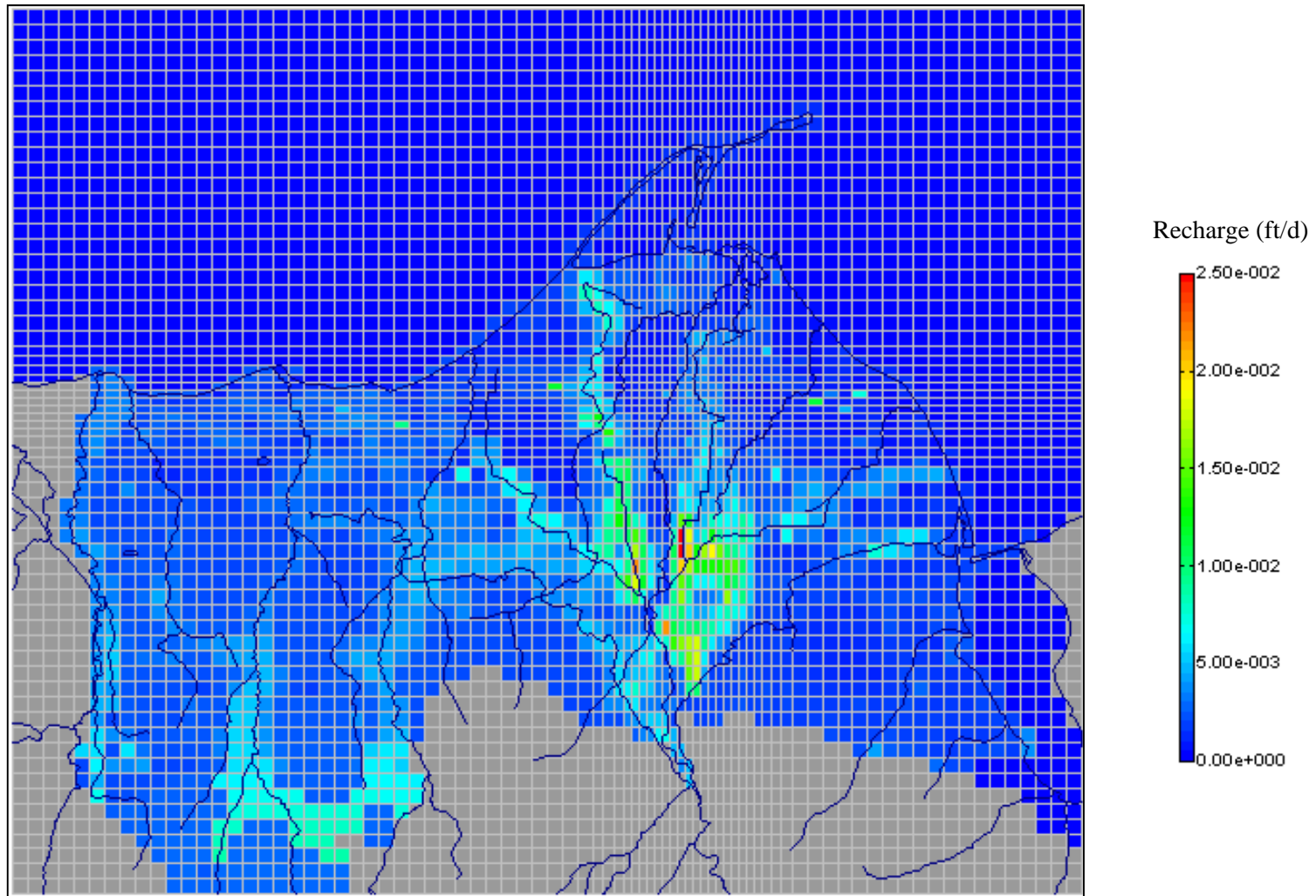


**Figure 4-7**  
**Distribution of Steady-State Model Recharge**

Clallam County  
2008 Groundwater Model

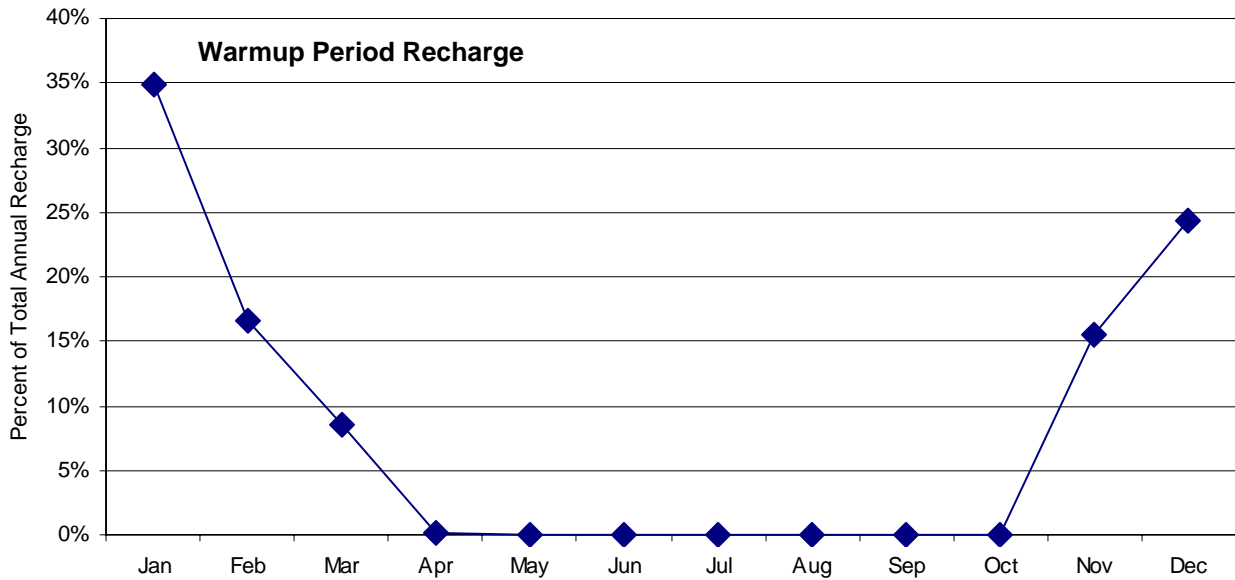
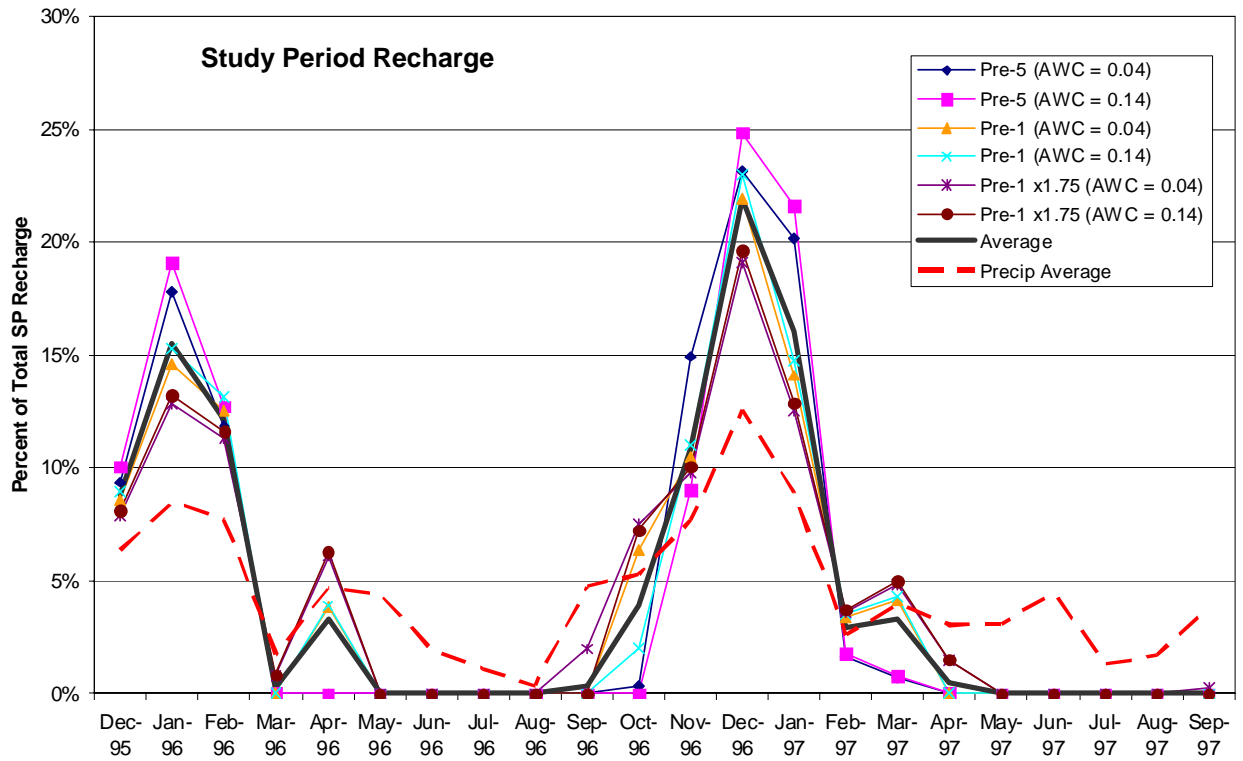
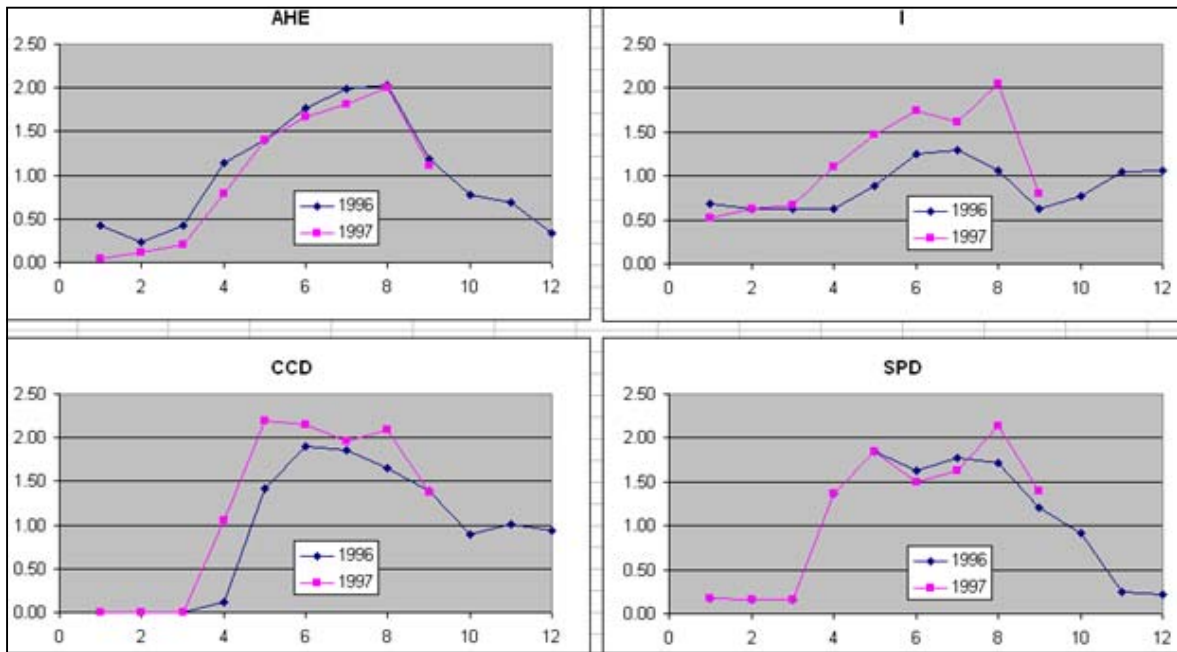


**Figure 4-8**  
**Transient Precipitation Recharge as Percent of Simulation Period Total**

### Monthly Irrigation Out-Takes (cfs)



### Geographic Irrigation Groupings

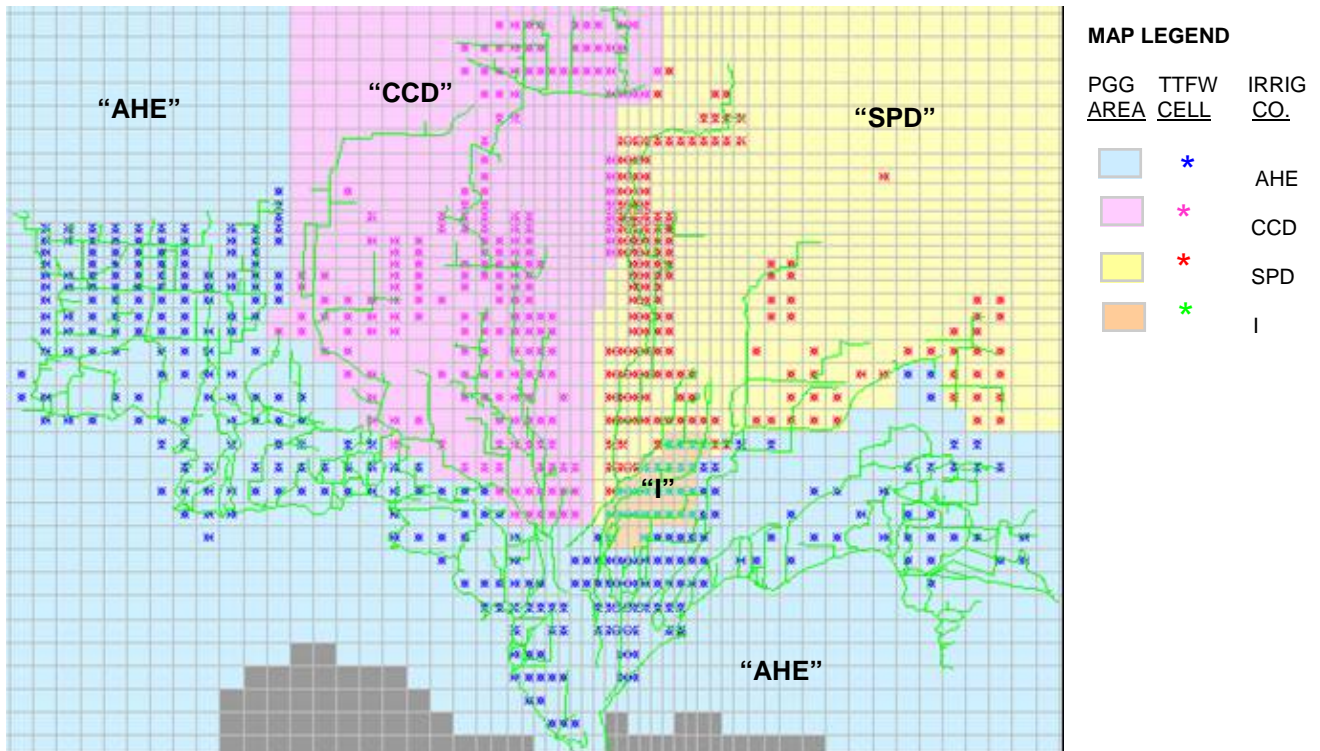
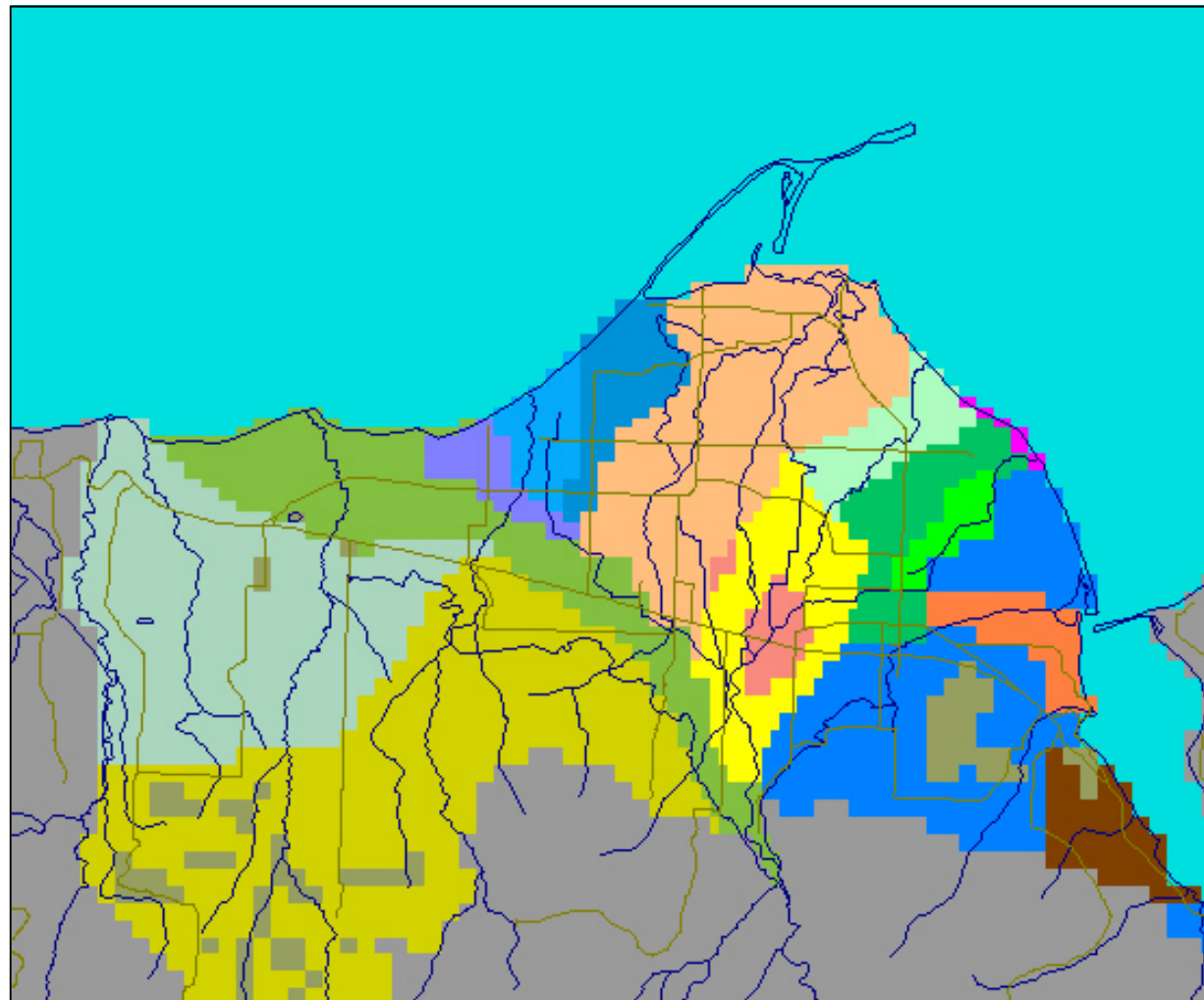


**Figure 4-9**  
Irrigation Out-Takes and Geographic Groupings for Recharge Estimation

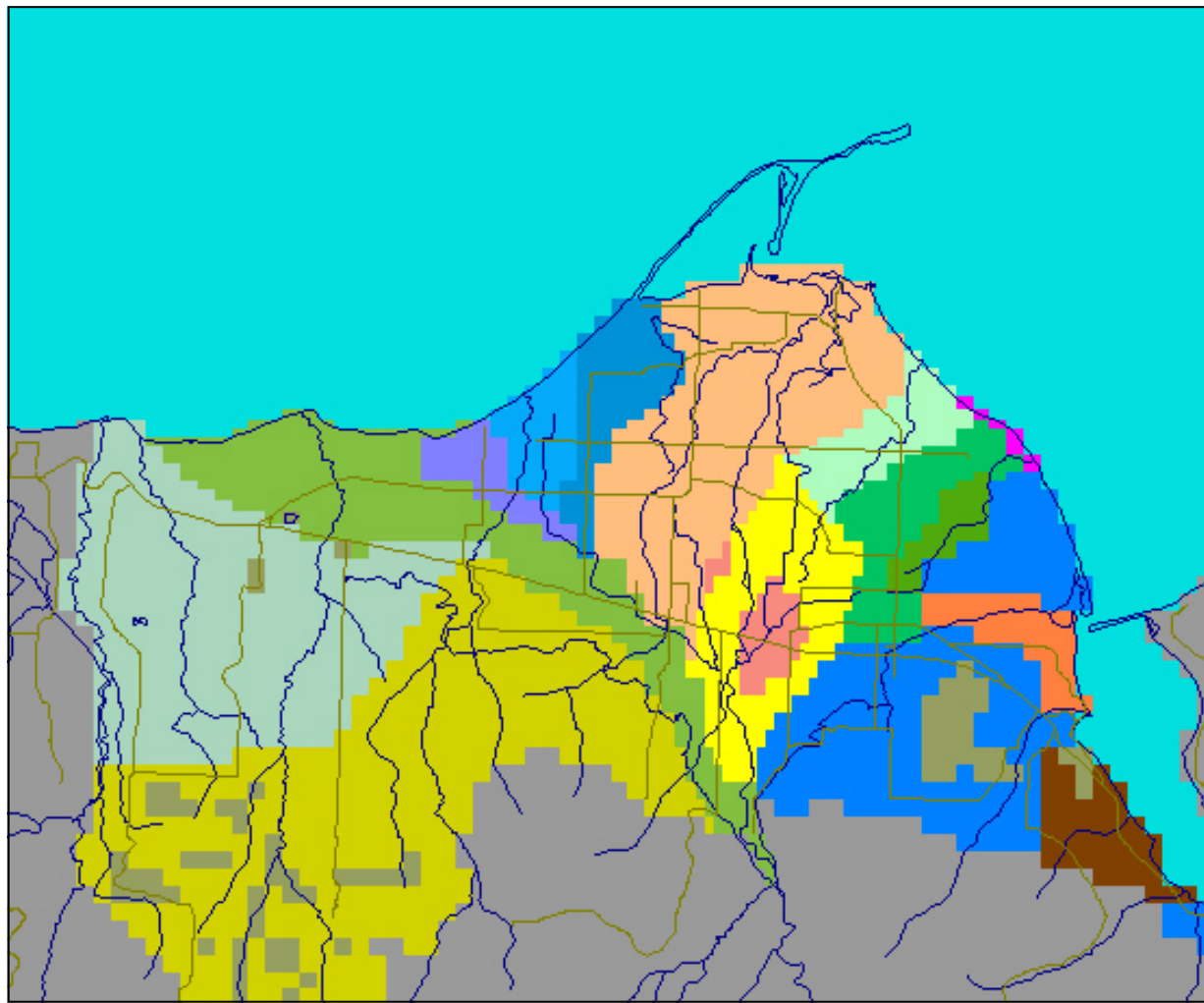


Zone	Value
	No Flow
1	22.00
2	7.000
3	20.00
4	400.0
5	100.0
6	10.00
7	250.0
9	15.00
11	11.00
12	20.00
14	100.0
15	30.00
16	80.00
17	40.00
18	75.00
70	4.000e-002
71	1.000
73	44.00
80	1.000e+005

**Figure 4-10**  
**Kh Zonation in Layer 1 of "Dung-7e" Model Realization**

Clallam County  
 2008 Groundwater Model





Zone	Value
No Flow	
1	18.00
2	7.000
3	15.00
4	400.0
5	100.0
6	10.00
7	250.0
9	15.00
11	20.00
12	20.00
14	50.00
15	30.00
16	60.00
17	30.00
18	75.00
70	4.000e-002
71	1.000
73	44.00
80	1.000e+005

**Figure 4-11**  
**Kh Zonation in Layer 1 of "Dung-7g" Model Realization**

Clallam County  
 2008 Groundwater Model



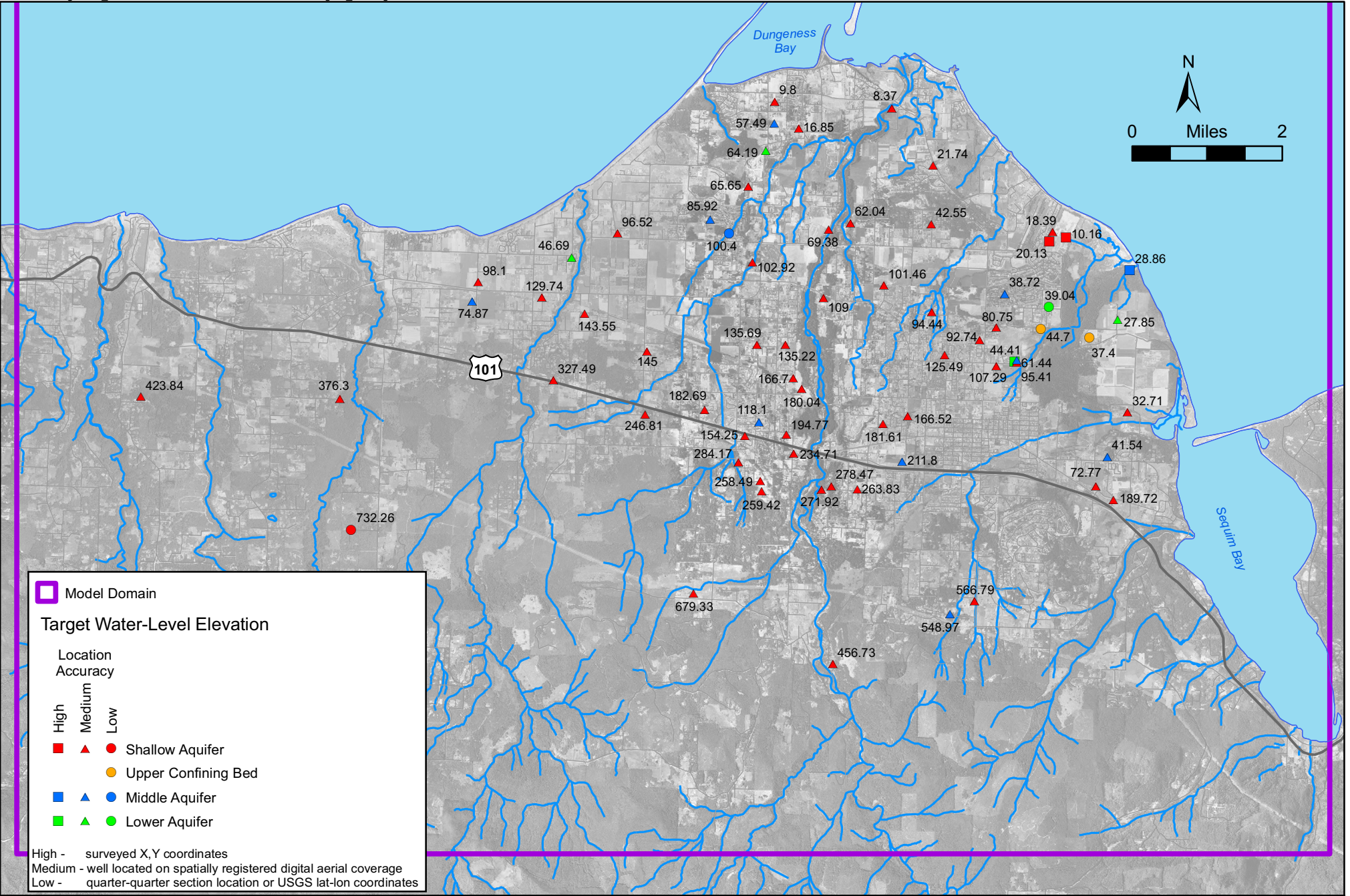
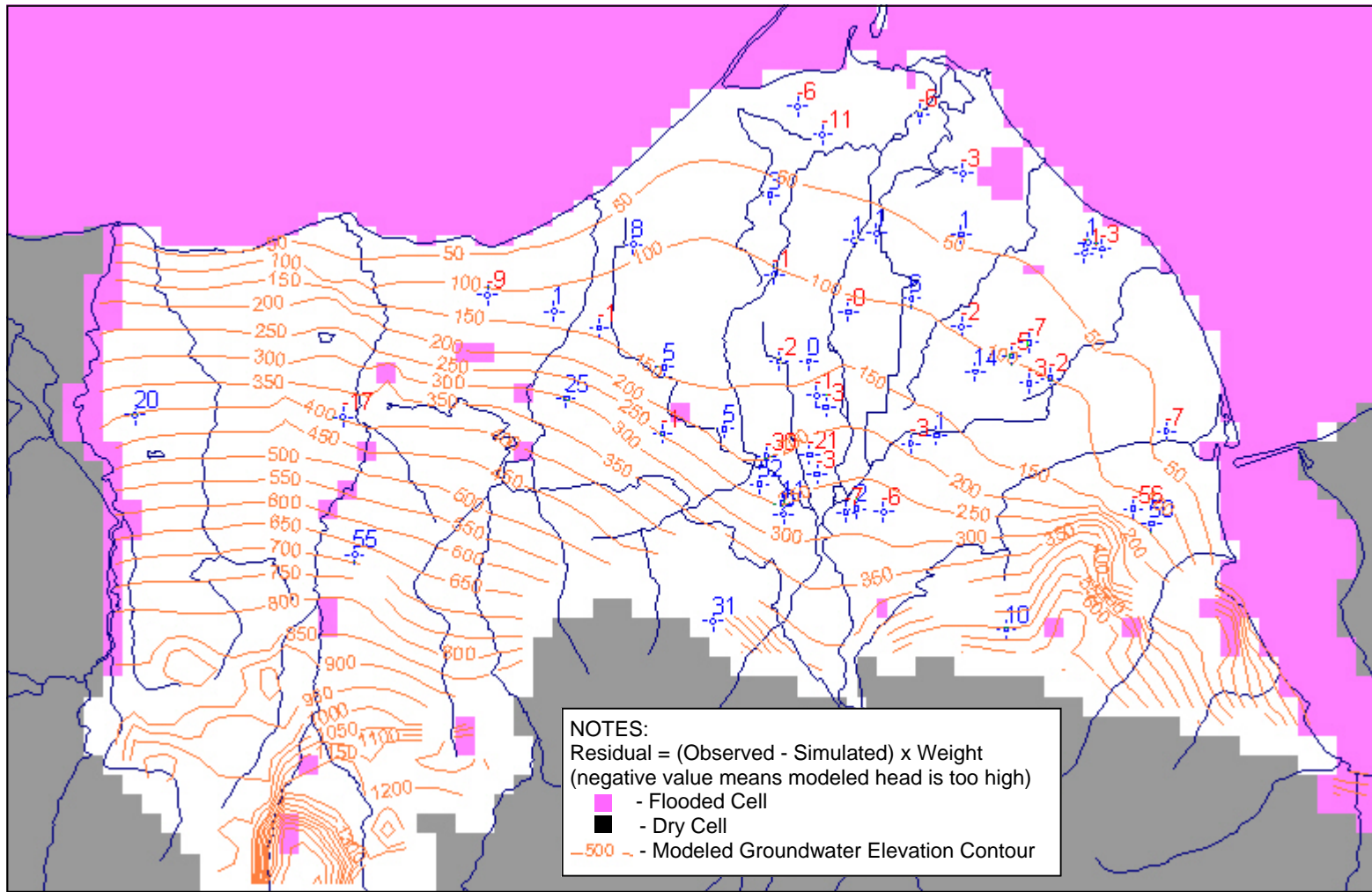
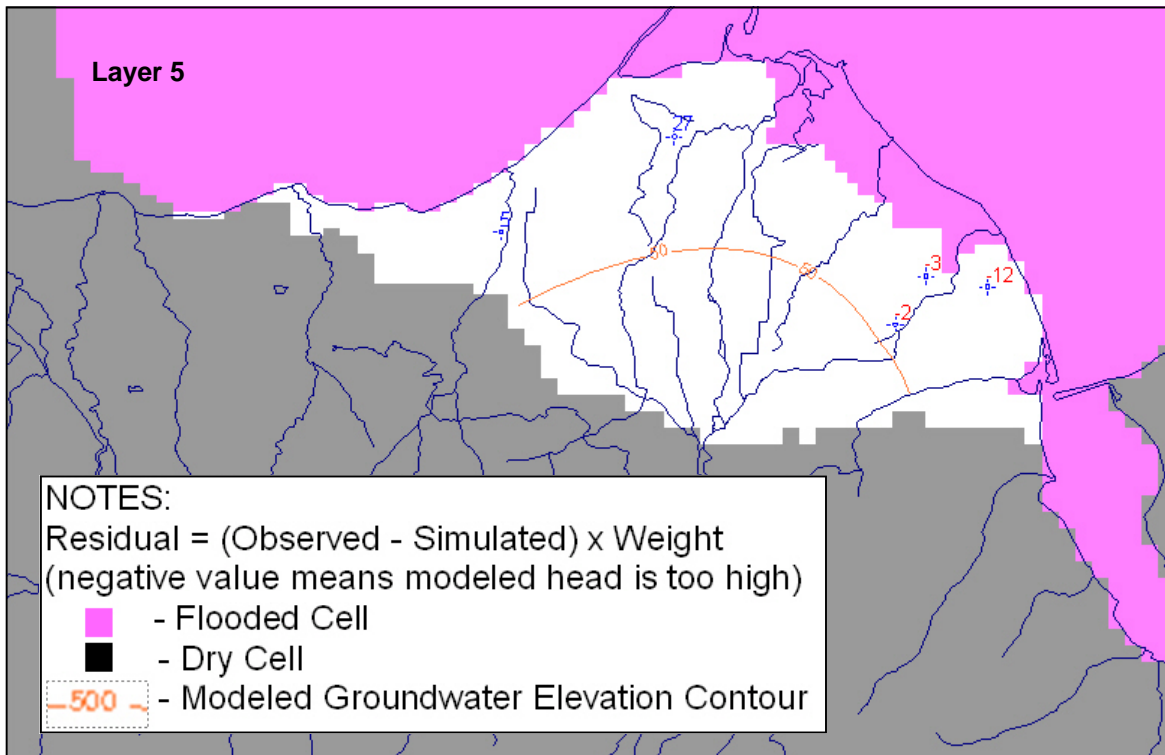
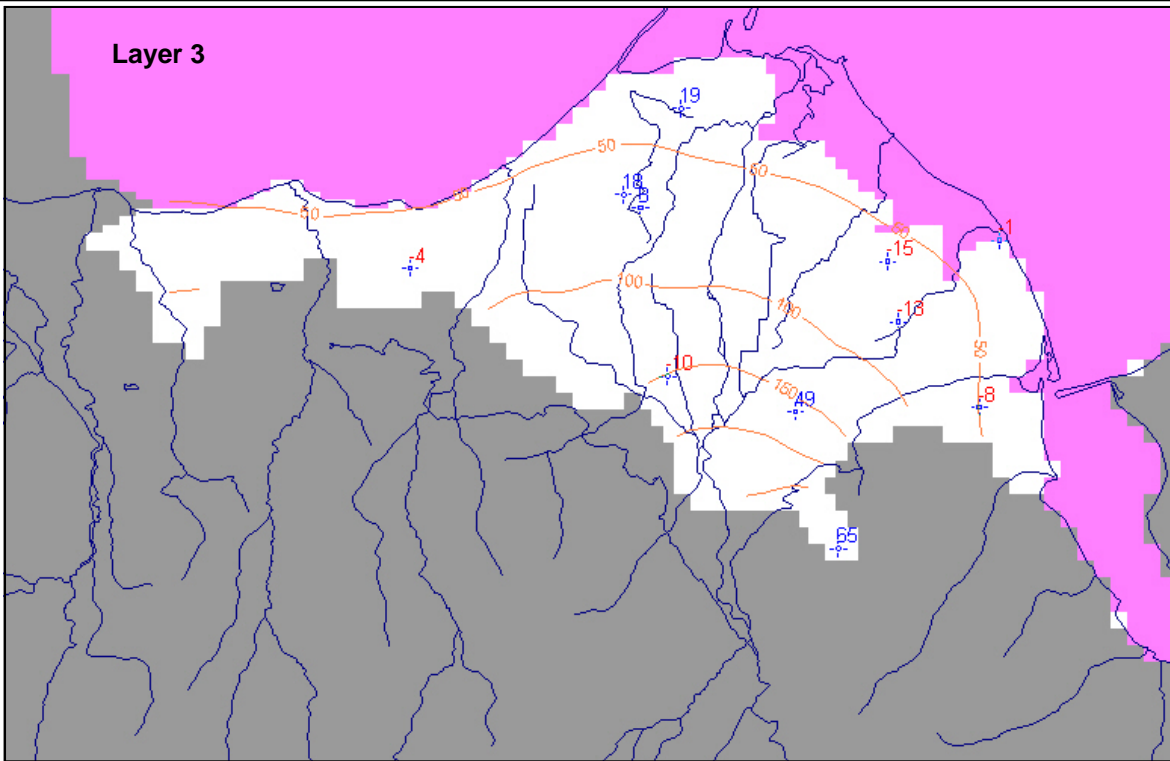


Figure 5-1 Model Water-Level Target Values



**Figure 5-2**  
**Head Target Residuals for Steady-State Model Realization “Dung-7e” (Layer 1)**



NOTES:  
 Residual = (Observed - Simulated) x Weight  
 (negative value means modeled head is too high)

- Flooded Cell
- Dry Cell
- Modeled Groundwater Elevation Contour

**Figure 5-3**  
**Head Target Residuals for Steady-State Model Realization “Dung-7e”**  
**(Layers 3 and 5)**



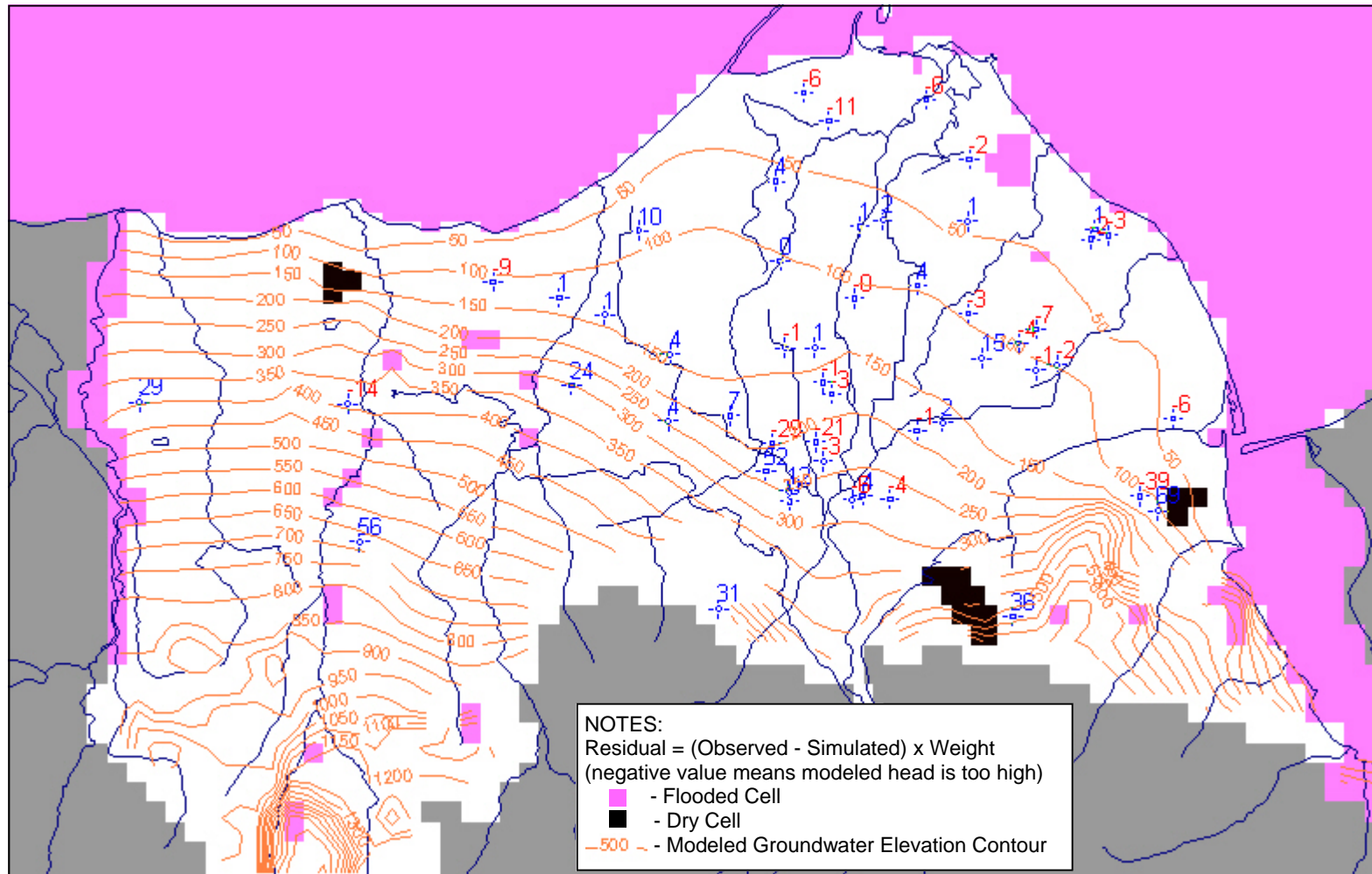


**Figure 5-4**  
**Head Target Residuals for Steady-State Model Realization “Dung-7g” (Layer 1)**

Clallam County  
 2008 Groundwater Model

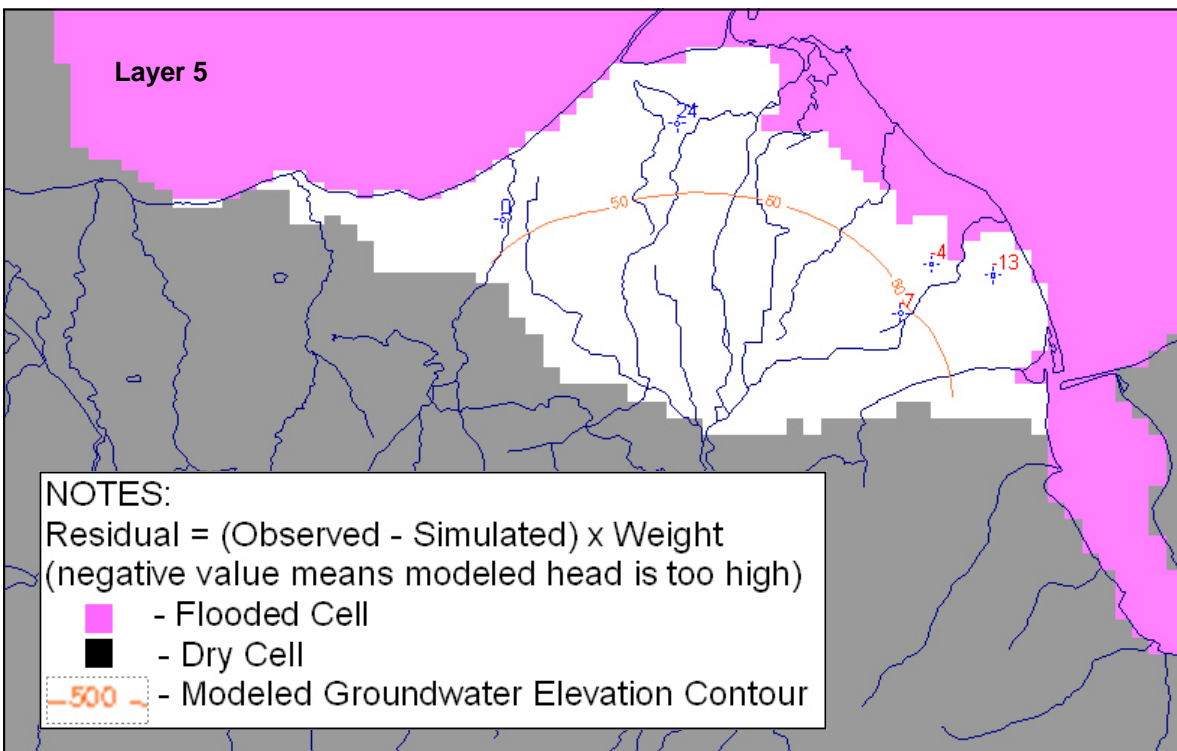
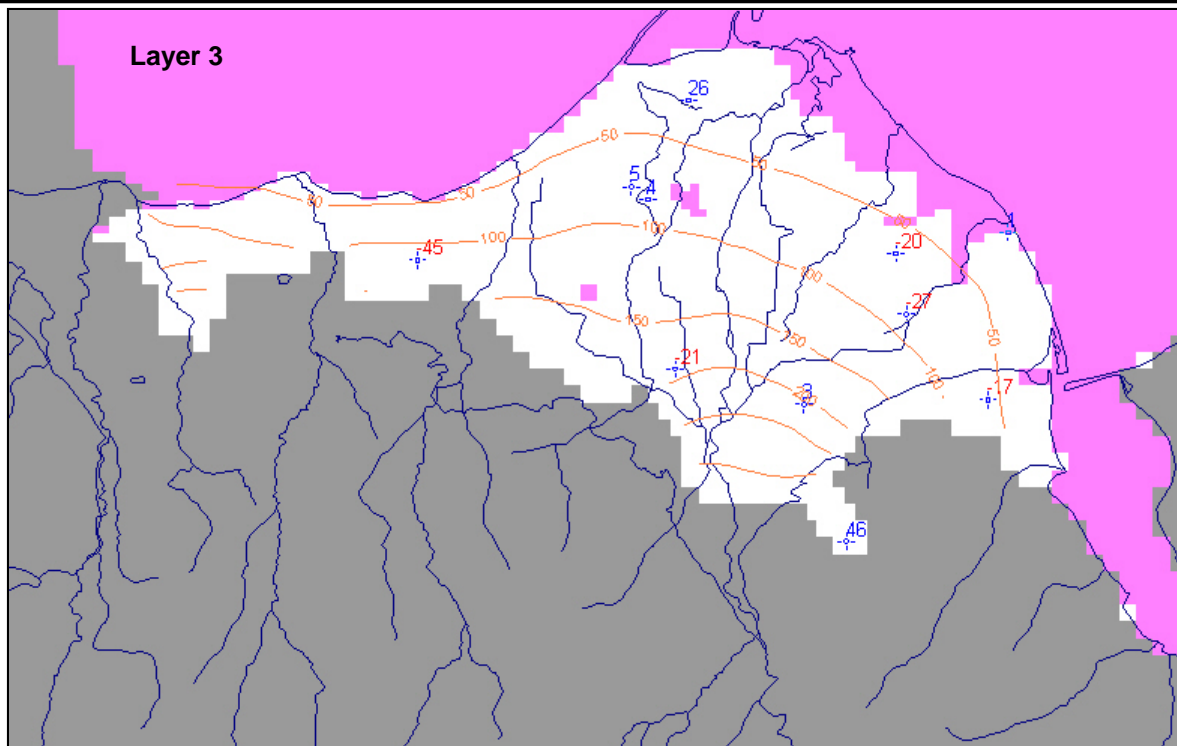
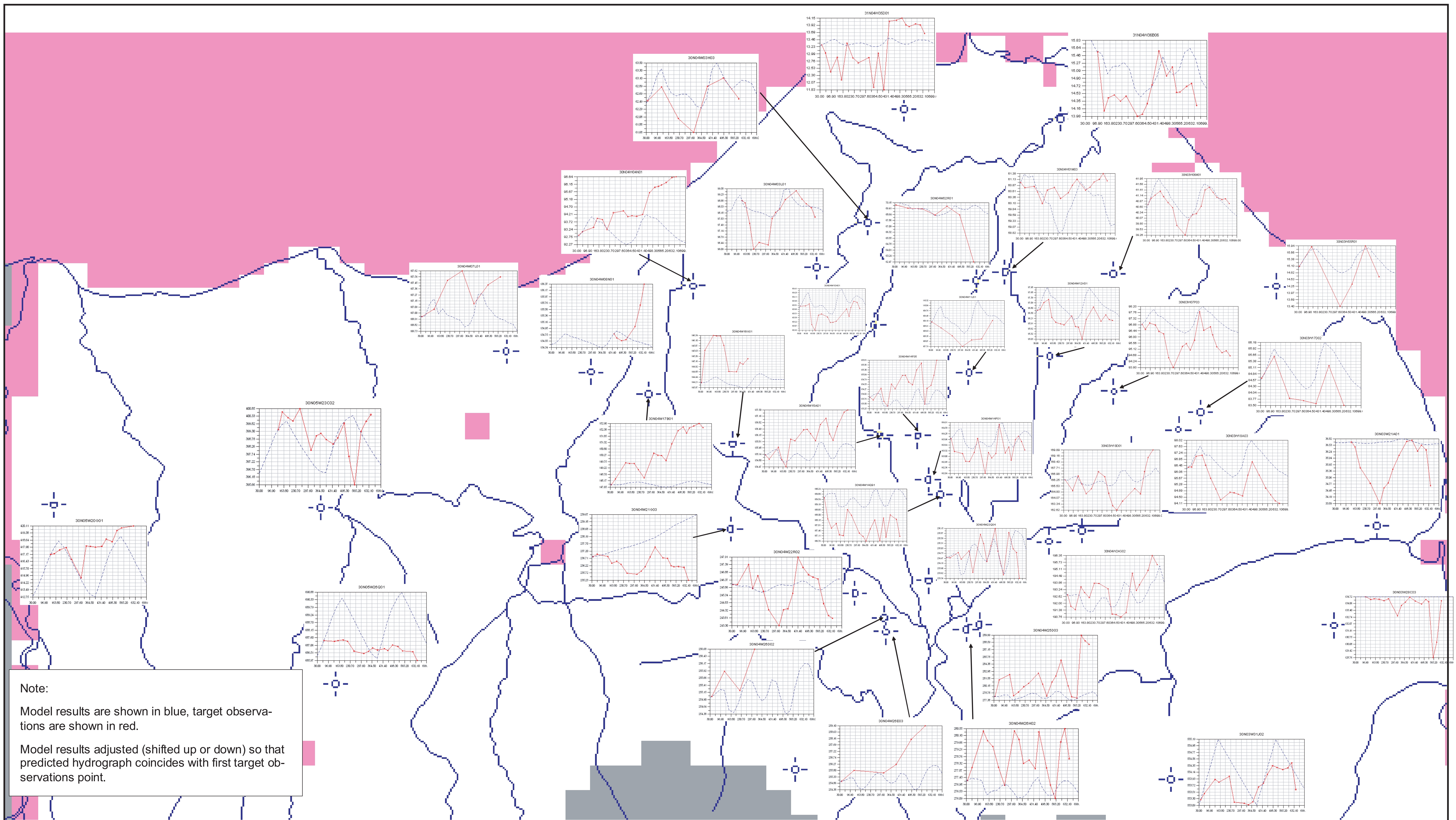


**Figure 5-5**  
**Head Target Residuals for Steady-State Model Realization “Dung-7g”**  
**(Layers 3 and 5)**



Note:  
 Model results are shown in blue, target observations are shown in red.  
 Model results adjusted (shifted up or down) so that predicted hydrograph coincides with first target observations point.

**Figure 6-1 Transient Target Predictions for the Shallow Aquifer for Model Realization "Dung-7e"**  
 (Model Run: DUNG-TR-7E-CAL1; Specific Yield = 0.15; Storativity = 0.0002)

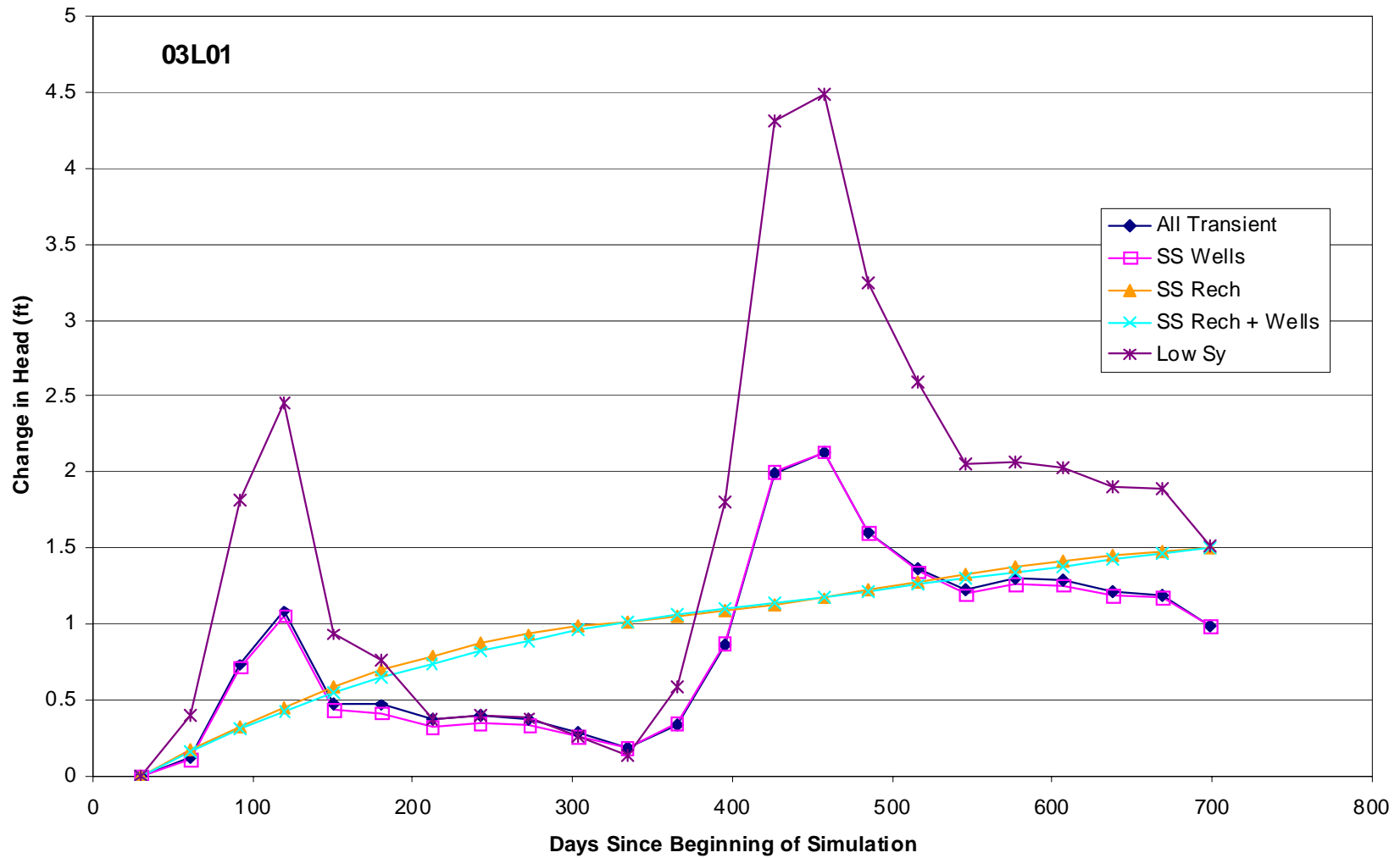


**Figure 6-2**  
**Sensitivity Analysis on Transient Boundary Conditions**

Clallam County  
 2008 Groundwater Model



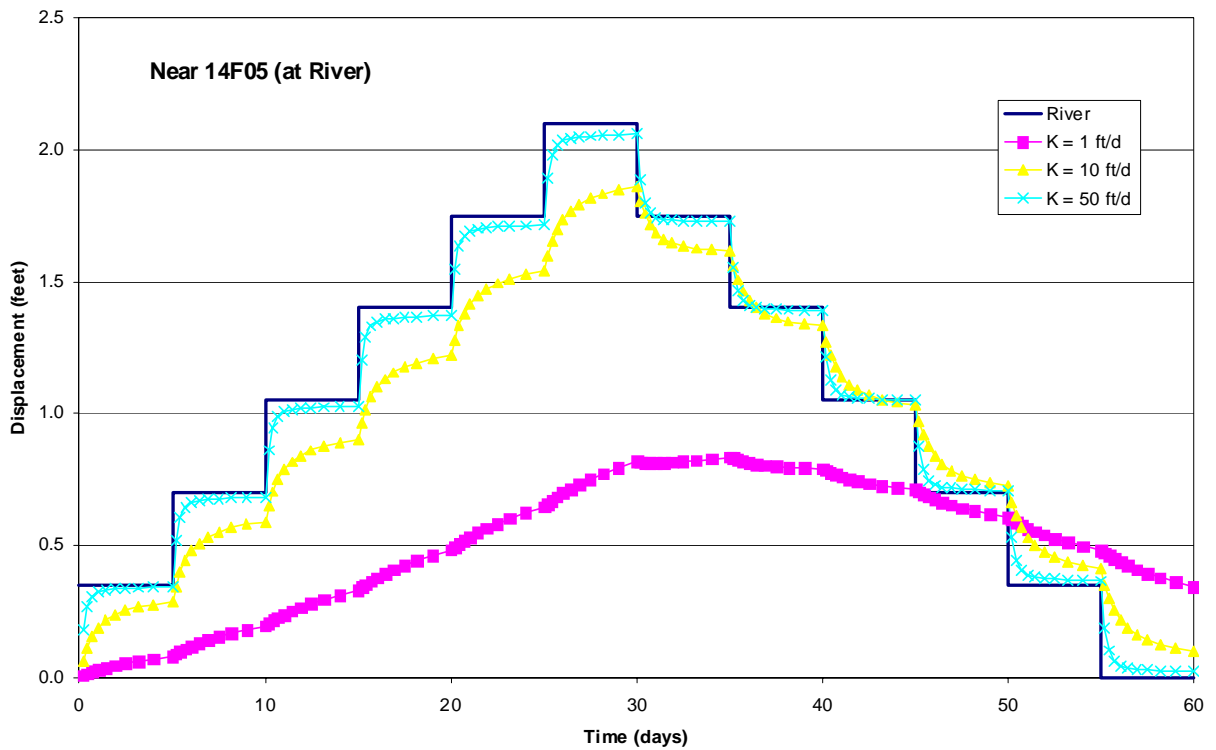
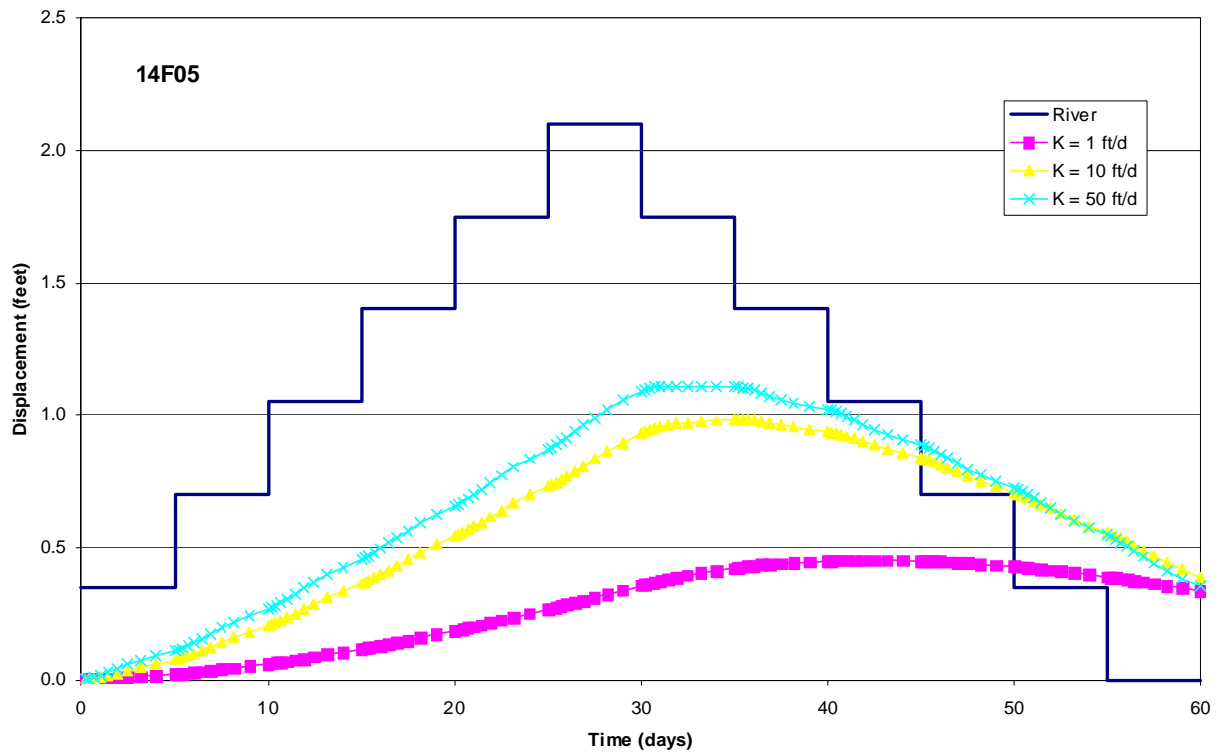


**Figure 6-3**  
**Transient Sensitivity to Dungeness River Streambed  $K_v$**

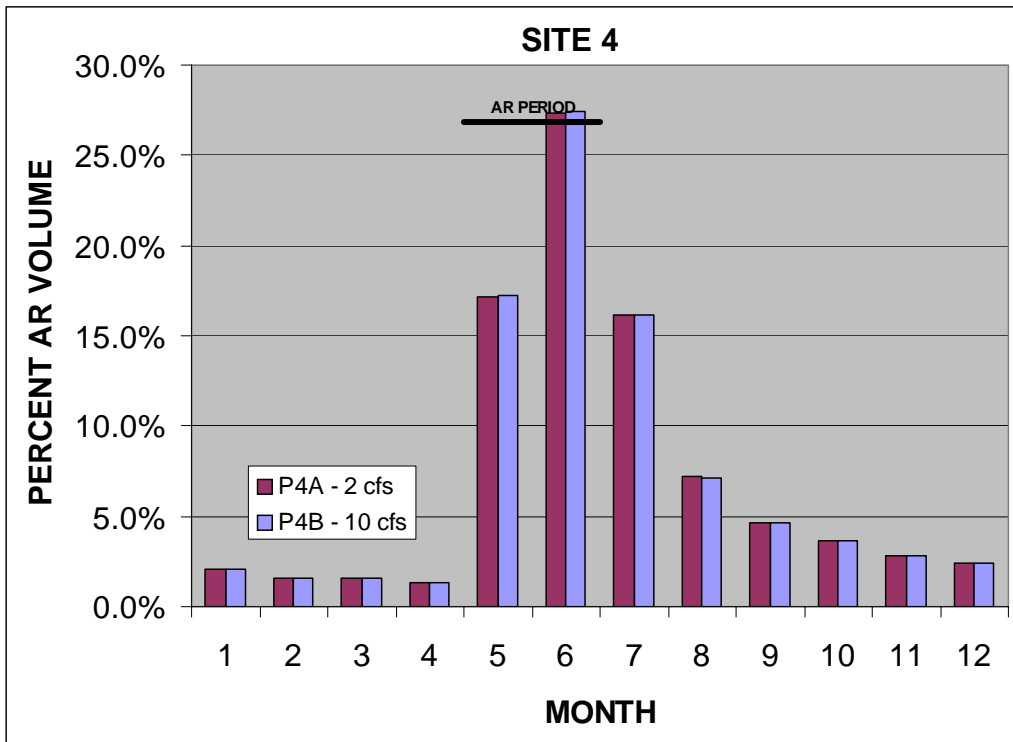
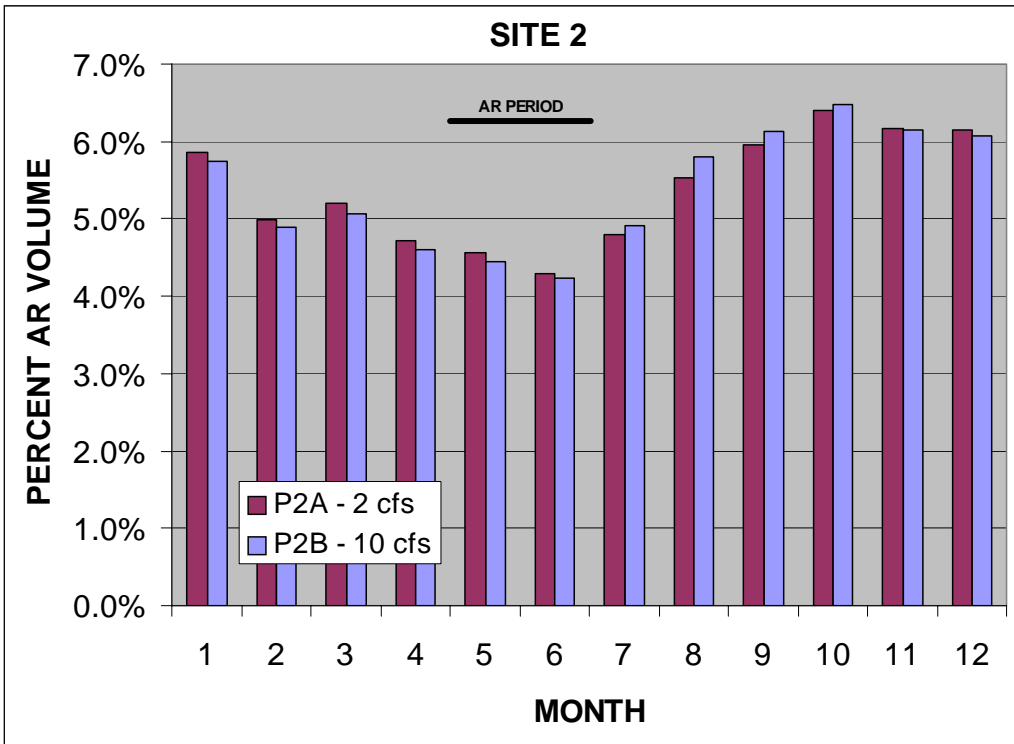
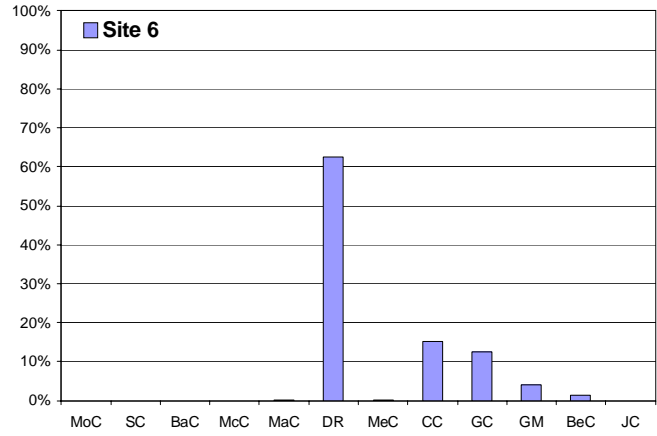
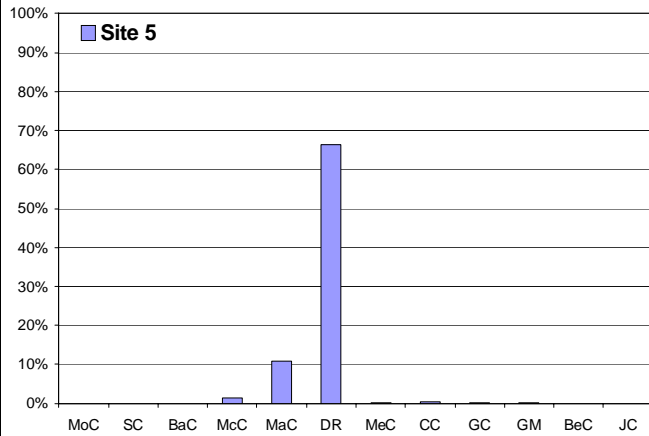
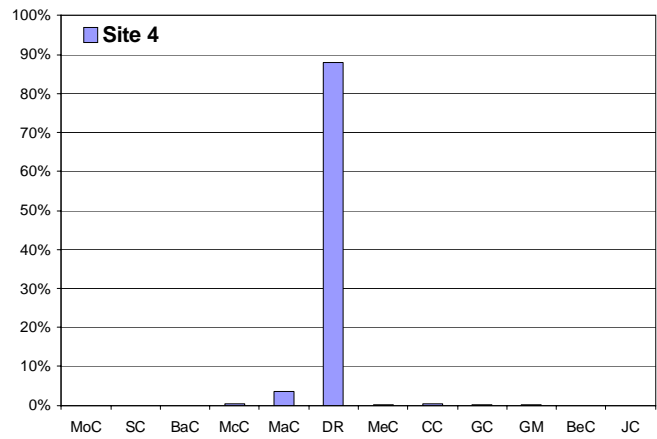
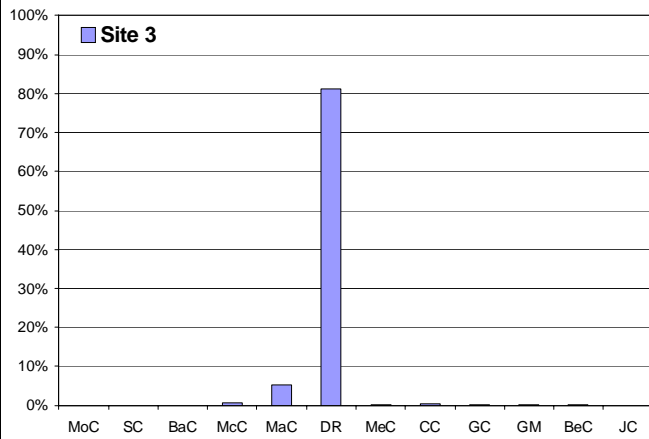
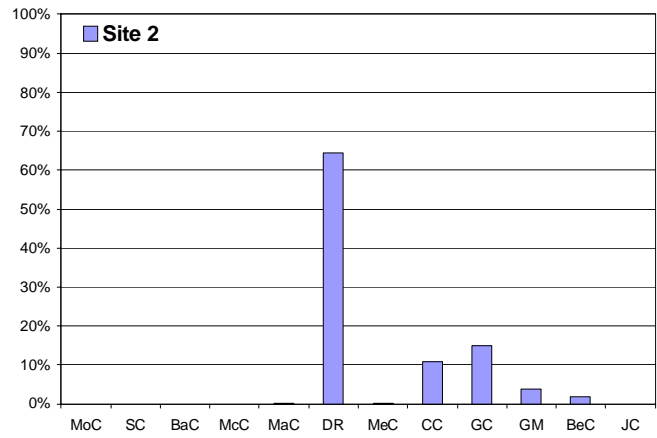
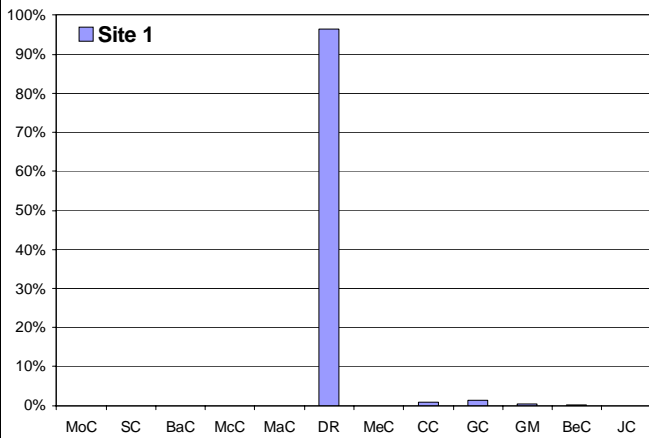
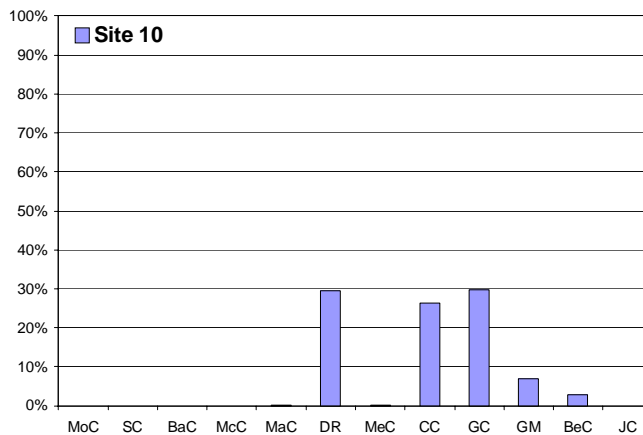
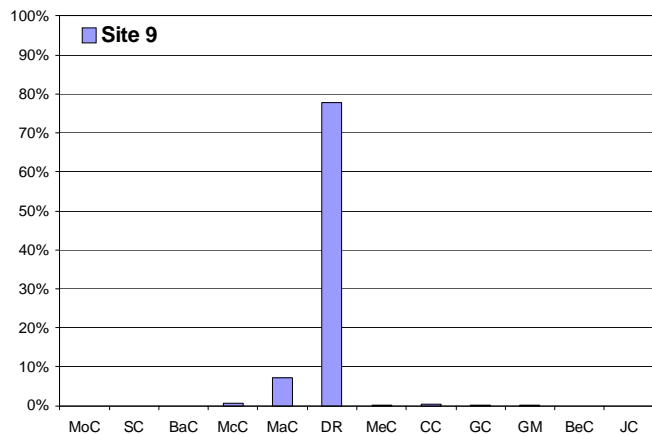
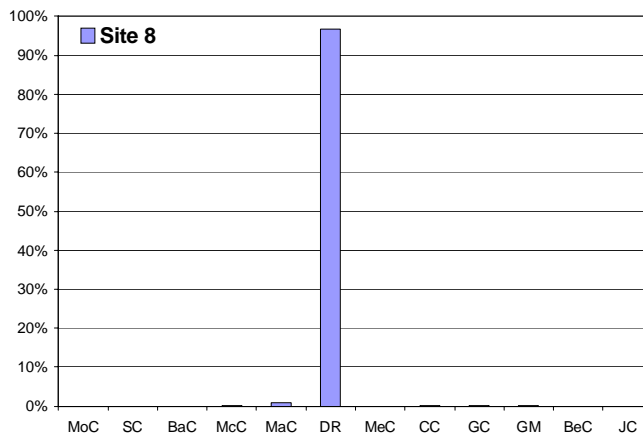
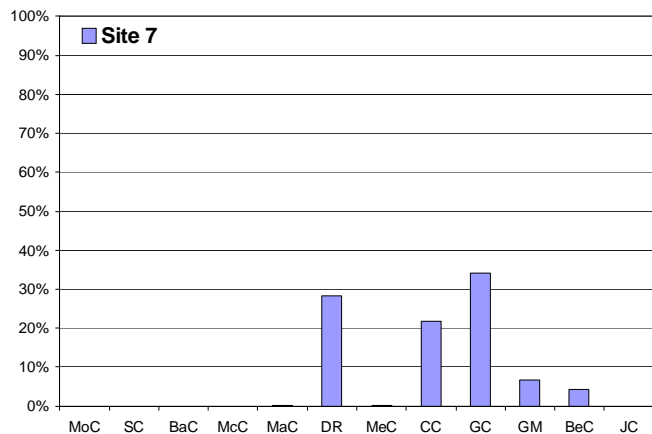


**Figure 7-1**  
**AR Discharge to the Dungeness River at Two Rates of AR**



**Stream Abbreviations:** MoC = Morse Creek; SC = Siebert Creek; BaC = Bagley Creek; McC = McDonald Creek; MaC = Matriotti Creek; DR = Dungeness River; MeC = Meadowbrook Creek; CC = Cassalery Creek; GC = Gierin Creek; BeC = Bell Creek; JC = Johnson Creek

**Figure 7-2a**  
**Stream Augmentation from Steady-State AR (Model Realization "Dung-7e")**



**Stream Abbreviations:** MoC = Morse Creek; SC = Siebert Creek; BaC = Bagley Creek; McC = McDonald Creek; MaC = Matriotti Creek; DR = Dungeness River; MeC = Meadowbrook Creek; CC = Cassalery Creek; GC = Gierin Creek; BeC = Bell Creek; JC = Johnson Creek

**Figure 7-2b**  
**Stream Augmentation from Steady-State AR (Model Realization "Dung-7e")**



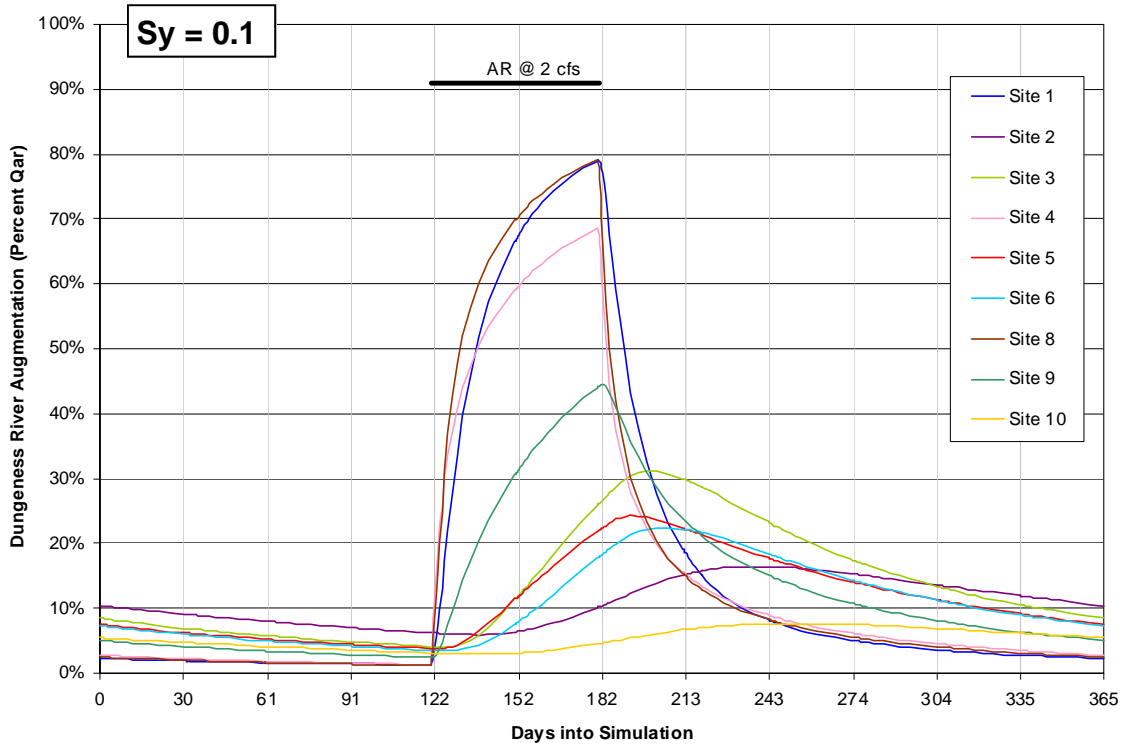
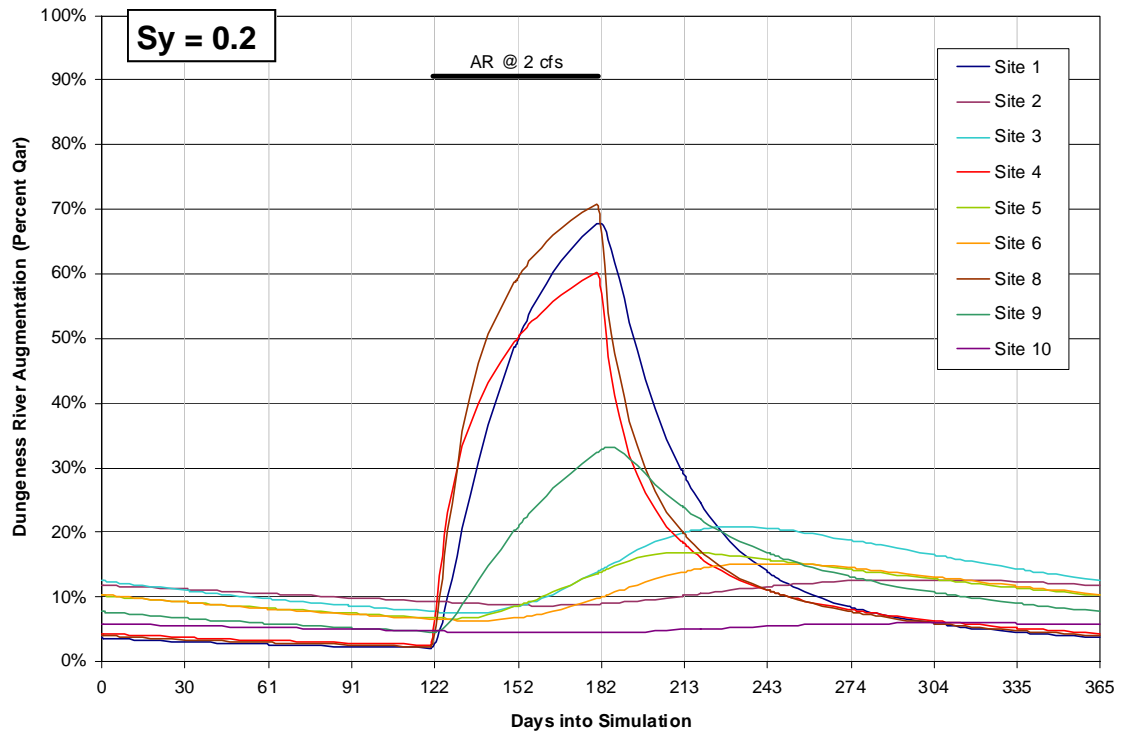
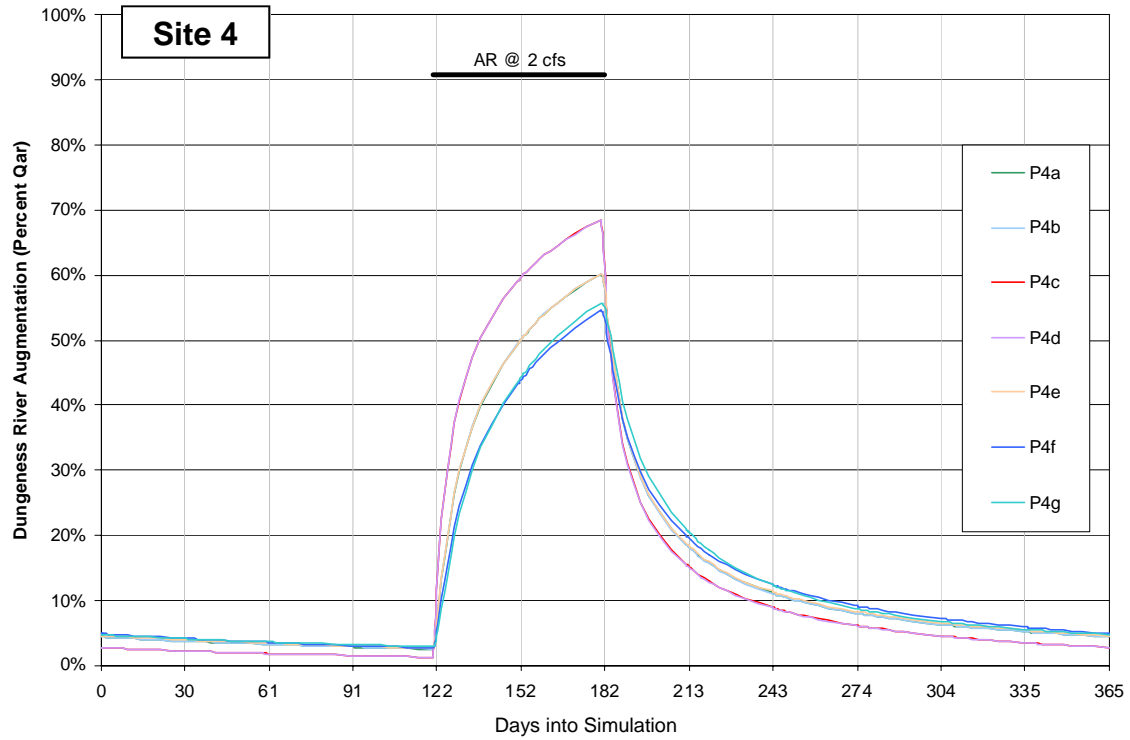
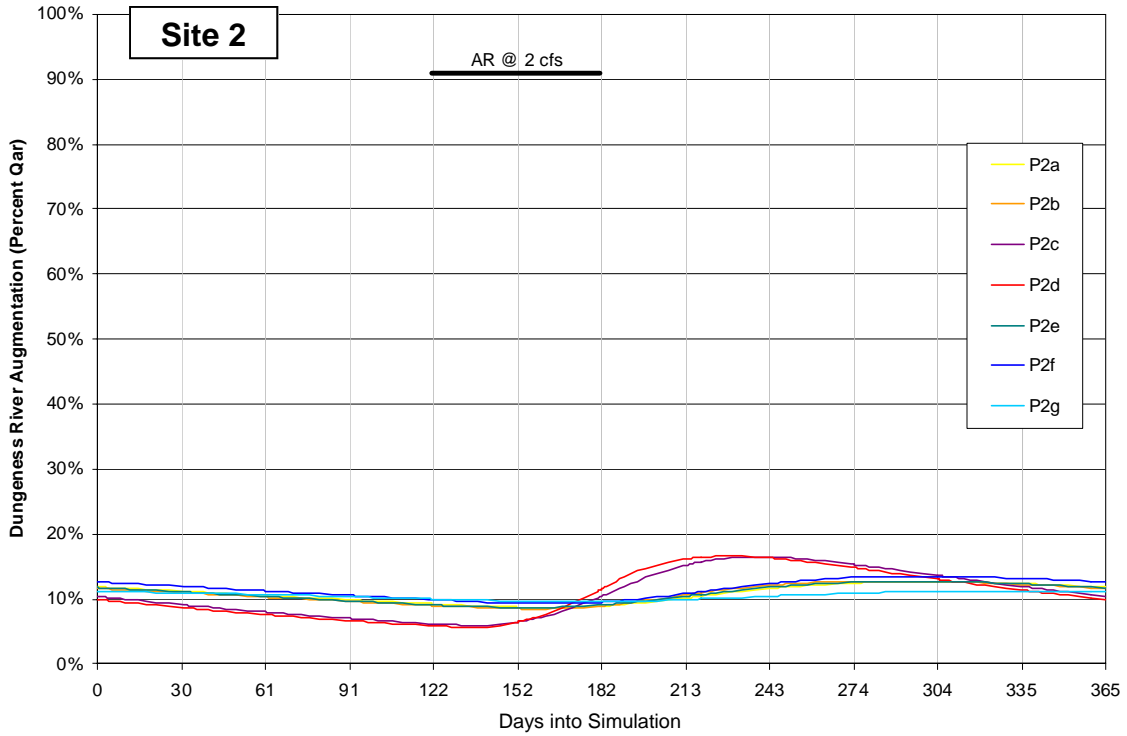


**Figure 7-3**  
**Dungeness River Augmentation from AR (Model Realization "Dung-7e")**



NOTE: See Table 7-1 for explanation of model run ID's.

**Figure 7-4**  
**Model Sensitivity to Key Hydraulic Properties: Sites 2 and 4**

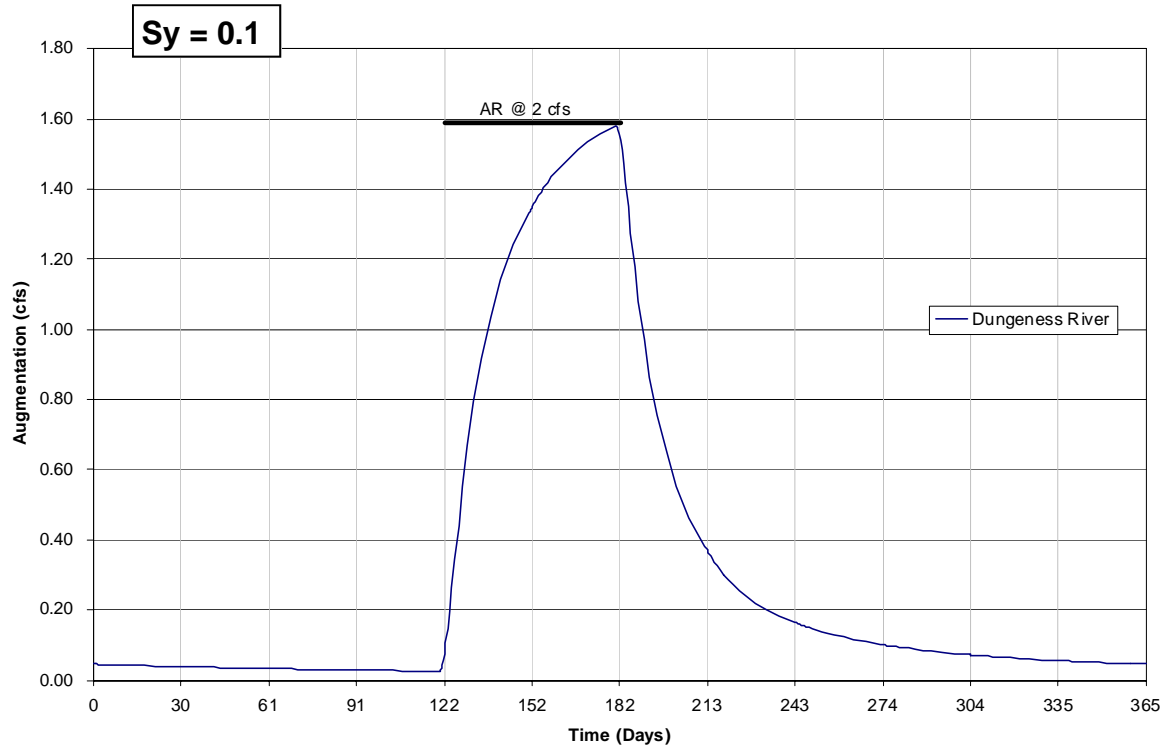
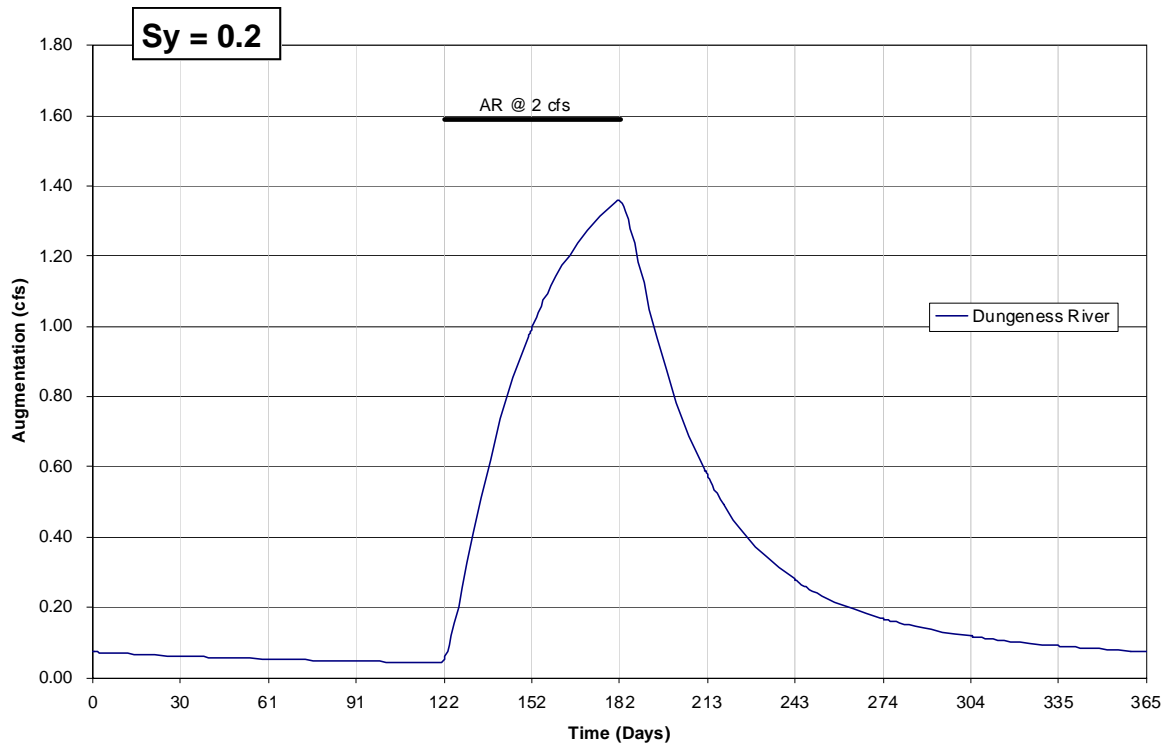


**Figure 7-5**  
**Stream Augmentation from Site 1 AR (Model Realization "Dung-7e")**

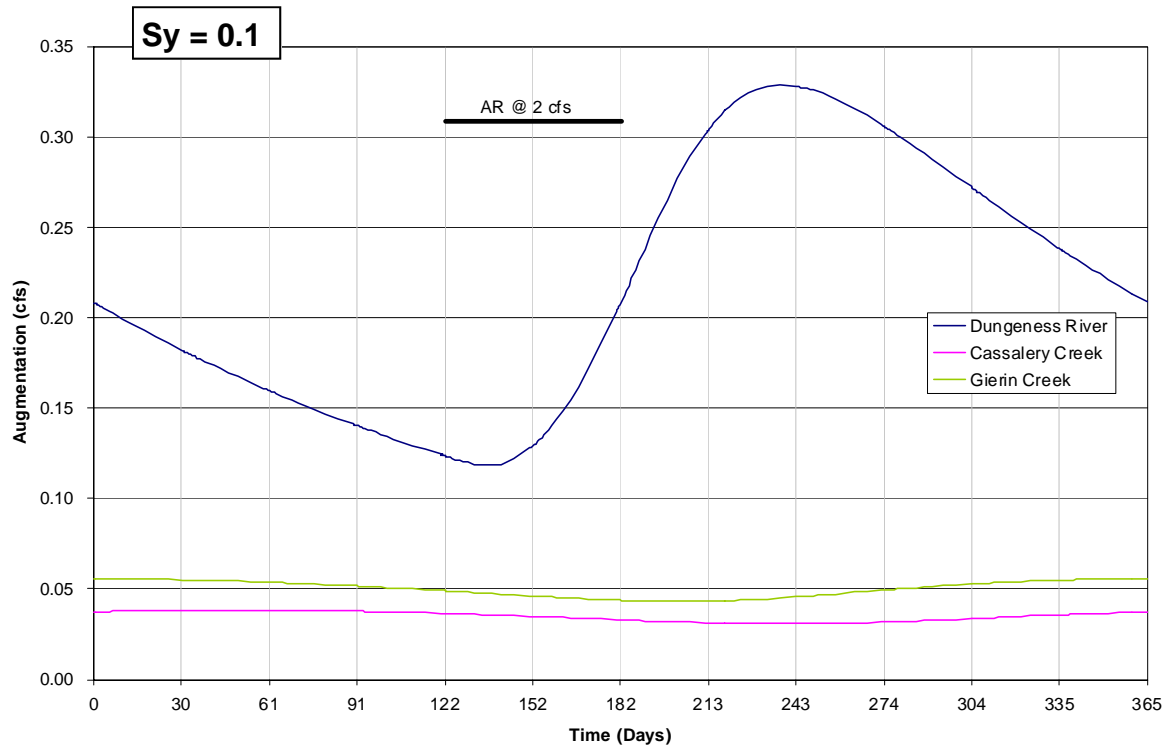
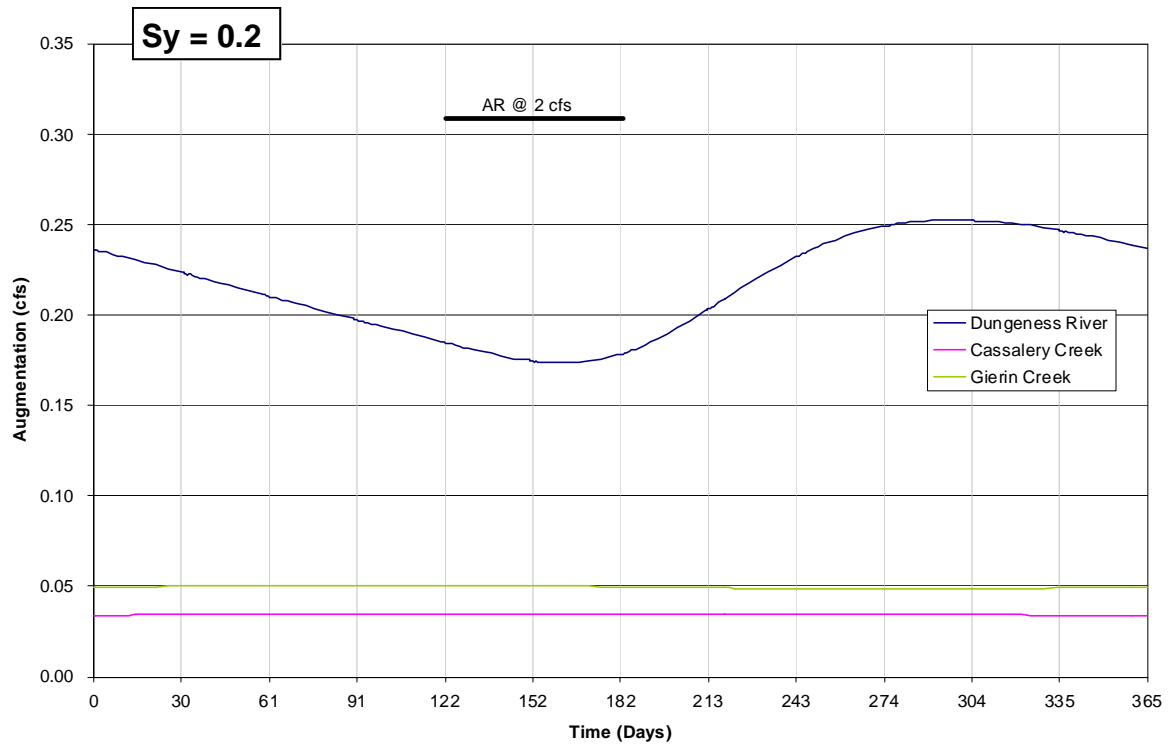


**Figure 7-6**  
**Stream Augmentation from Site 2 AR (Model Realization "Dung-7e")**

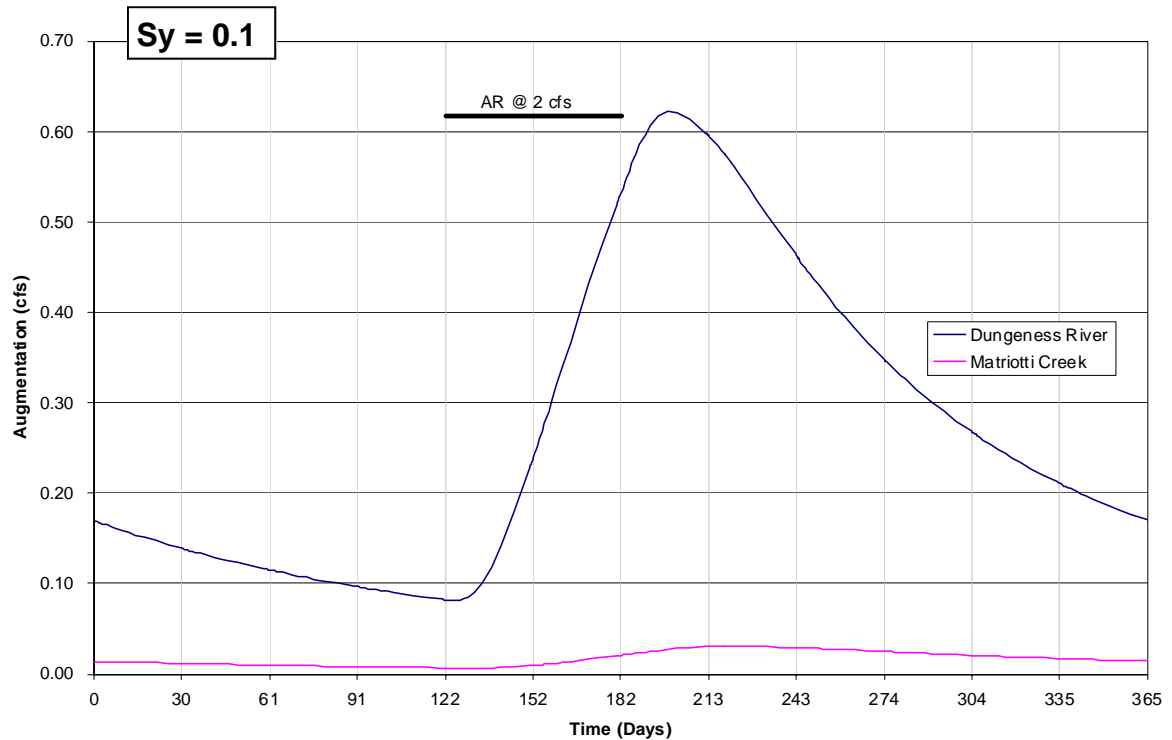
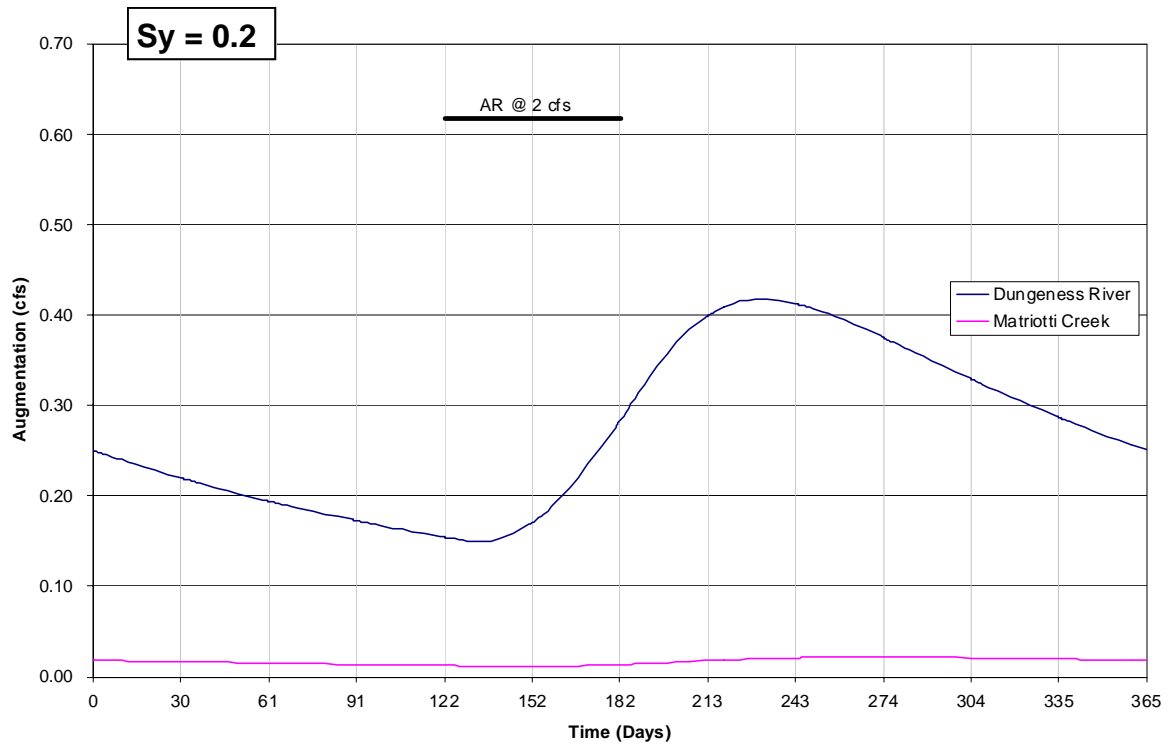


**Figure 7-7**  
**Stream Augmentation from Site 3 AR (Model Realization "Dung-7e")**

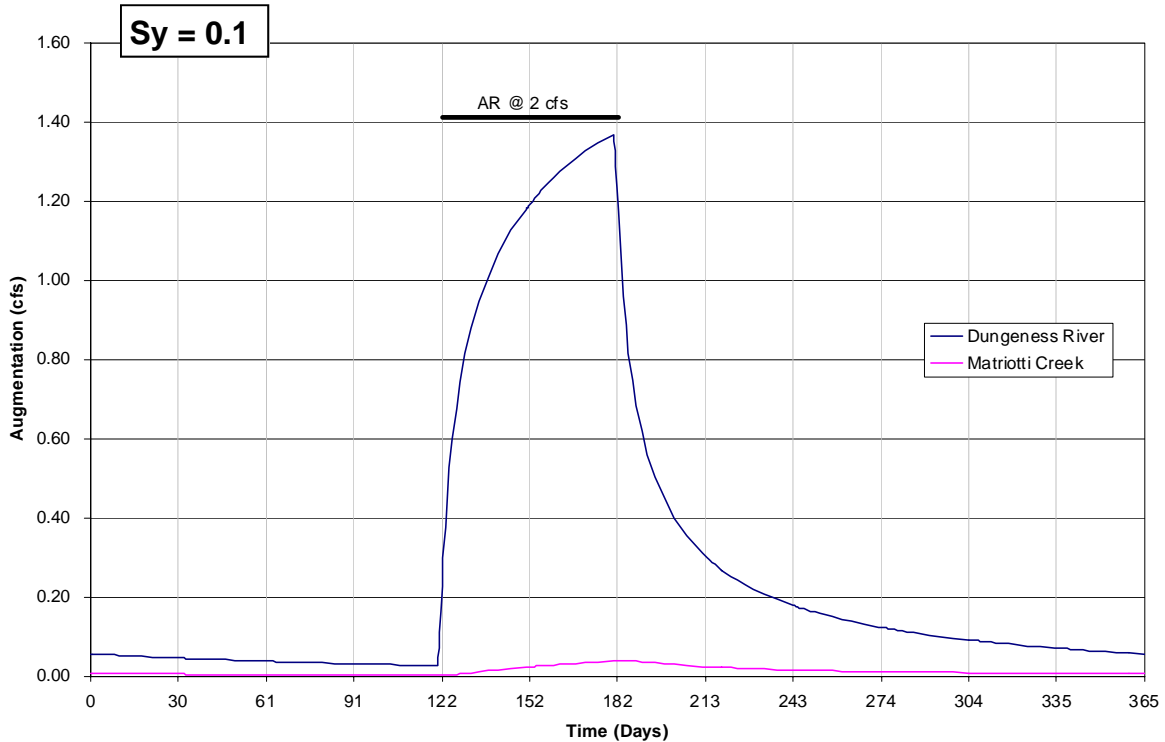
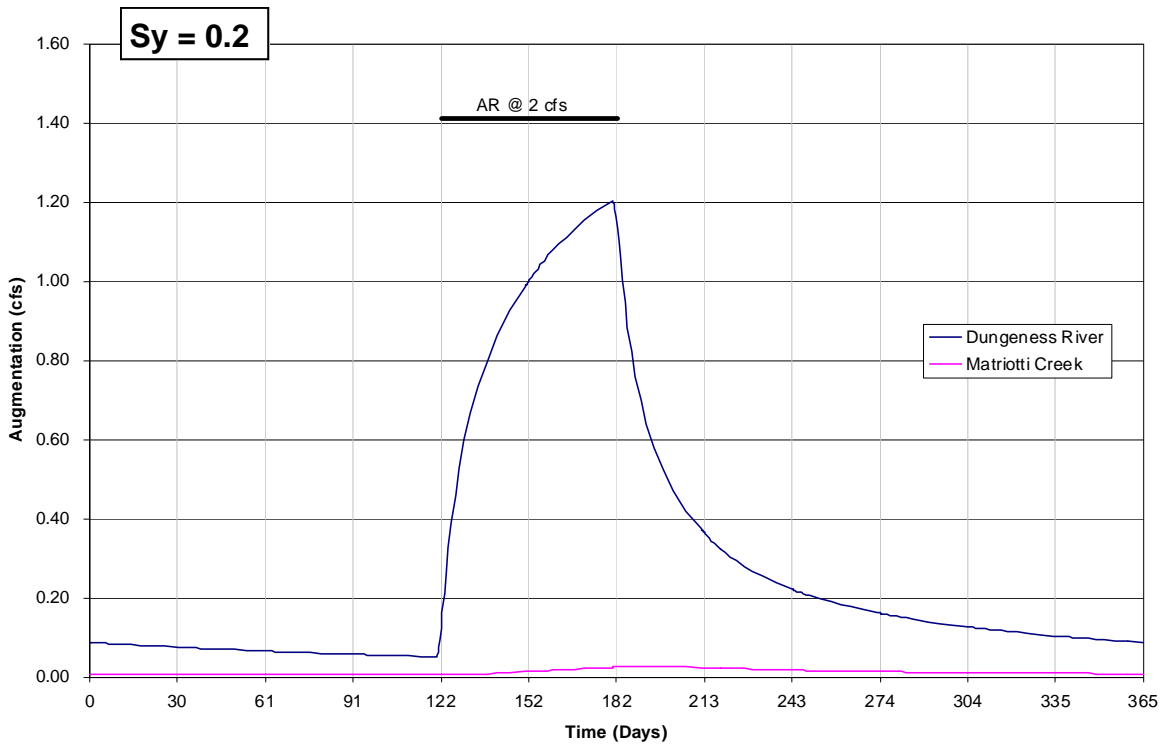


**Figure 7-8**  
**Stream Augmentation from Site 4 AR (Model Realization "Dung-7e")**

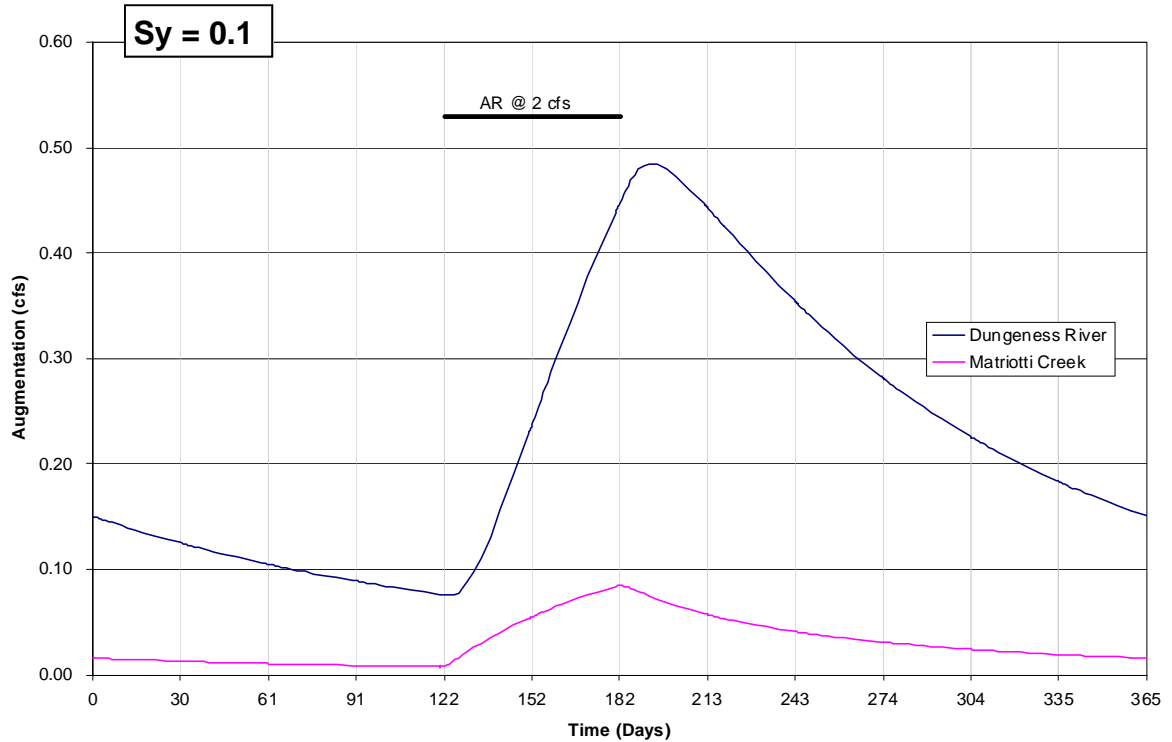
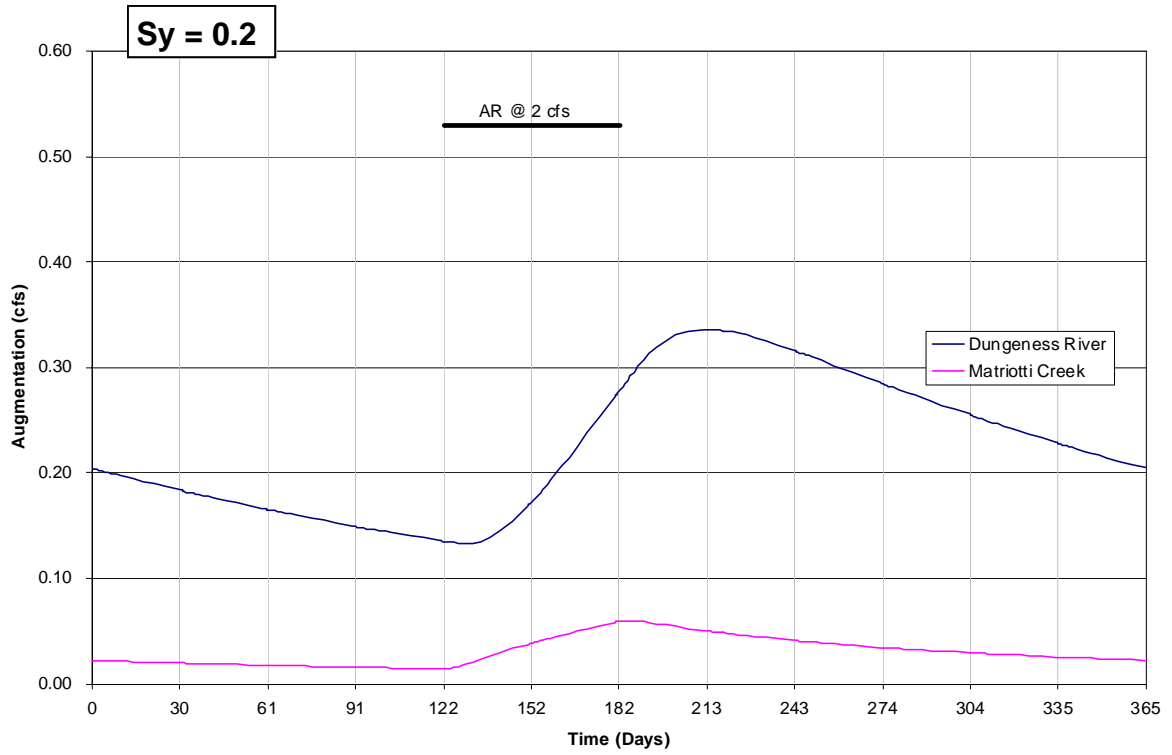


**Figure 7-9**  
**Stream Augmentation from Site 5 AR (Model Realization "Dung-7e")**

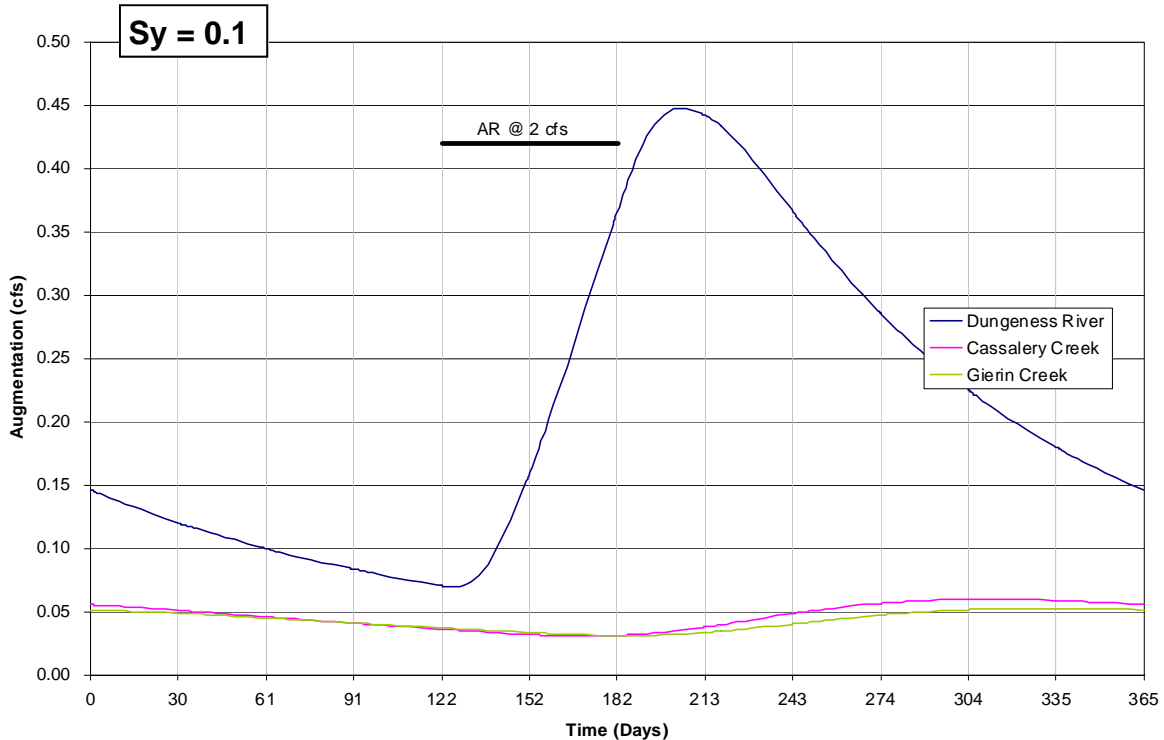
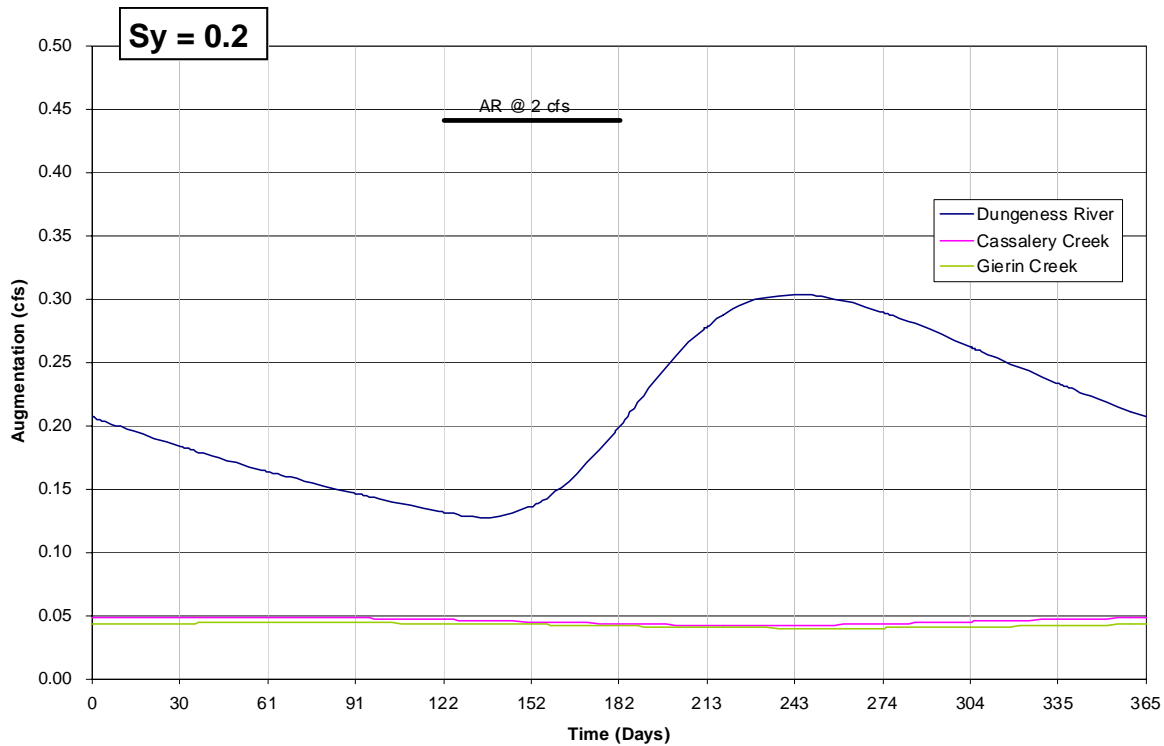


**Figure 7-10**  
**Stream Augmentation from Site 6 AR (Model Realization "Dung-7e")**



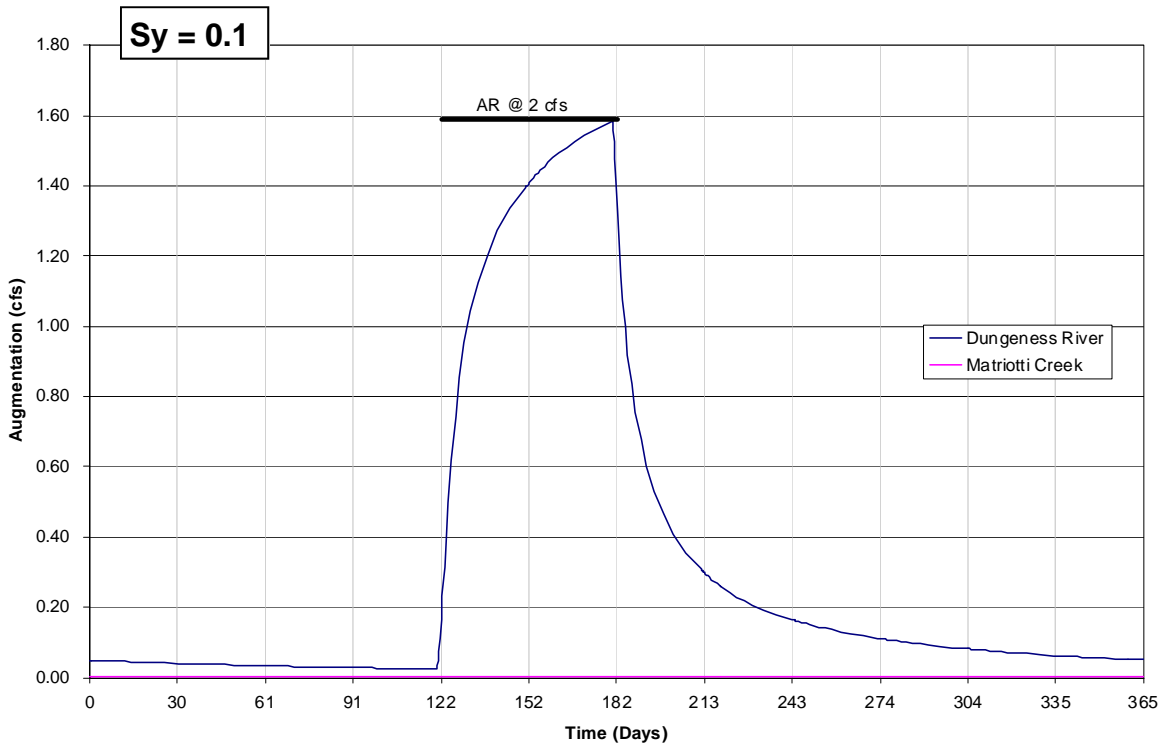
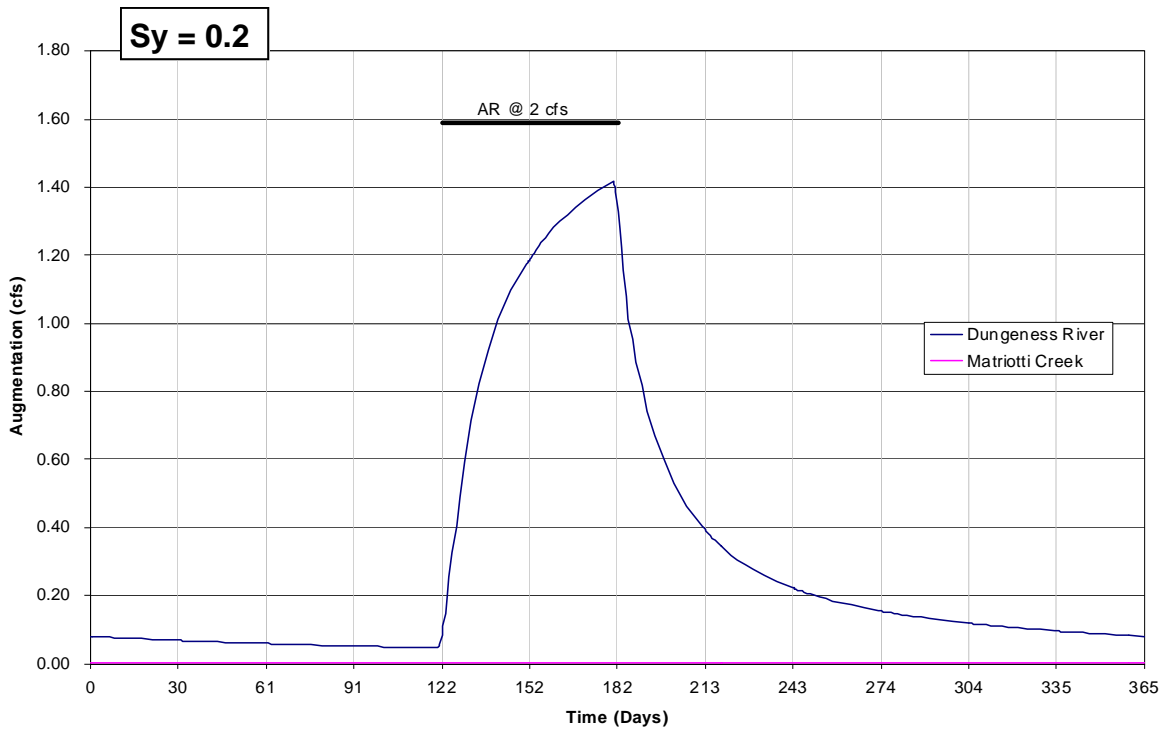


**Figure 7-11**  
**Stream Augmentation from Site 8 AR (Model Realization “Dung-7e”)**

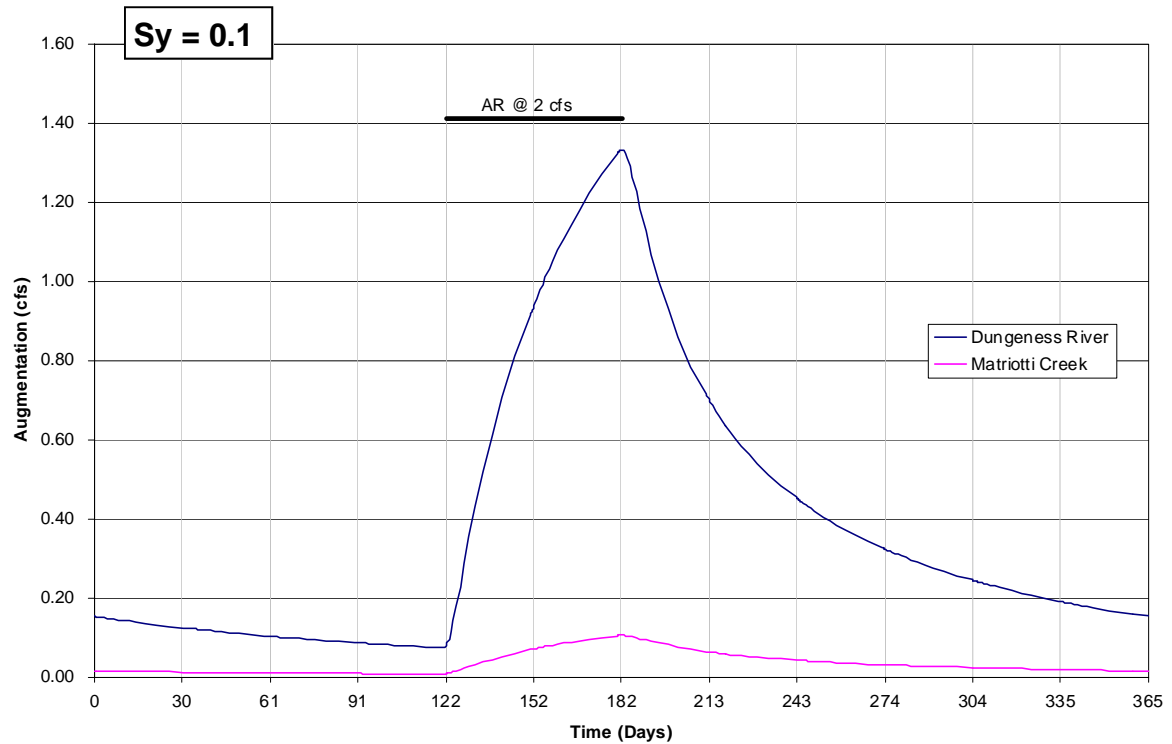
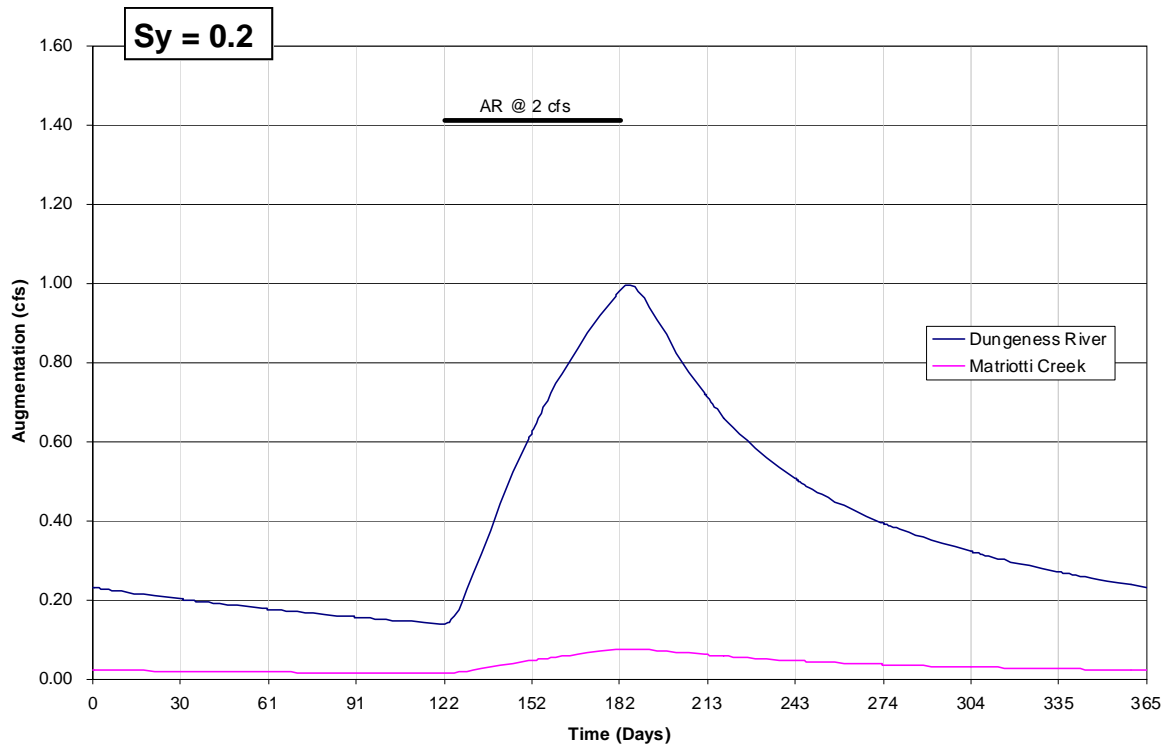


**Figure 7-12**  
**Stream Augmentation from Site 9 AR (Model Realization "Dung-7e")**

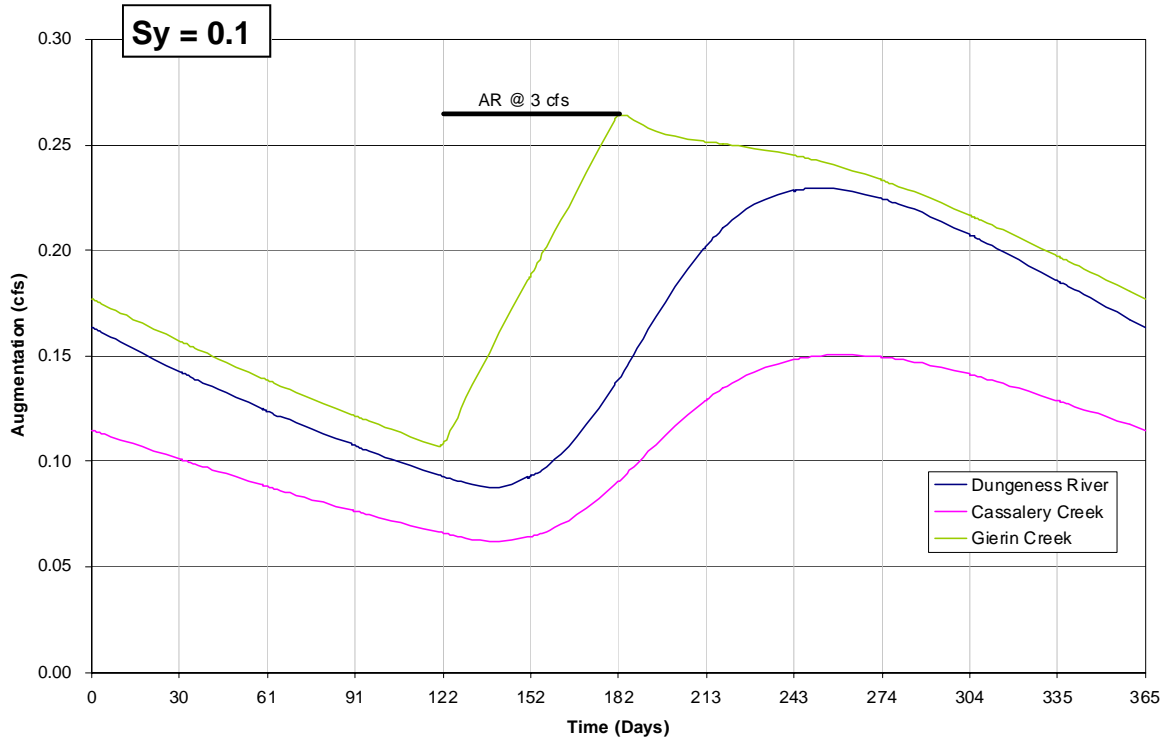
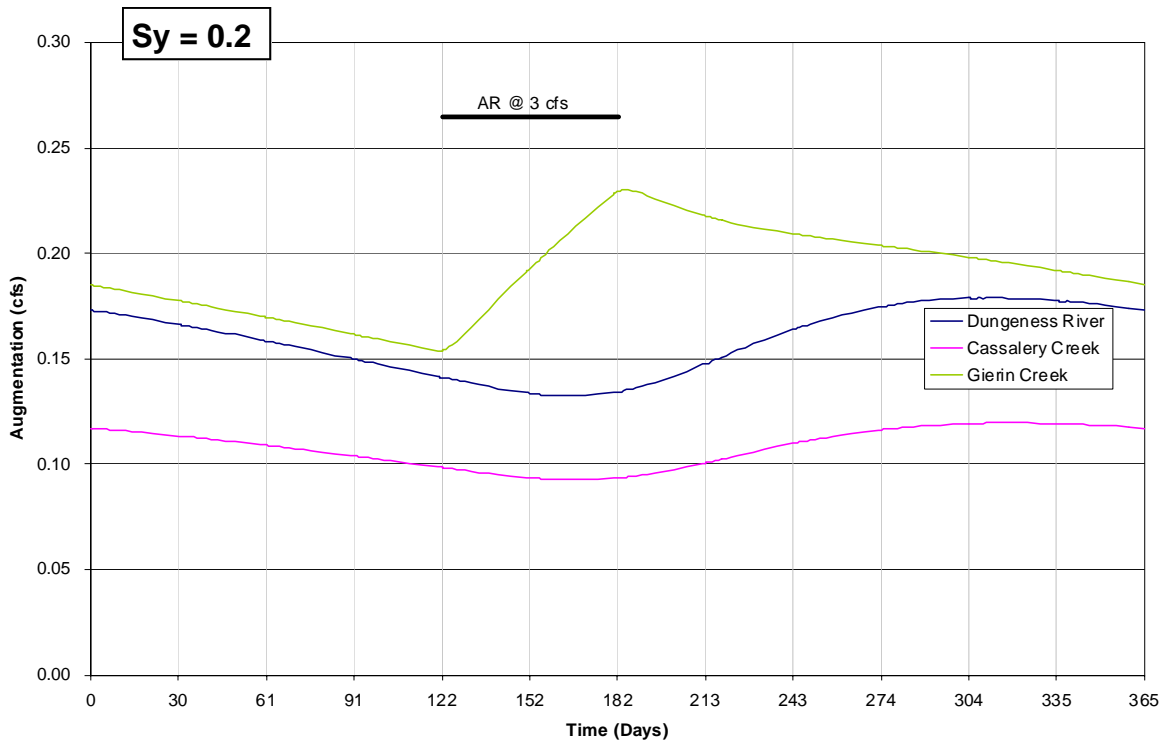
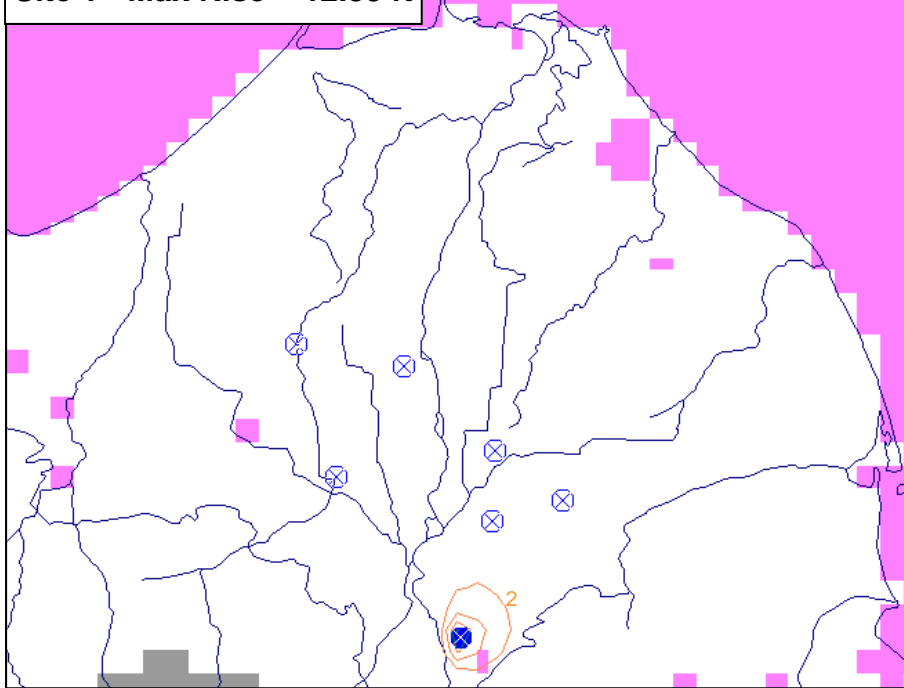
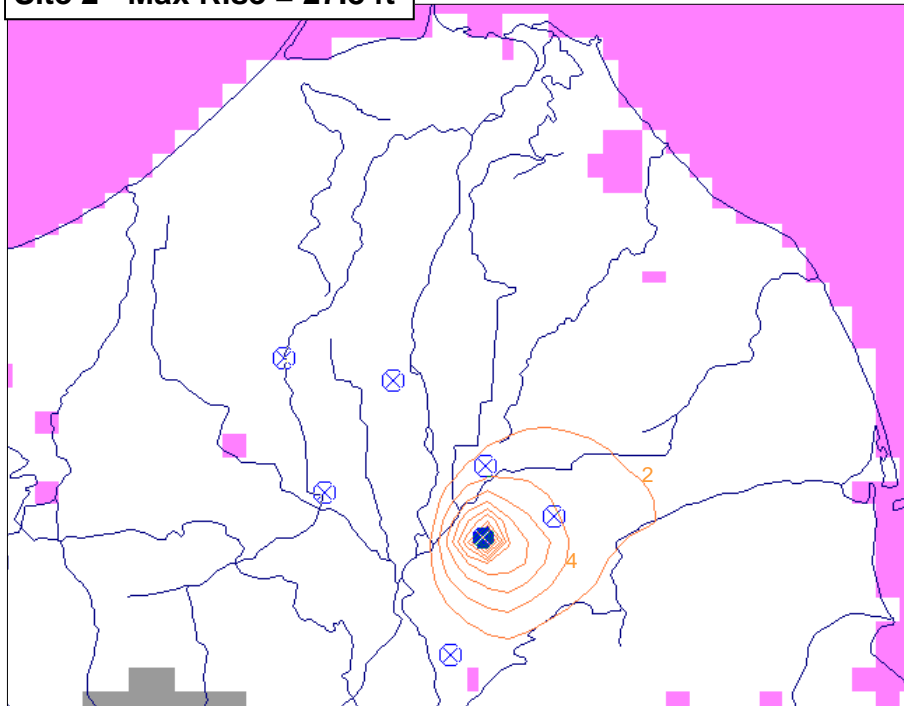


**Figure 7-13**  
**Stream Augmentation from Site 10 AR (Model Realization "Dung-7e")**

Site 1 - Max Rise = 12.85 ft



Site 2 - Max Rise = 27.8 ft



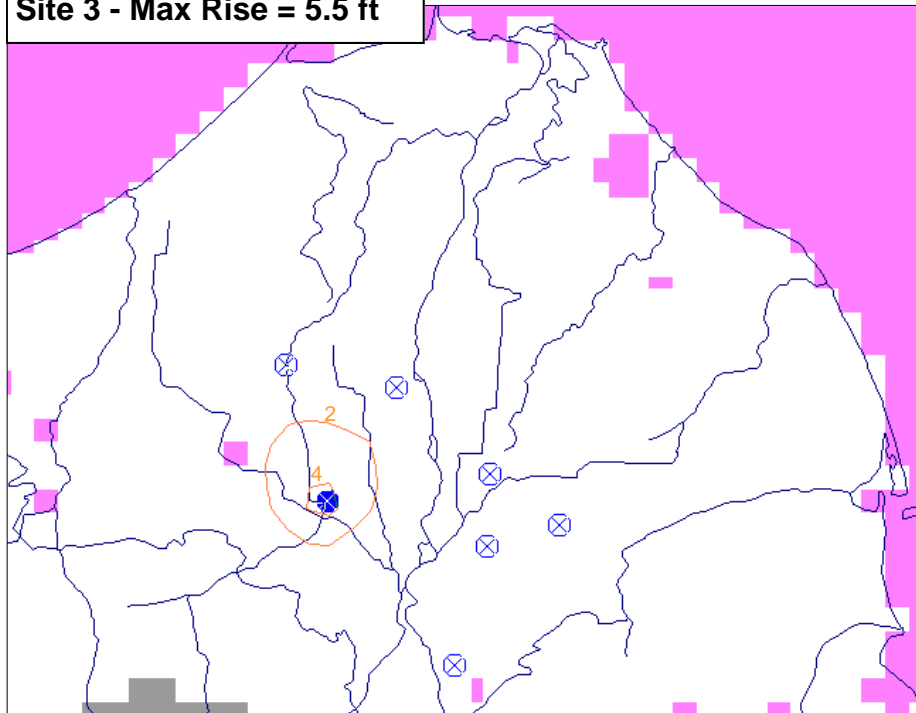
NOTES:

Model Simulations  
Performed with Re-  
alization "Dung-7e"

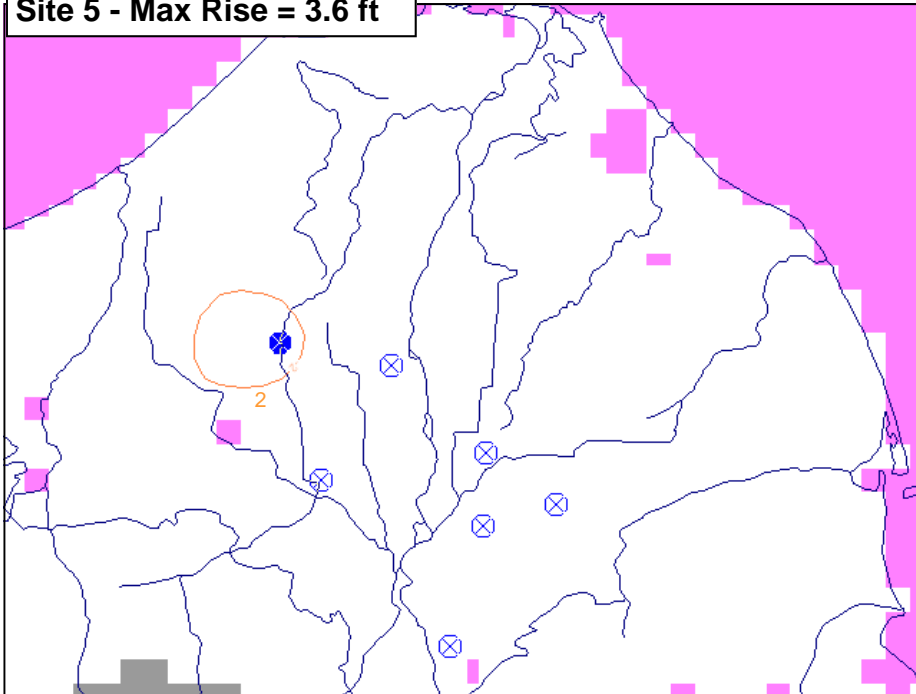
Contour  
Interval = 2 ft

**Figure 7-14**  
**Steady State Mounding from 2 cfs AR at Sites 1 and 2**

Site 3 - Max Rise = 5.5 ft



Site 5 - Max Rise = 3.6 ft



NOTES:

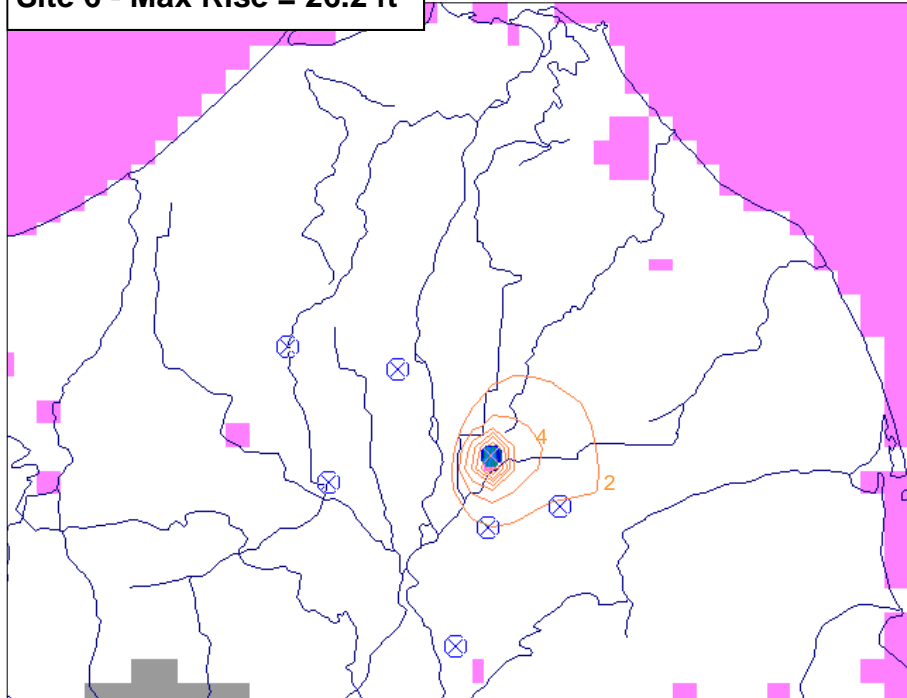
Model Simulations  
Performed with Re-  
alization "Dung-7e"

Contour  
Interval = 2 ft

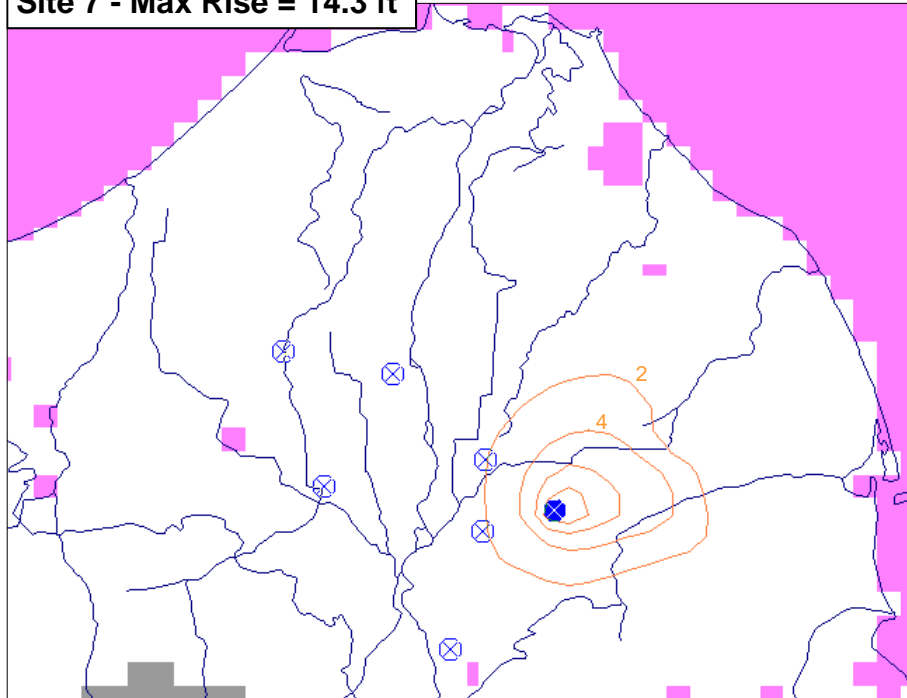
No map prepared  
for Site 4: Max Rise  
= 1.9 feet.

**Figure 7-15**  
**Steady State Mounding from 2 cfs AR at Sites 3 and 5**

**Site 6 - Max Rise = 26.2 ft**



**Site 7 - Max Rise = 14.3 ft**

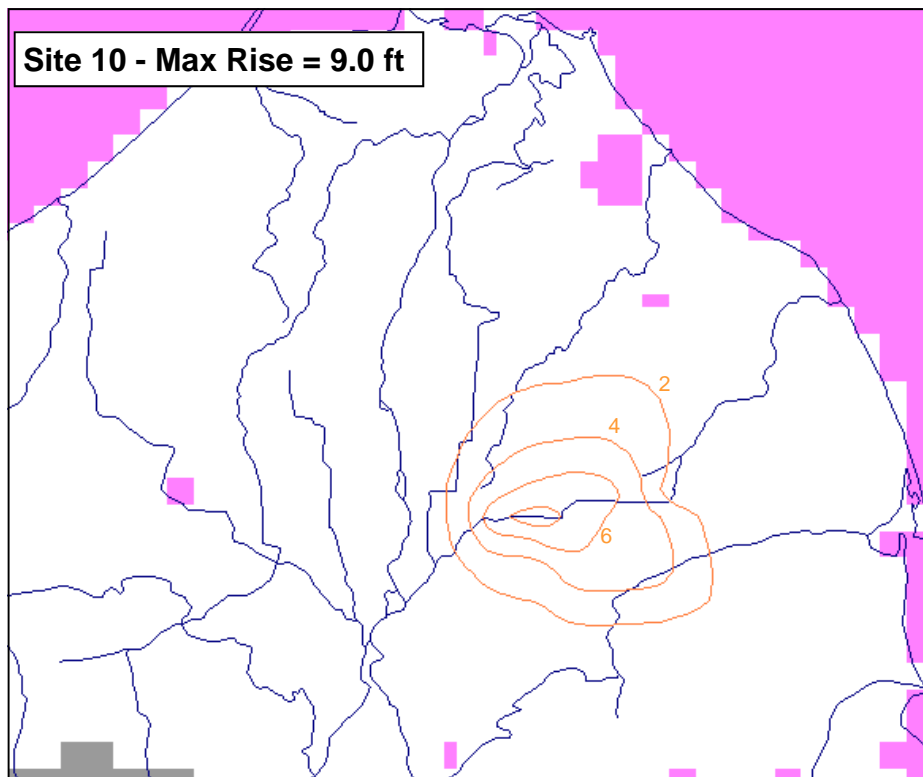
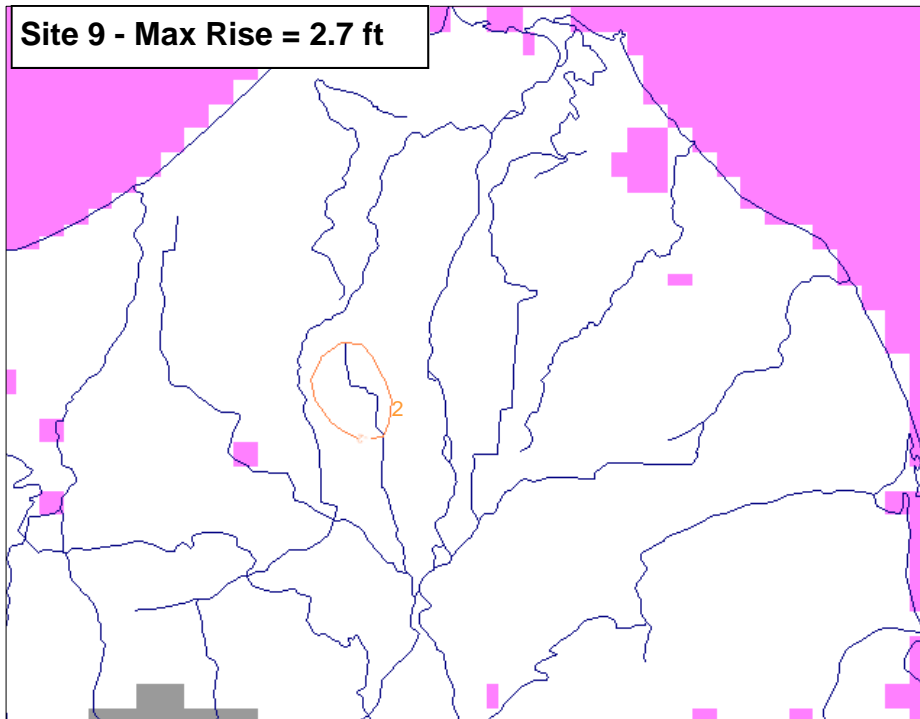


**NOTES:**

Model Simulations  
Performed with Realization "Dung-7e"

Contour  
Interval = 2 ft

**Figure 7-16  
Steady State Mounding from 2 cfs AR at Sites 6 and 7**



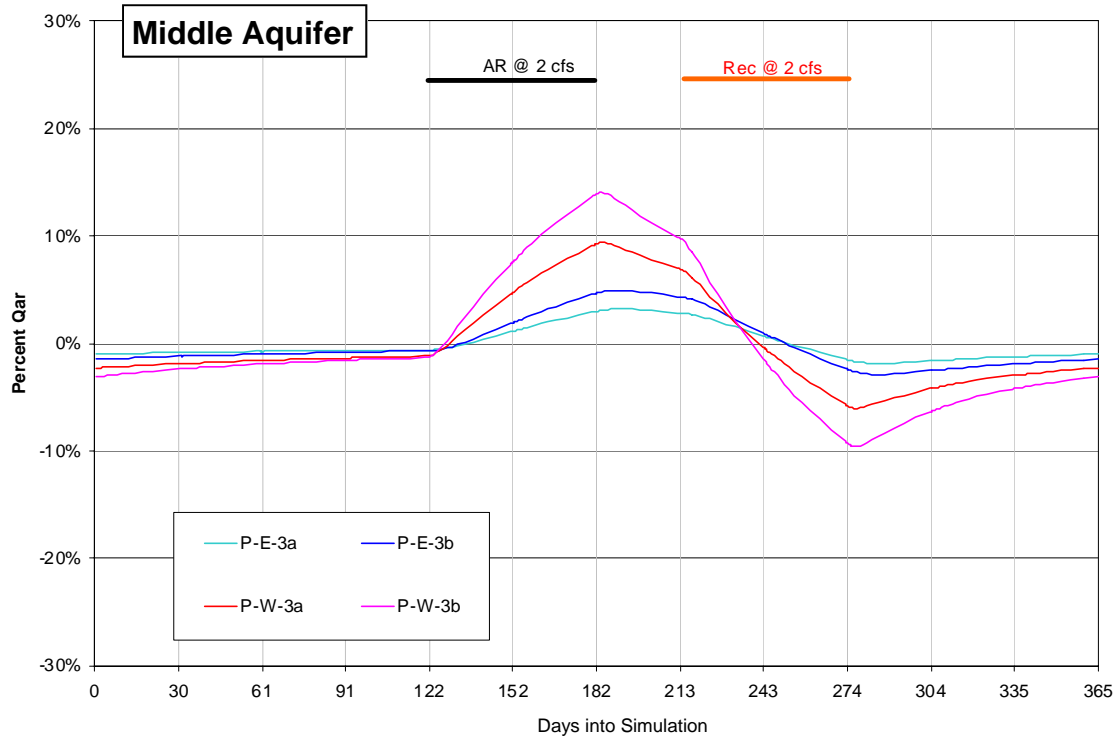
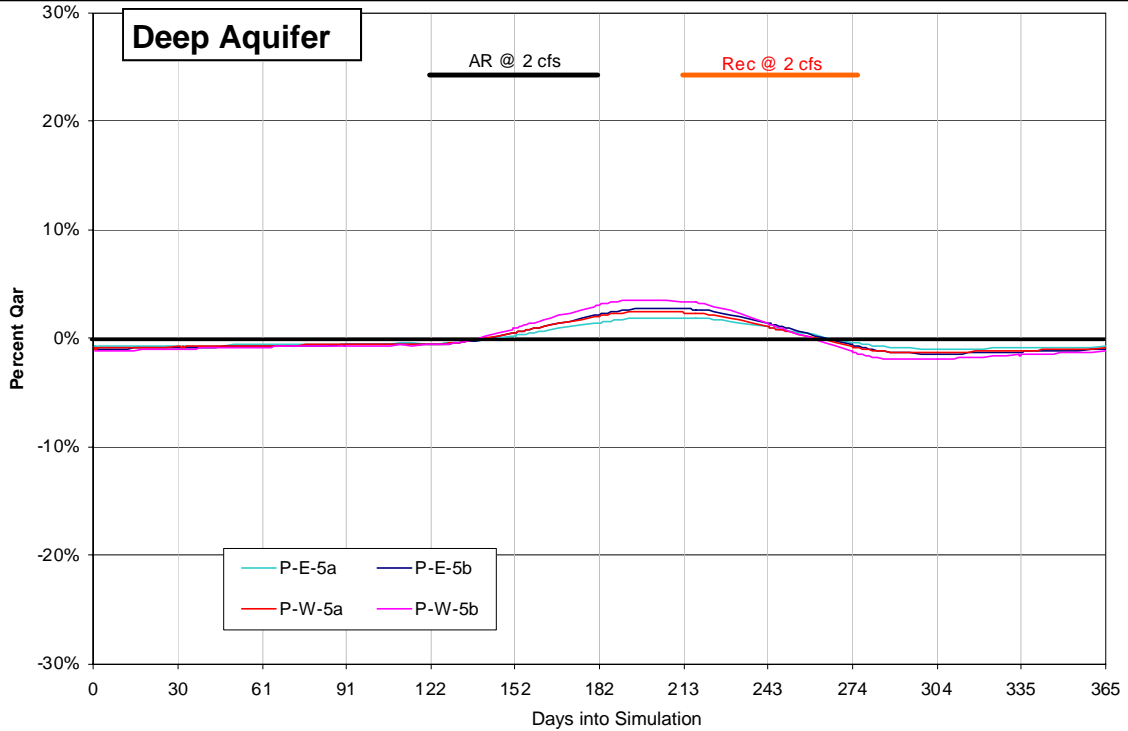
**NOTES:**

Model Simulations  
Performed with Realization "Dung-7e"

Contour  
Interval = 2 ft

No map prepared for  
Site 8: Max Rise = 2.7  
feet.

**Figure 7-17  
Steady State Mounding from 2 cfs AR at Sites 9 and 10**

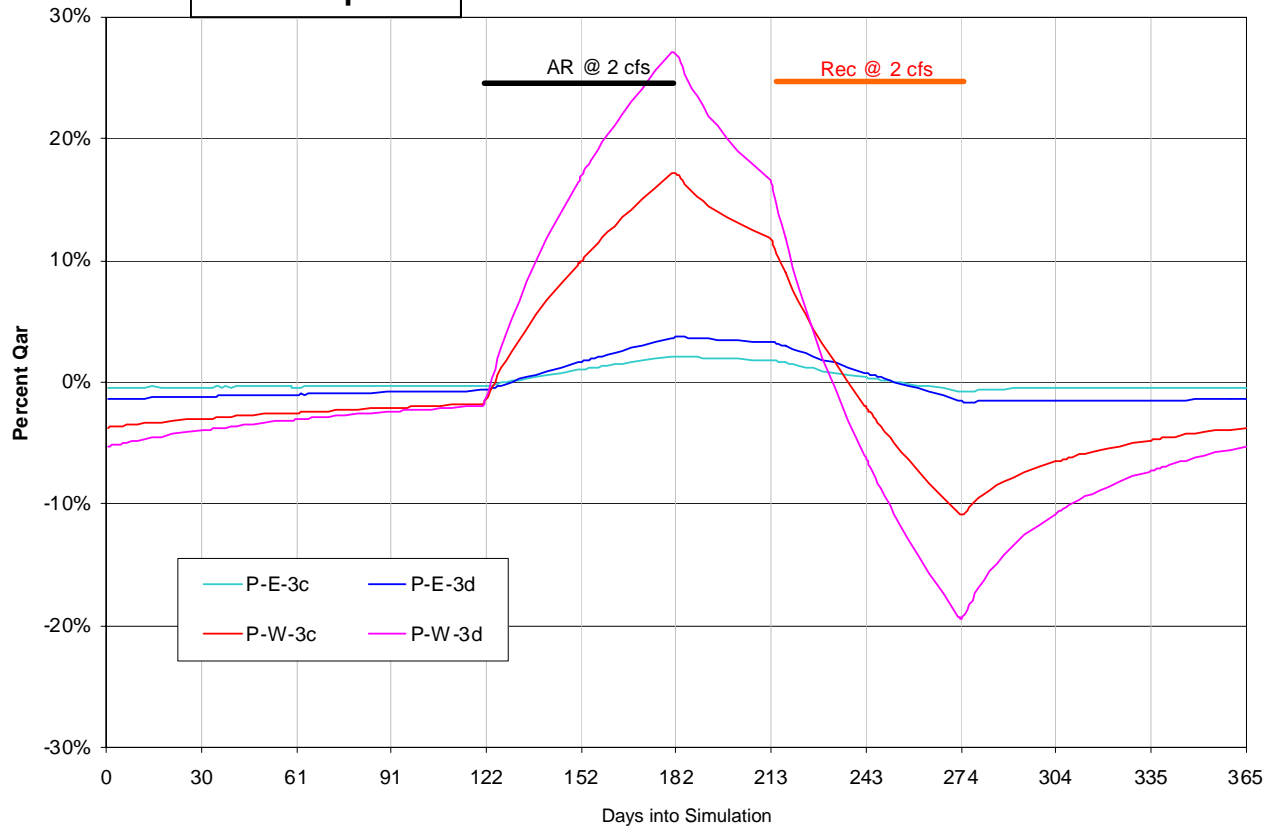


NOTE: See Table 7-4 for model run name ID's.

**Figure 7-18  
Dungeness River Augmentation from ASR (Model Realization "Dung-7e")**



### Middle Aquifer



NOTE: See Table 7-4 for model run name ID's.

**Figure 7-19**  
**Dungeness River Augmentation from ASR (Model Realization "Dung-7g")**

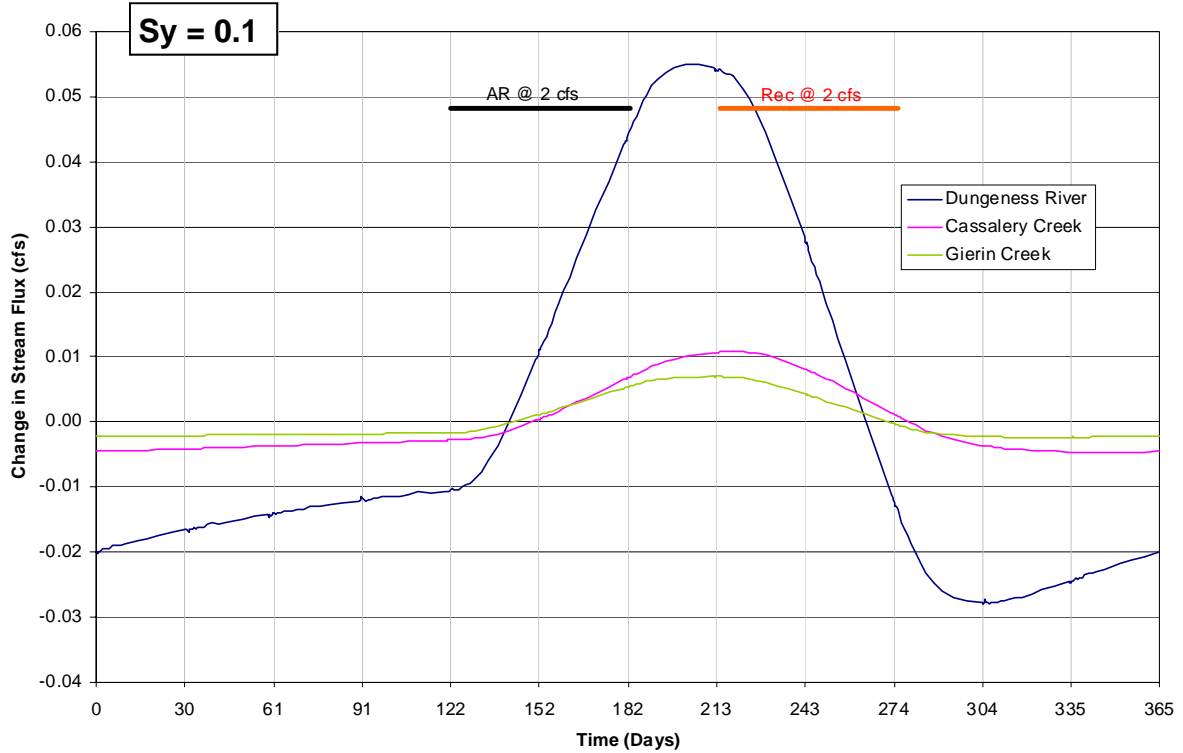
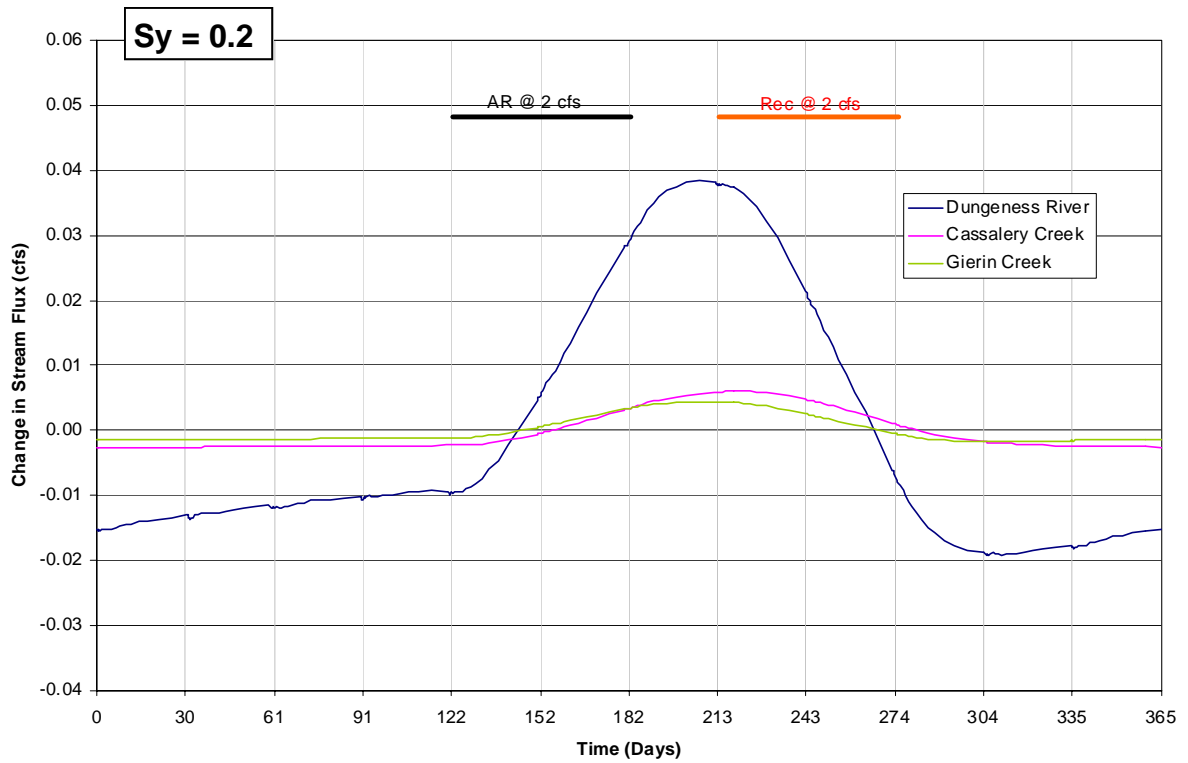


**Figure 7-20**  
**Streamflow Augmentation from East-Site ASR in Layer 5 (“Dung-7e”)**

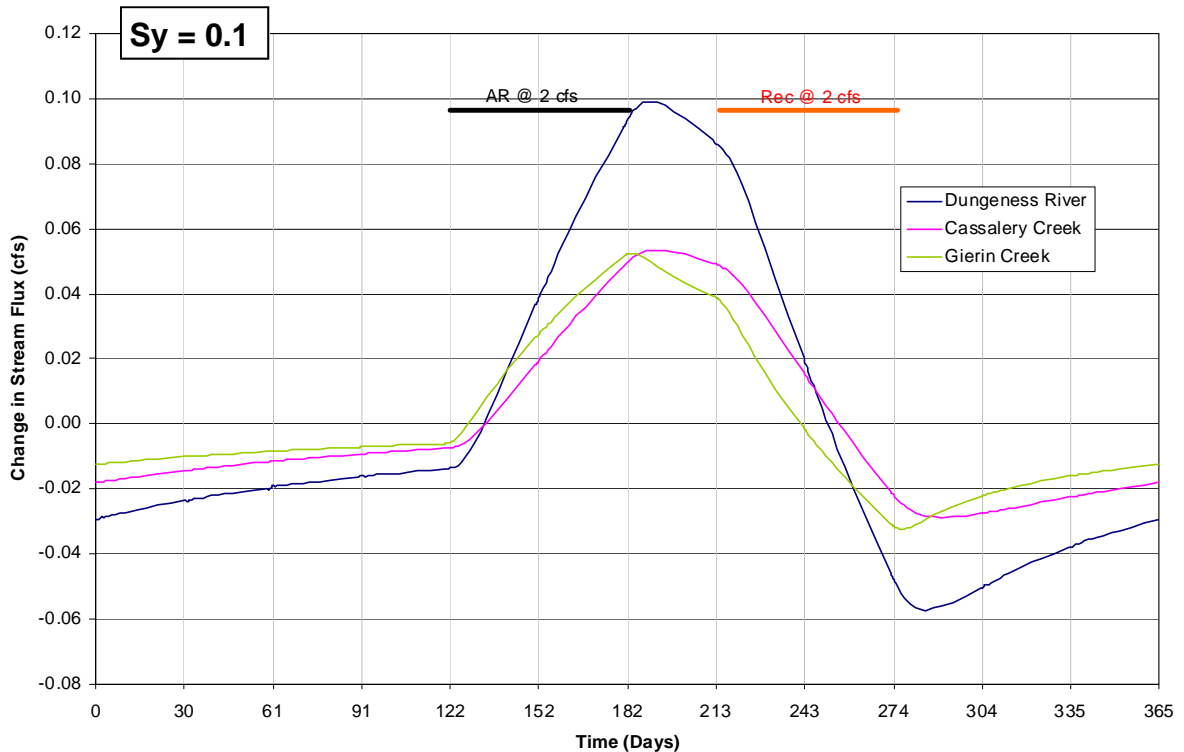
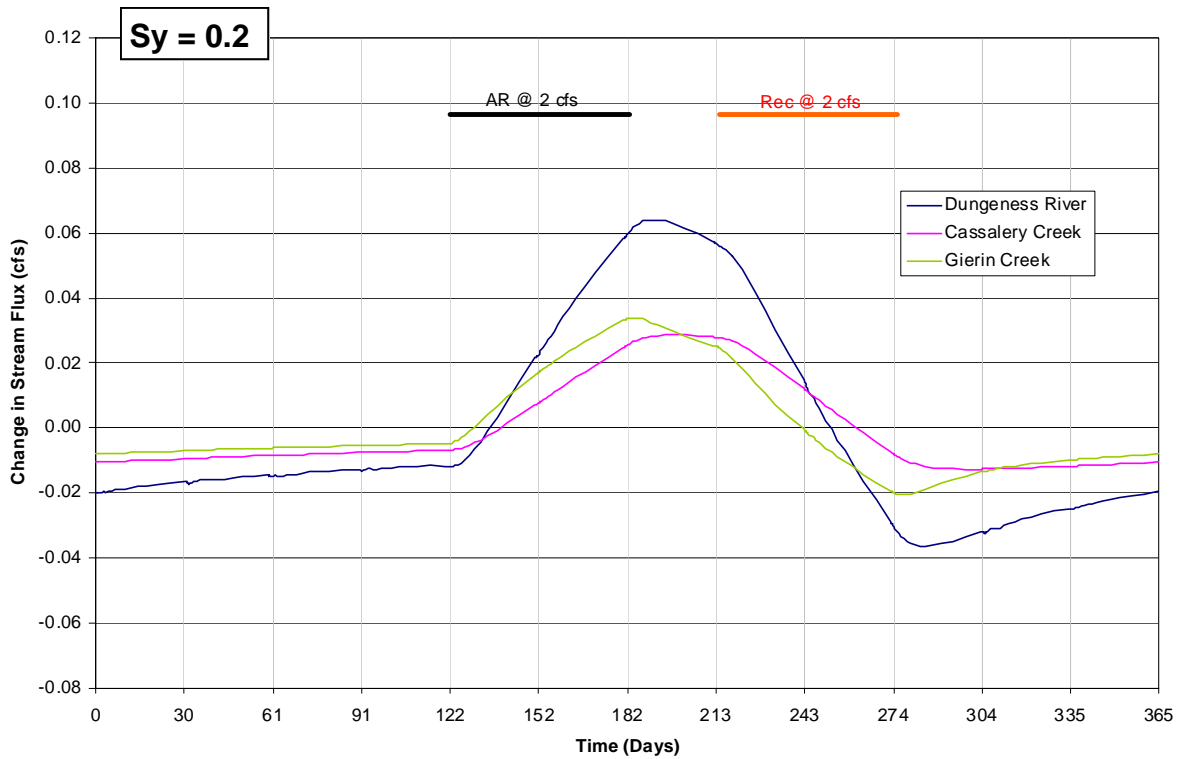


**Figure 7-21**  
**Streamflow Augmentation from East-Site ASR in Layer 3 (“Dung-7e”)**

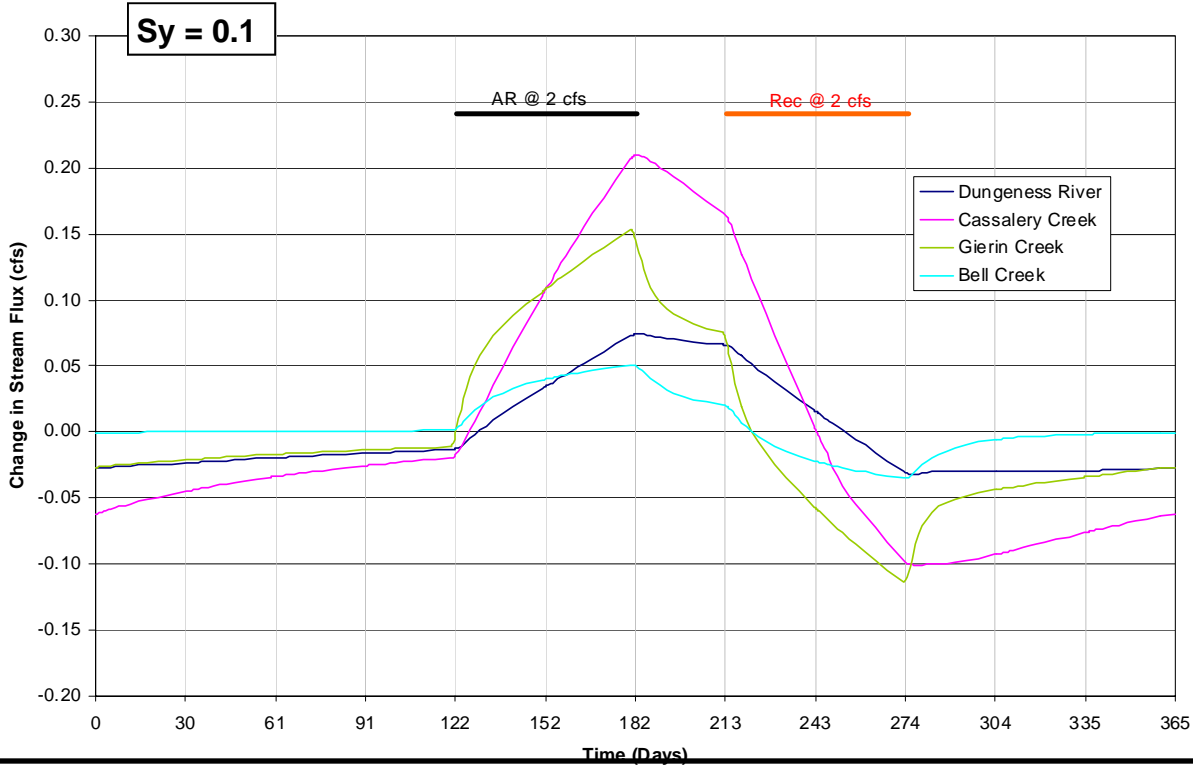
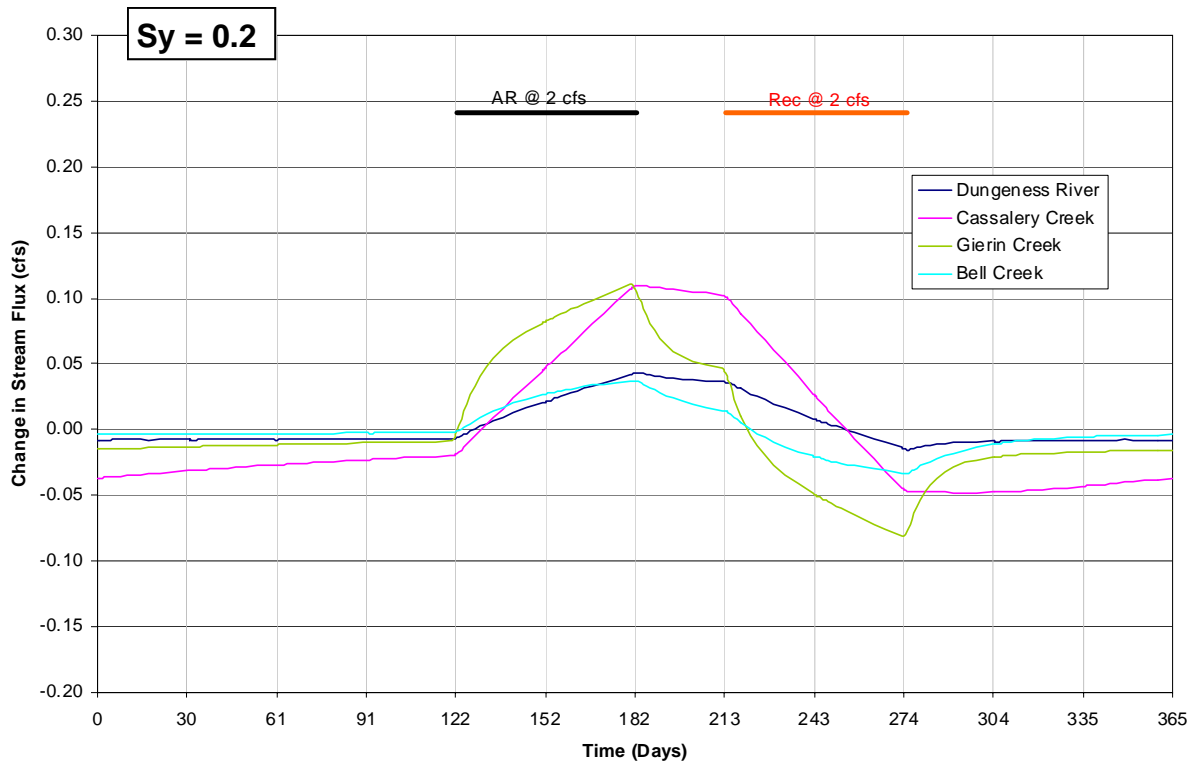


**Figure 7-22**  
**Streamflow Augmentation from East-Site ASR in Layer 3 (“Dung-7g”)**

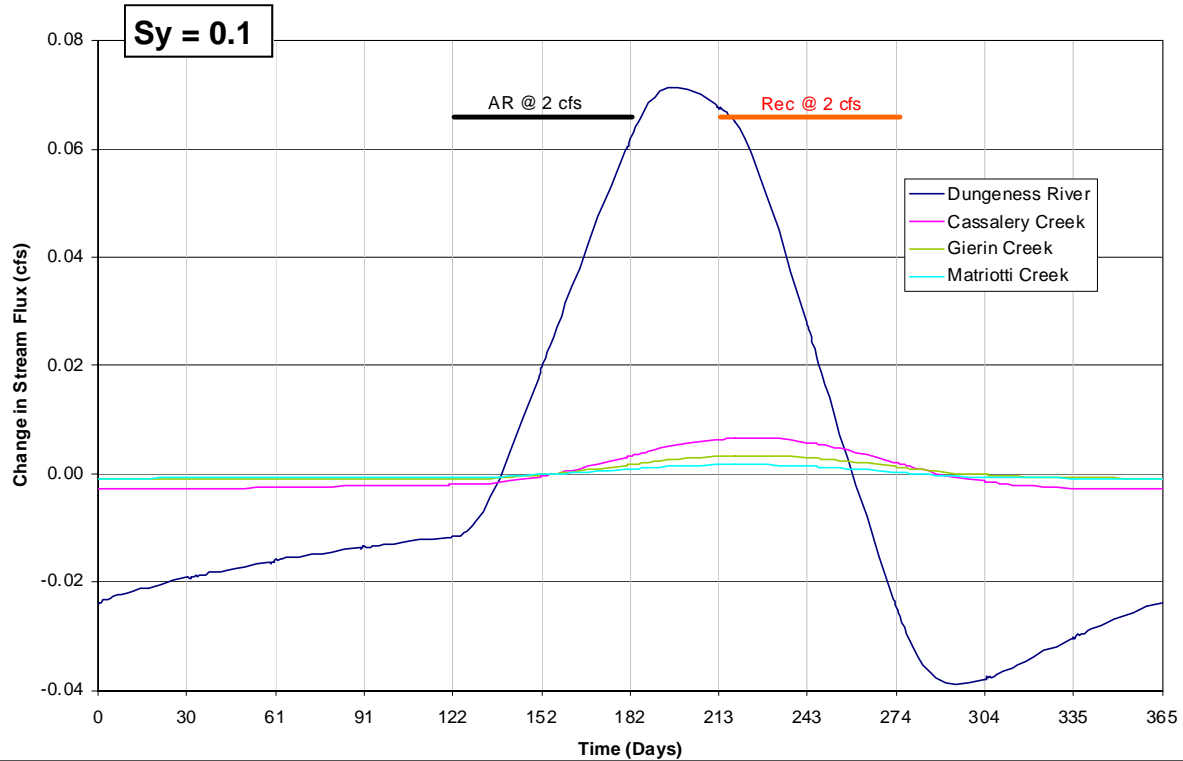
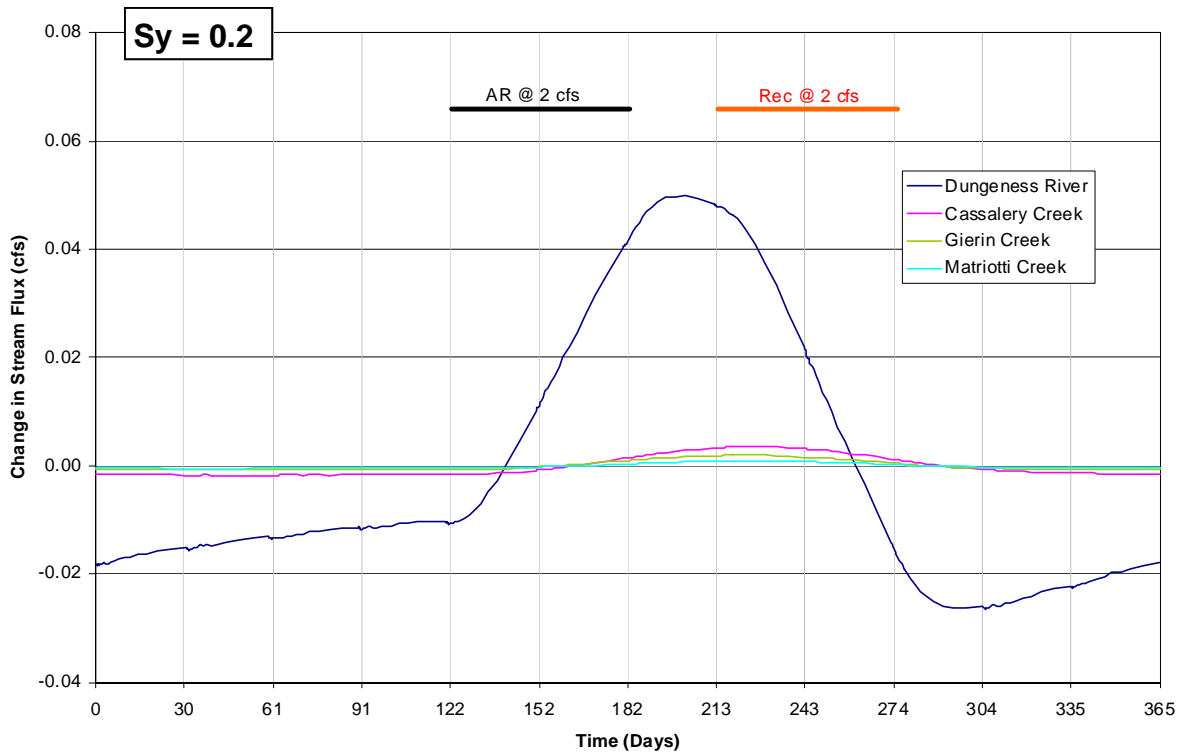


**Figure 7-23**  
**Streamflow Augmentation from West-Site ASR in Layer 5 (“Dung-7e”)**

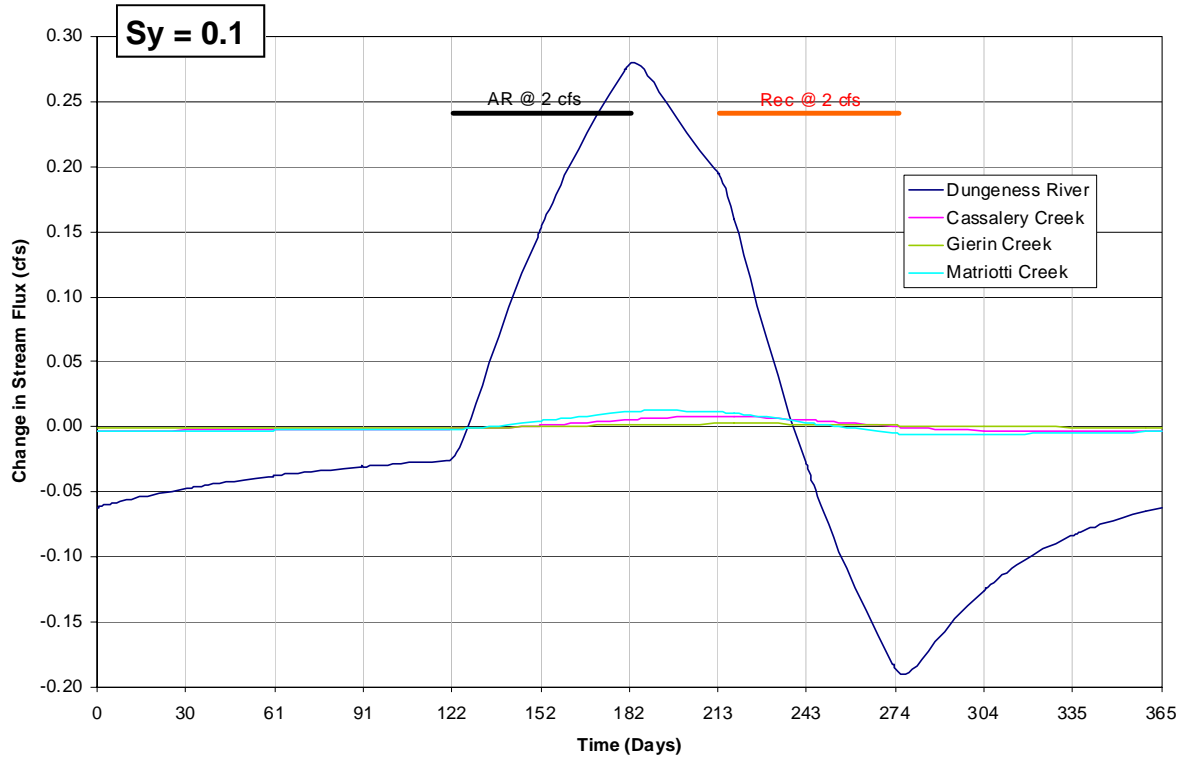
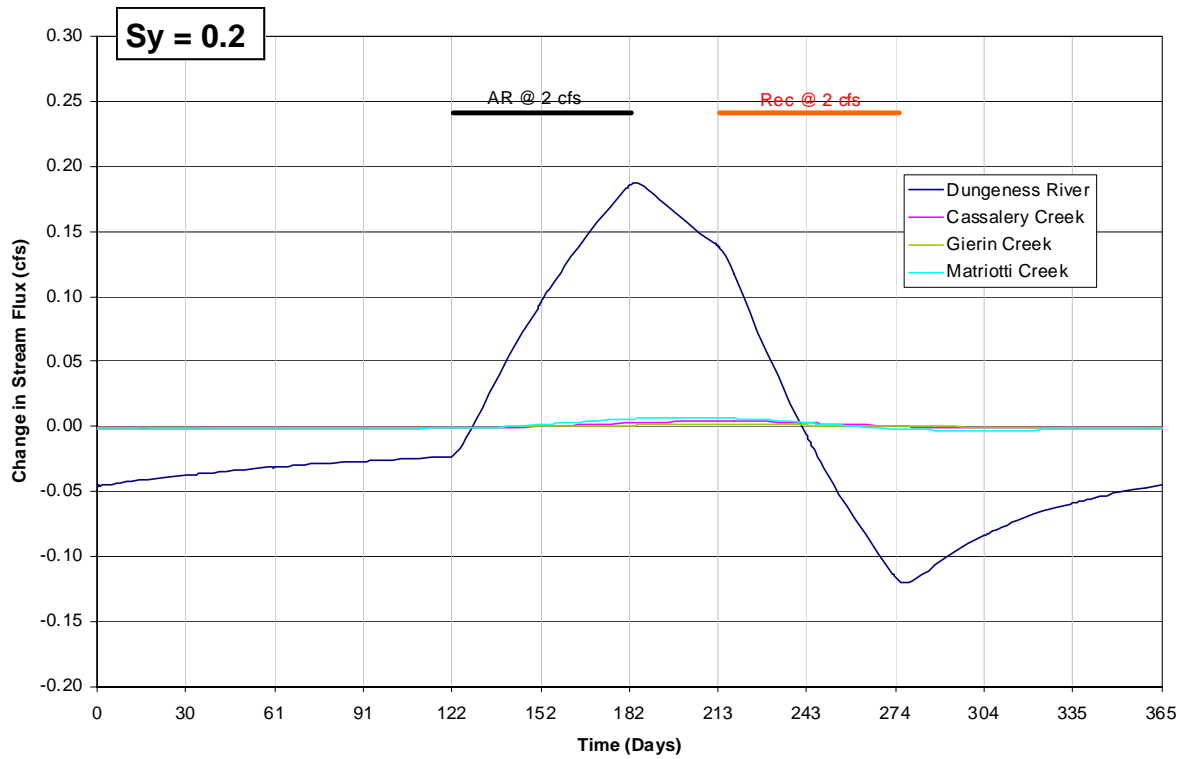


**Figure 7-24**  
**Streamflow Augmentation from West-Site ASR in Layer 3 (“Dung-7e”)**

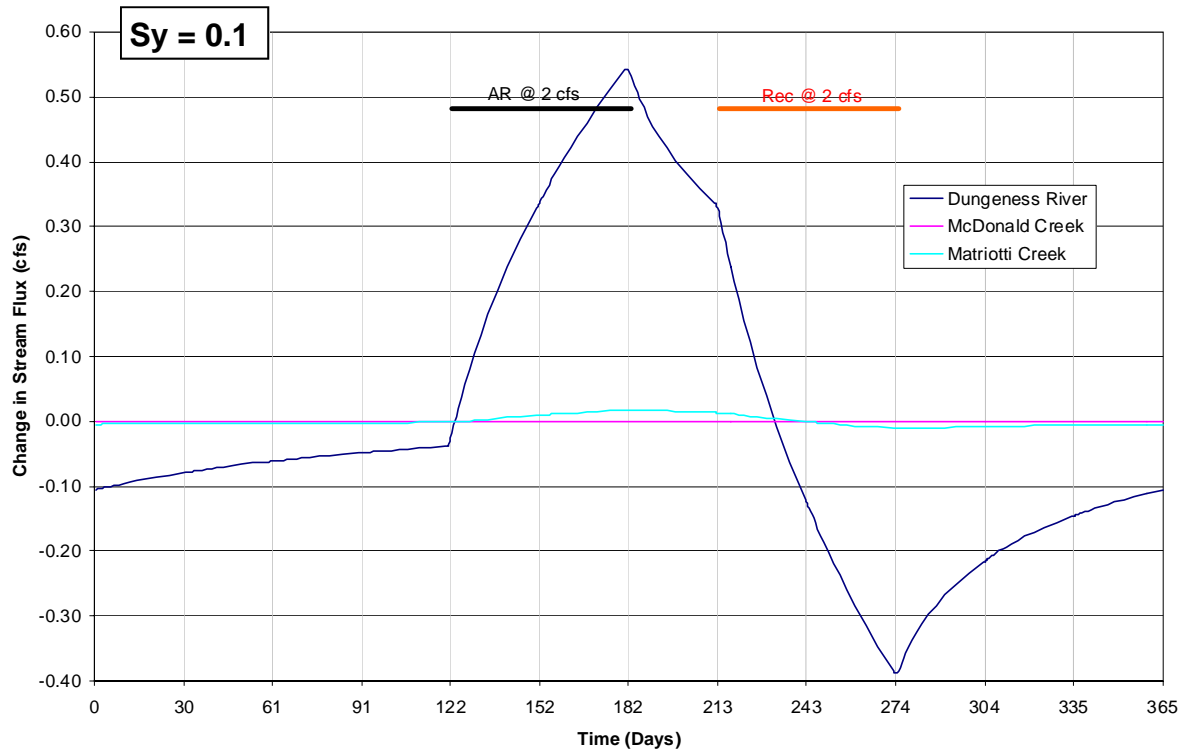
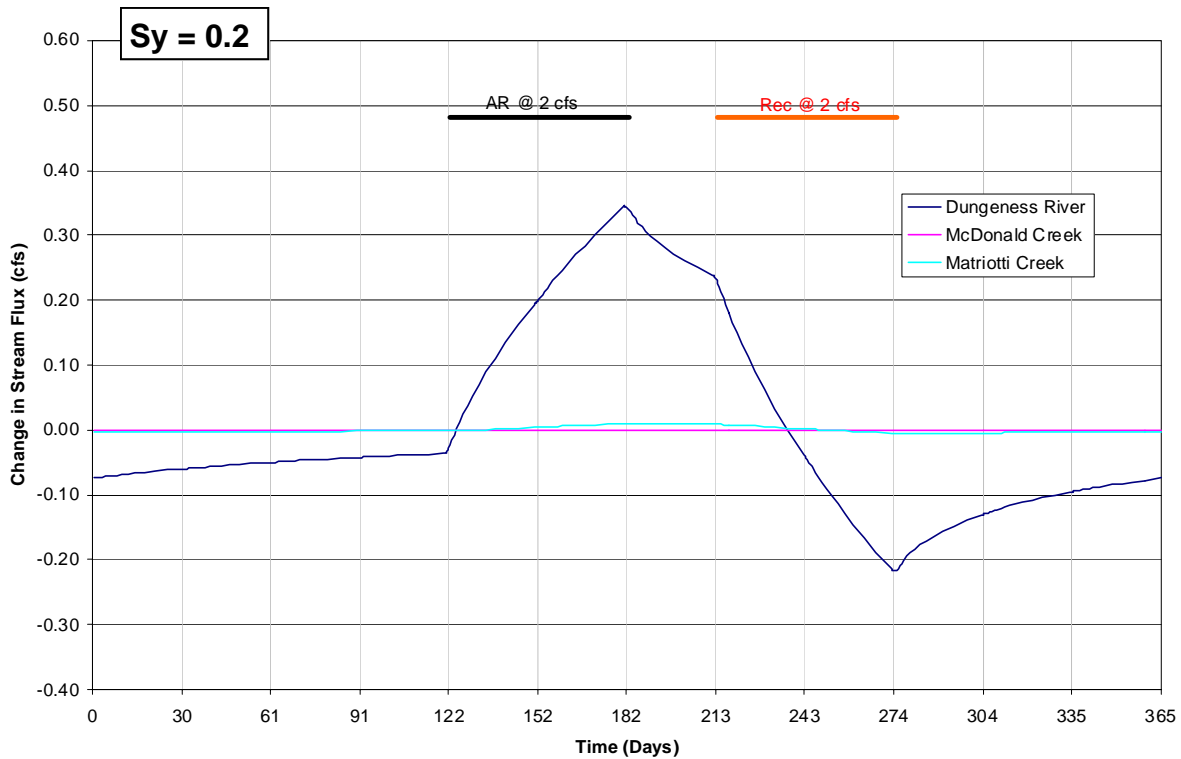


**Figure 7-25**  
**Streamflow Augmentation from West-Site ASR in Layer 3 (Dung-7g)**

## **APPENDIX A**

### **MODEL LAYERING, BEDROCK DISTRIBUTION AND MARINE CONNECTIONS**



## APPENDIX A

### MODEL LAYERING, BEDROCK DISTRIBUTION AND MARINE CONNECTIONS

During model refinement, PGG first redefined layer elevations over the entire model domain and then performed three subsequent localized adjustments. This process is documented below. **Figures A-1** through **A-4** show the elevations of the model layer interfaces, and **Figures A-5** through **A-7** show the saturated thicknesses of the model layers.

#### Initial Definition of Model Layer Elevations

PGG initially defined model layer elevations over the entire model domain with the approach described below. All elevations are in NAVD88. Reference to work performed by the USGS pertains to Thomas et al (1999). USGS GIS coverages for this analysis were provided by Clallam County. Abbreviations used in this appendix include: TTFW (work performed by TetraTech Foster-Wheeler for the 2003 model), GV (Groundwater Vistas), Xsec (cross section), L1 (e.g. “layer 1”), L1-Top (top of layer 1), L1-Bot (bottom of layer 1), etc.

1. The top of layer 1 was defined based on the average value of the Lidar points within each model cell. To define the bottom of layer 1, the following approach was used:
  - a. The extent of L1 (USGS Figure 18) was divided into various polygons: the area defined by L2-top contours (USGS Figure 20), areas where L1-Bottom will be defined by land surface minus L1 thickness (USGS Figure 18), the area without either source of data, and the area occupied by bedrock (“unit is absent” on USGS Figure 18).
  - b. Bring “top of L2” contours (USGS Fig 20) into GIS.
  - c. Generate a set of L1-Bot contours from land surface elevation and L1 thickness map (USGS Figure 18) and bring into GIS map. Generate contours by subtracting USGS thickness value, as defined by the midpoint of the thickness range in each zone, from the land surface, as defined as an average value for each cell using the (predominantly Lidar) Puget Sound DEM<sup>1</sup>. For bedrock areas, a dummy thickness of 100 feet was used
  - d. Generate a set of L1-Bot contours from TTFW model to be used in areas not covered by USGS Figures 18 and 20.
  - e. Combine the contour maps onto one map, with the L2-top contours left in place, the L1-Bot contours calculated from L1 thickness filling in the rest of the extent of L1 and the bedrock areas, and the TTFW contours filling in the areas of insufficient data. Hand-smooth the three sets of contours into a single set of contours to define the bottom of L1. Feather (or “smooth”) the data sets into one another to address inconsistencies between the coverages. The highest accuracy is available where the USGS defined L2-top contours, moderate accuracy is likely achieved in areas where USGS only defined L1 thickness and in areas defined by TTFW near their cross sections and any other (unreported) areas of their investigation, and the least accuracy is achieved where TTFW had to define elevations with no additional investigation.

---

<sup>1</sup> <http://www.ocean.washington.edu/data/pugetsound/psdem2005.html>

- f. Digitize and regrid the hand smoothed continuous contour set. Define average values per cell. This becomes the new (initial) layer 1 bottom.
  - g. Bring the new L1-Bot into GV and compare to USGS Figure 20. Immediately inland of the coast, where contours do not fill the entire land area (e.g. no contours off the coast for interpolation), manually go through cells and make sure that boundary effects of the contouring algorithm provide values that are consistent with USGS Figure 20. Individual cells were manually adjusted.
  - h. Determine which cells have centroids falling within the bedrock region and designate these cells as “inactive” within GV.
2. Define the Bottom of Layer 2
- a. Define L2 bedrock cells from USGS Figure 19 areas where the upper confining bed is absent.
  - b. Define “ND” (no data) cells from USGS Figure 19, obtain TTFW values for cell thickness from their model for these ND cells.
  - c. Define thickness of unit 2 for each model cell based on the midpoint value for each thickness range polygon shown on Figure 19 (e.g. use “75” for a “50-100” range).
  - d. Subtract thickness from L1 bottom elevations derived above, using the USGS thicknesses where available, a dummy value of 75 feet for bedrock, and TTFW thickness values elsewhere, to obtain L2 bottom values per cell.
  - e. Bring new L2-Bot distribution into GV and touch up distribution where needed. TTFW areas had some stand-alone outlier values of thickness (sometimes single cells) that PGG made consistent with neighboring values. In most cases, it turned out that these corrections were in areas that TTFW defined as occupied by bedrock (USGS had designated “insufficient data”), and therefore TTFW paid little attention to elevations.
  - f. It is worthwhile to note that PGG tried an alternative approach that preferentially used the L3-top contours defined by the USGS (USGS Figure 22) to define L2-Bot, and calculated values (L1-Bot minus thickness) elsewhere. This was problematic, however, because PGG’s redefinition of L1-Bot required some smoothing to provide consistency between the 3 datasets considered, and we observed multiple cells where the USGS definition of L2 thickness was not preserved when the contoured value of L2-Bot was subtracted from the new value of L1 bot. As L2 is an aquitard and is always saturated, its actual bottom elevations are far less important than L1. Instead, thickness is the key parameter - which PGG captured from USGS Figure 19.
3. Define the Bottom of Layer 3
- a. Define bedrock cells from USGS Figure 21 areas where the middle aquifer 2 is absent.
  - b. Define “ND” (no data, of “not defined”) cells from USGS Figure 21, obtain TTFW values for cell thickness from their model for these ND cells.
  - c. Define thickness of unit 3 based on the midpoint value for each thickness range polygon shown on Figure 21.

- d. Subtract thickness from L2 bottom elevations derived above, using the USGS thicknesses where available, a dummy value of 50 feet for bedrock, and TTFW thickness values elsewhere, to obtain L3 bottom values per cell.
  - e. Bring new L3-Bot distribution into GV and touch up distribution where needed. Only one spot was identified (cells 21,41 and 21,42) – this is a tiny area where the USGS said the unit was absent. PGG made thickness in this location similar to neighboring locations (25 feet) and recalculated bottom elevation values.
4. Define the Bottom of Layer 4
    - a. Make a master map for the lower confining bed that defines its entire extent, where L4 is occupied by bedrock, and where insufficient data occur (USGS Figure 23).
    - b. Obtain from USGS point values of lower confining bed thickness from USGS interpretation of the wells used to prepare their cross sections (included in the USGS GIS coverage). Contour these L4 thickness values in USGS area of L4 extent.
    - c. Contour L4 thickness values from TTFW.
    - d. Hand-generate a master contour map of aquitard thickness that honors the USGS contours within their definition of upper confining bed extent and TTFW contours in USGS area defined as “no data”.
    - e. Using GIS, re-grid L4 thickness based on PGG’s master contour map and all of the points with thickness values obtained from the USGS GIS. From this new grid, obtain average thickness values for each model cell. All cells with centroid occupied by bedrock were assigned a thickness value of 100.
    - f. Subtract new L4 thickness values from bottom of L3.
  5. L5 bottom was simply calculated as 100 feet lower than L4 bottom.
  6. To estimate the bottom of the undifferentiated deposits, PGG took TTFW’s definition of L6-Bot for all model cells and compared these values per cell with the new L5-Bot elevations. PGG used the TTFW values as long as L6 was represented as at least 50 feet thick. Where the TTFW L6 bottoms were less than 50 feet below the PGG L5 bottoms, PGG redefined them as L5-Bot minus 50 feet.
  7. The undifferentiated deposits (L6) was originally modeled as a single layer by TTFW. This meant that modeling L6 as an aquifer put the aquifer materials in direct contact with the lower aquifer in L5 without an intervening confining unit. In order to allow use of L6 to represent an aquifer, the layer was divided into 3 layers (from top to bottom – an aquitard, an aquifer, and another aquitard). The following procedure was used to split up L6 into L6, L7 and L8:
    - a. If the thickness of the original L6 is <300 feet, divide the layer evenly in 3.
    - b. If the original L6 is >500 feet, the middle layer (aquifer) will always be 200 feet below the top of the original L6 and 100 feet thick
    - c. If the original layer ranges from 300-500, the top of the middle layer (aquifer) will trend downward from a minimum depth of 100 feet below the top of L6 (when the

total thickness is 300 feet) to a maximum depth of 200 feet (when the total thickness is 500 feet). The thickness will always be 100 feet.

8. Bottom of bedrock, for bottom model layer, was prescribed as 500 feet below bottom of the undifferentiated deposits (original L6 or updated L8). Note that model sensitivity analysis later indicated that bedrock had relatively little influence on model results, and the model layers representing bedrock and the bottom aquitard in the undifferentiated deposits were later removed.
9. After defining layer elevations, PGG imported bedrock designations for model cells into layers 2 through 4 into GV from our GIS analysis (bedrock in L1 had already been defined in GV, as noted above). The USGS bedrock definition for various layers has gaps west of McDonald Creek. So, after importing the USGS bedrock distributions, PGG also imported the TTFW coverages west of a chosen model column. For layer 2 PGG imported TTFW bedrock designations west of column 26, and made inactive the small channel of non-bedrock materials that parallels Sequim Bay near the south and another east-west channel that predominantly just overlies bedrock. For layer 3, PGG imported TTFW bedrock west of model column 25. For layer 4, PGG imported TTFW bedrock west of column 21.
10. Because layer elevations were not defined for offshore areas, PGG estimated layer elevations by extrapolating the north-south dip of hydrostratigraphic units characterized in the USGS report. The USGS north-south cross sections that showed significant dip included I-I' (0.74%), G-G' (0.5%), and H—H' (1%). Section F-F' showed no dip but was relatively short, and section E-E' had insufficient detail and length to assess dip. From the northern terrestrial coastline, PGG applied a dip of 0.75% to the contacts between layers. This dip was extrapolated to the northern extent of the model domain. Beneath Sequim Bay, PGG assumed flat layering, and extrapolated contact elevations on the west side of the bay eastward to the easternmost active model cell.

#### First Refinement of Model Layer Elevations

During initial testing of the model layering described above, PGG identified 47 cells where the surface-water (river/drain) heads were below the bottom of layer 1. This predominantly occurred in areas where layer 1 overlies bedrock in layer 2 (43 of 47 cells), or where USGS defined “insufficient data” (along and west of Siebert Creek), or in areas where USGS contouring of L2 top had to be “smoothed” with other sources of data. PGG also realized that its initial definition of river/drain elevations (based on the lowest lidar elevation value in the model cell) provides the “downstream” river/drain elevation, not a river/drain elevation representative of the overall cell itself. A more representative river/drain elevation would be the average between the downstream and upstream river elevation of that cell (essentially the average between the downstream river elevation of that cell and the downstream river elevation of the next upstream cell). PGG recalculated the river/drain elevations accordingly, imported the new river/drain values into the model, and performed the following layer bottom adjustment:

1. Identify the cells that have surface water heads beneath the bottom of layer 1 and identify how much higher the bottom of L1 is relative to these river/drain cells.
2. Plot these elevation differences on a map viewable in GV.

3. Prescribe a distribution of L1 bottom correction (reduction) that will offset L1-Bot to below the river/drain heads. Corrections generally ranged from 50 to 100 feet in the vicinity of the streams.
4. Recalculate the bottom of layer 1 by subtracting the corrections from the previous distribution of L1-Bot values.
5. Recalculate the bottom elevations of all underlying layers using the procedure outlined above.

### Second Refinement of Model Layer Elevations

During calibration, PGG noted some difficulty in matching several head targets and therefore reviewed target well logs a little closer and made two local layering adjustments. These adjustments were made within GV, and are therefore not reflected in any of the spreadsheets maintained by PGG for layer elevations.

1. 30N04W17P01 is 70 feet deep and is predominantly clay down to a 4-foot-thick water bearing zone (62-66 feet) overlying more clay. It is located just east of McDonald Creek. USGS Xsec F-F' runs about a half mile away to the west. Closest to the well, in the immediate vicinity of SR101, the Xsec suggests that bedrock may be about 80 feet below land surface at an elevation of 220 feet msl immediately west of the creek. The Xsec shows the upper confining unit absent in this vicinity. At the target cell, the model represents bedrock in L3 with L2 active as an aquitard with a bottom elevation of 127 feet msl. The bottom elevation of L1 at the same cell is 202 feet mwl. PGG extended the bedrock distribution in L2 one cell north to the target cell (39,29) and increased the L1 bottom elevation from 202 to 220. This caused a small improvement in the target residual.
2. Another well, near the south bedrock boundary, is 30N/04W-34M04 (ACA629 in cell 51,37). The model prediction here is about 55 feet too low. The well is only 24 feet deep and no log is available. USGS Xsec H-H' shows the nearest well (34E01, just 1 Q section to the north) to have no more than 20 feet of unconsolidated sediments over bedrock. This cell has 77 feet of L1 aquifer over bedrock in L2. This is an area where the bottom elevations were not specified by the USGS, thickness was specified in ranges, and PGG hand contoured a surface for the bottom of L1 based on land surface elevation minus center value of thickness zone. Given the variation of top elevation per cell, there is room for this being off, especially in steep terrain. PGG raised cell 51,37 bottom by 61 feet and tapered off the adjustment by 2 cells in all directions – the bottom contours are still smooth. This fixed the target residual issue at this model cell

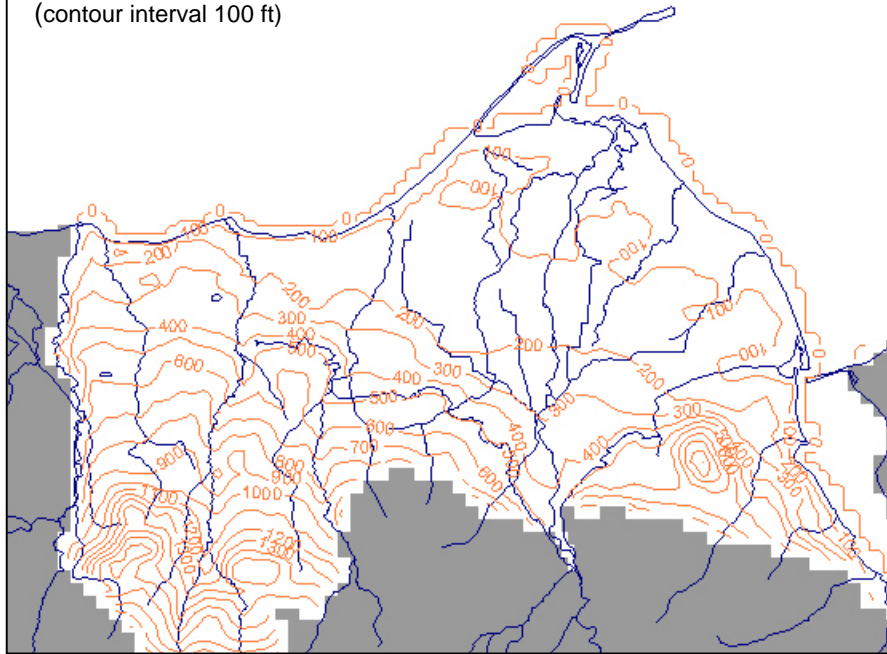
### Third Refinement of Model Layer Elevations

During calibration, PGG encountered flooded cells in the area around south Sequim Bay. PGG therefore checked the model L1 thicknesses against those shown on USGS Figure 18 and made changes to make them consistent. Prior assignments of L1 bottom in this area was based on hand contouring based on L1 top minus thickness, but it was simplified somewhat. The following table summarizes the changes made. The first string of characters specifies the original thickness, the change, and the final thickness respectively (e.g. “11 + 64 = 75”). The second string of characters specifies the top elevation of the cell (to which the new thickness was applied) and the new bottom elevation:

	<b>C73</b>	<b>C74</b>	<b>C75</b>	<b>C76</b>	<b>C77</b>	<b>C78</b>	<b>C79</b>
<b>R53</b>	11+64=75 322/247	n/a	n/a	n/a	n/a	n/a	n/a
<b>R54</b>	63+12=75 398/323	5+45=50 271/221	33+17=50 215/165	18+57=75 123/48	17+8=25 43/18	n/a	n/a
<b>R55</b>	115 - OK OK	45+30=75 369/294	7+68=75 261/186	23+52=75 188/113	28+22=50 107/67	n/a	n/a
<b>R56</b>	190 OK	193 OK	111 OK	75 OK	81 OK	10+10=20 31/11	n/a
<b>R57</b>	Bedrock	Bedrock	186 OK	153 OK	212-90=122 394/272	117 OK	10+10=20 5/-15
<b>R58</b>	Bedrock	Bedrock	Bedrock	Bedrock	Bedrock	119 OK	10+10=20 54/34

PGG then ran the GV grid correction routine to ensure that all cells in layers 2 and below had a cell thickness of at least 10 feet. Many of the cells fixed in L-1 had bedrock (inactive) beneath them in L2, and GV will not perform a grid correction on inactive cells (nor does it have any bearing on model function). Note that these local grid elevation changes were made within Vistas, and were not tracked in PGG's grid elevation spreadsheets. Ultimately, the changes did not fix the problem with localized flooded cells, and PGG instead increased the hydraulic conductivity in this area during calibration to reduce the occurrence of flooded cells.

**Top of Layer 1**  
(contour interval 100 ft)



**Bottom of Layer 1**  
(contour interval 100 ft)

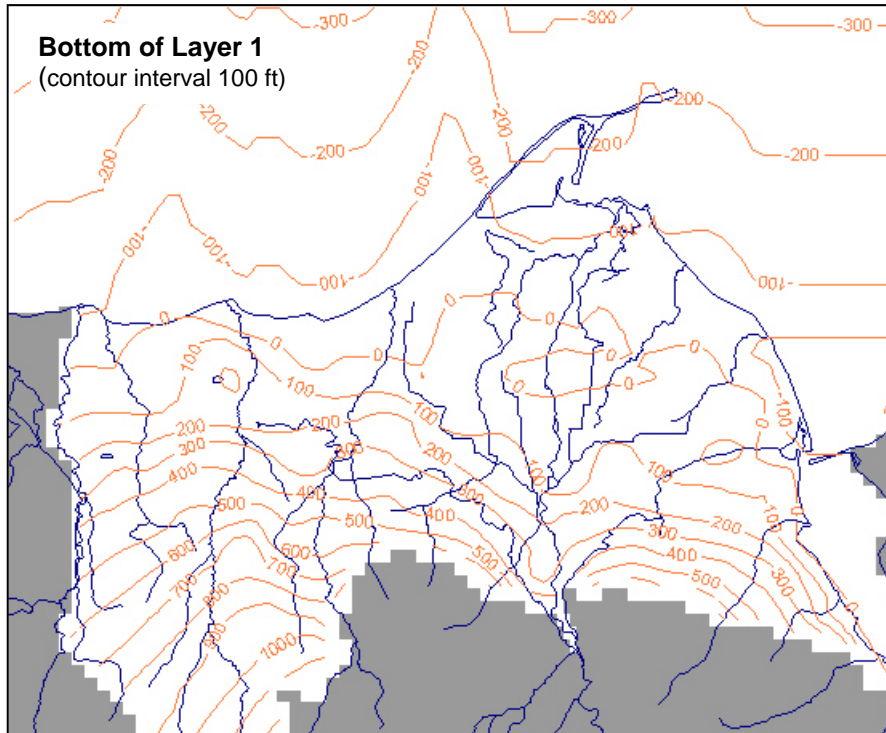


**Figure A-1**  
**Layer 1 Elevations**

Clallam County  
2008 Groundwater Flow Model



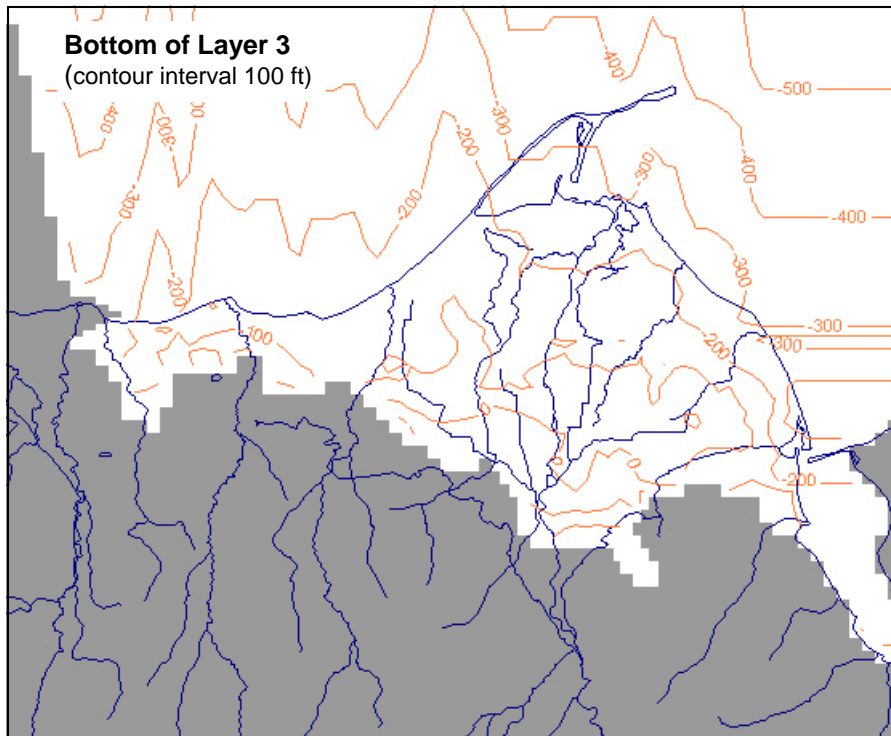
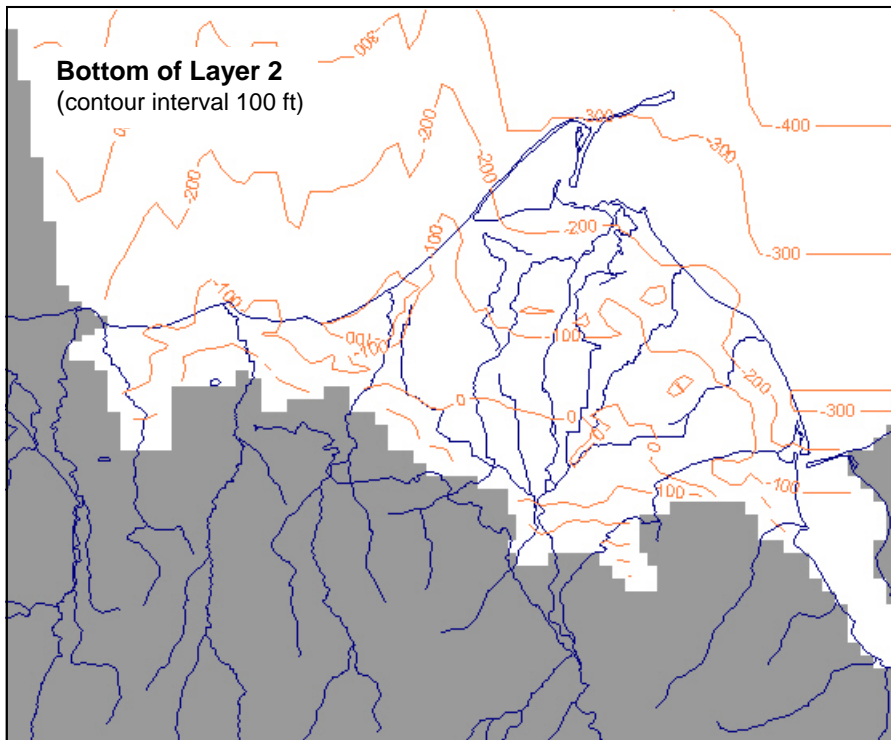


**Figure A-2**  
**Bottom Elevations of Layers 2 and 3**

Clallam County  
2008 Groundwater Flow Model





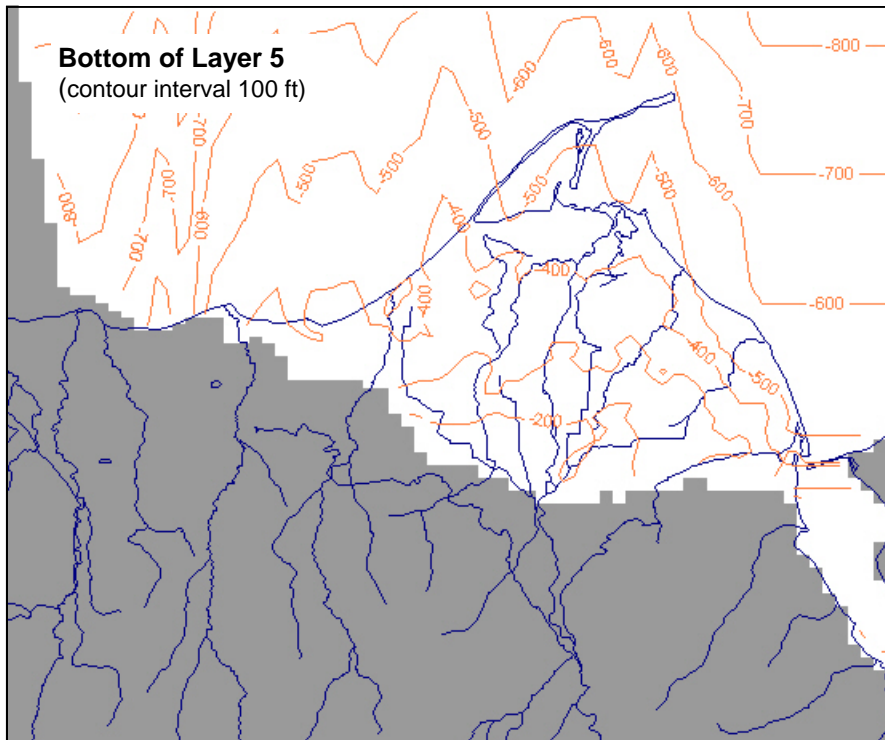
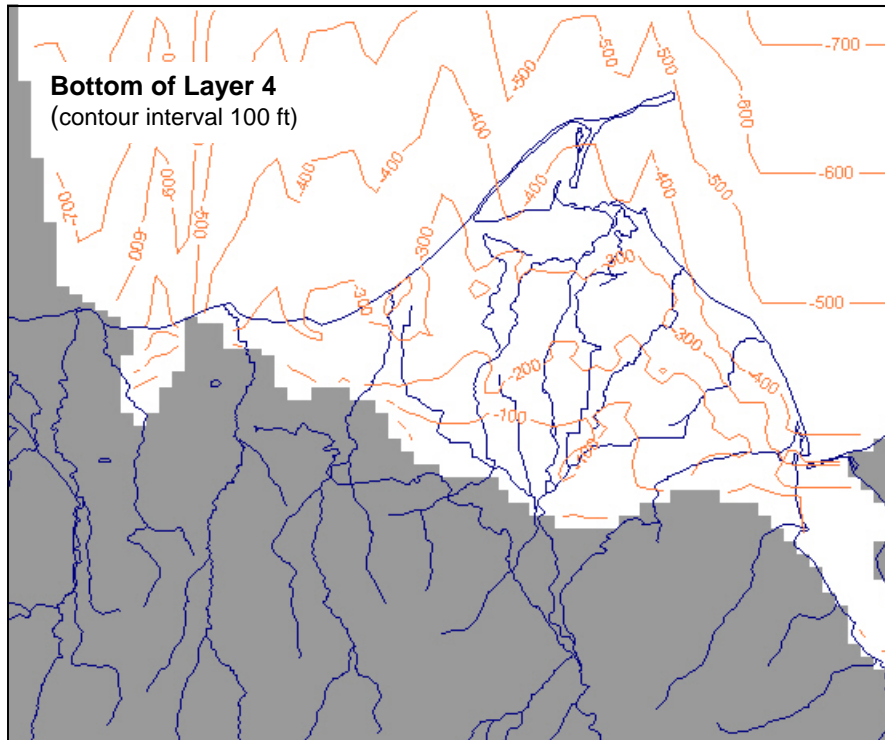


**Figure A-3**  
**Bottom Elevations of Layers 4 and 5**

Clallam County  
2008 Groundwater Flow Model



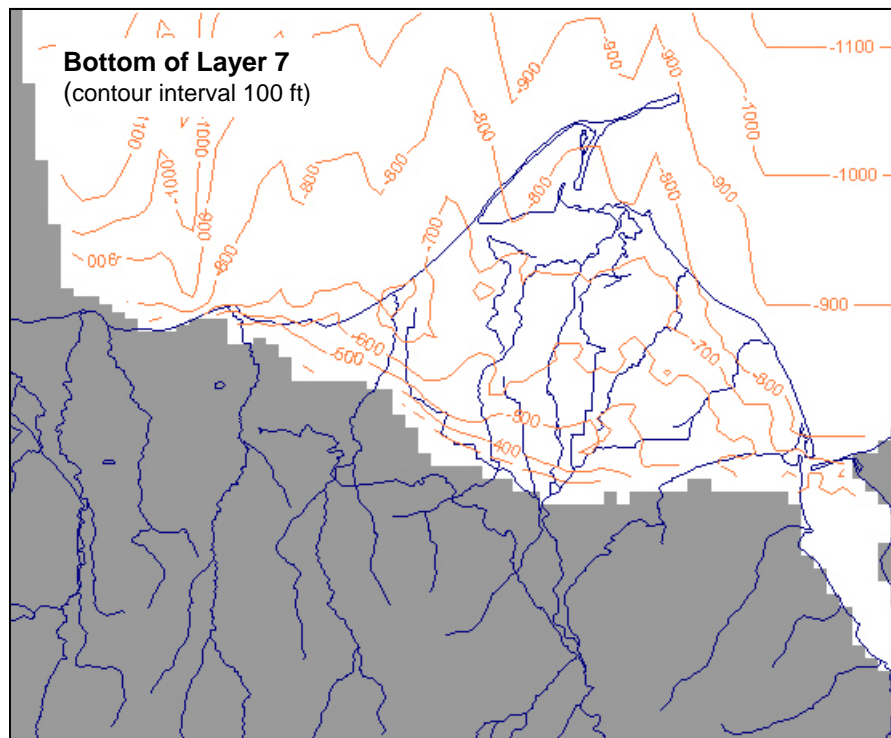
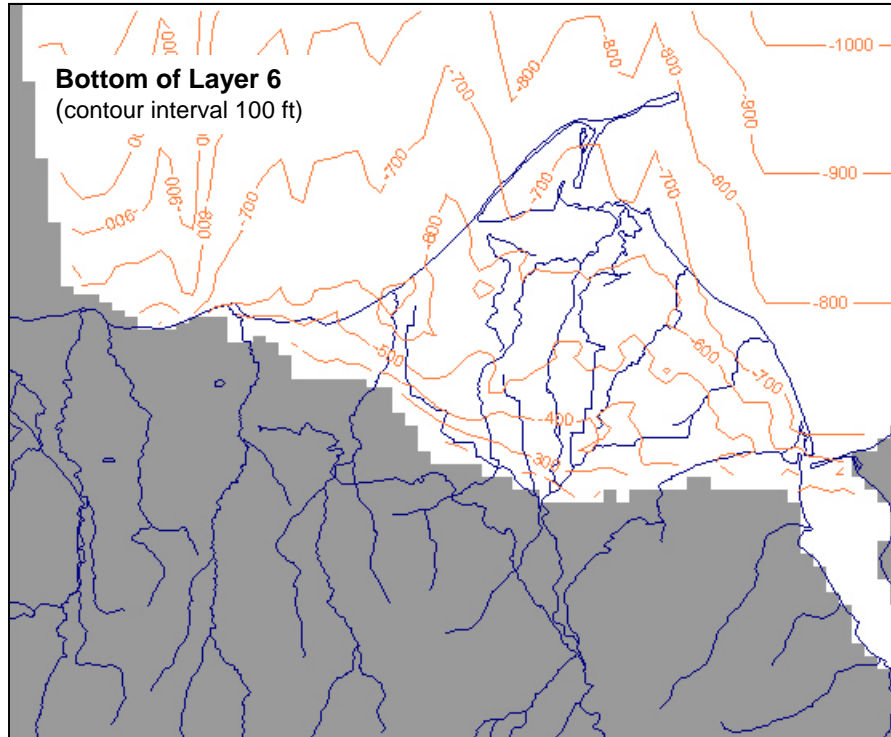


**Figure A-4**  
**Bottom Elevations of Layers 6 and 7**

Clallam County  
2008 Groundwater Flow Model



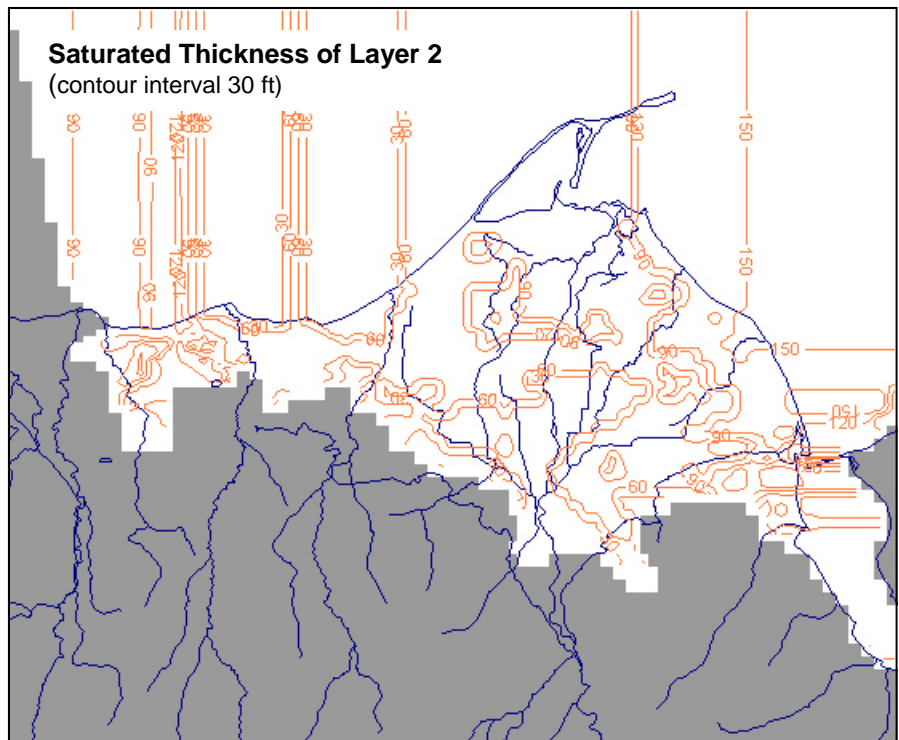
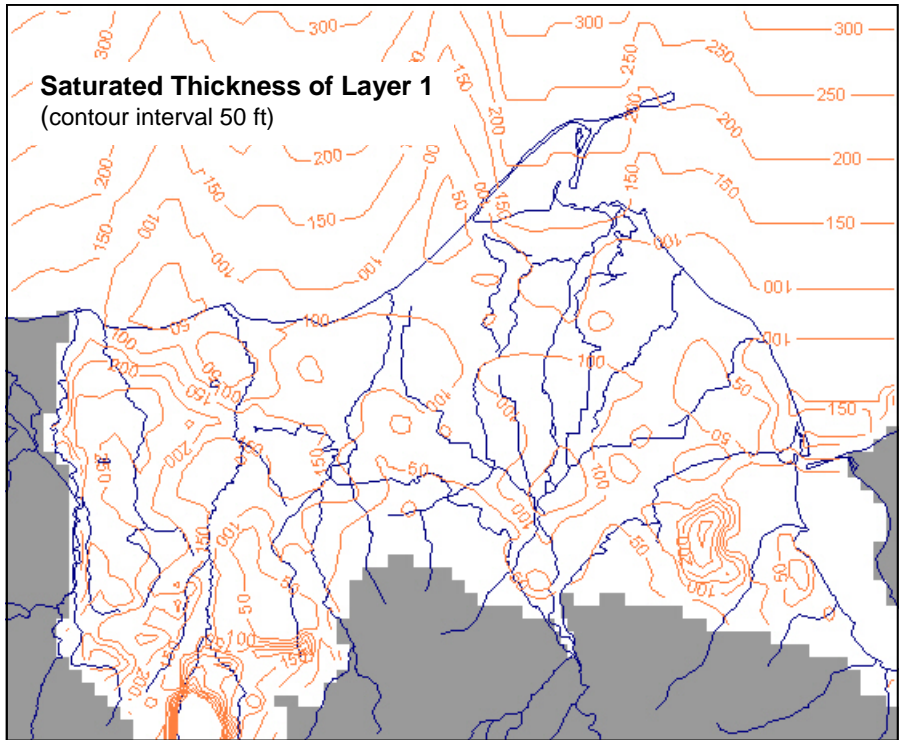


**Figure A-5**  
**Saturated Thickness of Layers 1 and 2**

Clallam County  
2008 Groundwater Flow Model



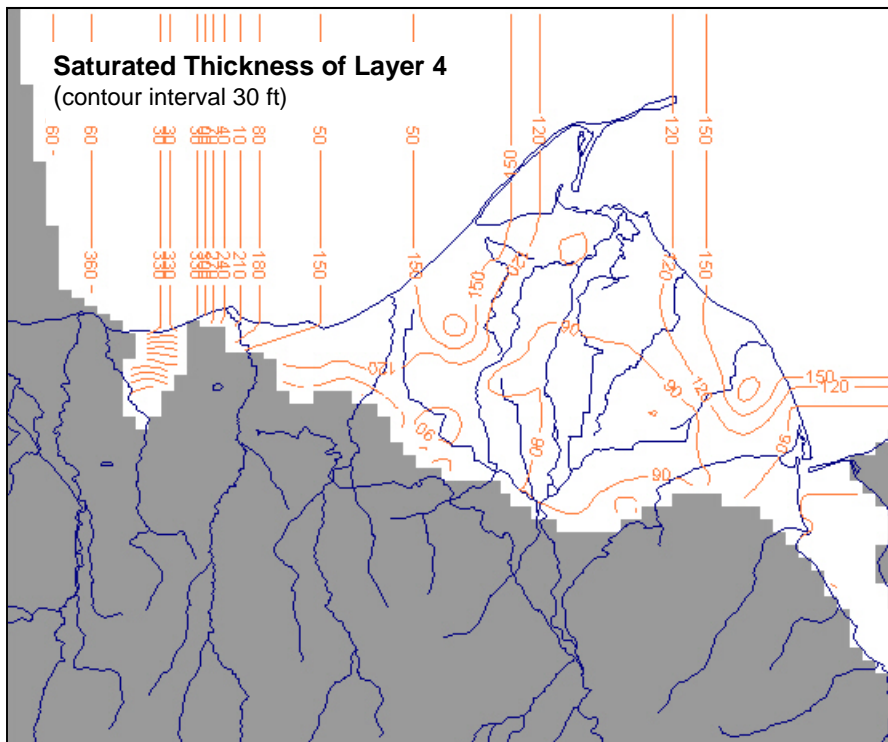
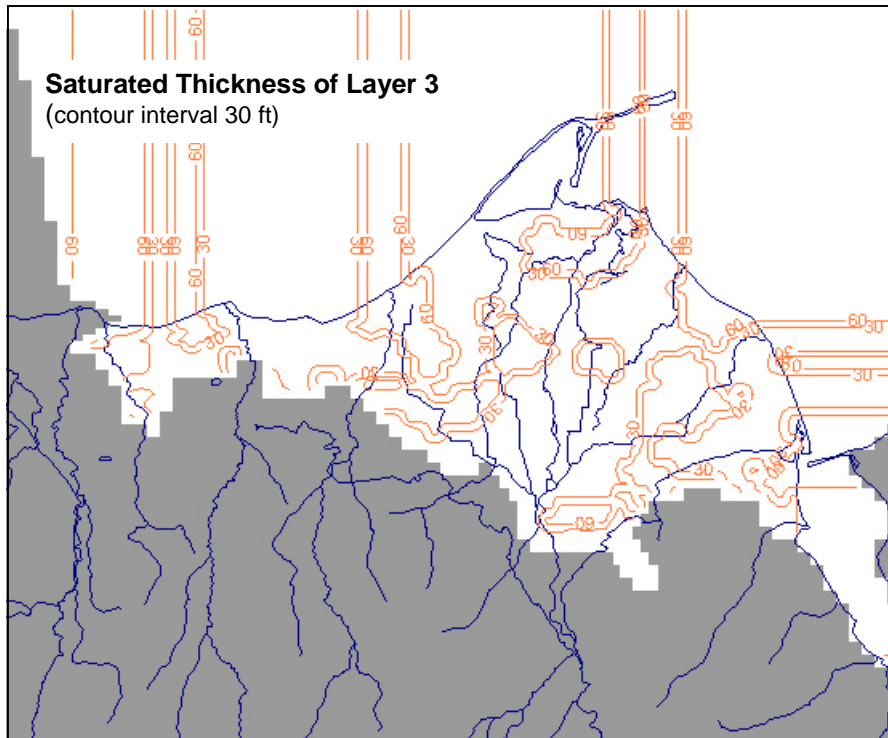


**Figure A-6**  
**Saturated Thickness of Layers 3 and 4**

Clallam County  
2008 Groundwater Flow Model



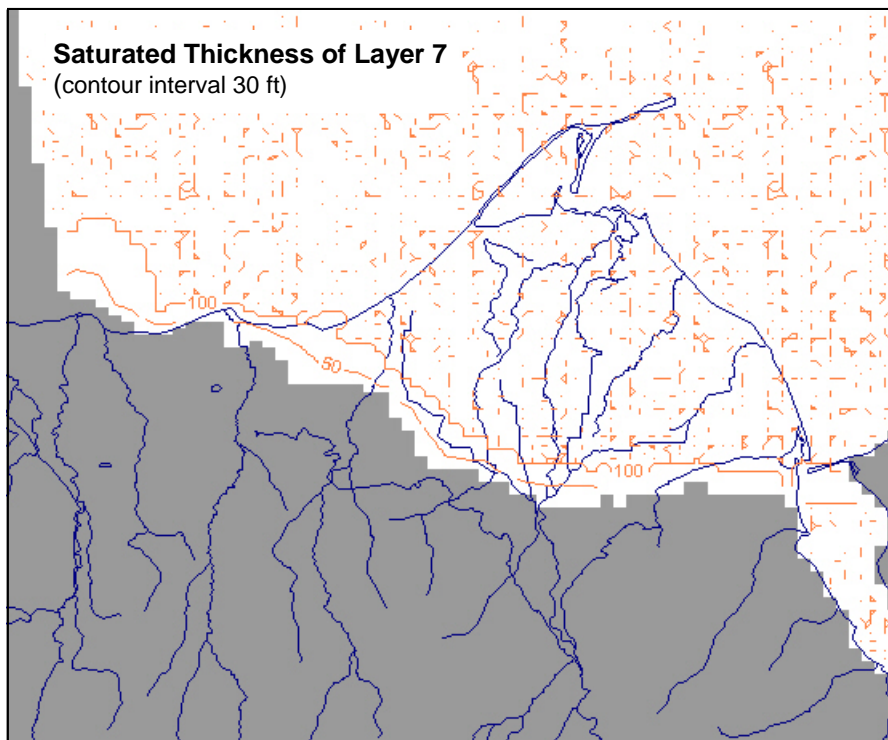
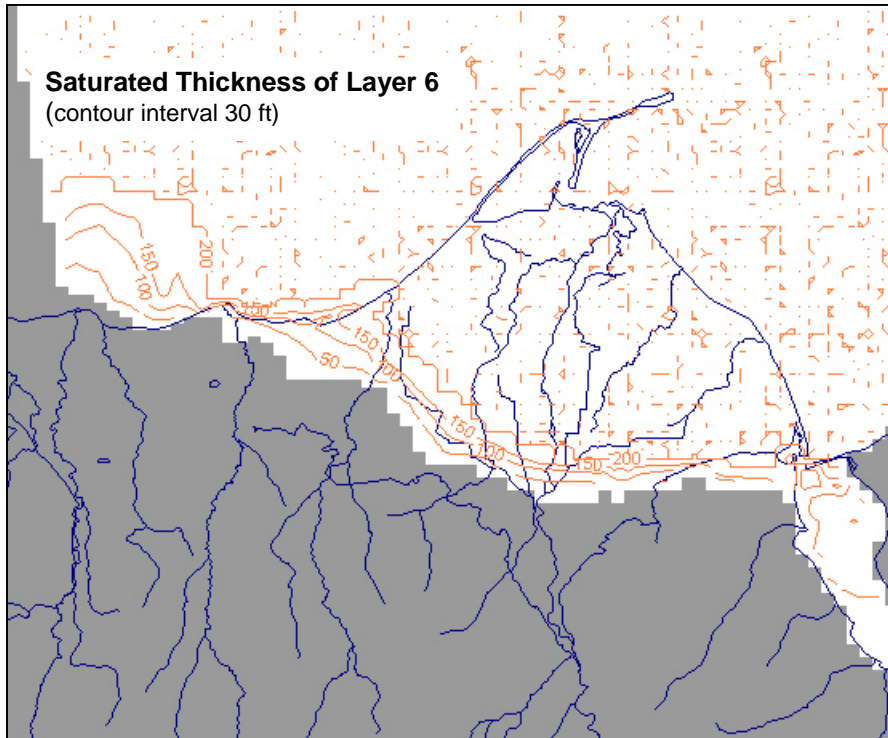


**Figure A-6**  
**Saturated Thickness of Layers 6 and 7**

Clallam County  
2008 Groundwater Flow Model



## **APPENDIX B**

### **ANNOTATED LIST OF DIGITAL DOCUMENTATION**

## APPENDIX B ANNOTATED LIST OF DIGITAL DOCUMENTATION

The following list describes the digital files PGG has made available with this report.

Dung-SS-7e-Final.gwv – This is the final version of the steady state model (realization 7e) to be used for future simulations. The recharge in this version has been changed from the calibration values to the long-term average defined by the USGS. Note – solver needs to be changed to Modflow 88/96 – see *Dung-SS-7e-MF88-example.gwv*.

Dung-SS-7e-Final.hds – Head output for the above mentioned model realization.

Dung-SS-7e-initial.hds – Initial heads for running Dung-SS-7e simulations.

Dung-SS-7e.gwv – Version of the steady state model (realization 7e) used for calibration. Has targets included, and used midpoint value between study period and long-term average recharge. Note – solver needs to be changed to Modflow 88/96 – see *Dung-SS-7e-MF88-example.gwv*.

Dung-SS-7e.hds – Head output for the calibrated model realization 7e.

Dung-SS-7e-MF88-example.gwv – Model version that includes solver settings for running the model in Modflow 88/96. Use these settings and the SIP solver. Make sure you check your mass balance at the end of any run.

Dung-TR-7e-WU.gwv – transient warmup run set up for study period calibration using realization 7e. Use *Dung-SS-7e.gwv* to produce initial heads for this run.

Dung-TR-7e-Cal-1.gwv – transient calibration run set up for study period calibration using realization 7e. Use results of *Dung-TR-7e-WU.gwv* as initial heads for this run. Note that the transient targets included in this model are not the absolute values, but have been translated within Groundwater Vistas so that the first target value corresponds with the model value at that time (thus providing a “head displacement” target. To replace these translated targets with absolute values of head, use the spreadsheet *PGG Transient Targets.xls* (see description below).

Dung-TR-7e-Cal-1.hds – head output from transient calibration model referenced immediately above. Check actual model to discern S and Sy values used during that calibration run.

Dung-SS-7g-Final.gwv – This is the final version of the steady state model (realization 7g) to be used for future simulations. The recharge in this version has been changed from the calibration values to the long-term average defined by the USGS. Note – solver needs to be changed to Modflow 88/96 – see *Dung-SS-7e-MF88-example.gwv*.

Dung-SS-7g-Final.hds – Head output for the above mentioned model realization.

Dung-SS-7g-initial.hds – Initial heads for running Dung-SS-7g simulations.

Dung-SS-7g.gvw – Version of the steady state model (realization 7g) used for calibration. Has targets included, and used midpoint value between study period and long-term average recharge. Note – solver needs to be changed to Modflow 88/96 – see *Dung-SS-7e-MF88-example.gvw*.

Dung-SS-7g.hds – Head output for the calibrated model realization 7g.

PGG Regen of TTFW Transient Pumping.xls – This file contains a regeneration of the transient pumping rates that were intended to be used by TTFW, but were not actually found in their calibrated transient model. PGG obtained the monthly pumping values from a TTFW spreadsheet (rather than the calibrated model) and then used an external database to sum the pumping of multiple wells per model cell. Note that steady state pumping was taken directly from TTFW version of the model, and can be exported from any of the steady state (SS) versions of the model noted above.

Model Targets with AS Revised Locations.xls – This spreadsheet contains steady state targets for study-period calibration. Use the “Targs-AS-Coords” sheet for steady state targets. Other sheets include well data from USGS database, explanation of USGS data codes, data from City of Sequim, data from Drost report, data from prior TTFW spreadsheet (“Avg DTW”), a preliminary weighting scheme developed by PGG.d data.

PGG Transient Targets.xls – spreadsheet used to prepare input files for transient targets for transient calibration. Note – use sheet called “AS Coords” for the targets with their coordinates updated by Ann Soule (the other similar sheets were for previous, less accurate coordinates). Export this sheet into the transient calibration model (*Dung-TR-7e-Cal-1.gvw*) to obtain absolute target values for any further calibration.

Updated Dungeness Cells 07-08.xls – This spreadsheet has the final Dungeness River dimensions that PGG estimated using GIS, measuring river length per cell and river elevation via lidar. However, note that during calibration, heads and bottom elevations were reduced by 4 feet to mitigate for cell dimension inaccuracies. Therefore, if you want the values used during model calibration, it is best to extract the data from the actual model. However, this spreadsheet does document the lidar elevations and channel lengths estimated by PGG per model cell.

PGG Rivers and Drains adjusted to mid cell lidar.xls – This spreadsheet has the final river and drain dimensions and elevations for every stream except the Dungeness. It was used as input for calibration. Note that hydraulic conductivities of streambed and drainbed were varied during calibration, and these values are embedded in the model. It is best to just extract the river and drain definitions from the model, as this will ensure the most up-to-date cell specifications. During calibration, cells may have been added or removed from the specifications on this spreadsheet.

Transient Dungeness v7.xls – This spreadsheet takes the steady state Dungeness River definitions from a prior version of the model (Dung-7c... same as Dung-7e but with riverbed conductance set to 1 ft/d rather than the current value of 10 ft/d) and applies monthly stage offsets to generate model input for the monthly stress periods. This input was used for both the warmup and the calibration versions of the transient model. The same data are embedded in the models themselves.



Corrected Model Recharge 5-10-08.xls – This spreadsheet contains PGG’s recharge calculations for steady state recharge. It is a bit complex. The sheet called “recharge” has the USGS recharge values interpolated onto the model grid by spatial weighted averaging in GIS. Some of the model cells do not have USGS recharge coverage, so PGG has to estimate recharge using the USGS regression equations, USGS soil type per cell, and slope per cell (from NRCS soil type slope definitions). TTFW’s definition of septic and wastewater recharge is also included in a separate sheet, although wastewater recharge for Sunland was later moved to a different cell (it can be observed in the actual model, as it stands out). Various sheets allow export of longterm (LT) or study period (SP) recharge for precipitation, wastewater/septic, irrigation, all combined for the steady state model.

Total Transient Recharge.xls – This spreadsheet contains all the calculations used to generate transient recharge per stress period. It identifies the recharge regime of each cell and the irrigation company classification for each cell with irrigation recharge. It applies different equations for each different type of irrigation regime. Be sure to check the “comments” in the cell headings to understand the different classifications. Also, I’ve included a folder that has all the files for which recharge was exported for both the study period and the warmup period. This spreadsheet uses long-term precipitation recharge to generate the warmup period monthly recharge values. A second spreadsheet, called Total Transient Recharge Warmup=SP.xls, was used to generate warmup recharge using the study period precipitation values.

Recharge Stress Period Files – This folder contains input files for Vistas that have the total recharge per stress period imported to the model. Steady state recharge distributions are also included. Note that the “HiRech” monthly files were used for the warmup model, and are based on study period precipitation recharge. Files named “Rech-month” were also generated for the warmup model, but use longterm precipitation recharge. Files named “Rech-0196” were the calibration period recharge for the referenced month (e.g. January 1996). Files named “PGG-xxxx-Recharge” are all steady state, and are specified to contain precipitation, irrigation, septic, or all combined.

Maps – the folder titled maps has all the map files PGG used during model development.

Cyclic Steady State.doc – explains the procedure used to run the model multiple times in series within Modflow Surfact (a similar procedure could be used with plain Modflow).